Provision of Flexibility Services by Industrial Energy Systems

Zur Erlangung des akademischen Grades

Doktor der Ingenieurwissenschaften

von der KIT-Fakultät für Wirtschaftswissenschaften des
Karlsruher Instituts für Technologie (KIT)

genehmigte
Dissertation
von

Julian Rominger, M. Sc.

Tag der mündlichen Prüfung:	26. Juni 2020
Referent:	Prof. Dr. Hartmut Schmeck
Korreferent:	PD Dr. Patrick Jochem

Abstract

Energy is needed for production processes at manufacturing plants. These lead to a considerable direct and indirect energy demand. To reduce the environmental impact and energy costs, many manufacturing plants invest in local power generation, storage, or employ demand response. On the one hand, the complexity of energy management increases for industrial energy systems with a large number of controllable energy technologies. On the other hand, a potential arises for reducing energy costs through the provision of local and external flexibility services such as the reduction of the peak load to save grid fees, the participation on energy markets, or the provision of control reserve to stabilize the grid frequency.

Short-term plant deployment, such as day-ahead scheduling, is an essential energy management tool for the cost-effective provision of energy, i.e., electricity, heating, and cooling. The aim is to use local energy devices in a cost-optimized manner, taking into account technical and contractual constraints. A prerequisite for this scheduling is a forecast of the energy demands and a detailed modeling of energy devices, markets and contracts. Furthermore, related revenues, costs, and conditions of the provision of local and external flexibility services have to be modeled.

For the provision of external flexibility services, many industrial plants rely on virtual power plants to aggregate and commercialize the offered flexibility, e.g., on control reserve markets. A manufacturing plant with a high number of energy devices can aggregate flexibility locally for the direct provision of control reserve and save fees usually paid to the external virtual power plants.

This work identifies, analyzes, and assesses possible flexibility services for an industrial production site in Germany. Furthermore, simulations of a battery storage providing selected flexibility services are introduced. Results for the battery storage indicate that it is most profitable to combine several flexibility services in a multi-use model instead of providing a single flexibility service.

A methodology is presented which examines an energy system of an industrial plant of the automotive industry consisting of a multitude of controllable and non-controllable generators, consumers and storage facilities. For the case study, a multi-objective optimization problem is developed, which minimizes total energy costs through the dispatch of flexible energy technologies and the provision of flexibility services in a multi-use model. The optimization problem is modeled as a mixed-integer linear program. Results show that the provision of several flexibility services at the industrial plan can decrease energy costs by 12%.

In addition, scenarios are modeled and evaluated that examine the potential of local aggregation as opposed to the aggregation by virtual power plants. Results show that local aggregation of flexibility of the pool of energy technologies and direct commercialization on control reserve markets without an external aggregator show the greatest cost reduction for the case study.

Kurzfassung

Produktionsprozesse zur Fertigung sowie unterstützende Prozesse und Einrichtungen führen zu einem direkten und indirekten Energiebedarf. Um die Umwelt- und Kostenbelastung der Produktion zu reduzieren, investieren viele Industrieunternehmen in eigene Energieerzeugungsanlagen, Energiespeicher oder flexibel steuerbare Energieverbraucher. Mit einer Vielzahl an steuerbaren Energieanlagen steigt einerseits die Komplexität des Energiemanagements, andererseits ergeben sich auch Potenziale zur Energiekostenreduktion durch den lokalen Einsatz von Flexibilität oder durch das externe Angebot von Flexibilität auf Energiemärkten und für Energiesystemdienstleistungen.

Für das Angebot von Energiesystemdienstleistungen setzen viele Industrieanlagen auf Aggregatoren, um die angebotene Flexibilität zu aggregieren und beispielsweise als Regelleistung zu vermarkten. Eine direkte Vermarktung ohne einen externen Aggregator kann Vermarktungsgebühren sparen, aber kann auch das Vermarktungspotenzial verringern.

Die kurzfristige Anlageneinsatzplanung ist ein wesentliches Werkzeug des Energiemanagements zur kostengünstigen Bereitstellung von Energie, d.h. von Strom, Wärme und Kälte. Dabei gilt es, Eigenanlagen unter Berücksichtigung der technischen und vertraglichen Randbedingungen kostenoptimal einzusetzen. Voraussetzung hierfür ist eine Prognose der Energiebedarfe und eine detaillierte Modellierung der verschiedenen Energieanlagen, -märkte und -verträge. Die Modellierung beschreibt die Menge an möglichen Ausprägungen der Einsatzplanung aller Energieanlagen inklusive der Erbringung von Flexibilitätsdienstleistungen sowohl für das lokale Energiesystem als auch für die Wertschöpfung auf Energiemärkten.

Im Rahmen der Arbeit werden mögliche Flexibilitätsdienstleistungen identifiziert, analysiert und auf eine Umsetzbarkeit in einem Industriestandort bewertet. Für einen stationären Batteriespeicher werden weiterhin Betriebssimulationen aufgestellt, die Erlöse und entstehende Kosten der Erbringung von Flexibilitätsdienstleistungen durch einen Batteriespeicher bewerten.

Des Weiteren wird ein Modell vorgestellt, das ein Energiesystem eines Automobilwerkes bestehend aus einer Vielzahl an steuerbaren und nicht-steuerbaren Erzeugern, -verbrauchern und -speichern abbildet. Hieraus wird ein Optimierungsproblem entwickelt, das einen Einsatzplan der steuerbaren Energieanlagen als Ergebnis hat, mit dem die notwendigen Energiebedarfe kostenminimal gedeckt werden und zusätzlich Erlöse durch das Angebot von Flexibilitätsdienstleistungen erzielt werden können. Das Optimierungsproblem wird als gemischt-ganzzahliges lineares Programm modelliert. Die Ergebnisse zeigen, dass die größten Einsparungspotenziale in der Flexibilitätsvermarktung auf kurzfristigen Strommärkten, der Regelleistungsvermarktung und in der Lastspitzenminimierung liegen.

Es werden außerdem unterschiedliche Szenarien der Aggregation mit oder ohne einem externen Aggregator modelliert und evaluiert. Es wird gezeigt, dass für den ausgewählten Industriestandort geringe Einsparungen durch eine Vermarktung ohne einen externen Vermarkter möglich sind.

Acknowledgments

First, I would like to thank my supervisor Prof. Hartmut Schmeck for the opportunity to pursue my doctoral research at the Karlsruhe Institute of Technology and at the FZI Research Center for Information Technology, the received advice and guidance, and the support during the research project *SmartFlex*.
Additionally, I would like to express my gratitude to Patrick Jochem for his valuable advice and comments as well as to Prof. Orestis Terzidis and Prof. Philipp Reiß for serving on my thesis committee.
For constructive feedback, research related and non-related discussions, accommodation, and memorable moments at the FZI, I would like to thank Birger Becker, Fabian Rigoll, Manuel Lösch, Fabian Kern, Sebastian Steuer, Kevin Förderer, David Wölfle, and Mischa Ahrens.
Furthermore, I would like to thank Dominik Becks and colleagues at the BMW Group for the constant support during the research project at the department of Energy Services. In particular, I am grateful for the support and the interesting insights received from Michael Müller-Ruff, Alexander Funke, Jens Berger, Sascha Brinkmann, Tina Benirschke, Thomas Schmid, Thomas Weber, Matthias Mitterhofer and Richard Wisbrun. Especially the practical application of my research at BMW production plants increased my motivation to pursue the research project and the finalization of my thesis.
Finally, I would like to express my gratitude to my wife Tomoko, our daughters, and the rest of our families for their belief in me and their continuous support.

Contents

Symbols and Indices

Abbreviations

AC	alternating current
ACE	area control error
aFRR	automatic frequency restoration reserves
AHU	air handling unit
BG	balance group
BMS	battery management system
BNetzA	Federal Network Agency (German: *Bundesnetzagentur*)
BOI	boiler
BRP	balance responsible party
BSP	balancing service provider
BSS	battery system storage
CCCV	constant current constant voltage
CHI	chiller
CHP	combined heat and power
COP	coefficient of performance
CO_2	carbon dioxide
CP	control pilot
DC	direct current
DER	distributed energy resources
DEM	demand
DOD	depth of discharge
DSO	distribution system operator
DSM	demand side management
DOF	degrees of freedom
DR	demand response
DCO	dry cooler
DU	deadband usage
D-1	day-ahead
EE	energy efficiency
EEG	Renewable Energy Act (German: *Erneuerbare-Energien-Gesetz*)
EER	energy efficiency ratio
EEX	European Energy Exchange
EPS	emergency power system
el	electric
EMS	energy management system
ENTSO-E	European Network of Transmission System Operators for Electricity
EMO	energy market optimization

EnWG	Energy Industry Act (German: *Energiewirtschaftsgesetz*)
EPEX	European Power Exchange
EPS	emergency power system
EU	European Union
EV	electric vehicle
EVSE	EV supply equipment
EPS	emergency power system
FCR	frequency containment reserve
GC	gradient control
GHG	greenhouse gases
HN	heating network
HT	peak periods (German: *Haupttarifzeit*)
HVAC	heating, ventilation and cooling
IGCC	International Grid Control Cooperation
ICT	Information and communication technology
KWKG	Combined Heat and Power Act (German: *Kraft-Waerme-Kopplungsgesetz*)
LEO	local energy optimization
LP	linear program
LPO	local peak optimization
mFRR	manual frequency restoration reserves
MBC	market-based charging
MILP	mixed-integer linear program
MINLP	mixed-integer non-linear program
MOL	merit order list
MOO	multi-objective optimization
NLP	non-linear program
NP	non-deterministic polynomial time
NT	off-peak periods (German: *Nebentarifzeit*)
OCPP	Open Charge Point Protocol
OEM	original equipment manufacturer
OF	overfulfillment
OTC	over-the-counter trading
P2H	power to heat
POR	permissible operation range
PP	proximity pilot
PV	photovoltaics
P2X	power-to-products
P2H	power-to-heat plant
RES	renewable energy sources
RQ	research question
RTP	real-time pricing
SCADA	Supervisory Control And Data Acquisition
SOC	state of charge
SOE	state of energy
TOU	time-of-use
TSO	transmission system operator

VFD	variable frequency drive
VPP	virtual power plant
V2G	vehicle-to-grid
WIND	wind power plant

Symbols

C	cooling power in W
c	cost in EUR
E	energy in Wh
F	flexibility power in W
G	gas consumption in W
L	required electric power for ventilation in W
M	energy necessary for mobility of EVs in Wh
P	electrical power in W
p	probability function in %
Q	thermal power in W
r	revenues in EUR
SOC	state of charge in %
T	time interval in h
x	binary variable
γ	cost in EUR/Wh
Δ_t	timestep interval in h
η	efficiency in %
ν	frequency in Hz
π	price in EUR
τ	energy price in EUR/Wh
υ	capacity price in EUR/W

Indices

a	energy technology
b	device
i	CHP plant including dry cooler
j	boiler
k	EPS
l	BSS
m	EV
n	AHU
o	chiller
p	P2H plant
t	time step

1 Introduction

The German chancellor Angela Merkel called the problem of climate change "a question of fate for mankind" at the United Nations Climate Change Conference in 2017 [319]. To cope with the challenge of climate change, the German government set out strict targets concerning the emission of greenhouse gases (GHG). It aims to reduce national GHG emission, measured as carbon dioxide equivalents, by 55% by 2030 compared to the reference year 1990. As of the publication of this work, GHG emissions have declined by around 36% until the year 2019 [143]. Around 20% of GHG emissions can be accounted to the industrial sector. For the industrial sector, the German government set the target to reduce GHG emissions until 2030 by 49-51% [121]. To achieve these targets industrial sites such as manufacturing plants have to increase their energy efficiency for industrial processes and switch to the use of renewable energies for heat production and electricity generation.
Next to governmental targets, industrial sites have faced continuously increasing energy prices over the last two decades in Germany. Foremost, the price paid by the final consumer for electricity has almost tripled from the year 2000 (5.79 Ct/kWh) to the year 2019 (17.02 Ct/kWh) [31].
As a consequence of these two developments, many industrial sites have invested in cleaner energy technologies for local generation, storage, and consumption. These investments enable the site to further control its power consumption from the public electricity grid, benefit e.g. from dynamic pricing, and hence lower the operational energy cost. If generation capacities exceed the demand, it is further possible to feed electricity into the grid and become an electricity *prosumer*. Furthermore, the flexibility to control the power flow from/to the electric grid enables industrial sites to participate in energy and reserve markets, which can generate additional revenues.
On the other hand, the energy manager of industrial sites faces a more complex energy system with a high number of technologically heterogeneous devices. The technical complexity of these devices and their dependencies make the use of an energy management system (EMS) indispensable. Especially, the ability to dispatch the controllable devices in an optimal manner considering the use of flexibility in the local energy system, as well as, the offer of flexibility to external markets is a challenge and requires a tool based on information and communication technology (ICT).
Due to the parallel developments of increased proliferation of wind and solar power plants and the phase-out of conventional power plants in Germany, leading to an increase in the intermittency of electricity generation, the value of flexibility in the energy system increases. As national energy systems take on a more decentralized, polycentric shape, industrial sites can profit from the role of *energy cells* by contributing to the national demand-supply matching and system stability. [148]

1.1 Problem description

From 2015 - 2018 the author conducted the research project *SmartFlex* for the FZI Research Center for Information Technology at the production plant of an original equipment manufacturer (OEM) of the automotive industry. The research project aimed at developing a *holistic optimization of local energy technologies for the commercialization of energy flexibility* at a production plant of the OEM, which serves as a case study in this work.
Over the past years, the OEM has invested in new energy technologies at its production plant to decrease energy costs for the external procurement of electricity to enhance its carbon footprint and decrease energy costs while

guaranteeing operational security of their production activities. The advantages of an active control of power demand by industrial microgrids is shown in several studies. [124, 312, 406]

On the one side, this development increases the level of complexity of the energy management of all controllable devices (1), on the other side, it increases the opportunities for reducing operational energy costs of the industrial plant (2) [362, 437]. In the following the resulting challenge (1) and the opportunities (2) are described:

(1) High degree of complexity of the energy management:

The investigated energy system at the production plant includes devices with multiple energy carriers. Based on information about the local energy demand, local electricity generation from intermittent renewable energy sources, external energy prices, contractual conditions, and energy targets, the energy manager of the industrial site has to decide, which plant to run at what time.

To illustrate this complexity, the control of one device, the combined heat and power plant (CHP), at the case study industrial site is explained. The CHP uses natural gas to generate electricity and supply heat simultaneously. As the level of heat supply is directly linked to the level of electricity generation, it is necessary to model the demand of both energy carriers to correctly adjust the thermal and electric power supply.

Depending on the thermal and electric power demand, the operation of a CHP results in different contractual conditions. For instance, if electric energy can not be used locally, it is fed into the public grid and has to be commercialized. Concerning thermal energy, no connection to a public grid or heat storage exists. Consequently, all generated heat has to be consumed on-site or emitted to the environment.

Furthermore, dependencies between the CHP and other devices exist. The CHPs at the production plant are, for instance, equipped with external dry coolers that can consume excess heat generation through a heat exchange process with the surrounding air.

(2) Opportunity to lower operational energy costs

Apart from the primary objective to meet the energy demand of the plant and provide the energy necessary to keep the production running, the energy manager is responsible for the reduction of energy costs.

Using the high number of controllable devices, the energy manager possesses the flexibility to control the amount of power that is obtained from or fed into the public grid, the load profile. Comparing the cost of different sources of energy such as local generators to cover energy demands, the energy manager can optimize energy costs by dispatching different devices. This optimization problem is generally solved in a classical dispatch problem. The heat production of the CHP at the case study, for example, can be replaced by the heat production of a gas boiler.

Furthermore, the flexibility to control the load profile enables the energy manager to provide services for various stakeholders in the national energy system, which can lead to a further reduction in energy costs [385]. The aggregator problem describes the optimization problem that maximizes revenues from the existing flexibility across multiple use cases [302]. By adjusting the electricity generation of the CHP, the energy manager can control the load profile of the industrial site.

Subject to the structure of the electricity bill, the energy manager can, for instance, profit from dynamic electricity prices provided by the supplier by moving power to less expensive times. In addition, it is possible to lower the peak electricity procurement from the public grid, alleviating the grid load for the distribution system operator (DSO).

Depending on the planned power profile, devices have the flexibility to adjust their electricity generation or consumption upon request. This flexibility can be further marketed on electricity markets or used to provide control reserve to stabilize the grid frequency for the transmission system operator (TSO).

To reduce operational energy costs, the energy manager needs to consider possible reductions in energy costs by the use of flexibility behind the meter, and possible revenues for the external offer of flexibility in front of the meter [385].

For the commercialization of flexibility services on external markets, the energy manager has the choice to either commercialize the flexibility of devices individually or as an aggregate [419]. Furthermore, the energy manager

can rely on an external aggregator, which combines multiple flexibility offers to fit market criteria, or use direct market access, consequently, saving fees paid to the aggregator.
To decide upon the optimal operational use of the given device, the energy manager has to solve the problem of the optimal dispatch of devices and optimal commercialization of their flexibility under changing energy demands and market prices. A tool that models all dependencies and calculates the optimal schedule of controllable devices such as the CHP can facilitate the job of the energy manager significantly.

1.2 Research questions

Along the described problem formulation, this thesis investigates and provides answers to the following research questions (RQ):

RQ 1 Flexibility services:
RQ 1.1: What are energy services that can be provided with the electrical flexibility of controllable devices of industrial sites?
RQ 1.2: How can the remuneration of the provision of these flexibility services be modeled?

RQ 2 Energy technologies:
RQ 2.1: How can the load profile and resulting flexibility of controllable devices commonly found in industrial sites be modeled taking into account multiple energy carriers and interdependencies among them?

RQ 3 Multi-use:
RQ 3.1: How can the provision of multiple flexibility services in combination with the economic dispatch problem be modeled for a microgrid in a joint optimization?
RQ 3.2: How can the ability of devices to provide multiple flexibility services ("multi-use") be modeled?
RQ 3.3: What is the contribution of flexibility services to the reduction of energy costs?

RQ 4 Flexibility aggregation:
RQ 4.1: What degrees of freedom in terms of aggregation of flexibility offers exist for the provision of control reserve?
RQ 4.2: What are possible aggregation models of flexibility offers and which one proves most beneficial for the case study?

To answer these research questions, this thesis presents a methodology to analyze and model the energy system of the case study industrial plant consisting of a multitude of controllable and non-controllable generator, consumer, and storage devices. This work also analyzes and models the different flexibility services that can be provided in energy systems.
This thesis develops an optimization problem, which results in a deployment schedule of the controllable energy devices. This schedule meets the necessary energy requirements given at the industrial site and minimizes total energy costs, which result from energy savings through the local use of flexibility and revenues through the external offer of flexibility to stakeholders such as the TSO. The optimization problem is modeled as a mixed-integer linear program and solved exactly. Additionally, scenarios are defined that model the effect of aggregation on the revenues of the provision of external flexibility.

1.3 Contributions of this work

This thesis complements, extends, and combines prior work, which mostly focuses on models of flexibility for single energy technologies or the provision of a single flexibility service in a multi-device energy system and is summarized in Chapter 4.
A comprehensive model for the flexibility of different energy devices despite their heterogeneous characteristics is presented in this thesis. To do so the findings of several works are combined and applied to a case study. Furthermore, the model includes the provision of several flexibility services, which have not been modeled adequately or have not been modeled in a joint optimization problem in the investigated literature. The optimization problem combines the dispatch problem with the aggregator problem, which results in an optimized schedule for the local and external flexibility utilization by available energy devices.
This work assess the feasibility to provide possible flexibility services by an industrial site in Germany, and to model them according to the given regulatory conditions in Chapter 3.
In-depth studies of two flexibility services for capacity-constrained energy technologies are laid out in Chapter 5. The studies extend the state of the art of simulations of battery storage systems (BSSs) providing frequency containment reserve (FCR) and commercializing their flexibility on electricity spot markets. The results of the simulations are also used as inputs for the model in Chapter 6.
A methodology is provided to mathematically model flexibility services and devices in an optimization problem that exploits flexibility to provide services that decrease local energy costs or increase profits from flexibility offers to external stakeholders in Chapter 6. Models of studied energy technologies in combination with the models of selected flexibility services is unprecedented. By applying the developed model at the case study, this work enables a realistic assessment of the monetary value of flexibility according to current regulations in Germany by analyzing the results of the optimization presented in Chapter 7.
In addition, this thesis explores the effects of aggregating control reserve offers according to current market conditions by comparing different scenarios.

1.4 Related publications and patents by the author

In the following, publications and patents by the author that relate to the contents of the thesis are listed:

1.4.1 Publications

Julian Rominger, Sebastian Steuer, Manuel Lösch, Katrin Köper, and Hartmut Schmeck
Analysis of the German Continuous Intraday Market and the Revenue Potential for Flexibility Options
In 2019 16th International Conference on the European Energy Market (EEM), Ljubljana, Slovenia, September 18th - 20th, 2019. [330]
This paper evaluates transactions of the Intraday Continuous power market from the years 2015 to 2017 to identify characteristics and analyzes structural changes in this period. Furthermore, an analysis of the revenue potential of different flexibility options in the market is performed based on two abstract device models given in [315]. The developed model is introduced in Chapter 5. Corresponding related work is shown in Chapter 4 and results appear in Chapter 7. Results are used in this work to estimate potential revenues of the flexibility service energy market optimization with a battery storage system. The content of this publication is based on a master thesis supervised by the author of this work [229]. The work of the publication has been extended and applied to the case study in Section 5.2.

Julian Rominger, Manuel Lösch, and Hartmut Schmeck
Utilization of electric vehicle charging flexibility to lower peak load by controlled charging (G2V and V2G)

IFAC Workshop on Control of Smart Grid and Renewable Energy Systems, 2019. [to be published] [329]
This paper analyzed the flexibility of EV charges from a charging cluster near Munich, Germany. In the publication, the authors ran simulations based on empirical charging data in order to evaluate the peak load reduction potential for different strategies. The content of this publication is used in this thesis to define the flexibility and model the energy technology of electric vehicles in Chapter 6. The content of this publication is based on work done throughout the research project *SmartFlex* between the FZI Research Center for Information Technology and the BMW Group.
The definition of flexibility of charge events is used to model electric vehicles in Section 2.4.

Fritz Bräuer, Julian Rominger, Russell McKenna, and Wolf Fichtner
Battery storage systems: An economic model-based analysis of parallel revenue streams and general implications for industry
In Applied Energy 239, April 1st, 2019. [54]
This paper evaluated the economic potential of a battery storage in a multi-use dispatch system at 50 different German small- and medium-sized enterprises. The battery storage system can pursue multiple revenue streams simultaneously by the provision of the following flexibility services: peak shaving, provision of frequency containment reserve and trading on short-term electricity markets. The publication presents an idea of the contribution of this thesis. It differs from this thesis in the choice and modeling of only a single energy technology, the battery storage system, as well as the simplified modeling and lower number of evaluated revenue streams or flexibility services. The author of this thesis contributed to the related work and assisted in the modeling of the flexibility service frequency containment reserve as well as the review of this work.

Emil Kraft, Julian Rominger, Vincent Mohiuddin, and Dogan Keles
Forecasting of Frequency Containment Reserve Prices Using Econometric and Artificial Intelligence Approaches
11. Internationale Energiewirtschaftstagung an der TU Wien, Vienna, Austria, February 13th - 15th 2019. [230]
In this publication, forecasting models of prices of frequency containment reserve have been developed using auto-regressive models as well as neural networks. The models are based on auto-regressive variables and exogenous econometric data. The content of the publication is not part of the contribution of this thesis; however, it is referenced in Chapter 4 as related work. The content of this publication is based on a master thesis supervised by Emil Kraft and the author of this work [285]. The publication was awarded the Best Paper Award at the conference.

Manuel Lösch, Julian Rominger, Sandeep Nainappagari, and Hartmut Schmeck
Optimizing Bidding Strategies for the German Secondary Control Reserve Market: The Impact of Energy Prices
In 2018 15th International Conference on the European Energy Market (EEM), Lodz, Poland, 27th - 29th June 2018. [251]
In this paper, the impact of automatic frequency restoration reserve (aFRR) energy prices on the activation of aFRR bids and the related profit potential were investigated. Based on an ex-post simulation of the aFRR market's auction results and actual aFRR calls, the publication showed how the selection of the energy price greatly affects the share of activation and therefore the total profit potential. Furthermore, the consideration of activation costs of a balancing service provider's technical unit allows improving aFRR bidding. Based on the methodology of this publication a simulation has been developed to describe the relation of aFRR energy price and call probability in Chapter 3. Furthermore, the publication is referenced in Chapter 4 as related work. The publication differs from the work of this thesis in the utilization of a different temporal resolution of aFRR call data and in the investigated period of market data. Furthermore, this thesis implements the methodology suggested in the publication to esti-

mate the correct energy price based on a given activation cost. The author of this thesis contributed by reviewing and testing the implemented methodology as well as using a slightly different approach in this work.
The methodology of the publication is applied to analyze and model automatic frequency restoration reserve (aFRR) in Sections 3.5 and 6.3.

Julian Rominger, Patrick Ludwig, Fabian Kern, Manuel Lösch, und Hartmut Schmeck.
Utilization of Local Flexibility for Charge Management of a Battery Energy Storage System Providing Frequency Containment Reserve.
Energy Procedia, 12th International Renewable Energy Storage Conference, IRES 2018, March 13th-15th 2018, Düsseldorf, Germany. [331]
This paper investigates the application of degrees of freedom, as well as, the utilization of flexible local power units for the charge management of a battery storage system providing frequency containment reserve at an industrial site. The developed model is introduced in Chapter 5. Corresponding related work is shown in Chapter 4 and results in Chapter 7. Results are used in this work to estimate the cost of the charge management of a battery storage system providing frequency containment reserve. The content of this publication is based on a master thesis supervised by the author of this work [254]. The model of the publication has been extended in Section 5.1.

Julian Rominger, Fabian Kern, and Hartmut Schmeck
Provision of Frequency Containment Reserve with an Aggregate of Air Handling Units
Computer Science - Research and Development, Special Issue Paper of the 6th DACH+ Conference on Energy Informatics, September 1st 2017. [328]
In this publication, a system architecture is presented that complies with German TSO standards to provide frequency containment reserve with an aggregate of electric motors of air handling unit blower fans in a robust way. A model has been developed by the author of this work to estimate the flexibility and power to be commercialized as frequency containment reserve provided by each electric motor. The content of the publication is referenced in Chapter 4 as related work and used for the modeling approach of the HVAC system in Chapter 6.
The work of the publication is used to analyze and model FCR in Sections 3.5 and 6.3.

Julian Rominger and Csaba Farkas
Public charging infrastructure in Japan - A stochastic modeling analysis
International Journal of Electrical Power & Energy Systems 90, September 1st 2017. [327]
In this publication, the author presented a stochastic model that is capable of modeling the EV motion based on traffic data. Through this model, the charging need at a charging station has been determined to investigate whether a given number of chargers is sufficient to meet the charging needs. The content of the publication is not part of the contribution of this thesis. The publication is referenced in Chapter 4 as related work. The publication is based on the master thesis of this author during the Master of Science program *Management and Engineering of Environment and Energy*.

1.4.2 Patents

Dominik Becks, Alexander Funke, and Julian Rominger
Verfahren zum Betreiben eines elektrischen Energiespeichers für eine Regelleistungserbringung
DE 10 2018 205 112 A1, Patent issued October 10th 2019. [33]
This invention relates to an innovative way of providing frequency containment reserve with a battery storage system while simultaneously assisting a charging station or charging park. The battery can provide an alternative power source to the grid for use cases such as high power charging or charge management. The content of the

publication is not part of the contribution of this thesis; however, the regulation for a stationary battery to provide frequency containment reserve is also used and modeled in Chapter 5 and a multi-use of stationary batteries is given in Chapter 6.

Dominik Becks, Michael Müller-Ruff, and Julian Rominger

Method for Providing Control Power for Stabilizing the Grid Frequency of a Power Grid and/or for Fulfilling a Power Schedule, Control Device for a Technical Installation, and Technical Installation

WO/2019/025075, Patent issued February 8th, 2019. [32]

This invention relates to the algorithm implemented in the control of an aggregate of air handling units that guarantees the robust provision of frequency containment reserve in case of temporary unavailability of individual air handling units. The content of the publication is not part of the contribution of this thesis; however, it is referenced in Chapter 4 as related work. The algorithm has been developed by the author of this work during his master thesis of the Master of Science program *Industrial Engineering and Management* at the Karlsruhe Institute of Technology.

Alexander Funke, Jens Berger, and Julian Rominger

System for Reducing Load Peaks in an Electrical System

WO/2019/007631, Patent issued January 11th 2019. [133]

The invention relates to an algorithm for controlling a load of an electrical system through the dispatch of a battery storage system. The idea of the patent is to charge or discharge the battery intelligently within 15-minute periods based on a short-term forecast, which prevents to exceed a peak power limit. The peak power is calculated as an average value of 15-minute periods, thus a temporary overshot can be balanced with a temporary undershot. The content of the publication is not part of the contribution of this thesis; however, it is referenced in Chapter 4 as related work for the use cases of battery storage systems.

Dominik Becks, Michael Müller-Ruff, Julian Rominger, and Tillmann Laux

Erbringung von Primärregelleistung

DE 10 2016 217 748 A1, Patent issued March 22nd 2018. [34]

This invention relates to the provision of frequency containment reserve with an aggregate of air handling units at several manufacturing plants of the BMW Group. The content of the publication is not part of the contribution of this thesis; however, the publication is referenced in Chapter 4 as related work.

1.5 Structure of the thesis

Chapter 2 provides fundamental knowledge on energy systems, the electrical energy system in Germany, the role of an industrial site within this electrical energy system, relevant energy technologies, and the mathematical modeling and optimization used to answer the research questions. Chapter 3 gives a detailed description of possible flexibility services that can be provided with devices of introduced energy technologies. The flexibility services are assessed concerning the feasibility to be provided by an industrial site. If feasible, the flexibility service is described in detail and later modeled in Chapter 6. Chapter 4 presents an analysis of related work of modeling approaches of energy systems, energy technologies, and a variety of applications of the dispatch problem in connection with the above-mentioned flexibility services. Chapter 5 provides simulation models for two flexibility services by a BSS. This is necessary due the lack of adequate modeling in the existing literature and due to special regulatory conditions for a BSS. Chapter 6 describes the optimization model to solve the Day-Ahead scheduling problem that combines the classical dispatch problem with the aggregator problem at a case study industrial site. Chapter 7 evaluates the developed model.

2 Background and Basic Theory

To optimize the dispatch of controllable devices to provide services on the one side for the local energy system and on the other side for the national electrical energy system, certain fundamentals are necessary. This includes basic knowledge of the German energy system, as well as, basic knowledge of modeling and optimization.
This chapter provides theoretical fundamentals of

1. Energy systems,
2. the electrical energy system (in Germany),
3. the role of an industrial site within the electrical energy system,
4. typical energy technologies that can be found within an energy system of such an industrial site, and
5. the mathematical foundations for modeling energy systems and solving the dispatch problem.

Thereby, the reader should understand the fundamentals of energy systems from Section 2.1 and especially the electrical energy system in Germany. Hence, in Section 2.2 the value chain of the commodity electricity in the German electrical energy system - generation, markets, transmission, and distribution - is explained. Furthermore, the energy technologies that can be found at the industrial site to provide services are described in Section 2.4. Section 2.5 provides basic information on optimization problems with the focus on the dispatch problem.

2.1 Energy systems

An *energy system* is for example defined as *all components related to the production, conversion, delivery, and use of energy* [63]. Hereby, energy can take up different forms such as electricity, heat, or fuels.
The main challenge in energy systems is the adequate treatment of spatial-temporal imbalances in the provision and consumption of energy [265]. This means that energy consumption and production varies over time and is often not produced where it is consumed. Furthermore, technical constraints of involved devices of various technologies have to be considered.
The scale of an energy system depends mainly on the number, heterogeneity, and spatial dimensions of devices used for production, conversion, and subsequent delivery of energy to the final user. To limit the scale of the energy system, it is common practice to set boundaries confining the modeled energy system [363]. Depending on the chosen system boundaries, energy systems can range from continents to countries, to industrial sites, or just single households. In this work, the energy system of an industrial site encompassing several devices is modeled.
Generally, an industrial site in Germany used to play the role of a large consumer and rarely of a producer or supplier of energy: The majority of electrical and thermal energy has been produced in large power plants that use transmission and distribution grids to carry the energy to demand centers. Therefore, the majority of energy systems of industrial sites were designed in a simple way as most forms of energy can be procured and delivered externally.
Several developments have led to an increase in local energy production and conversion technologies in industrial energy systems and a more decentralized energy supply in general. These developments include for example

1. the liberalization of energy markets on a European level [151],
2. the continuous increase in electricity costs in Germany from the year 2000 on [97],

3. advances in technologies for decentralized energy conversion [182, 320, 416], and
4. intentions to lower the carbon footprint [48].

The aspect of decentralized generation at an industrial site defines the term of a distributed energy resource.

2.1.1 Distributed energy resources

Distributed energy resources (DERs) are normally small in size (kW to a few MW capacity range), adaptable in structure, and installed close to customer load demand. DERs generally utilize renewable sources of energy for electricity generation, provide alternative means to derive electrical power to the external procurement of electricity, and can include non-generation devices that enable enhanced energy management. Emerging and existing DER technologies are primarily direct current (DC) generation sources (e.g. photovoltaic (PV)), rectified high-frequency alternate current (AC) sources (e.g. micro-turbines), conventional generation sources with especially high efficiencies due to the local energy use (e.g. CHPs), and storage systems (e.g. batteries) [79]. DERs represent sources, sinks, and converters of energy. DERs on the demand side can often be found within small scale energy systems, which are referred to as energy cells or microgrids.

2.1.2 Energy cells and microgrids

The notion of energy cells was first introduced by [36, 220] who referred to energy cells as a group of technical devices that are composed of elements of the energy supply system and elements of communication and automation systems. An energy cell enables devices to communicate among each other and with elements outside of a cell through gateways. Furthermore, an energy cell should include service platforms for the provision of services such as the communication of energy data. For Buchholz [64] the term energy cell originates from the idea to increase efficiency in balancing of the load profile: *Smart Supply Cells* in the distribution level support the TSO to reduce the complexity of power system operation by intentions to self-balance their electricity balance and offer system services [65]. Khattabi et al. [220] further specify the functions of these energy cells to include site-related energy management, dispatch functions, forecasting of local demand and of available generation, the participation of each single generator, battery, consumer, or of the cluster of distributed generation, storage or consumption in energy markets and ancillary services.
Similar to the definition of the energy cell is the definition of microgrids. Several different definitions appear in the literature [79, 155, 189, 197, 302, 311]. This work treats microgrids according to the definition of the U.S. Department of Energy Microgrid Exchange Group: "A microgrid is a group of interconnected loads and distributed energy resources within clearly defined electrical boundaries that act as a single controllable entity with respect to the grid. A microgrid can connect and disconnect from the grid to enable it to operate in both grid-connected or island mode." [378]
Based on the definition, the term microgrid holds a high level of congruence with the term energy cell. A major difference lies in the possibility of islanding, which is not given for energy cells, while the ability for communication and automation is not a condition for microgrids.
This work refers to the German energy system or the national energy system as the energy system that comprises all technical and economic effects of power exchanges with external networks of energy carriers such as the electrical grid. The local energy system refers to the energy cell defined by a given industrial site, the pool of devices - producers, consumers and storage facilities - and the existence of an energy management system (EMS) that enables communication and automation.

2.1.3 Energy system modeling

A model is a theoretical representation or description of systems or processes. A model of an energy system can describe involved energy devices, interrelations among devices, and energy flows within, into and out of the system. Models differ greatly in terms of the selected temporal resolution, spatial resolution, and the complexity of a model. The author of this work limits the boundaries of the analyzed energy system by the actual geographic boundaries of the industrial site. The energy provided by external sources (or to external sinks) is integrated into the model as simple energy sources (or sinks); consequently, the level of detail is reduced for these components.
In the proposed model of this work, for example, the procurement of electricity from the public grid is modeled as an energy source that can be tapped to meet electrical energy demand; however, the model does not account for the composition of technologies that are responsible for this electricity generation.
[289] differentiates between simulation-based and mathematical programming models. While simulation-based models include predefined operation strategies for individual devices, mathematical programming models represent the given energy system through an optimization problem including an objective function and constraints.
The model in Chapter 6 is formulated as a mathematical programming model as this representation facilitated the analysis of the contribution of different energy services to lower the energy cost (RQ4). A more detailed reasoning for the choice of the optimization method is given in Section 2.5.
The modeling of microgrids can be used for different applications [135]. These include, primarily:

1. **Optimal design** - The design of a microgrid in terms of power technology selection and sizing depends highly on the expected energy demands and objectives concerning e.g. the cost-effectiveness or the environmental impact of the microgrid. This problem is mostly used for strategic planning and supports investment decisions.

2. **Siting** - The correct allocation of energy devices and grid infrastructure such as power lines directly influence the power reliability and power quality (see Section 2.2.2) of the microgrid. The siting problem is considered to be part of strategic planning; i.e., it is done several years or decades ahead of the actual application.

3. **Dispatch** - Dispatch describes the process for operational and short-term planning of existing power resources while energy demands are covered. The dispatch problem includes one, or more than one objective function, e.g., minimizing operational costs and/or environmental impact. Dispatch problems are often also referred to as unit commitment and scheduling problems. It is done with a timeframe of months, days or even minutes ahead of the simulated power flow.

4. **Aggregator** - The aggregator or virtual power plant maximizes profits on energy markets by bundling a group of energy resources and flexible loads subject to operational and market-based constraints [302, 419]. This optimization problem is hereafter defined as the aggregator problem.

Further long-term planning problems can include market design problems or siting of new power plants [12].
The increase of complexity in the design of local energy systems of industrial plants leads to elaborate calculations to decide on how to run plants and how to commercialize their existing flexibility. Especially plant parameters, such as partial load operation, minimum operation time, and minimum downtime make it inherently difficult to plan the energy system operation without the help of a model of an energy system and an associated optimization. The problem solved with the methodology in this thesis is a combination of the short-term dispatch and aggregator problem of the energy system of an industrial plant.

2.1.4 The dispatch problem

The challenge to decide for a diverse portfolio of dispatchable devices of various technologies under which conditions to dispatch which power plant is called the dispatch problem. The term *dispatch* describes the planned

power output or consumption of controllable energy devices to satisfy the load of the energy system and further requirements defined in the modeling process. Thus, the dispatch problem includes at least a model of all relevant devices, energy balances, and loads. Depending on the defined objective, the dispatch plan results in a schedule for defined controllable devices. Generally, the selected objective minimizes costs under the condition that energy demands are covered. The mathematical model of the dispatch model is elaborated in Section 2.5.
The dispatch problem requires the knowledge of the technical characteristics, the availability, and the state of the modeled units. The dispatch problem is then solved for single snapshots or time slots of the energy demand.

2.1.5 The aggregator problem

An aggregator or virtual power plant (VPP) conducts a different schedule optimization. The aggregator or VPP gathers different DERs or energy cells in a pool. From the pool, it collects flexibility offers. Flexibility offers define the potential to adjust the electrical load profile of respective DERs or energy cells.
Based on these offers and the possible combination, the aggregator places bids on electricity and ancillary service markets and schedules DERs according to the bid acceptance. The bids are done based on market price forecasts, expected revenues from reserve markets, and the underlying cost structure of reserve calls of individual devices [263, 419]. Therefor, the aggregator often uses an actual model of the underlying energy technology of the device [365].
Next to market-based use of flexibility, an aggregator can utilize the flexibility offers for other non-market-based means [365]. The individual market-based and non-market-based use cases that can be satisfied with flexibility are referred to as flexibility services in this work.
As the energy system of an industrial site generally has electricity flows with entities outside, it is necessary to also introduce the electrical energy system that the industrial site is connected to.

2.2 Electrical energy system

The main task of the electrical energy system is to ensure a safe supply of electricity or electrical energy. Electricity is a secondary energy source because it is produced by converting primary sources of energy such as lignite coal or solar energy. This conversion is done in power plants and referred to as electricity generation. The generated electricity is then transported to the end-user or consumer through a power grid.
In general, electricity is available as AC or DC. While in AC circuits voltage and current are alternating their direction with a nominal frequency, in DC circuits, voltage and current are not alternating; i.e., the flow of electric charge is unidirectional [343].
An industrial site generally takes the role of an electricity consumer. To provide services for the electrical energy system as an industrial site, it is necessary to explain the framework of the energy system, specifically the regulatory, technological and economic framework. Hence, this section covers the topics of Energy policy in Section 2.2.1, the electricity grid in Section 2.2.2, and the markets for electricity in Section 2.2.3. Each section is described with a focus on Germany, as this is the country the case study is located at.

2.2.1 Energy policy in Germany

In Germany, the Federal Ministry for Economic Affairs and Energy is mainly responsible for the design and control of implemented energy policies. Due to the linkages with other sectors, the ministry closely coordinates policies with the Federal Ministry for the Environment, Nature Conservation and Nuclear Safety, or the Federal Ministry of Transport and Digital Infrastructure. [192]
Two main developments have to be emphasized that have transformed the German electrical energy system: the liberalization of the industrial sector related to the generation and transmission of electricity and the political

program *Energiewende*. These have led to strong changes in the regulatory framework fo the electrical energy system

Liberalization of the German electricity sector

Until the liberalization of the German electricity sector in 1998, the electricity industry was characterized by vertically integrated companies. These companies were responsible for generation, transmission, distribution, and sale to the end consumer. The liberalization of the German electricity market, triggered by the EU Directive 96/92/EC in 1996 [151], broke up this system and split up utilities to allow competition in the various sectors. As a result, large electricity supply companies (utilities) spun off their activities of electricity generation, grids, and sales into separate companies. For the first time, the directive enabled competition in the areas of generation, trading, and sales. Upon the implementation of the directive, electricity trading between different market participants was carried out in market-economy structures in a transparent manner.
Electricity grids, on the other hand, were regarded as a natural monopoly, in which remuneration is regulated [423] as the characteristics of electricity as a homogeneous, immaterial, and difficult to store commodity are taken into account. Since electricity can only be transported on the grid, a comprehensive infrastructure is necessary. This is provided by the grid operators, who are also responsible for the stability of the electrical energy system. It is generally regarded as not macro-economically valuable to open up competition between grid operators as several electricity grids for distribution would have to be constructed. [151]

The *Energiewende* of the electrical energy system

In the past decade, energy policies in Germany have been closely related to the so-called program *Energiewende* (energy transition). The Energiewende describes the German path towards an environmentally friendly, more self-sufficient and secure, and socially acceptable energy system. The targets of the Energiewende include a decrease of GHGs, an increasing share of power generation from renewable energy sources (RES), and the phase-out of nuclear-based power generation by the end of 2022. Among other policies, the Energiewende is supporting the electricity generation by RESs like wind and solar power in order to replace conventional power plants. This has led, for instance, to an increase in electricity generation by RES from 15.1% in 2008 to 46% in 2019 [131].
Figure 2.1 depicts (a) the traditional organization of the energy system and (b) the expected changes to the energy system due to the Energiewende. The figure suggests that decentralized electricity generation and storage capacities are increasing and conventional generation is decreasing because of the Energiewende. Furthermore, it can be seen that the power flow has changed. While the traditional grid structure saw electric power generated on high voltage levels and distributed to consumers in low voltage levels, decentralized generation across voltage levels causes this power flow to be at least temporarily reversed into a bidirectional system.
According to [393], these recent developments in the German electrical energy system have led to and will lead to

1. the reduction of electricity generation from large power plants in the transmission grid,
2. a simultaneous rapid increase in the number of DERs, especially at the distribution grid level,
3. the associated need to make greater use of the flexibility of generation and consumption, and
4. the expansion and construction of modern and intelligent measuring and control systems.

Regulatory framework of the electrical energy system

In the German electrical energy system, a clear separation is made between the electricity markets and the electricity grid. The energy market allows free competition and free price formation for the trade of electrical energy for each market participant. The grid sector provides the necessary infrastructure for the physical fulfillment of

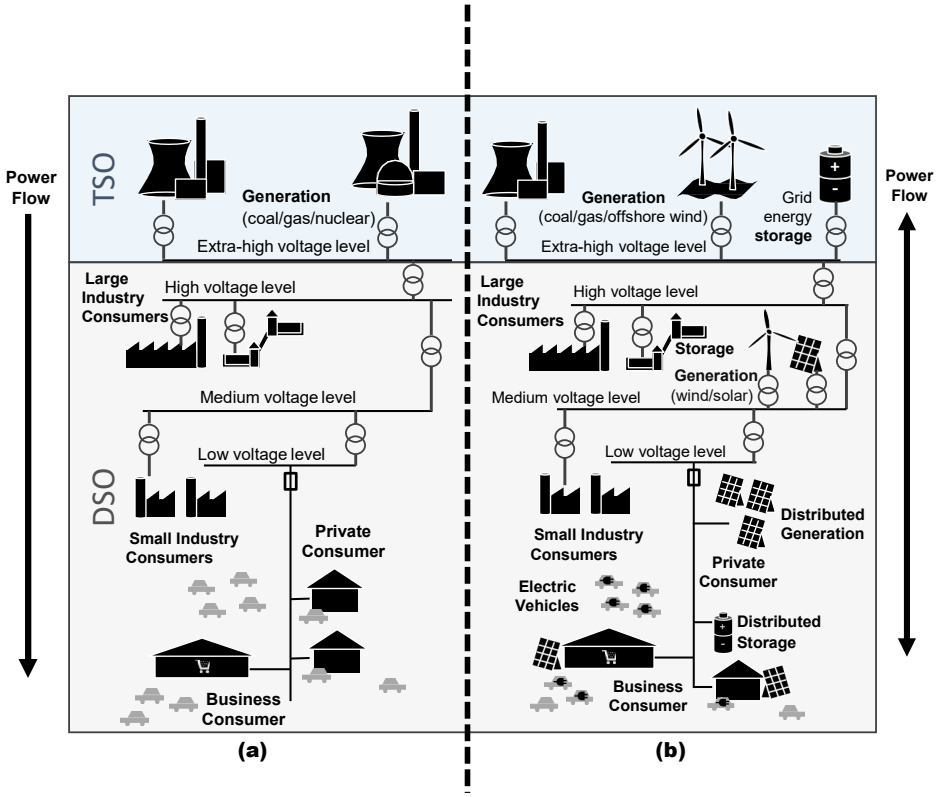

Figure 2.1: Visualization of the general electricity grid layout for an individual control area in Germany
The types and their respective voltage level of electricity generation and consumption before (a) and after the *Energiewende* (b) based on [289]. Furthermore, system operation responsibilities by the TSO and DSO are shown depending on the voltage level.

the traded energy transactions and thus forms the basis for a functioning electricity market to fulfill the delivery of electricity to consumers. As required by a European directive, the activities surrounding transmission and distribution have been unbundled from all other businesses in the value chain of electricity provision.

Energy regulation in Germany is mainly subject to the Energy Industry Act (German: *Energiewirtschaftsgesetz*, hereinafter EnWG). The EnWG deals with the structure of electricity and gas markets and came into effect in 1998 as a consequence of the above mentioned European directive. The law is directed towards the liberalization and deregulation of the German electricity and gas markets. The EnWG declares reliability of supply, fair pricing and environmental protection as its objectives. RES are privileged under the Renewable Energy Act (German: *Erneuerbare-Energien-Gesetz*, EEG) and the Combined Heat and Power Act (German: *Kraft-Waerme-Kopplungsgesetz*, KWKG) of 2000. System operators are obliged to provide access to energy suppliers producing energy exclusively by RES and to issue a feed-in tariff for the electricity generated in such plants.

The Federal Network Agency (German: *Bundesnetzagentur*, BNetzA) acts as the leading regulatory authority on the federal level supervising the TSOs and larger DSOs with cross-border activities or more than 100,000 customers.

The Incentive Regulation Ordinance (German: *Anreizregulierungsverordnung*) exists to regulate the sector of electricity grid system operation (see Section 2.2.2). The Ordinance ensures that consumers benefit from fair grid fees and that the prices paid by end consumers do not exceed the operators' real costs due to the monopoly [117].

2.2.2 Electricity grid

The power grid connects power generators and consumers and handles transmission, distribution, and voltage conversion. Typically, power grids can be divided into two classes:

1. Transmission networks, and
2. distribution networks.

Network operators operate the power grid. Depending on the voltage level, these are called Transmission System Operators (TSO) or Distribution System Operators (DSO). Generally, transmission networks carry electric power over long distance on so-called "very high" voltage grids. In Germany, the distribution network can further be divided into three levels: the high, the medium, the low voltage level. Transformers are used to connect the voltage levels. The grid responsibility depending on the voltage level of the TSO and DSO in Germany is also shown in Figure 2.1.
The German network infrastructure is part of the Synchronous Grid of Continental Europe with connections to neighboring countries [80]. Within the European Union (EU), the specific technical implementation of the electricity grid varies from country to country, however, it follows the principle of a separation into a transmission and a distribution grid [343]. With the exception of certain lines, the European electricity grid is an interconnected alternating current grid with a synchronous frequency of 50 Hz. This has the advantage that numerous controllable generators and power reserves are interconnected in this grid, which improves reliability and allows economies of scale [343].
The German electricity grid is divided into four control areas, each of which are monitored by individual TSOs (also shown in Figure 3.5). The four control areas within Germany originate from the four main utilities, which historically were responsible for generation and transmission of the commodity electricity (see also Section 2.2.3). The provision of the network infrastructure, the uninterrupted, and secure operation of the electricity supply are the main responsibility of the network operators.
Moreover, the German TSOs are part of the European Network of Transmission System Operators (ENTSO-E) which supervises the European synchronous grid area and issues network codes that regulate grid operation [80].
The system operators perform various measures for the safe and reliable provision and performance of the network infrastructure. In order to comply with the permissible parameters (current, voltage, and frequency), the network must be permanently monitored and controlled. This is currently done almost completely in the very high, high, and in some cases in medium voltage networks. The low-voltage networks generally lack monitoring devices.
To maintain the operational security of electricity supply, the network operators have to assure power quality and power reliability. Power quality can be defined as the variation of the electrical waveform from the predefined nominal values expressed by characteristics - amplitude, frequency, etc. . Power reliability refers to the probability of its satisfactory operation over the long run and the ability to supply adequate electrical services on a nearly continuous basis [234].
These two topics are broken down to four areas of responsibility of the network operators in this work [393]:

1. **Frequency control** - The containment and restoration of deviations of the grid frequency from its nominal value. This is done indirectly through the supervision of balance groups and directly through balancing activities.
2. **Voltage control** - Manual or automatic control actions designed to maintain the set voltage level. This includes the system services of reactive power supply and short-circuits current supply.
3. **Operational planning & scheduling** - This includes all responsibilities concerning the coordination of network operations such as capacity calculations, congestion forecasts, reserve planning, and congestion management. Congestion management is done by manual or automatic control actions designed to limit the

equipment loading. This work classifies operational planning & scheduling as a power reliability measure as suggested by [25].

4. **System restoration** - Re-establishing of the system operation and maintaining operational security after a blackout. Power plants realize this through black start capability.

In the following sections below, fundamentals concerning these four system services are explained. Chapter 3 gives a detailed explanation of individual system services, assesses the economic opportunities of an industrial site to provide these system services, and shows how they have been modeled in this work.

Table 2.1: System service responsibilities by the TSO and DSO according to [393]

	Power quality		Power reliability	
	Frequency control	Voltage control	Operational planning & scheduling	System restoration
TSO	x	x	x	x
DSO		x	x	x[1]

Frequency control

Frequency control is done through the balancing of electricity demand and supply. The balancing can occur in a preventive measure in the scheduling process before, or reactive measure in the rescheduling process after actual electricity generation. Generally, the latter is referred to as frequency control; however, in the following both preventive and reactive measures are elaborated.
The stable operation of the power supply system presupposes that the power balance of feeds, withdrawals, and losses in the overall system is maintained at all times as the electricity grid cannot function as energy storage. The TSO is responsible for observing and controlling the electricity transactions within its control area and electricity exchanges with other control areas to establish this balance.
The supervision and control is done through balance group management: Different electric power consumers and generators are aggregated to a virtual power balance, a balance group (BG). A BG is run by a balance responsible party (BRP), which is generally a utility that incorporates generation through their power plants and consumption by their electricity customers. Differences in power consumption and generation are to be matched by (electricity market) transactions of power quantities on the electricity markets by BRPs. In the control area of the TSO *TenneT*, for example, 2520 different BGs were registered in 2019 [374].
To fully avoid the occurrence of differences between feeds and withdrawals and consequent imbalances within a BG or the balance of a control area, one would have to precisely forecast the

1. individual and aggregated power consumption
2. feed-in by power generation including intermittent power sources such as wind and solar power plants, and
3. unplanned power plant outages or major events that can affect the grid stability.

Due to the forecast errors and the influence of external events, it can be very difficult to level the balance of a BG. It is crucial as a TSO to measure and monitor the power balance of the electrical energy system and ensure that it is kept in equilibrium by suitable control systems. These control systems must have access to controllable feeds or controllable consumption devices to be able to influence the power balance in a targeted manner [81]. Imbalances

[1] For system restoration, DSOs can actively participate in coordination with the TSOs.

within the sum of all BGs of all four control areas in Germany are recorded by the TSO as imbalance energy. An indicator of imbalances within the interconnected European grid is its frequency.
The frequency describes the number of oscillations of the alternate current of the grid and is set at a nominal value. The devices connected to the grid are set to operate at that frequency. In the European interconnected grid, the nominal frequency equals 50 Hz. From a technical point of view, the equilibrium state of the electricity balance is expressed this nominal frequency. In the case of an oversupply of electricity, the frequency increases above the nominal value and vice versa for an lack of power.
Large differences between the actual frequency and its nominal value can be caused, e.g., by forecasting errors of power supply and demand. This can include unplanned power plant outages, unexpectedly strong electricity demand for example due to special events, large deviations in the actual consumption of small-scale consumers from standard load-profiles to forecast their consumption, or unexpectedly high/low supply due to changing weather conditions from intermittent RES. Although forecasts of power generation of, e.g., intermittent power resources have improved over the last years [182], active continuous control of the power balance is necessary for a stable system operation [81].
To maintain the balance between generation and consumption, several market, penalty, and control mechanisms exist that contribute to this balance:

1. **Electricity markets** - Marketplaces connect entities selling and purchasing goods. As purchased quantities equal sold quantities at all times, electricity markets perform a balanced market-clearing between different BRPs. As sold quantities are usually generated in power plants and purchased quantities usually consumed, transactions on electricity markets contribute to the balance of electricity generation and consumption.
2. **Balance energy** - Quantities of electrical power are traded on electricity markets before actual supply or consumption. Thus, the traded quantities always rely on forecasts and may not equal the correct amount of power fed into or withdrawn from the electricity grid. The difference between the forecasted and net power balance per BRP is settled by the responsible TSO. This balance is compared to the net balance of the whole control area. If the BRP contributed to the imbalance of the whole control area, it has to pay a balance energy price. On the other hand, if by chance the BRP counteracts the balance of the control area, it receives a balance energy price for its net balance. The balance energy price is calculated per 15-minute trading interval and is derived from the cost of balance energy - the energy provided or withdrawn by balancing activities (see 4.).
3. **Instantaneous reserve** - Instantaneous reserve is the ability of an electrical system to cover fluctuations due to inertia. Within small deviations of the nominal utility frequency, the balance between electricity generation and consumption can be achieved by the inertia of the electricity system, in particular by the kinetic energy of rotating electrical generators and coupled steam or gas turbines. The instantaneous reserve can also be synthesized by power electronics of, for instance, a battery storage system [407].
4. **Balancing** - Balancing describes actions procured by the TSOs and performed by individual power plants or devices to maintain the system frequency at its nominal value. This is often also referred to as frequency control. In the European power system, the most prominent actions are those of balancing reserves. Balancing reserves are resources procured by the TSO for balancing purposes. The balancing power market generally offers three products for balancing reserves - frequency containment reserves (FCR), automatic frequency restoration reserves (aFRR), and manual frequency restoration reserves (mFRR). These products are presented in detail in Section 3.5.

Voltage control

Network operators are obliged to maintain the network voltage in a voltage band of +/- 10% of the nominal network voltage in their respective networks [93]. Compliance with the voltage bands is essential for the reliable operation

of equipment and generation systems. Furthermore, it is necessary to limit the voltage drop in case of a short circuit [88].
Especially in distribution systems characterized by time-varying power generation and demand from DERs, voltage conditions can easily vary from nominal conditions; however, it is important to assure nominal voltage levels to guarantee security of supply and operation of power electronic equipment. In order to keep the power system voltages at all buses in acceptable ranges in both normal and abnormal conditions, voltage control solutions are used in distribution systems [322].
A distinction is made between static and dynamic voltage maintenance. Static voltage control defines voltage control during normal grid operation. In case of a short-term interruption of normal grid operation due to, e.g., a short circuit that leads to a corresponding voltage drop, dynamic voltage control enables continuous operation of the grid [88, 317].
Static voltage control requires primarily a reactive power balance. Each consumer or generator connected to the grid influences the voltage in the grid located behind depending on the direction of the current flow. Static voltage control can be done at the source of electricity generation, such as large scale power plants or DERs or along the grid lines through the grid operators' resources or DERs located at facilities of consumers. The responsibility for static voltage control within its network is the responsibility of the respective system operator [88].
In AC grids, electricity can be divided into two classes of power, active power and reactive power, which is important to minimize losses during transmission and distribution. Reactive currents further influence the effectiveness of voltage control [393]. Active power provides the energy that is actually consumed by energy devices. Reactive power describes the lag between sinusoidal voltage and current waves in AC lines and occurs due to inductance and capacitance in a circuit. The relationship between active and reactive power is defined by the power factor of a circuit. High reactive power decreases the efficiency of power present in the distribution system, i.e., more power is consumed for the same work. Thus, network operators use power factor correction in order to avoid energy losses in the distribution system [88, 389].
Furthermore, system operators use adjustable local power transformers, the installation of further equipment, voltage-related redispatch, and DER control (e.g., through ripple control or control through smart meter gateways) for static voltage control [28, 130].
The increasing integration of fluctuating loads and generators, especially in the low-voltage grid, leads to an increase in the reactive power requirement for voltage maintenance [100]. The feed-in of reactive power by generation plants is already required today for the connection of generation plants in VDE-AR-N 4105 [389]. The integration of DERs into the voltage control scheme such as the Smart Grid Traffic Light Concept are currently discussed by relevant stakeholders [29].
Due to the lack of measuring equipment in low-voltage bands, a stable voltage-related operation is achieved by technical conditions for the grid connection of DERs [225]. The resulting costs for generators, e.g., due to a larger inverter sizing for photovoltaic installations or lost income due to the reduction of the fed-in active power, are currently not reimbursed.
Sufficient short-circuit power is required for dynamic voltage control. The provision of an adequate short-circuit power is essential for the detection of short-circuit events and for ensuring transient stability in the event of a sudden voltage change due to load drop or generation failure [231]. Today, short-circuit power is mainly provided by conventional generators; however, power converter-based systems can also generate these short-circuit currents if designed accordingly [88, 407]

Operational planning & Scheduling

Operational planning summarizes all activities concerning the planning of power flows in accordance with the transfer capacities of the transmission and distribution networks. In liberalized electricity networks, generation

and transmission services are unbundled but remain interconnected due to their physical nature. As with other infrastructure, the use of the power grid is constrained. The transmission and the distribution grid have limited transfer capacities. The possible transfer capacity is often defined as the maximum possible transmission of active power minus a reliability margin in accordance with the system security criteria. For the calculation of transfer capacity, several criteria are taken into account, such as thermal limitations, voltage limitations, and further technical limitations [105, 126].

For correct electricity flow and capacity calculations, system operators take into account the topology of the grid, generation and load patterns, network characteristics, and weather conditions.

Congestion management

A major task of the grid operators is the resolution of a grid congestion. A congestion occurs when the (planned) electricity flow exceeds the transfer capacity. To solve the problem of transmission capacities, system operators have implemented congestion management. Congestion management assures that planned power plant deployment matches the consideration of the topology of the electricity grid and is crucial for the efficiency of these interconnected systems. It is generally under the responsibility of the TSO [101]. Around 85-90% of congestion events occur in the transmission network [30, 83].

Various regulatory concepts for cost-efficient (electricity markets) and correct (electricity grid) electricity flows within networks have been proposed, analyzed and implemented. The two most prominent concepts include uniform zonal prices with redispatch or nodal prices. "Zonal" and "nodal" prices refer to the spatial resolution of prices on the electricity market [76].

In zonal price systems, the same price applies to an entire bidding zone. Price formation in a zonal price system purely depends on the demand and supply of electricity and does not take into account spatial grid information.

In nodal price systems, an individual price is determined for each entry or exit point of the transmission grid. Hereby, the transmission of electricity from the point of generation to the point of consumption is regarded in the price formation process.

The German power system follows the concept of uniform zonal prices. Nodal prices are used, for example, in the state of Texas of the United States, where different prices are indicated at 12.000 different nodes [37, 76, 299].

The price formation process has a direct influence on the congestion management. While congestion management in zonal price systems is done after price formation on the market, nodal price systems consider bottlenecks during the price formation process: Zonal price systems perform congestion management in a curative manner, while a nodal price system performs congestion management in a preventive manner during market-clearing [76]. An apparent problem of the zonal price system is the "Inc-Dec" strategy where market participants anticipate redispatch and change their price bidding accordingly (Producers in surplus regions offer below marginal costs as they anticipate to not have to produce due to redispatch measures) [181]. Nodal price systems, on the other hand, possess a higher complexity as the grid structure has to be included within the market mechanisms.

Active power flow management by the TSO can technically be achieved by adapting the network topology (e.g. switching actions) or the network properties (e.g. changes in transformer taps). On the other hand, market-based congestion management methods include the adaptation of nodal generation or load by market-based methods. In Germany, the cost-oriented redispatch of power plants is applied [50, 236]. The dispatch schedule of running power plants or power plants of the grid reserve capacity, which is communicated day-ahead is adjusted to fit the planned state of the grid. Currently, redispatch is only performed with large-scale power plants.

Feed-in management

Furthermore, a separate important measure of the German grid operators is the feed-in management of subsidized renewable energy sources. It allows grid operators to temporarily shut down or adjust the power generation of renewable energy plants and combined heat and power (CHP) plants (Section 13 EnWG, Section 3 KWKG). The curtailment of renewable energy plants is mainly due to the incapability of the grid to cope with these power

flows. Feed-in management as well as further emergency measure are generally done as a response to an already occurring grid congestion.
In 2018, costs related to congestion management amounted to 351,5 Mio. EUR and costs related to feed-in management amounted to 635,4 Mio. EUR. In total, close to a billion EUR is spent on these measures [400].

Future developments

Currently, congestion management and feed-in management are done in an uncoordinated manner. From 2021, the congestion management is reformed and combined with the feed-in management. It will include all DERs that are currently only controlled by feed-in management. This means, that small-scale devices down to a power of 0.1 MW will participate in redispatch measures [116]. DSOs are planned to be further involved in the redispatch process and a coordination between measures by TSOs and DSOs is enabled. TSOs have performed projects to include small-scale devices of varying technologies, e.g. batteries [371, 372], within the redispatch regime and establish platforms to collect electric power flexibility for congestion management [373].

Reserve capacities

One possible measure to guarantee power reliability and long-term generation adequacy is the creation of reserves. Power plants in the reserve are not allowed to participate in the electricity market. In the German power system, the EnWG provides for various mechanisms for the provision of reserve power so that there are always enough power plants available to step in, if generated electricity sold on the electricity markets does not match the demand to avoid drops in frequency and subsequent blackouts. These mechanisms are in particular the grid reserve, the capacity reserve, and the specific reserve of lignite-fired power plants [114]:

1. **Grid reserve** - The grid reserve is formed each year in the winter half-year in order to hold back power plant capacities for redispatch interventions of TSOs. The demand for electricity in winter months and the electricity generated in the wind farms in northern Germany are particularly high. Due to grid bottlenecks, the TSOs often have to perform redispatch measures. Since the phase-out of nuclear power will lead to the withdrawal of further power plant capacities from the market by 2022, particularly in southern Germany, this north-south divide is likely to worsen over the next few years.
2. **Capacity reserve** - The capacity reserve is intended to compensate for current account deficits in the German grid control network in the event of a threat to or disruption of the security or reliability of the electricity supply system because of the incomplete balance of supply and demand on the electricity markets. 2 GW of capacity is to be reserved by the TSOs according to the EnWG. From 2020 on this reserve is procured in a tender procedure for a period of three years [119].
3. **Reserve of lignite-fired power plants** - Furthermore, the EnWG states that decommissioned lignite-fired power plants form another safety reserve. Specific lignite-fired power plants have been moved to a safety readiness state for four years after decommissioning.

These power plants are manually activated by the TSOs [393], e.g., in the case of imbalances that cannot be covered by frequency control.
Different capacity mechanisms are explored by [187] who developed a model to investigate different capacity mechanisms such as capacity markets and strategic reserves.

System restoration

In case of a blackout due to, e.g., strong drops in frequency and subsequent disconnection of networks from the grid, the system has to be restored. The TSOs are responsible for system restoration if a blackout occurs in their control area.
Since electricity consumption and generation must be balanced at all times, reconstruction can only be carried out gradually and in a coordinated manner. To this end, smaller regions are first stabilized and gradually interconnected

in a network. Power plants are needed that have the function of "islanding" in the event of a fault or can be started independently of an existing power supply if no connected grid can provide start-up power.
Three power plant types with different characteristics are available to network operators to restore supply after a failure. Firstly, after a network breakdown, generating plants can switch to self-sufficient island operation and supply themselves with electricity for at least two hours. At a later point in time, synchronization with the grid and reconstruction of the grid can take place. All generating plants on the extra-high voltage grid must do this free of charge [390].
The grid island operational capability is the second type of supply reconstruction. This includes the regulation of the grid frequency in a grid island as well as the ability to balance load additions. This is required by all generating plants lower than or equal to 100 MW and is not remunerated [390].
The third form of provision of system restoration is the black start capability. Power plants capable of black starting can start up independently from a switched-off state and do not require any energy from the grid. They must be able to set up an independent grid and provide system services (frequency and voltage maintenance). Due to the high demands on the communication and protection system, black start capability is remunerated by the network operators in bilateral contracts [113]. In Germany, the network operators currently contract 4.7 GW of black-start-capable power plant capacity, with pumped storage power plants accounting for 3.5 GW and the largest share of black-start-capable power plants. In addition to run-of-river and pumped storage power plants, the black start capability can also be provided by specially equipped conventional power plants (e.g. gas turbines), provided they have an appropriate emergency power supply. The technical potential of conventional generators including hydro power is more than 10 GW [113, 190, 228].

2.2.3 Electricity markets

Well-functioning wholesale markets are pivotal for competition in the electricity sector. Spot and forward markets are crucial for meeting suppliers' short and long-term electricity needs. In addition to bilateral wholesale trading or over-the-counter trading (OTC), electricity exchanges play a key role in the German electrical energy system. They create a reliable trading forum and at the same time provide important price signals for market participants in other areas of the electricity industry [68]. The acting parties on these electricity exchanges or markets are BGs or specifically their BRPs. The electricity generated or consumed has to be purchased or sold on electricity markets prior to actual generation or consumption to avoid balance energy fees (see Section 2.2.2).

Acting parties on the electricity markets

Within BGs different types of electricity consumers and generators exist. According to [357], these mainly include

1. small-scale consumers such as households,
2. large-scale consumers such as industrial customers,
3. small-scale (renewable) generators,
4. generators, and
5. EEG-generators[2].

BRPs use different methods to commercialize and balance the customer segments. While the electricity consumption of small-scale consumers is calculated from synthetic standard load profiles, individual forecasts are done for large-scale consumers and renewable generators. The power schedule of controllable generators is mostly optimized in dispatch problems to optimize profits. Renewable generators under the EEG subsidy are aggregated and commercialized under the balance group of the individual TSOs.

[2] EEG generators describe the exclusive group of generators that receive constant premiums under the Renewable Energy Act (EEG).

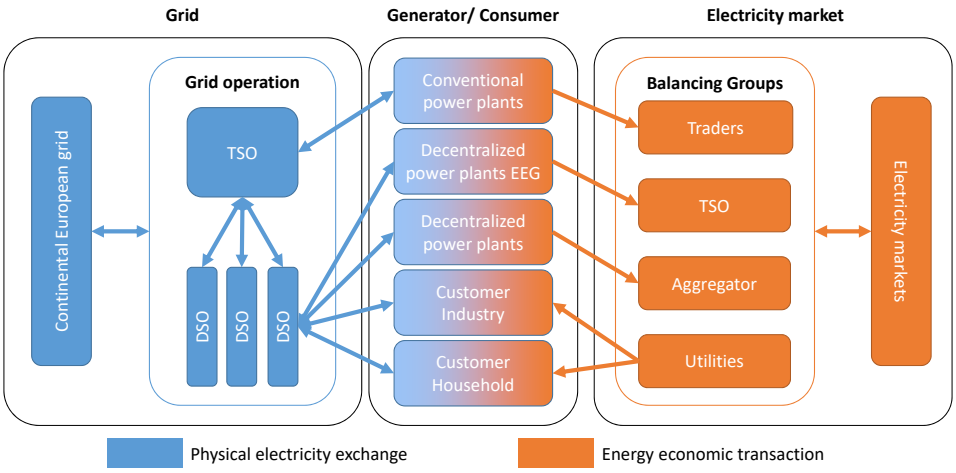

Figure 2.2: Interdependencies of electricity market and grid for Germany partly based on [393]

A BRP generally pools several of the mentioned customer groups together in one or several BG. An energy supplier, e.g., often has industrial customers and at the same time household customers. While for the first group the BRP can use synthetic forecasts for the correct procurement of energy, individual forecasts have to be made for industrial customers.

Aggregators

An aggregator forms in most cases a BG and controls a VPP comprised of various DERs. A VPP is a network of IT-interconnected independent DERs of smaller capacity, which is controlled by suitable communication. The network of DERs achieves characteristics similar to conventional large power plants in terms of the ability to control and plan power output through aggregation and decentralized communication. Aggregators form a balance group, in which they pool small-scale and EEG generators and commercialized them on electricity markets. Furthermore, aggregators pool DERs for the commercialization on ancillary service markets.

Electricity trading

Electricity is traded on different marketplaces. Predominantly, two options exist: Bilateral trading over-the-counter (OTC) or trading on electricity exchanges.

Over-the-counter trading

Bilateral contracts for the supply of electricity are negotiated between a buyer and a seller. This allows for great flexibility in contract design [423]. Trade intermediaries (so-called brokers) play an important role in bilateral wholesale trade. Brokers serve as intermediaries and bundle information on demand and supply of electricity trading transactions. On electronic broker platforms, the pairing of interested parties on the supply and demand side is formalized and the chance of a two-party agreement is increased. Stock exchanges can also act as a broker for OTC-trading. The European Energy Exchange, e.g., offers OTC clearing.

OTC trading takes up a majority of the energy traded (see Figure 2.3). In 2017, around two-thirds of electricity of the German power market was purchased through OTC (65%) generally with a lead time between one week and one year [68].

Moreover, direct trading is possible in electricity exchanges. One distinguishes between the derivatives market and the spot market in electricity exchanges.

Futures market

The largest platform in Europe is the European Energy Exchange (EEX). The derivatives market is used to trade long-term electricity transactions, so-called futures. Futures determine future electricity supply for periods from a

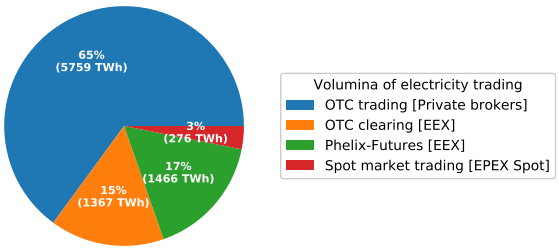

Figure 2.3: Traded volume of electricity for the German power market in 2016 [68]

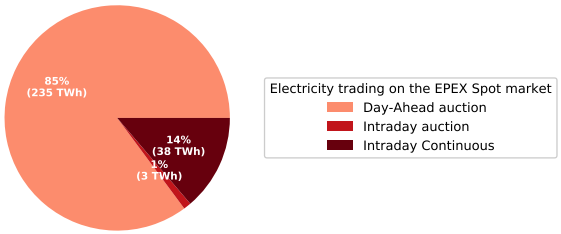

Figure 2.4: Traded volume of electricity on EPEX Spot markets in 2016 [68]

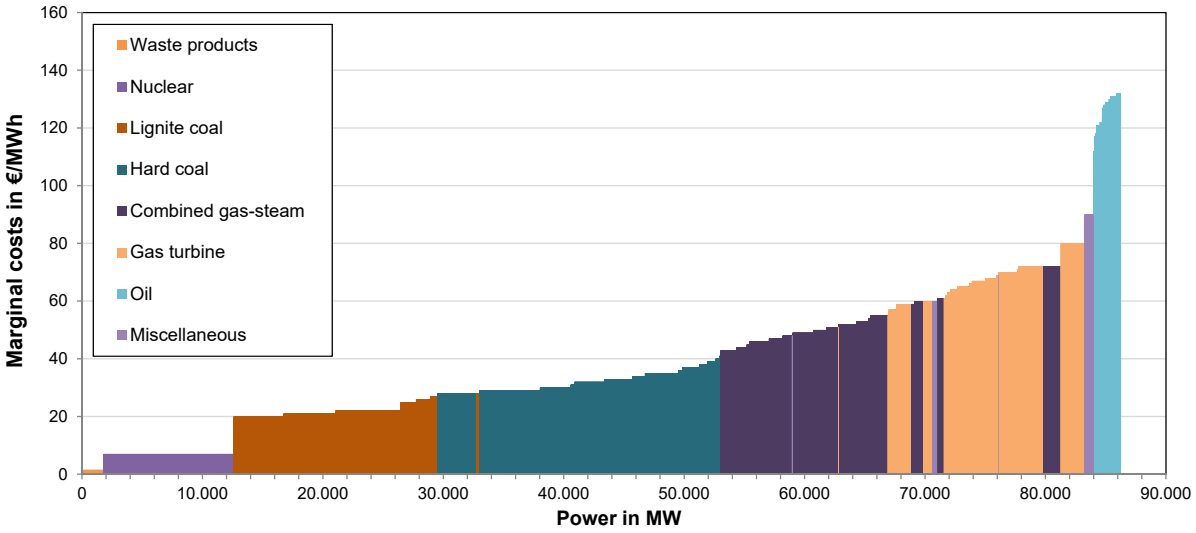

Figure 2.5: Average merit order list (MOL) of electricity generation by conventional power plants in Germany in 2018 based on [98]

week up to six years after actual trading. The largest European spot market is the EPEX SPOT where Germany, Luxembourg, Austria, Switzerland, Belgium, the Netherlands, France, and the United Kingdom participate [151]. The EPEX SPOT distinguishes between the Day-Ahead auction, the Intraday auction and the Continuous Intraday market. In the following, the auctions, as well as the continuous trading are explained in detail as they are relevant for Chapter 6.

In 2018, the exchanges EEX recorded 236 and EPEX Spot 203 registered members [68]; however, not every company needs its own access to the electricity exchange; rather, a BRP can also make use of services offered by registered traders. Larger utilities often bundle their trading activities in a group company that has a corresponding exchange registration.

The Merit Order List

The sorted marginal cost curve is called a merit order list (MOL). It can be used to determine which power plants are the most cost-effective for meeting a given demand for electricity at any given time.

Figure 2.5 shows the MOL of conventional power plants in Germany in 2018 according to [98] with a CO_2 emission certificate price of 16 EUR/ton. It is visible that the operational cost among dispatchable power plants in the electrical energy system varies significantly. Generally, investment costs or costs that arise after the decommissioning of the power plant are not included in the MOL. As renewable energies receiving the EEG subsidy are prioritized the MOL is matched with the demand curve of the residual load, i.e., the difference between the total electrical load and the electricity generation by renewable energies.

Day-Ahead and Intraday auction

Trading on the Day-ahead auction works according to the marginal pricing principle. All market participants place a bid for desired products - periods - in which they want to buy/sell electricity. For each product, BUY bids are sorted in descending and SELL bids in ascending order taking into account the bid quantities. The intersection of the resulting two curves determines the market-clearing price. This price is treated as the marginal price or "pay-as-cleared" price meaning all participants have to buy/sell the bid quantity for this marginal price. This allows participating power plants to bid the marginal costs for the generation of electricity. The default trading unit is one hour; however, blocks of longer duration are also traded. All bids must be submitted by 12:00 of the previous day and results are published at around 12:40 [107]. Similar to the Day-Ahead auction, the Intraday Auction works the same; however, it allows the trade of 15-min. products. The Intraday Auction for 15-min. products takes place at 15:00. The results are published at 15:10. The auction also functions as the opening auction for the following continuous trading.

Intraday Continuous market

The Intraday Continuous market enables trading on a more short-term basis. Intraday trading starts at 15:00 for hourly products and at 16:00 for the 15-minute products (see also Figure 2.6). Electricity can be traded up to 5 minutes before physical delivery. Price formation on the Intraday market works according to the pay-as-bid system. Buyers and sellers continuously submit bids to an order book and are automatically merged into a transaction if a match between a BUY and a SELL price is reached. The resulting price is the price of the transaction, which may differ from transaction to transaction for a quarter-hour product [107].

Day-ahead optimization

Day-ahead (D-1) operational planning determines the optimal schedule of controllable devices of the energy system with respect to a given objective function [112, 138, 145, 336]. In this context, day-ahead refers to a daily optimization a day prior to the actual energy flow. Typically, D-1 approaches are performed due to gate closure deadlines of different energy markets such as the Day-Ahead market and control reserve markets [429]. The time of the optimization is generally determined by the earliest gate-closure time of involved markets [41].

Due to the short-term nature of the, e.g., forecasts of energy demands, forecasts of electricity generation from renewable energies, and market conditions on electricity and control reserve markets, a day-ahead optimization has been chosen for this work. To realize all considered markets, the optimization of the model introduced in this work is to be performed before the earliest gate-closure time of modeled products, the gate-closure time of the frequency containment reserve, which occurs at D-1, 8 a.m. (see Figure 2.6).

The market design of the German power system allows for sequential trading on individual electricity markets as well as markets for frequency control [149]. As this work focuses on the participation of an industrial site in short-term electricity trading, the opportunities for participation and the analysis of trading is done in Chapter 3; however, mainly focus on the markets displayed in Figure 2.6.

2.3 The role of an industrial electricity consumer

As depicted in Figure 2.1, industrial production plants are often located on medium to high voltage levels in the distribution grid. According to [347], electrical energy at manufacturing plants is used as direct energy for production processes and as indirect energy for activities to maintain the correct environment for production. Due to the organization of the electricity grid and the electricity markets, the industrial site interacts directly and indirectly with many different stakeholders within the national electrical energy system as shown in Figure 2.7.

The conventional set-up is shown in Figure 2.7 by the connections in black lines. It comprises the electricity supply and grid value chain: The industrial site holds a connection contract with the connected DSO and purchases energy from a supplier. The supplier forecasts its customers' load profile and sources the energy through the BRP based on

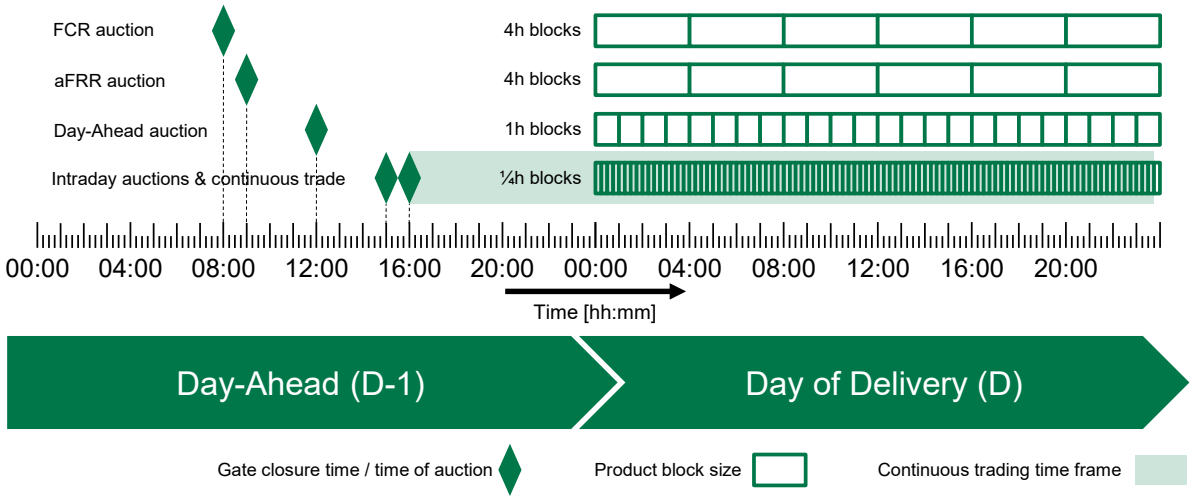

Figure 2.6: Gate-closure times and product durations of modeled electricity and reserve control products in this work [106, 108, 394]

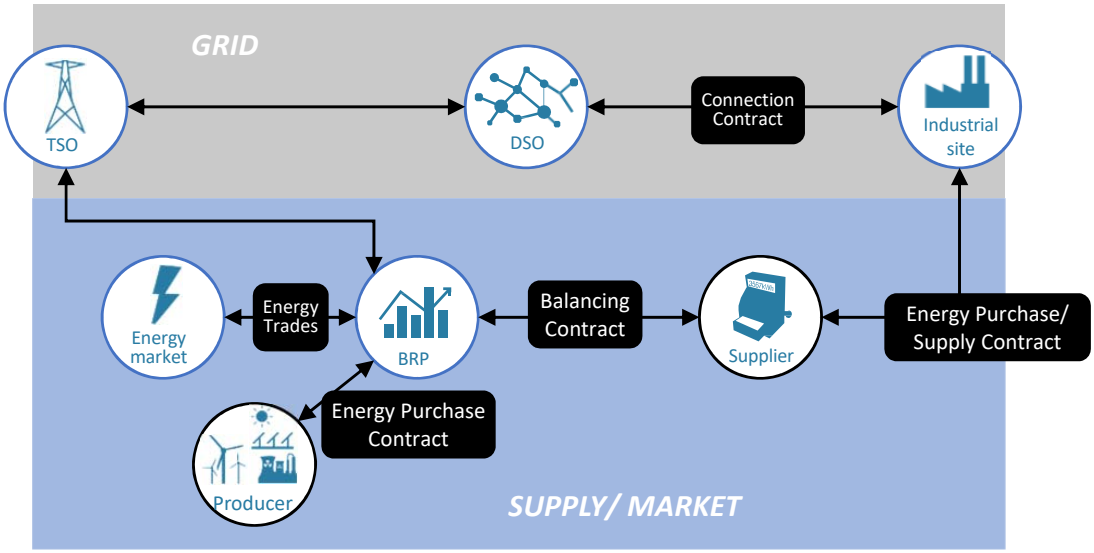

Figure 2.7: Roles in the grid and electricity supply value chain surrounding an industrial site based on the concept in [385]

a previously arranged contracts. The BRP purchases energy directly from producers or trades energy on electricity market places as described in Section 2.2.3. The BRP communicates the scheduled energy purchases with the corresponding TSO and intents to balance the respective balance group. The actual consumption is measured using energy meters by the DSO and communicated to the TSO [385].

2.3.1 Flexibility services

An industrial site generally plays the role of a large-scale consumer. It purchases electricity OTC or on electricity markets using its BRP. The operation of their own devices enables these sites to control their level of electricity exchange with the public grid. Industrial sites can further participate in the energy system by providing and commercializing this flexibility to adjust their load profile.

This work identifies possible use cases for flexibility, hereafter referred to as flexibility services, of industrial sites. A flexibility service can be the use of flexibility within the local energy system or the offer of flexibility to external

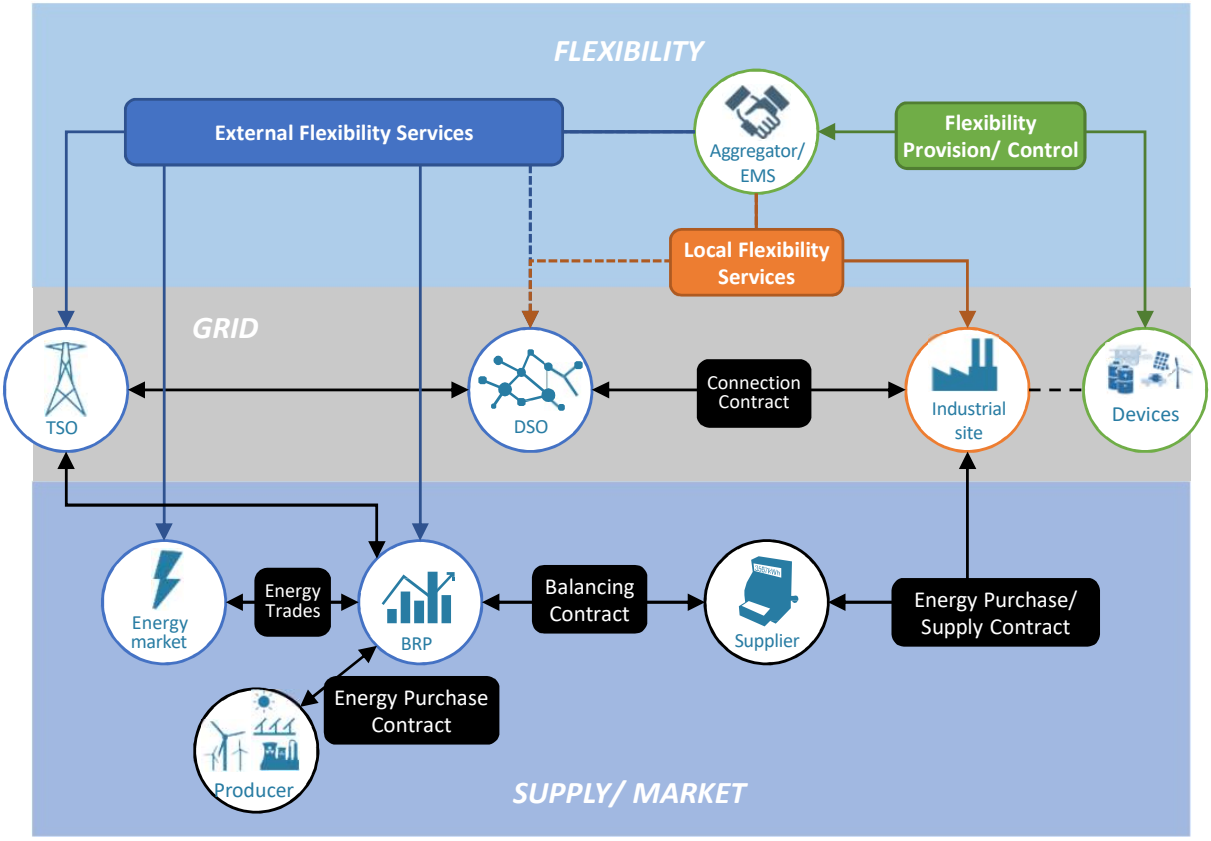

Figure 2.8: Roles in the flexibility, grid, and electricity supply value chain surrounding an industrial site as a prosumer offering flexibility based on [385]

entities such as the DSO, TSO, BRP, or on energy markets as depicted in Figure 2.8. The term flexibility and the mentioned flexibility services is discussed more closely in Chapter 3.

This work relates to the flexibility value chain provided in [385], which defines the role of an aggregator to collect flexibility and offer the flexibility either back to the industrial site as prosumer services, or to external players as external flexibility services. The flexibility services are provided by an aggregator (see Section 2.2.3), who controls devices at the industrial site. This work, furthermore, looks into the provision of flexibility without an external aggregator.

Next to the flexibility services provided to the DSO and the BRP as defined in [385], this work also considers offering flexibility services to the TSO. The utilization of flexibility for several flexibility services is referred to as multi-use.

In order to actively control the electric power flow with the public grid, flexible generation, storage, or consumption devices are necessary. Section 2.4 introduces typical energy technologies present at industrial site.

2.3.2 Electricity pricing for industrial sites

Operational energy costs at manufacturing plants in Germany often result from procured electricity, gas, and occasionally heat from the public grid as well as fees for transmission and distribution and surcharges and taxes. According to [31] the average electricity price for industries in 2019 in Germany equals 17.02 Ct/kWh. Figure 2.9 shows the composition of this electricity price. Data from [31] was broken down into costs related to the procurement (power sourcing) and network charges share given at the case study for the year 2017. It is visible that the actual price of the commodity electricity only contributes around 30% to the electricity final price. The residual

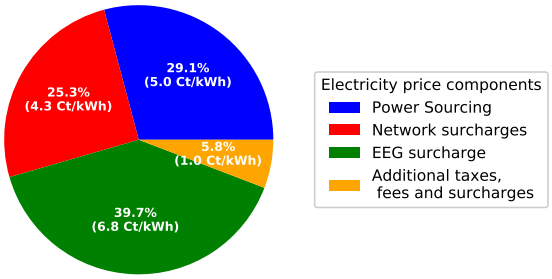

Figure 2.9: Average price composition of externally procured electricity for industries in Germany according to [31] for the year 2020

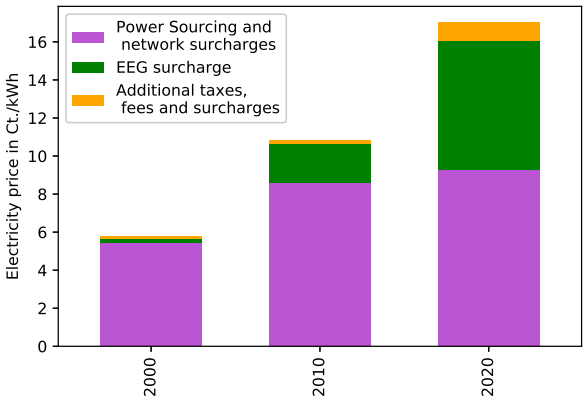

Figure 2.10: Development of electricity price for medium-sized industrial enterprises in Germany according to [31] from the year 2000 to 2020

amount is attributed to price components related to transmission and distribution, subsidies for renewable energy technologies (EEG surcharge), taxes, and further surcharges.
Figure 2.10 shows the development of the electricity price from the year 2000 to the year 2020. Even inflation-adjusted prices lead to a total increase of 65%. This can be mostly attributed to the increase in surcharges and fees, especially the EEG-surcharge as visible and lead to a financial burden for industrial sites [31]. In Germany, so-called "electricity-intensive" industries, for which electricity costs amount to at least 14% (or 20%, depending on the industry) of the gross added value, can apply for an exemption of up to 90% of taxes and surcharges. In 2020, 4% of the total number of companies applied for this exemption [118].

Power Sourcing

Industrial production plants are generally not run by energy companies. The supply of electricity is usually procured externally from a supplier. Mainly the conditions for the procurement of electricity are settled in bilateral contracts between the industrial company and the supplier. The procurement often includes long-term power purchases of quantities of energy through OTC or futures trading for yearly or quarter-yearly base (24h) or peak (8:00-20:00) products [68]. These quantities are generally procured for fixed energy prices. Residual quantities of electricity are then balanced on the EPEX spot markets such as the Day-Ahead market or the Intraday market by the BRP and costs are handed down to the customer.

Transmission and distribution grid charges

The grid fees pay for the use of the grid infrastructure, provision of the system services, and coverage of losses occurring during electricity transport. Transmission and distribution charges in Germany are issued by the corresponding system operator depending on the voltage level and contain charges paid for the amount of energy consumption (energy price) and charges paid for the maximum power consumption (power price) during a fixed period (generally a year).

Further surcharges and fees

Industrial consumers of electricity pay around 40% of net electricity prices for surcharges. These surcharges were implemented to finance inter alia the policy program *Energiewende*. Three main surcharges - the EEG, CHP, and Offshore surcharge - are introduced in the following. With the exclusion of the electricity tax, which can be reimbursed for the manufacturing industry and is not included in the above stated numbers, these account for 96% (7.398 Ct./kWh) of the surcharges in 2020 according to [31].

The **EEG surcharge** (renewable energy surcharge) finances the expansion of renewable energies. It provides the money to pay for the difference between feed-in-tariff and price on the electricity exchanges for electricity generated from wind, solar and biomass. Under the EEG, DER operators of these technologies receive remuneration rates set for 20 years for renewable power that is generated and fed into the grid. The tariff is paid by the TSO, who is responsible for commercializing the electricity on energy exchanges [120]. The **CHP surcharge** finances the decentralized expansion under the KWKG. CHP plant operators can qualify to receive premiums for decentralized CHP power generation [120]. The **Offshore surcharge** accounts for the costs of compensation paid for delays in connecting offshore plants to the grid or due to technical problems under the EnWG [120].

2.4 Energy technologies within industrial energy systems

Energy technologies refer to a type of devices that convert energy from one form to another. At an industrial production plant the devices are used to fulfill the needs of certain forms of energy of manufacturing processes and connected activities. This includes, for instance, the demand for electricity to run machines, provide lighting, ventilation, heating, cooling, and mobility.
In the following, the energy technologies that can be found at the case study industrial site are introduced with a brief technological description. Due to the different forms of energy and functions, these are introduced under the following categories: Electric power generators, electric power storage, electric power consumers, and thermal power production.

2.4.1 Electric power generators

Controllable electricity generators at the case study industrial site include CHP plants and emergency power systems (EPSs). Furthermore, renewable energy provided by a wind power plant (WPP) is generated on-site. This intermittent power source can be controlled to a limited extent; however, due to contractual reasons, this function is only used to a limited extent at the case study industrial site. In the scheduling problem, the WPP is, therefore, a non-controlled source of electricity.

Combined heat and power plant

CHP plants use the concept of co-generation to generate electricity efficiently following a combustion process while using the generated heat for local heating. The CHP plant converts chemical energy stored in the fuel into electric and thermal energy.
The heart of most CHP plants is an internal combustion engine, more specifically a gas, diesel, or petrol engine that drives a generator. The usable part of the heat generated in the combustion process is extracted from the exhaust gas, engine cooling water, engine oil or charge air, and is then fed for further use into the heating network. At industrial sites with high-temperature heating networks, the temperature level equals around 80 °C. For the industrial use aggregates with a nominal power of up to 10 MW_{el} are installed [43].
CHPs for industrial use can achieve electrical efficiencies of around 45% and at the same time thermal efficiencies of more than 40% leading to a total energy efficiency between 85% and 90%. CHP plants generally need a minimum power level to operate. For industrial plants, this often equals around 50% of the nominal power. CHPs show changing thermal and electrical efficiencies depending on the power level [196]. The power coefficient defines the ratio of electrical and thermal efficiency. It is generally higher at nominal power [318]. Especially in the German market, high electric efficiencies are requested by customers due to the high price of electricity.
CHPs can be equipped with dry coolers, which allow the discharge of thermal energy if necessary. Especially during times when thermal demand levels are rather low (in the summer), a dry cooler allows CHPs to run even at

high power levels. The dry cooler disposes excess heat away from the CHP and avoids overheating. A bypass of the return allows for additional flexibility in the operation.
Limits to the operation are minimum run and minimum down times, which define time intervals that the engine has to run once started or rest once stopped.

Emergency power system

The EPS generates electrical energy. It is mostly used as a back-up device to avoid the loss of power supply. In most cases, it mainly consists of an internal combustion engine and a generator. A fuel such as fuel oil, diesel or gasoline is used to drive the internal combustion engine and convert chemical energy to mechanical energy. The generator assures the conversion to electrical energy.
For the EPS, a fuel tank or other form of fuel supply is needed that can be tapped without the use of electric power. The size of the fuel tank and the calorific value of the fuel determine the desired period of emergency power that the system can provide. Generally, an EPS guarantees minimum power necessary for providing a safe environment for building occupants (e.g. lighting, protection of equipment, et cetera) and can partly provide the continuity of operations in case of a black-out. System maintenance and the replenishing of the fuel tank are crucial to guarantee the functionality.
The control of emergency power systems is generally limited. Often the power level of the EPS cannot be controlled, i.e., the EPS can only be turned on or off and the operator has to respect a minimum operation time.

Wind power plant

In contrast to direct solar energy used for photovoltaic, wind energy is an indirect form of solar energy, as the sun's activity creates air currents on the earth's surface. These fluctuating air currents or winds can be used technically by WPPs, which convert the kinetic energy contained in the flowing air masses into electrical energy. The energy of the wind is first converted into mechanical rotational energy by the rotor blades and then into electrical energy by a generator [169].
A wind turbine with a horizontal axis and three rotor blades is the most common design and found at the case study site. It consists of components such as: Rotor blades, rotor hub, rotor brake, blade adjustment mechanism, electric generator, frequency converter, and gearbox [169].
In order to protect wind turbines from overload, part of the power must be throttled at wind speeds above the nominal speed. The power control is realized by pitch control, which changes the rotor blade angle [169]. Many sites such as the target site also experience operation restrictions due to shadow casting or noise pollution by WPPs.

2.4.2 Electrical storage

This section covers the technological fundamentals surrounding batteries and their application in stationary storage systems and electric vehicles. This work focuses on lithium-based batteries, as this is the technology used at the case study site.

Batteries

Batteries consist of one or more electrochemical cells. Electrochemical reactions take place in these cells when charging, which are reversed during discharging. The individual cells consist of a combination of two electrodes (cathode and anode) made of different materials, an ion-conducting electrolyte that enables charge transport, and a separator. During the process of charging, the electrical energy to be stored is converted into chemical potential, which can be reversibly released as discharge current.
The capacity is the possible energy storage of the battery and the maximum power refers to the maximum possible charging (or discharging) power. Batteries are charged and discharged with direct current and are used for a range

of use cases in mobile and stationary applications. While in the mobile sector, there is almost no alternative to the use of battery technology, stationary use is characterized by competition with other storage technologies, e.g. pumped storage [360]. The current charge level is given by the *state of charge* (SOC). Several different methods for the estimation of the SOC in Li-ion batteries exist [222]; however, generally, the SOC is a value calculated by the *battery management system* (BMS).
Efficiencies are a key characteristic of batteries: The overall efficiency refers to the efficiency of the battery from the charging to the discharging process under consideration of losses in the power electronics. The self-discharge of a battery characterizes the decrease in the state of charge over a period of the fully charged battery, in particular due to chemical reactions within the battery.
Further parameters describe performance indicators of batteries: The *cycle stability* refers to the maximum number of charging and discharging operations possible during the lifetime of the battery storage device until it shows a degradation that amounts to 20% of the initial capacity (cyclical aging). The *calendar life* is the number of years the battery can be used, regardless of the degradation caused by the electrical load on the system (calendar aging). The *volumetric energy density* is the amount of energy that can be stored per volume. The *depth of discharge* refers to the maximum usable capacity of the total capacity of the storage system. It is expressed as a percentage of the total capacity. The *C-rate* is an indication of the discharge time of the battery and is calculated from the maximum battery power divided by the battery capacity. A C-rate of 1 results in a complete discharge of the cell in one hour, whereas a C-rate of 2 results in a discharge time of half an hour [51, 193].

Lithium-based batteries

All battery types that are based on Lithium (Li) chemistry are summarized under Li batteries. These include, on the one hand, Li-ion systems with different active cathode materials (iron, manganese, cobalt) and Li-metal systems. Li-ion batteries have currently reached the highest level of technological maturity of all battery technologies [51]. Li-ion batteries are characterized by high overall efficiency (around 90%) as well as high power and energy density. Furthermore, Li-ion systems, depending on the active materials used, have a long calendar life and cycle stability as well as high discharge depth. The self-discharge of Li batteries is low at 1 to 3% per month compared to other technologies. A disadvantage of Li-ion batteries is the high reactivity of the cell chemistry, which can trigger a thermal runaway in the form of a fire. This generally happens at high battery temperatures at extreme ends of the battery capacity. This requires a complex temperature and charge management [75].
Li-ion batteries are generally controlled by a BMS to control the electric charging of individual modules and cells. To avoid the rapid degradation of batteries, charging follows a regime of constant current and a regime of constant voltage (CCCV) depending on the SOC level of the battery. When applying CCCV charging, the maximum charging rate decreases exponentially from a certain state of charge (SOC) (generally 80%): Li-ion batteries show SOC-dependent charging efficiencies, which worsen at extreme ends of the capacity band. The BMS intends to avoid these extremes [51].

Battery storage systems

Battery storage systems (BSS) are large scale battery systems generally engineered by an interconnection of multiple smaller batteries. For the grid-connected operation of stationary battery storage systems, power converters are required, which convert the grid alternating current into direct current during charging and the direct current from the battery into alternating current during discharging. Main applications are in combination with the use of intermittent renewable energies (e.g. feed-in management, grid integration, PV self-consumption systems) as well as system services such as frequency control [360].

Electric Vehicles

Electric vehicles (EV) in the broad sense include all means of transportation that are driven by an electric motor. In the following, the term EV focuses on cars, which can draw energy from the electric power grid and store it in a battery. This definition excludes hybrid and fuel cell vehicles without grid charging options [177]. For applications in EVs, the most important requirements towards the employed battery technology are high power and energy density, high cycle stability, and fast charging capabilities (high C-Rate). Li-ion batteries are currently the most preferred technology as they match most requirements.
The transfer of electricity from/to the battery is done by the process of charging and discharging, which mainly happens cable-based at stationary charging stations. The proliferation of wireless charging technology is still low [223] and is therefore not considered in this work.
The definitions of charging stations and charging modes are not uniform: Charging stations and charging modes are classified according to the place, the charging power, the possibilities of communication, and the type of current flow. Table 2.2 describes the different charging modes defined in IEC 61851, which can be differentiated by their charging power and type of communication [191]. Proximity pilot (PP) communication refers to the communication of the charging station to charge with the correct current to prevent electric arcs at the electric contacts. Control pilot (CP) communication allows the charging station or EV supply equipment (EVSE) to charge at different currents using pulse width modulation.
Table 2.3 shows another classification depending on the defined places of charging. The definition is derived from the national platform for electric mobility [296]. The column "Modes" represents the relation to Table 2.2.

Table 2.2: Classification of charging modes according to [191]

Mode	Description
Mode 1	AC 1- to 3-phase charging generally at 230 V up to 16 A without communication
Mode 2	AC 1- to 3-phase charging generally at 230 V up to 32 A with PP-communication
Mode 3	AC 1- to 3-phase charging generally up to 290 V and 250 A with PP/CP-communication at specific EVSE
Mode 4	DC charging up to 100 V and 400 A with external AC/DC converter

Table 2.3: Classification of charging location according to [296]

Type	Description	Modes
Simple socket	'Schuko' socket	1 & 2
Wallbox	Simple or smart charging in private homes	2 & 3
Charging at work	Parking spaces on company premises for fleets or employee's vehicles	2 & 3
Semi-public charging	Charging points on privately owned public areas, e.g. at supermarkets	2 & 3
Public charging	Charging points located in public spaces, e.g. for lantern parking	2 & 3
DC fast charging	Public fast charging stations DC	4

Furthermore, several standards exist for communication between involved entities (e.g. vehicles, infrastructure providers, energy companies, and billing service providers). A communication standard for the exchange of charging profiles between vehicle and EVSE is explained in IEC 15118. The communication flow between various charging stations and higher-level central management authority usually of a charge point operator is specified for instance in the Open Charge Point Protocol (OCPP) [292]. The charge point operator can then connect the EV chargers or provide information from the chargers to a fleet energy management system, a distribution network operator, or an e-mobility provider.

This work concentrates on the use case "charging at work", as this work focuses on the energy management of industrial sites, which either provide charging infrastructure for their employees or own vehicles to travel between facilities. It is assumed that controlled EV charging and discharging with predominantly Mode 3/4 AC or DC charging stations is done. The communication of charging schedules by an EMS with individual charging stations and the corresponding vehicles could be done with standards OCPP and IEC 15118.
Furthermore, vehicle-to-grid (V2G) capability is assumed, i.e., the EV can both be charged and discharged. In reality, V2G capability is not yet a widespread functionality of neither vehicles nor charging station; however, actions of vehicle manufacturers and charging stations point into the direction [49, 292].

2.4.3 Electric power consumers

This section covers technologies that function as electric power consumers and whose electric power consumption can be controlled to change the load profile of the industrial site. According to Friedrichsen [132] especially suited for demand response are devices of technologies that possess some kind of energy and product storage, which achieves a decoupling between electricity consumption and the actual purpose of the underlying process. In other words, even with a short interruption of the electricity consumption the purpose can still be supplied. Friedrichsen especially points out electricity consumption of batch production processes or indirect energy consumption of industrial sites. Indirect energy consumption is defined as demand that stems from not directly production-related processes in this work. It includes, e.g., the provision of heating, ventilation, and cooling (HVAC). This work focuses on these processes, as these devices tend to offer a great potential according to Stadler [353]. Furthermore, this work does not include a model of batch production processes and their inter-dependencies with other production processes.
This work focuses on the electric power consumers air handling units (AHUs) used for the purpose of ventilation and compression chillers for the purpose of cooling as part of the HVAC system. Furthermore, electric vehicles have been introduced in Section 2.4.2 and a power-to-heat plant is introduced in Section 2.4.4.
HVAC systems have the objective of creating comfortable indoor conditions in buildings. The feeling of comfort mainly concerns conditions of air quality, temperature, pressure, air movement, and humidity. The HVAC system of a building generally consists of

- a ventilation system, which pushes fresh air into and retrieves used air from the building,
- a cooling system, which is used to cool down the building, and
- a heating system that is used to heat the building.

At the target site, heating and cooling are utilized for establishing comfort of the working force in both office and production buildings, as well as, to satisfy thermal energy demand of production processes. This distinction does not exist for the purpose of ventilation, which is deployed for the same means in office and production buildings. The HVAC system implemented at the target site is an air-water-system. Air-water systems have, in addition to an AHU system, an additional cold and hot water circuit to remove the cooling load.
This work treats the provision of ventilation, cooling, and heating individually, although an adjustment of the energy consumption of the ventilation system has an influence on the transfer of cooling or heating to the desired space. This assumption was taken as a thermodynamic model of these processes would go beyond the scope of this work. Ventilation is provided by air handling units installed at each building, cooling is provided by a chiller, heating is supplied by individual devices introduced in Section 2.4.4.

Air handling units

The AHU is a central part of the HVAC system and mainly responsible for ventilation. It is responsible for the regulation and circulation of the airflow and can comprise the following components: Air filters, heat exchangers, humidifiers, fans or blowers, and further heat exchangers for heat recovery.
The majority of the electric power consumption of an AHU (and of the whole HVAC system) can be attributed to the electric motors driving the fan or blower. The electric motors use electrical energy and convert it to mechanical energy to create an airflow. An AHU uses a supply motor and supply duct to push fresh supply air into the building and an exhaust duct and an exhaust motor to withdraw used exhaust air from the building. The majority of supply and exhaust air motors of an AHU are controlled via variable frequency drives (VFD). VFD enable the activation and deactivation as well as the modification of the power consumption of individual motors within the configured allowable power consumption range.
Moreover, the response time, ramp speed and controlled variables can be set by the VFD. Furthermore, the current power consumption of the controlled electric motors can be measured, thus making the VFD a central part of the concept of power control and power measurement [288, 328].
At the case study, the main control input for the power consumption of the AHUs is the outside temperature and the atmospheric pressure within buildings.

Chiller

In industrial environments, the majority of chillers for active room cooling are electrical compression machines. Thermally driven absorption chillers are less widespread.
A compression refrigeration machine consists of an evaporator, a compressor, a condenser, and an expansion valve to reduce the pressure. It works like a reversed heat pump at two different pressure levels. A refrigerant flows between the evaporator and the condenser. In the evaporator, the refrigerant absorbs ambient heat at low pressure, evaporates, and thereby cools down the cooling medium. After the pressure increases in the compressor, the refrigerant releases the absorbed heat in the condenser before it is expanded again to a low-pressure level in the expansion device. Industrial compression chillers generally employ a number of compressors, which are turned on and off depending on the difference of return and flow temperature.
The energy required to operate a compression chiller is therefore mainly derived from the power that has to be supplied to the compressor for the pressure stroke. The efficiency of electric compression chillers is indicated by the energy efficiency ratio (EER), which is the ratio of the cooling capacity generated to the electricity used. The maximum thermodynamically feasible values for EER can be derived from a Carnot cycle. The EER increases with a decreasing lift (temperature lift between condenser inlet temperature and evaporator inlet temperature), i.e., cooling from lower temperatures (e.g. in winter months) requires less electricity than from higher temperatures (e.g. in summer months) if the ambient temperature is used as the condenser inlet temperature [16, 152].
Absorption and adsorption chillers use heat to generate cooling in sorption cycles. Refrigerants are dissolved in a carrier medium (absorption) or deposited onto a solid carrier medium (adsorption). The separation of the refrigerant (condensing) - in order to close the circuit - takes place by means of thermal energy [16, 152].
Circulating air cooling units with a cooling register are often used to maintain cold temperatures. This cooling register is supplied with cooling from the refrigerating machine. In most cases, refrigeration machines consist of one or more compressors, which are switched on as required. In rare cases, speed-controlled systems are also available [16].
At the case study a central cooling system is installed: All parts of the chiller are installed in one compact unit. Furthermore, the entire system can be switched on or off by the energy management system. Individual compressors of the refrigerating machine cannot be controlled. This would require an intervention in the internal system control, which is usually not desired from the operator's and the manufacturer's point of view [154].

2.4.4 Thermal power production

This section describes the technologies responsible for the production of thermal power. The CHP plant has already been introduced in Section 2.4.1. Further technologies include gas-fired condensing boilers and a power-to-heat plant.

Gas-fired condensing boiler

A boiler is a device used for high-temperature heating. One type of boiler is the condensing boiler. Condensing boilers can achieve efficiencies higher than 95% fuel efficiency. This style of boiler includes a sealed combustion area, combustion draft inducer, and a secondary heat exchanger. Gas boilers obtain heat energy from the combustion of natural gas and transport the heat energy via the heat transfer medium water. Boilers generally can be operated in a flexible manner from a given minimum power.

Power-to-Heat

Power-to-heat (P2H) describe the conversion of (surplus) electricity (from renewable energies) to thermal energy in the form of heat.
There are different means to convert electricity into heat: The two main technologies are electric boilers and heat pumps. Electric boilers are often in the form of electrode boilers, which is also the technology used at the case study. Heat pumps are usually air- or ground-sourced. Large-scale heat pumps often use geothermal energy or waste energy from other processes. [45].
For electric boilers, the thermal efficiency defines the conversion rate of electrical energy to thermal energy (thermal efficiency), while for heat pumps the coefficient of performance (COP) is the key performance characteristic. The COP describes the relationship between the employed electrical energy and the usable thermal energy. Generally, electric boilers can reach a thermal efficiency of close to 1, the COP of heat pumps ranges from 1 to 5 depending on the employed technology, configuration, and ambient conditions [15].

2.5 Mathematical foundations for modeling and optimization of energy systems

This section summarizes mathematical foundations for the modeling and optimization of scheduling problems of energy systems [86]. Optimization is often assigned to the field of Operations Research and describes the development of abstract mathematical models for practical problems to make optimal decisions. The abstract mathematical models are also referred to as optimization problems. Optimization determines the maximum (or minimum) of a function f defined in a state space S [209]. The decision making process is done with a range of different solution algorithms. The development of efficient solution algorithms is a core area of the field "algorithm engineering" of computer science.
According to [96], the following steps are taken for a typical optimization project:

1. Identification and analysis of the problem
2. Determination of objective(s)
3. Formulation and implementation of the mathematical model or optimization problem
4. Input data acquisition
5. Solving modeled problem with input data for the determined objectives
6. Evaluation of the solution

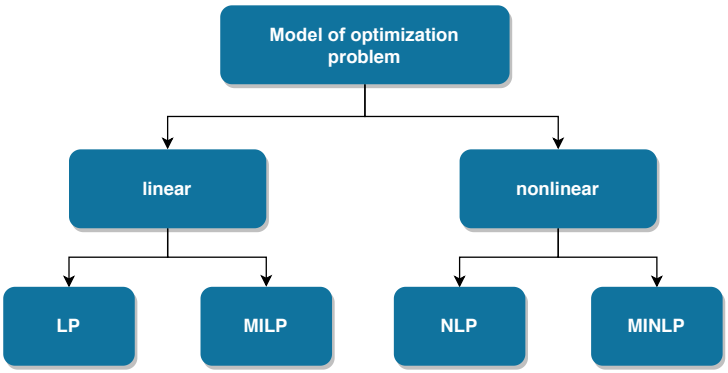

Figure 2.11: Branch tree of problem formulation classes commonly used for scheduling or dispatch problems according to [153]

In general, a mathematical optimization model with a single objective consists of the objective function z to be minimized (or maximized), m inequality and o equality constraints [359]:

$$\min z = f(x) \tag{2.1a}$$

subject to

$$g_i(x) \leq 0, \ \forall i \in [m] \tag{2.1b}$$
$$h_j(x) = 0, \ \forall j \in [o] \tag{2.1c}$$

Hereby, x is an n-dimensional vector containing all relevant decision variables. The decisions to be made in optimization are equal to a variation of the variables representing the degrees of freedom of the optimization problem. The evaluation of individual decisions is performed using the objective function(s). The task of the optimization is to find an assignment of values to the decision variables leading to an optimal value of the objective function(s). A solution algorithm of an optimization problem minimizes (or maximizes) the value of the objective(s) or cost function in compliance with all constraints m, o [300].

2.5.1 Model classes and solution algorithms of optimization problems

Optimization problems can be classified according to many criteria, whereby the classifications vary greatly depending on the literature. Thus, in this work, distinctions are made according to the model class of the optimization problem and corresponding solution algorithms or paradigms. Accordingly, these distinctions are described in the following.

Fig 2.11 shows a possible model classes of optimization problems in the form of a branch tree. These different model classes can include exclusively linear functions as objective and constraints (linear). In contrast to linear models, nonlinear models of optimization problems have a nonlinear objective function and/or at least one nonlinear constraint (nonlinear). Furthermore, both classes can be divided into problems that contain only continuous variables (LP, NLP) or problems that are integer programs, i.e., these problems contain integer or binary variables (MILP, MINLP) [96, 209].

The model class should be selected according to the adequacy to represent the problem at hand. A universally valid and feasible procedure or solution algorithm of defined optimization problems of all mentioned model classes does not exist. Rather, different solution algorithms have established themselves for certain model classes. Nevertheless, these must be examined on their applicability depending on the problem formulation [209]. For example, solving a complex optimization problem with a large number of variables and constraints usually involves a long computing

time such that the optimization is not feasible. A reduction of the computation time can be achieved by simplifying the model or by using enhanced utilization of computers applying methods of parallel and distributed computing. The preliminary investigation to what extent optimization problems and solution algorithms can be applied for the given real problem is therefore necessary.

Linear program

The "simplest" mathematical problem formulation or model is the purely linear program (LP), which only features linear constraints and a linear objective function. Furthermore, all variables must be continuous. The most prominent solution algorithm for this optimization problem is the Simplex method. Besides, other methods exist, such as solving the dual problem (Duality Theorem), the inner-point method or the ellipsoid method. Nevertheless, the linearity condition means that often compromises have to be made in the modeling of complex real problems that cannot be modeled exactly in an LP [300].

Mixed-integer linear program

In contrast to LPs, decision variables of mixed-integer linear programs (MILPs) can be integers. This allows a higher adequacy of the model for certain problems. For dispatch problems of energy systems, for instance, the on- and off- switching processes of part-load generators can be modeled using binary variables. A disadvantage is that in comparison to LPs, more complex solution methods are necessary that lead to a significant increase in computing time.
There are different solution algorithms with partly different approaches. Solution algorithms include, for instance, the branch-and-cut algorithm. Thereby, a relaxation of the optimization problem to a LP is done. The LP is solved and determines the initial search space of the branch-and-cut algorithm, which continuously narrows down the search space of possible solutions by combining the *branch and bound* and *cutting planes* algorithms. The branch-and-bound algorithm performs branching, i.e. it divides the search space and solves sub problems, and bounding, i.e. it eliminates branches that cannot contain global optimum. The cutting planes algorithm relaxes constraints (integer variables), solves the relaxed problem, and checks the feasibility of optimal solution. If a region of the search space proves infeasible, it is cut off. While the branch-and-bound algorithm creates two new sub-problems for each non-integer value of an integer variable, the branch-and-cut adds a linear inequality that excludes the non-integer value (as done by the cutting planes algorithm) [209].
Complexity classes are used to classify the computing time of algorithms. The optimization of a MILP falls into the group of non-deterministic polynomial time hard problems. NP-hard problems can be defined as programs that all problems of complexity class NP can be reduced to in polynomial-time [227]. Furthermore, MILPs are also NP-complete meaning that they belong to the complexity class NP. Moreover, it is assumed that P $\neq$ NP, which would prompt NP-hard problems to not be solved in polynomial time, i.e., the computation time for MILPs increases exponentially with the number of variables in the worst-case scenario; however, the application of these problems shows that the possible exponential increase of the computation time is not the rule in most practical cases [209].
All linear problems are convex optimization problems, as objective function and constraints are linear and, thus, convex. Convex programming means that a local optimum solution represents a global optimum solution [209].

Nonlinear program and mixed-integer nonlinear program

Another large group of problems has to be modeled by nonlinear programs. Here, the objective function and/or the constraints can also be nonlinear, so that nonlinear dependencies can be modeled precisely. Objective functions and constraints are at least twice continuous and differentiable such as quadratic functions. As opposed to linear programs, nonlinear programs may possess multiple local and global optima.

Typical solution algorithms of nonlinear optimization problems without discrete variables (NLPs) consist of applications of numerical methods, such as the Newton method, the conjugate gradient method or modifications of these [358].
The main disadvantage of all nonlinear optimization models is the high computational time when using many variables. Moreover depending on the solution algorithm, non-convex models can lead to the dilemma that the optimality of a solution cannot be ensured, because the solution algorithms can get "stuck" in a local minimum. By a randomized variation of the initial values of the optimization, the problem of local solutions in nonlinear optimization problems can be contained [26].
A nonlinear optimization problem, in which discrete variables are also allowed (MINLP), requires extensions of the existing algorithms, which is occasionally by a further increase in computing time.
All above mentioned model classes represent smooth optimization problems; however, also non-smooth models exist. Non-smooth means that the objective functions or constraints are not differentiable. A possibility to apply the models above is if the problem can be relaxed to a smooth model [55].

Heuristics

As opposed to exact optimization that is possible for the above-mentioned solution algorithms, heuristics are designed to find a good solution among a large set of feasible solutions with less computational effort. Heuristics do not require a mathematical program of the optimization problem, as they encode constraints into a representation of the solution. They are useful approaches for optimization problems when solution algorithms are not able to find the optimal solution in the desired time [96, 135]. Heuristics often modify existing solution algorithms and are generally designed to solve a specific optimization problems. The solution algorithms mentioned above are guaranteed to find an optimal solution within a certain error bound, heuristics, on the other side, often cannot guarantee this [309].

Metaheuristics

Metaheuristics, on the other side, provide a more generalized approach as they often represent algorithms that can be applied to various optimization problems. This group of solution algorithms, which has emerged strongly in recent years, includes an almost unmanageable number of different representatives, such as the genetic algorithm, simulated annealing, particle swarm optimization, random walk, and taboo search. Many of these algorithms are nature-inspired [142].
One example for metaheuristics is evolutionary algorithms (EA), which use mechanisms inspired by biological evolution, such as reproduction, mutation, recombination, and selection to create candidate solutions and select the best among them using a fitness function.
Further optimization problems and solution algorithms exist that consider uncertainty, i.e. the lack of complete or precise information. Research in this field includes robust optimization, stochastic programming, or online optimization [289, 418].

2.5.2 Multi-objective optimization

Multi-objective optimization (MOO) refers to an optimization problem that consists of a vector of objective functions, i.e., that follows several targets simultaneously. As opposed to a single-objective optimization problem that result in a one-dimensional solution space, multi-objective optimization yields a set of Pareto-optimal solutions. Pareto-optimal solutions are solutions that are non-dominated. Dominance refers to the concept of comparing solutions by considering all objectives. In other words, a solution is called dominated, if there is another solution that is better in one objective without deteriorating another.

Several methods exist that can reduce the dimension of a Pareto-optimal solution space. One of these methods is the use of a scalarization function, which maps any objective function vector to a real-valued number [55].

2.5.3 Solving the implemented problem

In the case of large, mixed-integer optimization problems, the solution is generally provided in three steps:

1. **Modeling**: With the help of an algebraic modeling language, the optimization problem is formulated abstractly by declaring the variables, setting up the constraints (equations and inequalities), and the objective function.
2. **Compiling**: The compiler of the modeling language translates the source code and generates an output file in a format that can be further interpreted by a solver. The Mathematical Programming System (MPS) format is practically considered as the standard format and is accepted by almost all commercial solvers as well as several open-source solvers [156].
3. **Solving**: The solver finds an optimal solution to the optimization problem. Solvers are programs that contain solution algorithms. To shorten the computing time, the solver also transforms the optimization problem in the run-up to the optimization, for example, using the elimination of redundant restrictions.

2.5.4 Selection of the objective function(s)

For each optimization, an objective function to be minimized or maximized must be defined. Common objective functions of scheduling problems in energy systems include operation cost minimization, primary energy use minimization, CO_2 emission minimization or run time minimization. In the optimization of the operational planning of energy devices, the dispatch problem, usually the operation costs are minimized or the contribution margin is maximized. This optimization problem is combined with the aggregator problem which maximizes profits on energy markets in this thesis. Both problems are describe below.

Cost-minimizing dispatch problem in microgrids

In a microgrid, the main objective for the (economic) dispatch problem is satisfying the energy demand at minimal cost. Depending on the given input, it is decided which DERs to operate or energy sources to tap to satisfy energy demands in the most cost-effective manner.
Generally, only variable costs of individual devices are included in the objective function. For example, the variable costs for the operation of a DER including fuel cost, start-up cost, maintenance cost, et cetera are included in the objective function. Fixed costs, such as investment costs, are not taken into account in the objective function.
A template of the optimization problem is given in Equations 2.2. The operation of the individual devices is subject to system-related constraints as well as device-related constraints given by individual devices.
A typical system-related constraint is the fulfillment of energy demands: To guarantee the reliability of supply of thermal and electric power for manufacturing processes, the thermal and electric power demands specified in the optimization model for the industrial site is fixed for each time step and must always be fulfilled, i.e., the pool of available devices must provide the required electric and thermal power output. The source of the provision of heat and electricity has no influence on the quality of power and heat provision.
Device-related constraints describe parameters that influence the operation of individual devices. These can include, e.g., the availability of units, must-run units, allowable emission limits, minimum up times, minimum down times, ramp limits, et cetera.

Economic dispatch problem

Minimize operation costs (2.2a)

subject to

system-related constraints (2.2b)

device-related constraints (2.2c)

Aggregator problem

Maximize profits from flexibility services (2.3a)

subject to

aggregate flexibility offers (2.3b)

satisfy use case criteria (2.3c)

Profit-maximizing aggregator problem

An aggregator collects flexibility offers of several DERs and commercializes them as flexibility services. For an aggregator, the main goal is to maximize profits. A template of the optimization problem is given in Equations 2.3. Constraints include criteria given by individual flexibility services, e.g., the bid placement criteria of control reserve markets. Profits are included in the objective function and can originate from the provision of flexibility services by commercializing the flexibility on electricity and control reserve markets.
With given flexibility provided by an energy device, an optimal allocation of flexibility for these services is found, thereby, scheduling energy devices accordingly. The constraints of the related markets are given by market design criteria such as minimum bid sizes, product duration, et cetera.

The objective function in this work

As shown in Chapter 4 many publications consider only one of the two described problems. In Chapter 3, this work identifies several flexibility services that can be fulfilled at industrial sites. Each flexibility service is represented by a different revenue or cost function in the objective function of the aggregator problem. The objective function of the dispatch problem includes different cost functions for the operation of DERs. A weighted sum is used to map the different objective functions to a single-objective function. This is done by assigning a scalar value, a weight, to each objective function and creating a weighted sum of objectives: The total energy costs, therefore, result from the variable costs of the operation of DERs minus the variable revenues of the commercialization of flexibility of DERs. The prices or penalties paid or received for each flexibility service resemble the weights and are multiplied by the flexibility, i.e. the difference in power between planned and (possibly) adjusted load profile. The task of optimization is to minimize the total energy cost including revenues from flexibility services.
As opposed to the method of creating a weighted sum among objectives, more convoluted scalarization methods as described in Braun [55] can be applied.

2.6 Summary

Chapter 2 explains the fundamentals of energy systems in Section 2.1 and the electrical energy system in Germany in Section 2.2. This knowledge is especially important for the understanding of the following Chapter 3, which provides an analysis of possible flexibility services that a typical industrial site can provide. Furthermore, Section 2.4 described the energy technologies that can be found at the case study industrial site. Section 2.5 provides basic information on optimization problems with the focus on the dispatch and the aggregator problem. The description of technologies and the fundamentals of optimization problems are crucial to understanding Chapters 6 and 5, which describe the optimization problems in this work.

3 Analysis, Assessment, and Modeling of Flexibility Services

This chapter introduces and assesses identified flexibility services from the viewpoint of an industrial site with the aim to lower the total energy costs.
Section 3.1 defines the term *flexibility of energy systems* as it is used in this work and define a methodology to measure the feasibility and potential of flexibility service provision by industrial sites. Section 3.2 gives an overview of possible flexibility services that can be provided by energy devices and selects feasible flexibility services. Sections 3.3-3.6 describe the selected flexibility services in detail and provide methodologies for their modeling.

3.1 The flexibility of energy systems

In the following section, the term *flexibility* of energy systems and its meaning in this work is discussed. As a result of a literature review of definitions of the term, a methodology is derived that meets important aspects mentioned in the literature. This methodology is then performed in Chapter 6.

3.1.1 Definition

In this work, "flexibility" focuses on the flexibility of the load profile of an entity connected to the electric power grid. The load profile describes the exchange of electric power with the grid.
Several different definitions of the flexibility of energy systems exist in the literature that further describe the term flexibility:

1. Mauser et al. [266] define flexibility as the "set of all valid combinations of system inputs and condition-related outputs for all energy carriers." This implies that the entire number of feasible load profiles of an energy system represents its flexibility. To assess the flexibility of an energy system one would have to model all energy carriers including their system inputs and outputs.
2. Petersen et al. [315] define a "taxonomy for modeling flexibility in Smart Grids, denoted Buckets, Batteries and Bakeries" Buckets, batteries, and bakeries represent different energy devices that are modeled as MILPs. Buckets represent flexibilities that are storage systems that can be charged and discharged (such as a bucket that can be filled and emptied or a bidirectionally charging EV), batteries are flexibilities that can only be charged (such as a disposable battery or unidirectionally charging EV), and bakeries are electricity consumers that have a load profile which can be moved en bloc (such as a bakery or industrial processes that cannot be interrupted once started).
3. Eurelectric [110], on the other hand, defines flexibility "on an individual level" as "the modification of generation injection and/or consumption patterns in reaction to an external signal (price signal or activation) in order to provide a service within the energy system." According to this definition, the ability of a device, i.e. a generator or consumer, to deliver a service within the energy system needs to be modeled. Possible services that can be delivered with demand-side flexibility are defined inter alia in [385].
4. Tusar et al. [384] define so-called flex-offers indicating flexibilities in production/consumption start time and energy amount. The flex-offer gives information on the time flexibility interval (the difference of earliest and

latest start time), and the flexible and inflexible energy consumption/supply. Neupane et al. [298] also model flex-offers in the same way as [384]. The flex-offers contain a time and an amount of flexibility. The authors further define a process to generate the flex-offer from time-series data. Gerritsma et al. [144] also identify time flexibility of EV charging processes in a similar way.

From these above-mentioned definitions, the conclusion can be drawn that in order to model the flexibility of an energy system, it is mandatory to model all possible states of an energy system [266]. This can be done using mathematical modeling as in [315]. The use of the flexibility to deliver services within an energy system is described in [110]. Based on this definition, the term "flexibility service" is used to describe the use case that can be offered with the flexibility to adjust the electric load profile. [298, 384] describe modeling approaches for flexibility on the device-level. To include all aspects of mentioned definitions, this work follows the methodology, which is a result of this compilation of literature:

1. Create a model of the energy system of the target site as suggested by Mauser et al. [266]. The conversion of energy using devices, their interdependencies, et cetera are modeled using a mathematical formulation as used by Petersen et al. [315]. This is done in Chapter 6.
2. Model the possible flexibility services that can be delivered using the flexibility of devices as suggested by EURELECTRIC [110]. The flexibility services are introduced in this chapter.
3. Define an objective function that incorporates savings or earnings from the flexibility services within the total energy costs.
4. Optimize the operation of controllable devices according to the developed model using energy data from the target site and market data for the period 2015-17.

The flexibility of electricity consumers such as an industrial site has been primarily stimulated by demand side management strategies. Thus in the following, the term *demand side management* is described.

3.1.2 Demand side management

Demand side management (DSM) was introduced by Gellings et al. [141] as a series of activities by utility companies or system operators to achieve load profile changes on the demand side. In other words, DSM provides incentives that trigger the utilization of flexibility. Mauser [265] points out; however, that this typical demand side customer does not exist anymore as these entities move towards a prosumer status through the deployment of own generation and storage devices. With the advancement of electricity market liberalization DSM strategies are nowadays put in place by several different stakeholders inter alia system operators, utilities, or aggregators [35].
Resulting changes in load shapes are most prominently presented in [141, 417] and shown in Figure 3.1. In the following, each load profile adaption is described shortly. The application and consequence of an actual demand-side management strategy in the German national energy system is presented as well.

1. **Strategic conservation**: Through strategic conservation, the amount of electricity procured from the public grid is deliberately lowered. This adaption of the load profile is often done to reduce the share paid for power sourcing. The change can be done by energy efficiency measures, switches to other forms of energy, or the increase in local generation. Triggers for strategic conservation are, for instance, increasing electricity prices.
2. **Strategic load growth**: Strategic load growth increases power consumption on a long-term basis. It can be caused by favorable electricity rates presented by the supplier or the increase in prices of other forms of energy. This can cause a switch to electricity from competing fuels.

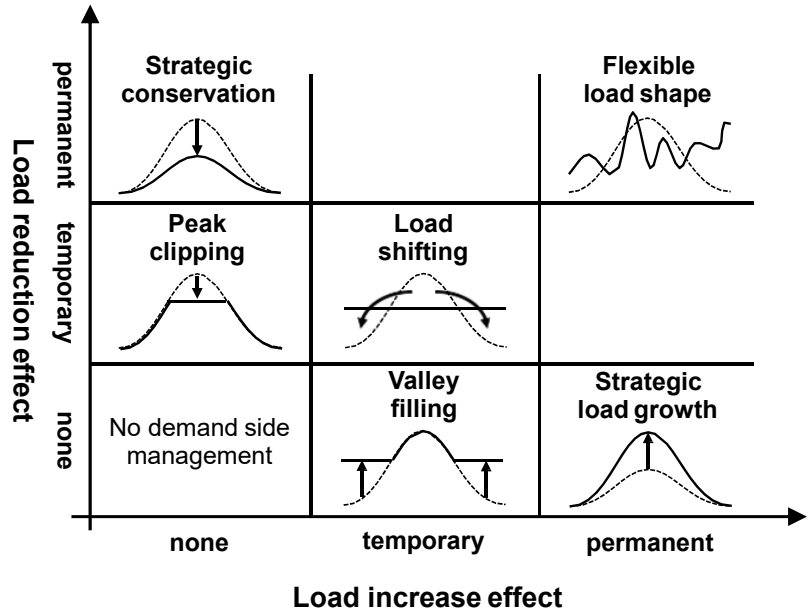

Figure 3.1: Load shape objectives caused by demand-side management strategies according to [141] as depicted by [265]

3. **Peak clipping or peak shaving**: Peak shaving decreases the maximum level of a load profile. This load change is generally performed to lower fees paid for peak pricing (see 3.1.3). In Germany, a share of the grid fees is paid for though peak pricing. At high full load hours[1], the share of grid fees based on peak pricing can reach up to 87 % [278].
4. **Valley filling**: Valley filling increases electricity consumption or decreases generation. Reasons for valley filling could be negative net electricity prices or the prevention of an electricity feed into the grid as this can spur further costs for commercialization. Furthermore, subsidies in Germany for certain energy devices are connected to the status of auto-producers - all generated electricity behind the meter is consumed behind the meter [123]. Another reason for a valley filling are reductions in grid fees for a flat load curve as defined in [122].
5. **Load shifting**: Load shifting moves loads from peak hours to times with less consumption leading to a flatter load curve. Triggers for this change in load profile are identical as for peak clipping and valley filling. The main difference is the actual shift in electricity consumption or generation. Load shifting is often done to move electricity consumption to less expensive times to profit, for instance, from dynamic power prices to decrease power sourcing costs.
6. **Flexible load shape**: According to [141] a load shape "can be flexible if customers are presented with options as to the variations in the quality of service that they are willing to allow in exchange for various incentives." Furthermore, [141] elaborates that fully flexible load shapes are only possible with electric power consumers that are possible to curtail or interrupt and an integrated energy management system that offers the choice to fulfill the desired service with a different energy carriers.

Many works in literature [35, 140, 307] follow the classification of DSM measures into the following categories:

1. **Demand Response (DR)** - changes in the electrical load profile by end-use customers as a response to prices, incentives, or signals. Depending on the flexibility and elasticity of the electricity demand of the customer, the customer changes its load profile through changes in demand or generation.

[1] The full load hour is defined by the division of the total yearly consumption by the yearly peak power.

2. **Energy Efficiency (EE)** - reducing the energy required for the provision of services or products.

Furthermore, the authors of [195] define strategic load growth as another category of DSM. [195, 307] further distinguish between **market-based DR** and **physical DR**. While market-based DR relies on market places where flexibility is traded and the provision remunerated, physical DR sends out binding requests for demand management, e.g., if the grid or parts of its infrastructure (power lines, transformers, substations, etc.) proves to be inadequate to deliver the necessary system services and the DR measures can increase the operational effectiveness of the grid.

3.1.3 Demand Response

This thesis does not consider strategic load reduction or strategic load growth DSM, but instead focuses on short-term market-based DR measures that currently exist within the German electrical energy system and that are suitable for the application at an industrial site. In this work, these DR measures are defined as flexibility services, as they use the available flexibility of the load profile to provide services for different stakeholders along the electricity supply chain. The energy manager of a manufacturing site can further decrease energy costs through participation in these market-based DR measures.
This thesis tests to what extent an industrial site alters its behavior according to these incentives. In the following section, different categories of incentives of DR strategies are introduced.

Incentive mechanisms for market-based demand response

The simplest incentive to spur DR activities is the electricity price which, in general, prices electricity consumption. [163] introduces the category of *time-based rates* DR which covers DR in connection with prices that change over time. As has been shown in Figure 2.10, the electricity price in the German markets is made up of many different price components. Still, most household and industrial customers receive *flat pricing*, i.e. the electricity price does not change regarding the time of consumption, or *block pricing*, specifically, only two different electricity prices exist. However, at times electricity contracts of industrial consumers include *real-time or dynamic pricing*. Additionally, in the near future, lawmakers force utilities to offer dynamic pricing [111].
[163] define the following pricing scheme categories, commonly used to spur DR:

- *block or time-of-use pricing* (TOU) - different unit prices for usage during different blocks of time,
- *critical or variable peak pricing* (CPP) - a previously specified high rate for usage designated by the utility to be a critical peak period, while a price discount received during non-CPP periods, and
- *real-time or dynamic pricing* (RTP) - price fluctuating in high frequency reflecting changes in the wholesale price of electricity.

Next to time-based rates DR, [163] also define incentive-based DR. Incentive-based DR is among others separated into

- *direct load control* - the DSM stakeholder (e.g. the DSO) gets direct access and control of the customer's devices. For market-based DR a remuneration is given to the customer, while for physical DR no remuneration is provided [307].
- *interruptible/ curtailable rates* - consumers receive discounted electricity rates, market-based rates, or payments defined in bilateral contracts [35] as compensation for accepting limited service interruptions.
- *capacity (market) programs* - customers guarantee to react to signals for capacity offered; however, loads are not controlled directly by the DSM-stakeholder but instead by the customer.

3.1.4 Local use of flexibility vs. external offer of flexibility

Next to the types of DR, this work distinguishes between the addressee of the flexibility services provided by the industrial site. Flexibility services can be used to deliver a service

- **within the local energy system**, e.g., actions that solve a local problem or reduce local electricity costs behind the meter.
- **within the national energy system**, e.g., in the form of system services. Hereby, the flexibility to change the load profile is offered to external entities in front of the meter. These can call up this flexibility if needed.

This work distinguishes between local use and external offer of flexibility. [305, 385, 386] specify different flexibility services that create value for different entities. This work defines flexibility services that are carried out behind the meter as services that can be used on-site without passing through a meter. They are carried out by the consumer within his or her premises and are primarily used to lower the consumer's electricity bill. [305] defines these as Prosumer Services. Local and external service are often also referred to as behind-the-meter and front-of-the-meter services [102].
Further services either carry out system services to solve problems outside of the prosumer's premises or interact with third parties through energy exchanges. In front of the meter flexibility services are not reflected on the actual energy bill but generate additional revenues.
The two different types of flexibility services can, therefore, be further defined as

1. **local flexibility services**- flexibility is used behind the meter to lower electricity costs or create non-monetary benefits.
2. **external flexibility services** - flexibility is offered to external entities in front of the meter to gain additional revenues or non-monetary benefits.

Local flexibility services feature only indirect control as no external entity such as a grid operator or the utility company is controlling the different devices while external flexibility services represent a mix of direct or indirect load control.
The following Section 3.2 summarizes all possible flexibility services that can be delivered by devices of introduced technologies. The flexibility services are classified according to the addressee in the electricity supply chain for the German electrical energy system and the actual value that they create. Furthermore, differentiation of local and external flexibility services is done.

3.1.5 Criteria for selection of flexibility services

In Section 3.2, individual flexibility services are introduced. These are assessed according to criteria partly stemming from the definition of DR in this work.
The criteria for selection the flexibility service for modeling are:

1. It is technologically feasible to provide the flexibility services with existing energy devices of technologies introduced in Section 2.4. This can include tests done at the case study industrial site or examples found in the literature.
2. It is economically viable to provide the flexibility services, i.e., a DR program exists that remunerates the utilization of flexibility in the German electrical energy system.
3. As of now sufficient data exists to correctly model the remuneration and provision of the flexibility service.

The identified flexibility services are selected for modeling if they fit all three criteria.

3.2 Identification and analysis of flexibility services

Table 3.1 describes possible use cases for flexibility, the flexibility services, in electrical energy systems. The basic structure of the table has been taken from work done by Battke [24]. His work is extended and elaborated in this chapter. If possible, relevant use cases are applied to the regulatory conditions of the German energy system as described in Chapters 1 and 3. The use cases are clustered according to the need of the flexibility service by a stakeholder in the electricity supply chain on the x-axis. The electricity supply chain has been taken from the smart grid architecture model [380] and combined with entities defined in [385] - thus covering areas:

- *Generation* which represents mainly fossil-fuel power plants located in the transmission grid such as nuclear, hard coal, lignite, or gas power plants,
- *trading* which defines market activities around balancing groups led by BRPs,
- *transmission & distribution* which covers system operation of electricity grids by TSOs and DSOs,
- the *retail* of electricity done by the supplier, who defines the electricity contract to the prosumer,
- *distributed energy resources*, which applies to all DERs installed mainly in the distribution grid. This also includes DERs behind the meter of the customer's premises, and
- the *prosumer* who primarily consumes electricity; however, can also act as a producer of electricity due to the installation of DERs.

On the y-axis, the flexibility services are classified by the source of economic value that they offer. The different classes of economic values include

- *power quality* which counteracts electrical disturbances to assure safe and efficient operation of the power system [241],
- *power reliability* which creates economic value by assuring an uninterrupted power supply,
- *portfolio or cost optimization* which defines market-based flexibility services that can save electricity costs or generate additional revenues, and
- *hybrid use cases for enhanced utilization of existing assets* which refers to the combination of different flexible energy devices to extend their functions or improve their operation.

The flexibility services that are classified in Table 3.1 are flexibility services that can be provided with a single device or a combination of devices of the described energy technologies in Section 2.4 found at industrial sites such as inter alia BSSs, EVs, or CHPs. Flexibility services that are selected for modeling in this work are marked in gray. These flexibility services and the modeling approach for the schedule optimization model from Chapter 6 are explained within the scope of this chapter.
Furthermore, the differentiation of local and external flexibility services is also visible in Table 3.1 by the separation of the double line. While flexibility offered to the BRP, TSO, and the DSO are external flexibility services (left side), local flexibility services include services for energy cost optimization based on energy supply contracts or flexibility services addressed at local DERs (right side). The flexibility service peak shaving represents an exception to the definition stated above in Section 3.1.4 as it is performed behind the meter and leads to the reduction in energy costs. It is remunerated by the DSO as it flattens the load profile of customers and decreases peak usage of grid infrastructure. Thus, it is categorized as a local flexibility service provided to the DSO.
Following Table 3.1, the individual flexibility services are introduced along with their sources of economic value to a stakeholder in in the electricity supply chain:

Table 3.1: Classification of flexibility services along the electricity supply chain based on [24].

Source of economic value		Source of remuneration in the electricity supply chain						
		Generation	Trading	Transmission	Distribution	Retail	DER	Consumption
		Conventional PP	BRP	TSO	DSO	Supplier	Intermittent RES, BSS, etc.	Prosumer
Power quality	Frequency			Load frequency control				
	Voltage			Voltage control			RES smoothing	End-consumer power quality
Power reliability	Operational planning			Redispatch & Reserve				
	System restoration	Emergency power and islanding		Black Start				Emergency power and islanding
Portfolio or cost optimization	Bilateral Agreement or single price		BG self-balancing		Peak shaving		FCR charge balancing for BSSs	
	Market dynamics		Energy market optimization			Real-time price optimization	RES buffering	
Hybrid use cases for enhanced utilization of existing assets	Fulfill legal specifications	Synthetic control reserve					RES firming	Local self-balancing
	Other	Improved load following			Load buffering			increase in self-sufficiency
		External flexibility services in front of the meter ←				→ Local flexibility services behind the meter		

Power quality

As described in Section 2.2.2, power quality is concerned with frequency control, voltage control, and reactive power compensation.

Frequency control

As mentioned in Table 2.1 frequency control is under the responsibility of the TSOs. For *frequency control*, the TSO employs different measures to control the grid frequency, which are primarily defined by the ENTSO-E that is further elaborated in Section 3.5.

The contraction of flexibility to use the mentioned measures is done as incentive-based DR: frequency control is currently organized as a *capacity market program* in Central Europe. Individual products and the implemented modeling in this work is explained in Section 3.5.1.

Voltage control

Voltage control is done both in the transmission grid by the TSO, as well as, the distribution grid by the DSO. For a typical large-scale industrial site connected high-voltage grid (see Figure 2.1), remuneration of these services is under the responsibility of the DSO.

Section 2.2.2 covers the fundamentals of this flexibility service. In contrast to frequency control, voltage control is often employed through technical specifications upon installation of energy devices (reactive power), transformer control, the modification of grid infrastructure, or as direct load control through ripple control signals. Due to the non-uniform system for remuneration among DSOs, voltage control is not considered further in this work.

RES smoothing

On the DER part of the electricity supply chain, RES smoothing [241] can be provided by flexible energy davices such as batteries. RES smoothing enables RES to generate electricity without any voltage sacks, flickering, or harmonic distortions. To avoid these distortions, DERs have to comply with different technical regulations upon installation [28]. The compliance with these regulations is not remunerated in Germany.

End-consumer power quality

On the consumption part of the supply chain, industrial consumers often operate microgrids. In these microgrids, power quality such as a constant voltage level have to be assured. Here, flexible energy devices can contribute to increasing local power quality. No data on the levels of current and power for individual phases at the case study industrial site has been available. The flexibility service is, therefore, not considered further.

Power reliability

The field of power reliability refers to possible measures that tackle problems requiring operational planning of grid operators, such as the violation of transfer capacities of grid lines, or system restoration, such as the restart of systems after blackout (see Section 2.2.2). The issues related to power reliability relate to all sections of the electricity supply chain that operate grids. These can be microgrids as for the parts Generation and Consumption or large-scale transmission and distribution grids as for the TSO and the DSO.

Emergency power & Islanding

A blackout within the energy system of a power plant or a manufacturing plant, can cause great harm to the operating equipment and endanger personnel. A blackout of a power plant can additionally have serious consequences for the grid operation.

To ensure safe shutdown and employee safety, one can operate emergency power "back-up" capacities that can establish minimum electrical services in case of a blackout of the micro-grid. These emergency power station as described in Section 2.4.1 can further be used to restart systems after a blackout. This work models the energy technology EPS in Section 6.7.3; however, it does not consider blackout scenarios in the model due to the difficulty to estimate the likelihood of a blackout scenario for an industrial site.

To operate independently of the distribution grid, independent power sources often have the capability to provide controlled islanding even though the electrical grid power is no longer available. Microgrids are often equipped with a microgrid controller that disconnects the local circuit from the grid and forces available generators to power the island grid [214]. The flexibility service of islanding is not considered in this work due to the lack of data and remuneration.

Redispatch

Congestion management as described in 2.2.2 is performed by both TSOs and DSOs when the equipment loading limits, often line transfer capacities, are exceeded. Energy resources, in particular, power plants, are obliged to report their power profile flexibility and adjust the planned profile upon request. They are remunerated with their variable costs for increasing or decreasing their power output. Recently, system operators intend to further integrate DERs into the redispatch process; however, at the moment, this service is limited to large-scale power plants. Due to the difficult market access for an industrial manufacturing plant to participate in this capacity program, redispatch is not considered in this work.

On the DSO level, the Smart Grid Traffic Light Concept has been introduced recently by the BDEW which integrates issues of redispatch, voltage control, and frequency control. It proposes a new concept that includes an "amber" phase which lies between a "green" (no critical network situation) and a "red" (critical network phase) phase. During the "amber" phase, the DSO can utilize the flexibility offered by market participants: The concept proposes a capacity program as with frequency control in which the DSO contracts flexibility beforehand, which is provided upon request by the DSO [29]; however, as the program is still in a concept phase, no data is available concerning possible earnings for an industrial site.

Capacity reserve

Greater harm can be caused by a blackout of the transmission grid, for example by an abnormal drop or increase in frequency in the transmission grid. To prevent this, the TSO holds capacities as described in Section 2.2.2 that can be ramped up or ramped down in case of such an emergency event. This capacity reserve can be TSO-owned capacities or incentive-based acquired capacities. In Germany, this capacity market program targets mostly large-scale power plants and is not suitable for an industrial prosumer with a comparably small power flexibility.

Black start

In order to start up conventional power plants such as a nuclear power plant, black start capacities are needed that provide a minimum power for ramping up to minimum power output. A BSS or an EPS, for instance, can assist in starting up conventional power plants in dysfunctional grids [415]. For black start capabilities for conventional power plants, close vicinity is necessary. This is generally not given for industrial sites and therefore not considered as a feasible flexibility service.

Portfolio or cost optimization

Portfolio or cost optimization includes flexibility services that are targeted either at generating profit through trading on electricity markets or at optimizing energy costs for an actual consumer of electricity.

Balancing group self-balancing

BRPs are the actors on electricity exchanges that purchase or sell electricity for their customers as explained in Section 2.2.3. BRPs have to pay imbalance energy fees if they deviate from their forecasted balance of electricity. This imbalance energy fee is calculated through the total balance of all balancing groups within the four German control areas and calculated from the cost of the energy price of provided mFRR and aFRR in this time slot.

This imbalance energy generally creates costs for the BRP. Due to the rise in weather-dependent DERs such as wind and solar within balancing groups, the accuracy of the forecasted electricity generation drops as compared to conventional power plants. The demand for short-term balancing of these forecast errors increases. To clear these errors from the electricity balance, the BRP can place bids on the short-term electricity markets. If own flexible

electrical devices are available, the BRP can use them to reduce the weather-dependent imbalances. The utilization of flexible energy devices for self-balancing is generally procured in bilateral contracts from the operator of the device. As no data from actual BRPs has been available, this flexibility service is not pursued in this work.

Energy market optimization

The BRP has an additional goal to generate profits through trading to reduce energy costs for its customers. Energy market optimization buys energy at low prices and sells it again when prices are high; however, trading can only be done if devices exist that can realize the traded energy. Energy market optimization continuously adjusts the schedule of devices. This adjustment is backed-up by trades. The profitability of energy market optimization depends, on the one hand, on market dynamics and, on the other hand, on the available flexibility.
In Section 3.6.1, this work shows how the flexibility of a BSS can be used to generate profits on short-term electricity markets.

Peak shaving

Section 2.3.2 explains the electricity pricing for consumers of electricity. A large share is taken up by the grid fees. A part of the grid fees is paid as a capacity price for the maximum electricity procurement from the public grid.
DSOs incentive consumers to lower this maximum electricity procurement. This is done by penalizing the maximum electricity consumption, thus utilizing the DR strategy of *critical or variable peak pricing*. The flexibility service *peak shaving* is further elaborated in Section 3.4.1.

Real-time price optimization

A further possibility to optimize energy costs is the actual electricity price paid for power sourcing.
The supplier issues the electricity contract with the consumer and, for large-scale electricity consumers, often contains some kind of dynamic pricing dependent on real market prices. If dynamic prices exist, flexibility can be used to alter the load profile to consume electricity when prices are low. The *real-time or dynamic pricing* DR strategy helps the supplier to consume electricity when it is cheaper on the markets. The flexibility service *real-time price optimization* is further investigated in Section 3.3.1.

FCR charge balancing for BSSs

For this flexibility service, devices utilize their flexibility to balance charge or discharge events of a battery. This use case can be applied to the charge management of a BSS providing FCR as shown in [331].
Results showed large potential for flexible devices to substitute market-based BSS charge management; however, regulatory conditions complicate a realization of this flexibility service. Thus, it is not pursued in this work.

RES buffering

RES buffering describes the process in which devices buffer or store energy produced from intermittent RESs to use it or sell it to the grid when the power prices are high. One can use devices that include buffer storage to bridge the gap between generation and consumption.
As many industrial sites have devices with a capability to buffer electricity consumption, this flexibility service is further discussed in Section 3.3.2.

Hybrid use cases for enhanced utilization of existing assets

The final source of economic value describes flexibility services that create economic value by improving the use and value of existing generation, transmission, or distribution capacity and thus avoid or defer additional investments.

Improved load following

The final power output of conventional power plants can often not be controlled to the desired extent. Quite often, the response of conventional power plants to power signals has often long reaction times, long rise times, or overshooting. To improve control characteristics of these power plants, they can be combined with faster and

flexible devices to improve exact load following. Thus, it is possible to balance fluctuations in demand while the power plant runs at its optimal load with maximum efficiency.
Nevertheless, due to unavailability of conventional power plants in many industrial sites, this flexibility service has not been considered further.

Synthetic control reserve

As described in Section 3.5.2 strict technical specifications apply to the delivery of control reserve, e.g. with respect to the gradient of a response to a signal. A flexible energy device can enable power plants to satisfy regulation compliance [179], e.g., by a combination with a fast-reacting, flexible energy device [217, 274]. Further applications exist that combine energy devices with electric power consumers to fulfill regulatory conditions [354]. This innovative flexibility service has not been considered as its application is rare at industrial sites.

Load buffering

Due to an increasing intermittent electricity generation through, e.g., PV and high-load electricity consumption through, e.g., EV charging at the lower-voltage levels, transformer ratings might not match the apparent load and generation levels of certain grid segments. Instead of installing new equipment, flexible devices such as storage applications could also be used to mitigate overloads at the transformer and might actually be cheaper in the long term [179]. The overloading of a transformer in the distribution grid is often modeled using the transformer hot spot temperature [225, 268]. This flexibility service requires a distribution grid model, which was not given for the case study, and is not considered further.

RES firming

Energy flexibility can be used to form the load profile of intermittent renewable energy technologies by "firming" or "flattening" it. An example is provided in [62], where Hawaii operators of wind and photovoltaic power generation capacity deploy battery storage capacities to fulfill legal requirements concerning the firmness of the electricity generation. This flexibility service is especially apparent in small grids with high penetration of RESs [259] and regulation stating a firm feed-in of RESs. As a firm feed-in profile is generally not required in Germany, under the current feed-in tariff program, this flexibility service is also not considered further. As more and more RES power plants are urged to commercialize their energy on electricity markets [139], RES firming becomes more interesting; however, it is to be merged with flexibility service BG self-balancing, as RES firming is generally done by the respective balancing group.

Self-balancing & increase in self-sufficiency

On the consumption level, the use of flexible consumption, generation, and storage can enable an increase in self-consumption through load shifting and valley filling. The use of local renewable energies, for instance, can be improved by storing renewable energy and releasing it at times when it is needed (high power consumption). In this case, it is done without the consideration of monetary incentives as in RES buffering.
Furthermore, to decrease the feed of electricity to the public grid, loads can be employed that transform electrical energy into other forms of energy, for example via P2X technologies. This self-balancing is often also done to fulfill legal specifications that presuppose the use of RES only behind the meter [89].
This flexibility service can easily be applied at energy systems of industrial sites that have renewable generation and is therefore further considered in Section 3.3.3.
As is visible in Table 3.1, many different flexibility services exist; however, as described above, only some are suitable for the application at an industrial site. Flexibility services marked in grey are selected for modeling in the scheduling model in Chapter 6 and is introduced in detail in the following. The modeling approach of the selected flexibility services is introduced in the following Sections 3.3 to 3.6.

3.3 Flexibility services for local energy optimization

In most cases, the main motivation for local flexibility services is to minimize energy costs; however, some cases include the increase in self-sufficiency or the decrease of the CO_2 footprint.
This section introduces the flexibility services *real-time price optimization*, *RES buffering*, and *self-balancing*, which are by the definition of Section 3.1.4 flexibility services used within the local energy system.
Real-time price optimization alters the load profile according to the energy prices given by the supplier. The flexibility service is introduced in Section 3.3.1.
RES buffering describes the shift of renewable energy to times when procurement of the energy from the grid is expensive. This flexibility service is introduced in Section 3.3.2.
Self-balancing describes the local balancing of generation and demand at times when generation exceeds local demand to avoid the feed of locally generated energy to the public grid. This is explained in Section 3.3.3.

3.3.1 Real-time price optimization

Real-time price optimization describes the flexibility service to shape the load profile according to dynamic electricity prices presented by the supplier. As explained in Section 2.3.2, industrial sites often have part of their electricity bill tied to dynamic prices on, for instance, short-term electricity markets. Generally, the difference between the procured (sold) energy and the actually consumed (generated) energy is priced with a dynamic energy price, e.g. the Day-Ahead market price, and passed down to the customer.
In this work, it is assumed that electricity procured from the public grid is priced according to the EPEX Day-Ahead auction for the German grid region.
Figure 3.2 gives an exemplary impression of the price development on the Day-Ahead auction. It shows the average prices on a weekly basis as a line plot in black and the span between the 5% and the 95% quantile of energy prices for the period of 2015-2017[2]. It is visible that price levels on weekdays vary greatly from the price level on the weekend; however, all days show a morning and evening peak. This reflects the typical duck curve. The duck curve can be defined as the power generation minus the amount of solar generation over the course of a day and earns its name from the form it takes up that looks like a duck. As only the residual load is traded on the Day-Ahead auction, the price curve displayed in Figure 3.2 takes up this form.
The monetary value of this flexibility service lies in the load shifting towards cheaper periods. For an industrial site with the possibility to shape its load profile, the responsible energy manager could save on average around 11 EUR by shifting 1 MWh from the more expensive evening to the cheaper noon period (see Figure 3.2).

3.3.2 RES buffering

A further flexibility service lies in the buffering of renewable energy technologies by storage or energy conversion devices generated e.g. by intermittent wind and solar. At the target industrial site, WPPs are installed with a rated power that equals 42% of the average power demand; however, as wind energy is intermittent the electricity is not generated in a price-controlled manner. Storage devices such as a BSS or energy conversion devices such as a P2H plant can be used to shift this energy to times when electricity generation or procurement (case: BSS) or heat production (case: P2H) are expensive. RES buffering refers to load shifting considering the amount of local generation by RES and the price of electricity.

3.3.3 Self-balancing

Self-balancing refers to the flexibility service that does balancing of local generation and load "behind-the-meter". Hereby, the load profile is shaped to avoid feeding electricity to the grid and to increase self-sufficiency. This

[2] As energy data of the case study has been available from the period 2015-17, most energy market data is also analyzed for this period.

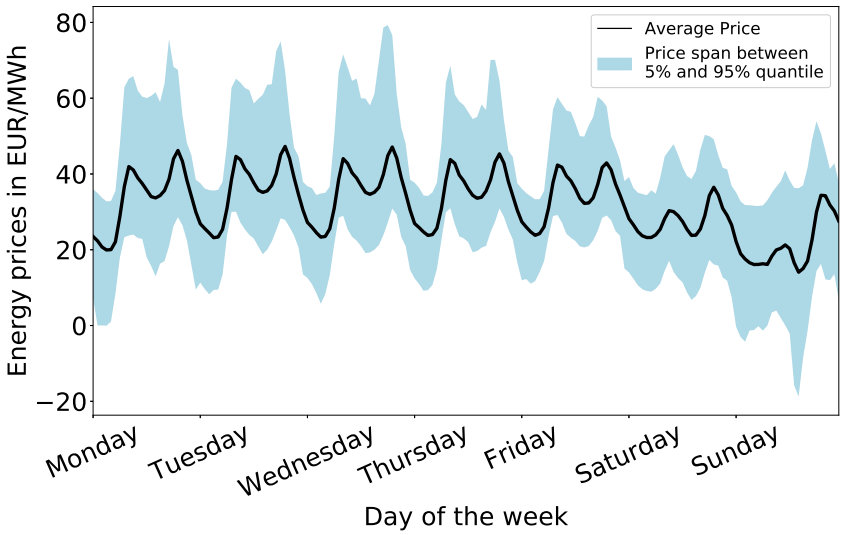

Figure 3.2: EPEX Spot Day-Ahead market auction results for the period of 2015-17
The black line depicts the average price, the blue shaded area the price range between the 5% and 95% percentile. Data is taken from [106] and extracted using [410].

can, e.g., avoid payments of marketing or low revenues of locally generated electricity on power markets. This self-balancing can be achieved with, e.g., storage devices. Self-balancing can also include valley filling (load is increased temporarily) to avoid mentioned costs.

3.3.4 Modeling approach for local flexibility services

As it is visible, the targets of the three local flexibility services *real-time price optimization*, *RES buffering*, and *self-balancing* are closely connected and often congruent.
As a MILP model has been chosen for the optimization problem, the modeling of the flexibility services is done by designing the objective function (Section 6.4). This work chooses a weighted sum of the different objective functions to overcome the challenge of having multiple objectives. Thus, for the above-mentioned local flexibility services, the cost of the electricity exchange with the public grid, and the design of the power balance are used to model the flexibility services.
For the flexibility service *real-time price optimization*, energy prices for power provision from the public grid are accounted for with Day-Ahead auction prices. For *self-balancing*, a penalty cost for feeding energy into the public grid is implemented and for *RES buffering*, feeding locally generated wind energy to the public grid is further penalized. The detailed model is given in Equation 6.15.
Due to the congruence of the flexibility services, the three use cases are summarized as the flexibility service *local energy optimization* and evaluated together.

3.4 Flexibility services for the distribution system operator

The change in the structure of the electrical systems through the *Energiewende* causes new challenges for the DSO (see Figure 2.1). Especially the move of electricity generation into the distribution system creates problems concerning the violation of power and voltage ratings. Furthermore, the lack of transparency of voltage, current, and power levels in the distribution system due to the poor measuring equipment aggravates this problem. The roll-out of measuring and communication devices, so-called Smart Meters, can help ease these problems [115, 218].

Table 3.2: Full-load hours and respective grid fees for the years 2015-17 of the case study

	2015	2016	2017
Peak electricity consumption (MW)	38.5	36.6	36.2
Full load hours (h)	4814.2	4753.7	4087.7
Peak grid fee (EUR/kWa)	71.18	85.86	111.66
Consumption grid fee (Ct/kWha)	0.41	0.50	0.65

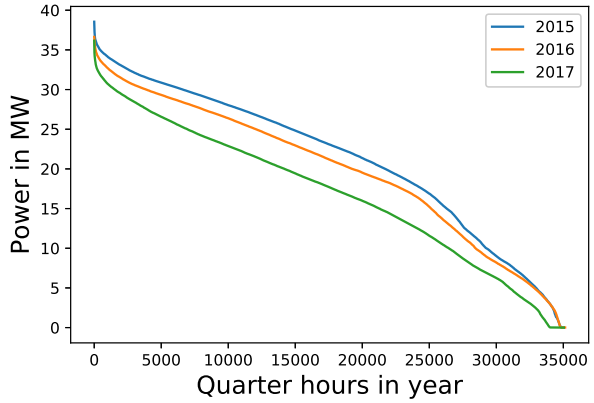

Figure 3.3: Load duration curves of the case study for the years 2015-17
Energy consumption per quarter-hour of a year is sorted in descending order.

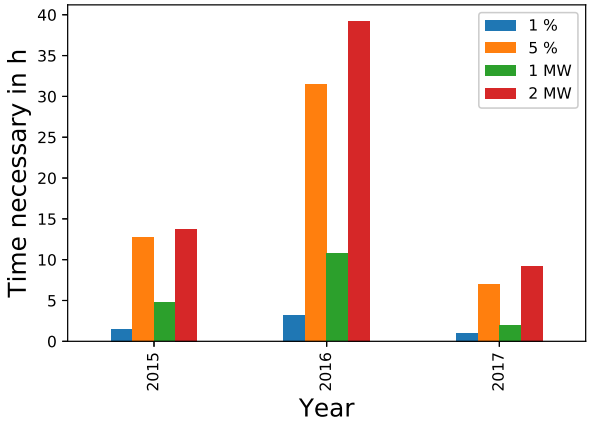

Figure 3.4: Hours necessary to reduce peak power to target value for years 2015-17
The bars display reduction by desired percentage of peak load or by an absolute value.

Once these problems have been correctly recognized, the flexibility of consumers can be employed; however, on the DSO-level rarely market structures exist that enable the DSO to utilize the flexibility of consumers. Several concepts for organized flexibility markets by DSOs [29] and the cooperation of these markets with other stakeholders exist.

One measure currently used to alleviate power violations on the DSO level is the cost structure of grid fees. Grid fees contain a peak grid fee, which penalizes the maximum power drawn from the grid within a month or year.

This section introduces the flexibility service *peak shaving* and shows its application and value with load data from the case study. The modeling of the flexibility service is explained in Equation 6.11.

3.4.1 Peak shaving

Peak shaving describes the flexibility, with which a peak consumption, such as the maximum power consumption from the grid, is actively reduced, thus avoiding additional charges and fees by grid operators. In Germany, DSOs generally bill annual capacity demand charges in EUR/kWa which account for the maximum power drawn from the grid within any 15-minute interval of the respective year. Additionally, they consider the individual voltage level and the specific consumption characteristics, the *full load hour*: In 2017, consumers at the high voltage level with fewer full load hours (< 2500h) pay 33.41 EUR/kWa, while consumers with a high number of full load hours (> 2500h) pay 111.66 EUR/kWa [54, 278]. For the case study, grid fees in 2017 amount to peak related grid fees of 36.2 MW · 111.66 EUR/MW = 4 Mio EUR and energy related grid fees of 36.2 MW · 4087.7 h · 0.65 Ct/kWh = 9.6 Mio EUR. Full load hours of the case study industrial site and the respective grid fees are visible in Table 3.2. 2015 shows the largest number of full load hours which means that this year had the "flattest" load profile. It is visible that the load profile of the case study industrial site generally fits the characteristic of full load hours > 2500 h.

Figure 3.3 displays the load duration curves for the target industrial site for the years 2015-2017. The load duration curve is a sorted list of the load profile. The load duration curves show that peak power levels only occurred for a small number of quarter hours per year.
Figure 3.4 analyzes the load profile curve of the single years by the hours necessary to produce a certain reduction potential in the maximum of the load profile. The reduction potential is either given in percent or in MW. It is visible that for a reduction by 2 MW only 10 hours of peak shaving would be necessary for the year 2017, while for the year 2016, the same peak shaving would require almost 40 hours. Nevertheless, the value of the peak shaving in 2017 would equal 223k EUR of reduction of grid fees, while in 2016, the remuneration would only lead to 172k EUR in energy cost reduction. In terms of time necessary for peak shaving, the load profiles of years 2017 and 2015 were more favorable to peak shaving than 2016.

3.4.2 Modeling approach of peak shaving in this work

The problem describing peak shaving by demand shifting can be generalized as a minimax problem as the maximum load is to be minimized [293].
To model this flexibility service, the procurement of power from the grid above the previous peak is penalized with the given peak grid fee. If the previous peak is exceeded, the new maximum of the load profile is set as a peak threshold.
This simplified modeling technique allows for a lean integration of the peak shaving problem into the unit commitment problem; however, shortcomings of this model exist. An initial peak threshold has to be defined prior to the first optimization. This might yield a non-optimal solution as a lower peak level might have been achievable or the initial peak level is set too low. This can cause unnecessary peak shaving. The mathematical model for the flexibility service peak shaving is given in Chapter 6.

3.5 Flexibility services for the transmission system operator

The TSO holds the responsibility for the continuation of grid services within its control area. This continuation can be disrupted by strong variations of frequency and voltage levels, as well as power levels that violate line or transformer ratings. In order to maintain stable grid operation, the structural changes to the German national energy system caused by the *Energiewende* lead to the necessity to compensate the gradual fade-out of conventional power plants which so far provide most frequency and voltage control.
This section introduces the flexibility service *frequency control*, which can be further divided into the products used for delivering frequency control that are modeled in this work - *frequency containment reserve (FCR)* and *automatic frequency restoration reserve (aFRR)*. Section 3.5.2 introduces FCR and Section 3.5.3 introduces aFRR. Both sections analyze technical requirements and market data of control reserve auctions for the years 2015-2017, explain market dynamics, and state how this price data has been adjusted to be used in this work.

3.5.1 Frequency control

The stable operation of the power supply system presupposes that the power balance of feeds, withdrawals, and losses in the overall system is balanced at all times with a tolerance of a few seconds as the electricity grid cannot function as energy storage. Therefore, it is crucial to measure and monitor the power balance of the electrical energy system and ensure that it is kept in equilibrium by suitable control systems.
These control systems must have access to controllable electricity generating or consuming devices in order to be able to influence the power balance in a targeted manner. From a technical point of view, the distance from the power equilibrium is expressed by the deviation of the grid frequency from its nominal set point of 50 Hz in the European synchronous area.

Forecasting errors of demand and supply, fluctuations of demand and supply within the minimum product duration of electricity markets, or the utilization of standard load profiles for certain customers, may lead to a deviation of the grid frequency from the nominal value.
TSOs utilize control reserves to limit and reduce these deviations. According to the European Transmission Network Code [103], they collectively employ three different reserve products that differ in activation times and ramp rates: primary, secondary and tertiary control reserve. Subsequent to control reserve, TSOs employ the use of interruptible loads, electricity trading activities, emergency capacity contracts with foreign TSOs, and manual load shedding in cooperation with DSOs [396, 401].
From frequencies lower than 49.8 Hz, emergency power reserves and storage pumps are activated. From frequencies lower than 49.0 Hz load shedding is started sequentially. At 47.5 Hz power plants are taken off the grid [129]. For frequencies higher than 50.2 all electrical generators, even if not prequalified as control reserves, are required to lower their generation [396]. Balancing service providers (BSPs) provide control reserve by changing their power consumption or generation.
Sections 3.5.2 to 3.5.4 provide a detailed analysis of the selected control reserve products and explain how these flexibility services are modeled in this work.

Mechanisms for frequency control

A distinction is made between positive and negative control energy. If the energy fed into the grid exceeds the energy withdrawn at the same time, there is excess power in the grid. In this case, the grid operator needs negative control energy, i.e. lower electricity generation or higher electricity consumption. If the demand for electricity is exceeding the actual generation, positive balancing energy is required. In this case, the grid operator needs additional energy to be fed into its grid or less energy to be consumed.
The ENTSO-E defines a system and operation handbook for national TSOs to follow. It defines the following control actions:

1. **Primary Control** has the aim to limit the frequency deviation and is activated within seconds in regard to the frequency deviation uniformly within all control areas of the European connected grid. The product procured for primary control by German TSOs is the frequency containment reserve (FCR).
2. **Secondary Control** replaces primary control and is activated automatically by individual TSOs. It has the aim of restoring the grid frequency to its nominal value. German TSOs procure automatic frequency restoration reserves (aFRR) for secondary control.
3. **Tertiary Control** initially complements and finally replaces the secondary control and is partially activated manually by individual TSOs. This is implemented as manual frequency restoration reserve (mFRR) in the German grid.
4. **Time control** corrects long-term time deviations of the synchronous area and is activated by all participating TSOs.

The control reserve products mainly differ with respect to their permissible activation time: It must be possible to fully activate the procured capacity within 30 seconds for FCR, 5 minutes for aFRR and 15 minutes for mFRR. Thus, these products possess different response and ramp-up times to counter disturbances in the grid frequency. While fast response through FCR contains the deviation from the nominal value, FRR helps in restoring the nominal frequency. In control theory, FCR is defined as proportional control and FRR as proportional-integral control [328]. Another essential difference is that FCR is continuously activated proportionally to the frequency deviation while aFRR and mFRR are activated on demand with their full capacity.
Furthermore, the TSOs implemented the tool of **interruptible loads** which they can use to even the system balance in case of a generation deficit. Interruptible loads can be used to complement or replace positive control reserve.

Interruptible loads are also used for congestion management. The use of this measure only occurs in case of exceptional frequency deviations [401, 402].
This work focuses on primary and secondary control or specifically FCR and aFRR as, from the viewpoint of an industrial site, these products are the most promising flexibility services in terms of expected revenues.

3.5.2 Frequency containment reserve

The actual demand for FCR is determined by the ENTSO-E, the European network of TSOs for electricity. As the European grid is a synchronous area, the provision of FCR is shared jointly by all the network operators belonging to the ENTSO-E. The total demand for FCR is determined by assuming a simultaneous failure of the two largest power plant units within the grid area. This corresponds to a total ENTSO-E reserve of $\pm$ 3 GW. The distribution to the grid operators involved is recalculated annually and is based on the proportion of electricity fed into the grid in the previous year. Currently, the demand for FCR of the German grid operators is 605 MW (as of August 2019).
The FCR provision is formed by individual electricity generators, consumers, and storage hereafter referred to as technical units. The technical units alter their power consumption or generation to contribute to a stable frequency. The activation of FCR is controlled solely by the mains of the grid frequency. If the frequency increases above the nominal value of 50 Hz, the electric power output of generating units is lowered or the power of consuming units is increased ("negative FCR") and vice versa for frequency values below 50 Hz ("positive FCR"). The frequency is measured at each individual technical unit with frequency meters to guarantee provision in case of a non-functionality of, for instance, communication systems. To ensure a fast stabilization of the grid frequency, FCR is thus deployed automatically and decentralized.

Market design and tender procedure

The provision of FCR is remunerated with a capacity price depending on the amount of power provided. A tender auction is organized by the responsible TSOs that procure the requested amount of FCR for a different product duration from BSPs. All possible BSPs place bids including the FCR power and the desired capacity price. BSPs are determined by the MOL of capacity prices and remunerated through marginal pricing or "pay-as-cleared" - the capacity price of the last position in the MOL is given to all BSPs.
Market design conditions of FCR and FRR auctions have undergone changes within the last years. Table 3.4 summarizes market conditions that were valid in the period 2015-2017 and Table 3.5 shows decided market conditions valid from July 2020. Due to the recent changes in market design, a methodology has been designed that fits available data of FCR prices in the period 2015-2017 to the current market design [104, 403].
BSPs are organizations that control at least one technical unit that has been successfully qualified to provide FCR by the responsible TSO. Due to the specification to place integer bids (in MW), technical units with a smaller prequalified FCR power can be combined to jointly form a bid. This combination is often done by VPPs as explained in 2.2.3.
Marketing for FCR takes place online on a common tender platform among TSOs of Germany, France, Austria, Switzerland, the Netherlands and Belgium as shown in Figure 3.5 including the German control areas and countries colored in dark green. The international cooperation allows for im- and export of FCR among the TSOs and therefore offers opportunities to lower the total expenditures for system operators.
The tender for FCR is done symmetrically, i.e., no separate tender for positive and negative FCR exists. Consequently, technical units generally have to be able to provide both positive and negative control reserves. Asymmetric provision of FCR is only possible if an adequate technical unit has been found that provides the contrary direction to jointly form a symmetric bid. This implies that participating power plants, for instance, cannot run at minimum or maximum power if they intend to provide FCR, as they have to be able to decrease and increase power generation.

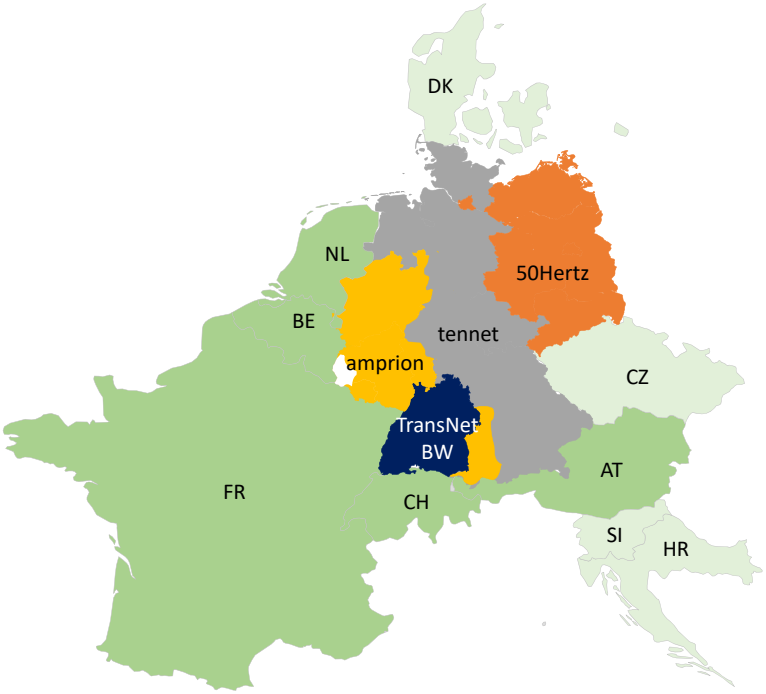

Figure 3.5: Map highlighting participating TSOs forming common FCR market or aFRR IGCC cooperation
Map displays German control areas (amprion, TransNetBW, tennet, and 50 Hz), countries that are involved in common FCR market and IGCC member operation states (darker green), and countries that are only IGCC member operation states (lighter green).

Still, thermal or hydroelectric power plants provide most FCR in Germany through the use of variable turbine speed governors [80, 395]; however, the decommissioning of conventional power plants results in market opportunities of new devices.

Technical specifications

FCR represents the fastest reacting balancing products to frequency deviations with a maximum idle time of 5 seconds and a maximum ramp-up time of 30 seconds. FCR is designed as proportional control: The FCR to be provided by each technical unit is calculated locally as a function of the frequency deviation from the nominal frequency or set point (50 Hz). Maximum FCR is provided at deviations of $+/-$ 200 mHz.
FCR control is done on the basis of seconds, i.e., the frequency meters measure the grid frequency every second and the corresponding FCR signal is calculated and communicated to the technical unit. This is referred to as the requested FCR ($P_t^{FCR\_request}$).
The FCR to be provided is calculated locally on the basis of the following equation as defined above:

$$\begin{aligned} P_t^{FCR\_request} &= P_t^{FCR} \cdot \frac{50 - \nu_t}{0.2} \\ P_t^{FCR\_request} &= \text{FCR power to be provided at time step } t, \\ P_t^{FCR} &= \text{FCR power bid at time step } t, \\ \nu_t &= \text{Grid frequency at time step } t. \end{aligned} \tag{3.1}$$

The technical unit can deliver FCR regardless of the voltage level; however, FCR ability has first to be prequalified by the connecting TSO of the control area. The prequalification is done based on rules stated in [399]. It includes standardized tests to test the response criteria of the FCR and in case of batteries the offered capacity or possible duration of activation. For special technologies, a documented technical concept is necessary.

Table 3.3: Key statistical indexes relevant for FCR provision
Mean (μ), respective FCR power (P^{FCR}) for $P_t^{FCR\_bid} = 1$ MW and standard deviation (s) of all grid frequency values (ν), values below 50 Hz (ν^+), and values above 50 Hz (ν^-).

	μ in Hz	P^{FCR} in MW	s
ν	49.9996	+0.0018	0.0206
ν^+	49.9840	+0.0801	0.0132
ν^-	50.0159	-0.0794	0.0132

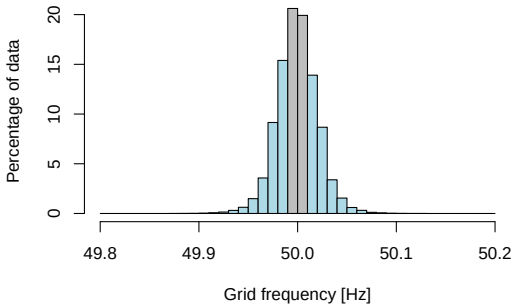

Figure 3.6: Histogram of grid frequency data over the period 2012-19
Data were taken from [379].

Figure 3.6 shows a histogram of the grid frequency over the years 2012-2016 as also published in [328]. It is visible that grid frequency is distributed symmetrically around the nominal grid frequency of 50 Hz. The area in gray depicts the so-called dead band ($+/-$ 10 mHz), which are grid frequency values that are not mandatory to fulfill for providers of FCR. Table 3.3 shows the mean (μ) and the standard deviation (s) of grid frequency values, and the resulting FCR power of a 1 MW FCR power bid. The lines ν^+ and ν^- display the frequency values relevant for the sole provision of either asymmetric positive FCR or negative FCR and can, therefore, be used as the expected call rate for positive ($p^{FCRPos} = 0.0806$) and negative ($p^{FCRNeg} = 0.0795$) FCR calls.

3.5.3 Automatic frequency restoration reserve

In the event of a greater disruption of the grid frequency, the total amount of FCR is not sufficient to re-establish the set point of 50 Hz and a frequency deviation remains. It is the task of the frequency restoration reserve to restore the nominal grid frequency. Furthermore, unlike the FCR, which is exclusively frequency-controlled, FRR takes into account imbalances among balancing groups of a control area. Each TSO operates a proportional-integral (PI) frequency controller, which automatically activates the necessary amount of aFRR and mFRR. The frequency controller takes into account power flows to/from neighboring control areas (the balance of the control area) and the grid frequency.
To not counteract FRR of other TSOs, European TSOs have established an imbalance netting process. This process has been extended to all operating member states of the International Grid Control Cooperation (IGCC). Figure 3.5 shows all operational member states of the IGCC. Imbalance netting is the process that allows avoiding the simultaneous activation of aFRR in opposite directions. As a result of the imbalance netting, the area control error (ACE) is sent to each individual TSO. Upon the ACE each TSO calls up individual BSPs.

Market design and tender procedure

aFRR products include next to a capacity price (υ) an energy price (τ). As indicated in Table 3.4 and 3.5, these two prices serve different purposes. Based on the merit order of capacity prices, bids are accepted, i.e., the appropriate technical units have to reserve capacity. The merit order of energy prices, on the other hand, determines the activation order of technical units.
TSOs procure FRR as positive reserves and negative reserves from BSPs in individual auctions. These products are currently procured on a daily basis through auctions for six products of a duration of 4h for the following day. As shown in Table 3.4 aFRR was previously procured for weeks with additional separation into HT (German: *Haupt-tarifzeit*) - time between 08:00h and 20:00h from Monday through to Friday - and NT (German: *Nebentarifzeit*) -

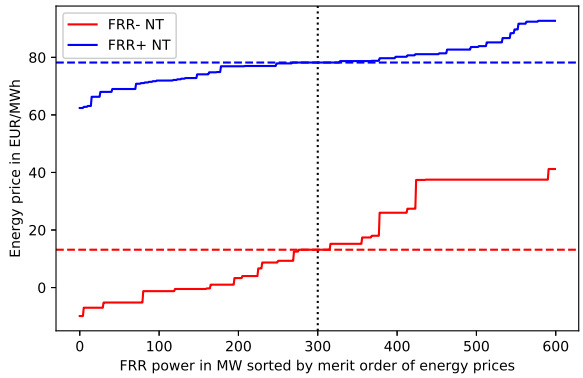

Figure 3.7: aFRR Merit Order List of calendar week 2 in 2015
Positive (blue line) and negative (red line) aFRR merit order list displayed for Nebentarifzeit(NT). Red and blue dashed lines show energy price at 300 MW position (black dotted line). Data were taken from [398].

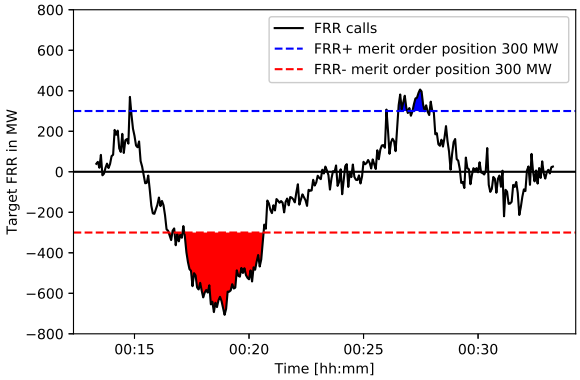

Figure 3.8: aFRR calls for an exemplary period
aFRR calls (black line) are displayed for a 30-minute period on Jan. 5th 2015. Red and blue dashed lines show aFRR calls for MOL position 300 MW. Shaded areas display periods of aFRR calls. Data were taken from [379].

time between 00:00h and 08:00, between 20:00h and 24:00h from Monday through to Friday, as well as all day on Saturday, Sunday and public holidays applicable to all of Germany.
Reserves are remunerated, on the one hand, for the provision of FRR by the capacity price (in EUR/MW), and, on the other hand, for the activated energy by the energy price (in EUR/MWh). The power demand (MW) for each product is allocated among reserves using the MOL of capacity prices. Activation, however, is done upon the merit order of energy prices. The demand for each FRR product is recalculated every quarter year by the TSO based on historic values in the past year; however, this procedure is currently under discussion [82] as occasionally these demands are adjusted based on special events such as high frequency deviations [401].
Remuneration of capacity prices is done pay-as-bid. Contrary to marginal pricing, this can lead to different bidding behavior, e.g., bidders try to guess the price of the marginally accepted offer to bid as closely as possible while controlling the risk of overbidding [207].
The remuneration scheme of aFRR offers the possibility for different types of bidding strategies. These include, e.g., a defensive strategy, which focuses on gaining revenues through capacity prices and rare but high-profit reserve calls. These participants try to place their bids towards the end of the MOL of energy prices [250].

Technical specifications

In case of a demand for FRR given by the ACE, the TSOs call the technical units according to the energy price merit order - the lowest energy prices are called first, the most expensive technical units activated last. This procedure is shown in Figures 3.7 and 3.8: Figure 3.7 shows an excerpt from the merit order list of positive and negative aFRR for the NT product of an exemplary week between 2015 and 2017. Figure 3.8 displays actual FRR calls that are sent with a frequency of four seconds of an exemplary week. As an example for both MOLs, the position of 300 MW is marked in each MOL. This correlates with an energy price of 16 EUR/MWh for negative aFRR and 79 EUR/MWh for positive aFRR in the y-axis of Figure 3.7. These individual bids were called once the FRR calls exceeded the capacity of 300 MW. The respective time of activation in the exemplary week of these technical units is shown in Figure 3.8 by the colored areas.

3.5.4 Modeling approach of FCR and aFRR provision

In this work, the provision of FCR and aFRR by individual technical units is modeled. Based on tests and actual prequalifications with energy devices, the prequalified power is known.

This work covers the following steps to model the commercialization of available flexibility as FCR and aFRR:

1. The remuneration of FCR and aFRR provision by capacity prices:
   As explained above FCR is remunerated by a capacity price; however, due to changes in market conditions, a methodology has been developed to adjust the available data on power prices for the year 2015-2017 to the current market design. This is explained below.
2. The remuneration of aFRR provision by energy prices:
   Next to the capacity price, aFRR bidding requires the provision of the energy price. Energy prices is remunerated for the activated energy of the energy device. This offers a second source of income for aFRR BSPs. The interaction and the correct selection of the energy price are discussed in Section 3.5.4.
3. The special case of FCR provision with a BSS:
   FCR can be provided by a variety of electricity generators and consumers that fulfill the above-mentioned criteria. Batteries possess fast response characteristics that make them extremely useful for the flexibility service FCR; however, limited capacities lead to the inability to provide symmetric FCR if the battery is completely discharged or charged. Therefore, TSOs have implemented a special regulatory framework to deal with FCR providers of limited capacities. The provision of FCR with a BSS is discussed in detail and simulated in Section 5.1.
4. The mathematical model of FCR and aFRR provision within a scheduling problem:
   The mathematical description for the provision of FCR and aFRR by individual energy devices and the power balance are given in Section 6.3.3.
5. The different possibilities of aggregation to deliver FCR and aFRR:
   As depicted in Table 3.5, the market design requires FCR BSPs to place symmetric FCR bids over a product duration of 4 hours and integer values of FCR bids. The same conditions applies to aFRR with the exception that aFRR allows asymmetric bidding. Especially with small-scale devices these temporal and size-wise bid requirements cannot be satisfied by the flexibility offer of an individual device at all times. Section 6.8 explains the possible scenarios of aggregation levels of flexibility offers and provides the mathematical model for each scenario.

Table 3.4: Conditions for reserve control products FCR and FRR over the period of 2015-17

	FCR	**aFRR**
Activation time	30 seconds	5 minutes
Participating TSOs	DE, FR, AT, CH, NL, BE	DE, AT
Tendered balancing power	1384 MW	+1882 MW/-1760 MW
Tender frequency	weekly	weekly
Tender gate closure	D-5[3], 3 p.m.	D-5, 4 p.m.
Product duration	1 week	1 week (divided in HT/NT)
Minimum bid size	1 MW	5 MW
Minimum bid increment	1 MW	

[3] The offset refers to the time interval between gate closure and first day of actual provision. D-5 means that gate closure occurs five days before provision.

Product symmetry	Symmetric bids	Asymmetric bids
Acceptance of bids	Merit order of capacity price	
Reserve activation	Mutual activation	Merit order of energy price
Remuneration	Capacity price in $\frac{EUR}{MW}$	Capacity in $\frac{EUR}{MW}$ and energy price in $\frac{EUR}{MWh}$
Remuneration method	Pay-as-bid	Pay-as-bid

Table 3.5: Conditions for reserve control products FCR and FRR valid from July 2020

	FCR	**aFRR**
Activation time	30 seconds	5 minutes
Participating TSOs	DE, FR, AT, CH, NL, BE	DE, AT
Tendered balancing power	1384 MW	~ +1882 MW/-1760 MW [4]
Tender frequency	1 day	
Tender gate closure	D-1, 8 a.m.	D-1, 9 a.m.
Product duration	4 hours	
Minimum bid size	1 MW	
Minimum bid increment	1 MW	
Product symmetry	Symmetric bids	Asymmetric bids
Acceptance of bids	Merit order of capacity price	
Reserve activation	Mutual activation	Merit order of energy price
Remuneration	Capacity price in $\frac{EUR}{MW}$	Capacity in $\frac{EUR}{MW}$ and energy price in $\frac{EUR}{MWh}$
Remuneration method	Pay-as-cleared	Pay-as-bid

Analysis of market development of FCR and aFRR products

FCR

Figure 3.9 depicts the auction results for FCR capacity prices in the analyzed period between 2015-2017. The black line shows the capacity weighted average capacity price of accepted bids of each week's auction, i.e., the bid's capacity prices are weighted according to the offered power. The blue dashed line represents the last accepted bid of the MOL of capacity prices, i.e., the marginal price. The shaded area depicts the difference between the minimum and the maximum accepted FCR bid.

It is visible that market forces have led to strong variations in the FCR prices with occasional peaks, but in general, a downward trend is visible. Seasonal plots show that capacity prices tend to increase towards summer, decrease throughout autumn and peak at year-end [285]. Both observations suggest that the FCR capacity price time series is a non-stationary process.

[4] Dynamic dimensioning per 4h product from December 2019 [397].

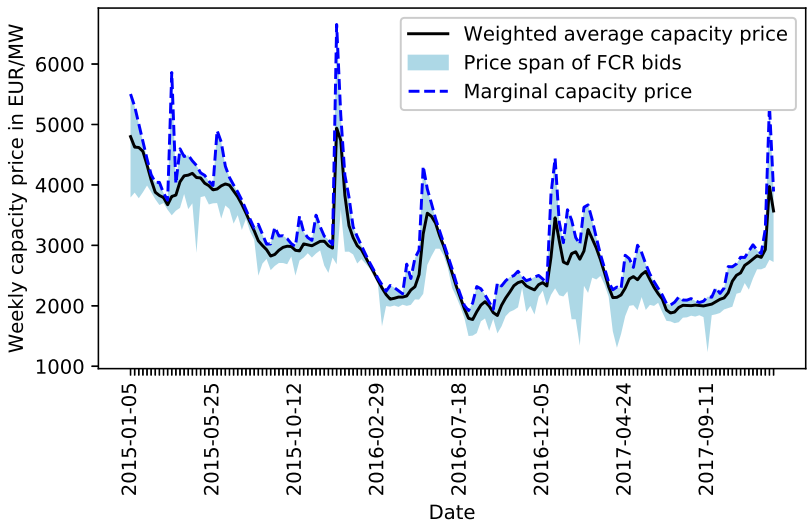

Figure 3.9: Auction results of capacity prices of FCR for the period of 2015-17
Black line displays average capacity price, blue shaded area displays the range between lowest and marginal capacity price shown as light blue dashed line. Remuneration method was pay-as-bid during the analyzed period. Data were taken from [398] and extracted using [410].

Kraft et al. [230] create forecasting models for FCR capacity prices. To develop the forecasting model, different exogenous variables were selected representing opportunity costs for reserve provision and scarcity in the market. In a regression analysis, the authors find that the exogenous factors with most explanation power for the FCR capacity price market development were identified as the price range of the previous tender and the planned unavailable capacity in Germany and France. This points to the influence of the supply side on the power prices and indicates a high price elasticity of supply and bidding behavior that is strongly guided by the previous auction results.

aFRR

Figures 3.10 to 3.14 show capacity weighted capacity prices, for all four aFRR products as black lines and the median of energy prices as a red line of weekly auction results.

It is visible that for all products capacity prices tend to decrease with occasional price spikes mainly correlated with weeks that include public holidays, e.g., at the end of the year. As there are hardly any changes in demand for control reserve, the price mechanisms are mostly supply-driven. Negative aFRR shows lower capacity prices than positive aFRR indicating that an abundance of negative reserves exists in the market. NT products are higher priced than HT products. This can be explained with fewer power plants available to deliver the aFRR as the demand is comparably low during NT periods.

The median of energy prices can be described as a time series with occasional peaks but no apparent trend. The overall level of the time series does not vary greatly among the four products; only negative aFRR NT has a slightly higher average level.

Figure 3.12 shows the development of the capacity weighted mean of the energy price. It is visible that an increase in the mean happened towards the year 2017 across all FRR products. No such development has been visible for the median as depicted in Figures 3.10 to 3.14. This leads to the conclusion that a share of market participants have increased their bids for energy prices or newly entered the market with high bids for energy prices. Box plots of energy prices of all four aFRR products for each year are displayed in Figure 3.15. It is visible that the upper end of the box has increased for every year for almost all products meaning that the 75% quantile has risen. Lösch [250]

explain this phenomenon with an increasing number of market participants that follow a defensive strategy of low call probability at the end of the energy price merit order.
As the remuneration method for both FCR and aFRR auctions was pay-as-bid in the period 2015-2017 (see Table 3.4), the weighted capacity price is used for capacity-related remuneration of flexibility offered by the industrial site. A different remuneration method, as has been implemented for FCR in July 2019 (pay-as-cleared or marginal pricing), would have led to different bidding behavior and is therefore not be considered for the given data.

Methodology for modeling FCR and aFRR capacity price remuneration

The data used in this work are FCR and aFRR prices from the period of 2015 to 2017 [398, 410]. In this period, product duration for FCR and aFRR prices was one week. Market clearing during this period for FCR worked with the merit order of capacity prices, and remuneration through the pay-as-bid method (see Table 3.4).
As visible in Table 3.5 the product duration of FCR and aFRR has decreased to 4h by 2020. Furthermore, this thesis assumes that different supply and demand of control reserve lead to significant price differences for 4h slots with in a week. In order to reflect this change, weekly FCR and aFRR capacity prices were adjusted to 4h intervals by multiplying FCR and aFRR results with a factor for each weekly 4h time slot as explained below.
As currently no auction data for 4h slots is available for FCR, these factors were calculated from aFRR auction results. 4h slots were implemented for aFRR in July 2018. Auction data was used from this date until December 2019. The number of weeks of auction data is represented by set K. The set L forms the set of all 4h slots of a week with a cardinality of 42. The following methodology was employed to calculate the 4h product factors:

1. Calculation of mean aFRR capacity price for each 4h-product of a week, $l \in L$, over all weeks $k \in K$.
2. Calculation of total mean capacity price over all 4h products of a week, $l \in L$, of all weeks $k \in K$.
3. Calculation of the individual factors f_l^{aFRR} by the division of 1. and 2. for each 4h-product of a week l of each aFRR direction.

$$f_l^{aFRR^-} = \frac{\frac{\sum_{k\in K}(\upsilon_{k,l}^{aFRR^-})}{|K|}}{\frac{\sum_{l\in L}\sum_{k\in K}(\upsilon_{k,l}^{aFRR^-})}{|K|\cdot|L|}}, \forall k \in K \tag{3.2a}$$

$$f_l^{aFRR^+} = \frac{\frac{\sum_{k\in K}(\upsilon_{k,l}^{aFRR^+})}{|K|}}{\frac{\sum_{l\in L}\sum_{k\in K}(\upsilon_{k,l}^{aFRR^+})}{|K|\cdot|L|}}, \forall k \in K \tag{3.2b}$$

4. Calculation of individual factors f_l^{FCR} for each 4h-product of a week, $l \in L$, for symmetric FCR by the mean of positive and negative aFRR 4h product factor.

$$f_l^{FCR} = \frac{f_l^{aFRR^-}}{2} + \frac{f_l^{aFRR^+}}{2} \tag{3.3}$$

The individual factors for the 4h slots can be seen in Figure 3.16. A factor of 2 shows that the average capacity price of this 4h-product is 2 times as expensive as the average capacity price of all 4h-products.
It is visible that capacity prices are highest on Sundays, especially in the afternoon (highest mean). This is mainly due to the high prices for negative FRR which also peaks during products for night hours (0h-4h), so in times of rather low electricity demand. Positive FRR is especially expensive during weekdays in morning (8h-12h) and afternoon (16h-20h) slots, so during peak electricity demand hours.
This could be due to the fact that during low demand fewer power plants are online or operate at high loads that could provide negative control reserve. Due to low electricity demand, the residual load that is covered by

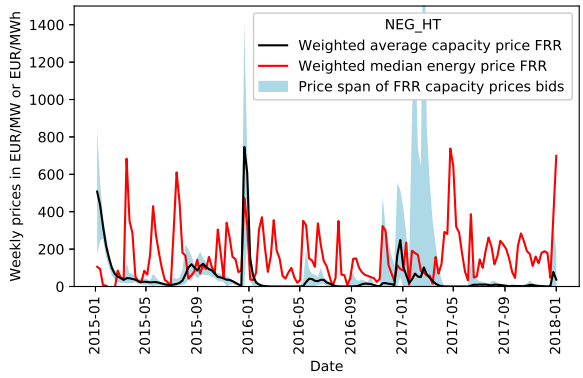

Figure 3.10: Auction results of negative HT aFRR for the period of 2015-17
Mean capacity prices (black line), capacity price range (blue shaded area) and median energy prices (red line) are displayed.

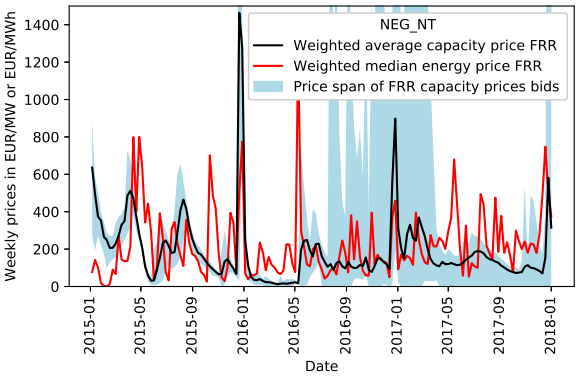

Figure 3.13: Auction results of negative NT aFRR for the period of 2015-17
Mean capacity prices (black line), capacity price range (blue shaded area) and median energy prices (red line) are displayed.

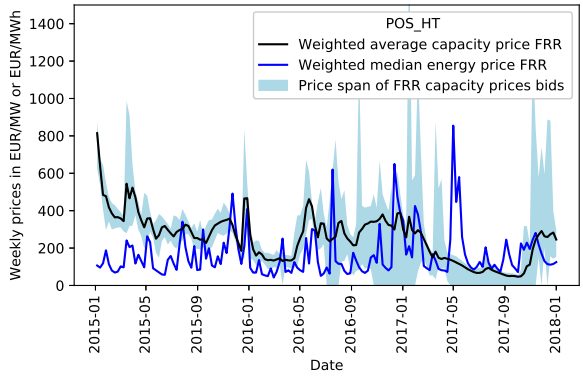

Figure 3.11: Auction results of positive HT aFRR for the period of 2015-17
Mean capacity prices (black line), capacity price range (blue shaded area) and median energy prices (blue line) are displayed.

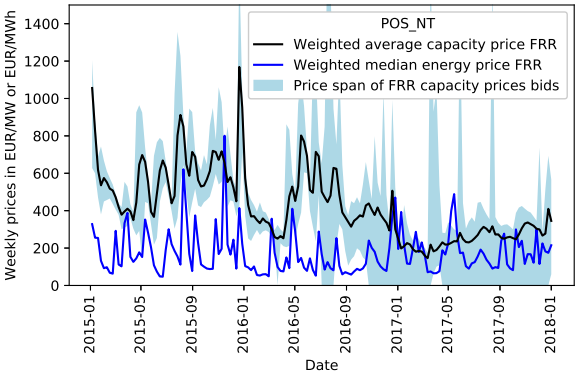

Figure 3.14: Auction results of positive NT aFRR for the period of 2015-17
Mean capacity prices (black line), capacity price range (blue shaded area) and median energy prices (blue line) are displayed.

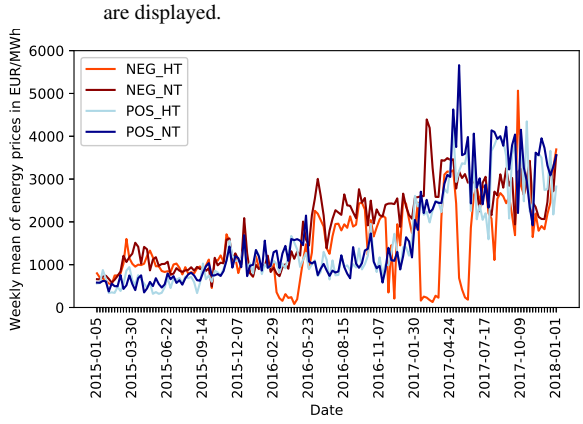

Figure 3.12: Auction results of mean energy prices of aFRR products for the period of 2015-17
The line NEG_HT displays mean energy prices for the product "negative aFRR HT".

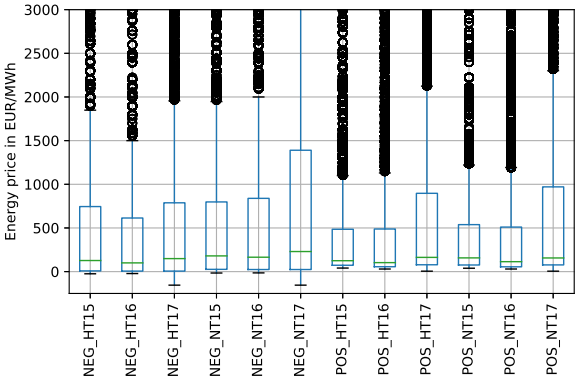

Figure 3.15: Box plot of energy prices for aFRR products for each year in the period of 2015-17
The box plot NEG_HT15 displays data for the product "negative aFRR HT" for the year 2015.

conventional power plants is low during these hours. On Sundays especially, electricity generation by renewable energies at times leads to a negative residual load, which consequently prompts a high demand for negative FRR. High electricity demand, on the other side, leads to high residual loads and many power plants operating at higher load. Furthermore, electricity prices, which are direct opportunity costs for power plant operators [208], are higher during these hours. Thus, it is understandable that prices for positive FRR are higher during these times (see Figure 3.2).

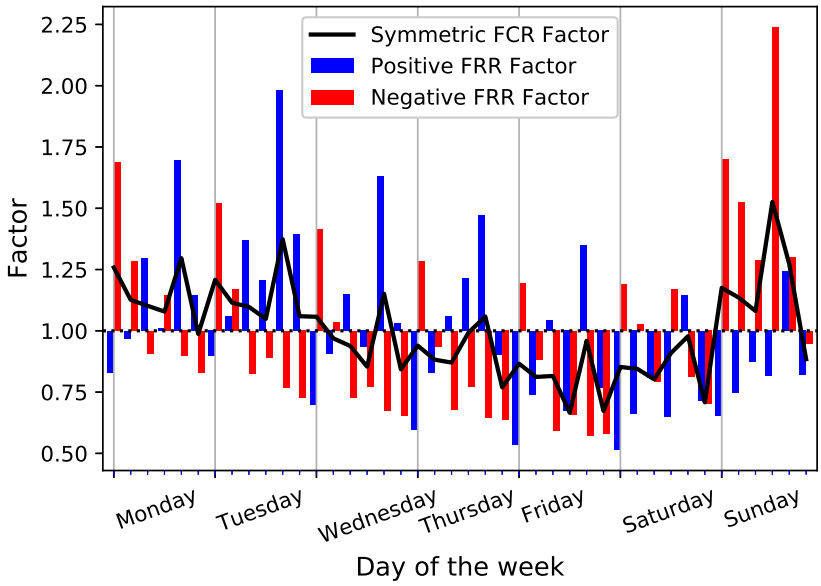

Figure 3.16: Results of factor calculation for resampling weekly capacity prices to 4h capacity prices
aFRR factors displayed as blue and red bars and FCR factor displayed through the black line. Bars pointing up indicate higher than average capacity prices while bars pointing down indicate lower than average capacity prices. The black line shows the average of the bar values for the indicated 4h slot. Data was taken from aFRR auction results of 4h-products from 07/18 to 12/19.

To resample aFRR and FCR prices, weekly capacity prices of week k in the period 2015-2017 were multiplied by the calculated 4h-product factors as indicated in Equation 3.4. To cope with HT and NT values for aFRR products, a weighted average depending on the duration of HT (duration = 60 hours per week) and NT (duration = 108 hours per week) price data was taken. The resulting 4h-aFRR and -FCR capacity prices were used in the model defined in Chapter 6. For a time step t that is part of week k and 4h-product l the following is valid:

$$\upsilon_t^{aFRR^+} = f_l^{aFRR^+} \cdot \upsilon_k^{FCR} \tag{3.4a}$$

$$\upsilon_t^{aFRR^-} = f_l^{aFRR^-} \cdot \upsilon_k^{FCR} \tag{3.4b}$$

$$\upsilon_t^{FCR} = f_l^{FCR} \cdot \upsilon_k^{FCR} \tag{3.4c}$$

The scheduling model in Chapter 6 employs the individual capacity prices per time step t. For the employed simulation a time step of 15 minutes has been chosen requiring the data to be resampled. The FCR capacity prices, for instance, are referred to as υ_t^{FCR} in the following. The prices originate from weekly auction prices multiplied with a 4h factor and further resampled to a time interval of 15 minutes.

Methodology for modeling aFRR energy price remuneration

A provider of aFRR can gain profits from the capacity price (υ_t^{aFRR}) as well as from the energy price (τ_t^{aFRR}), which is paid for the time of activation or call duration (T_t^{ACT}) during the time step t. This work further assumes that the actual activation of the providing technical unit incurs activation costs γ_t. These activation costs arise, for instance, from additional fuel costs for increasing power output for positive aFRR. Consequently, the total revenues for aFRR can be summarized in Equation 3.5.

$$r_t^{aFRR} = P_t^{aFRR}\upsilon_t^{aFRR} + P_t^{aFRR} \cdot T_t^{ACT} \cdot (\tau_t^{aFRR} - \gamma_t) \tag{3.5}$$

As the activation of reserves follows the energy price MOL, the following trade-off in optimizing an aFRR energy price bid can be recognized:

1. A higher energy price (τ_t^{aFRR}) increases the revenue per time step; however, results in a shorter activation time (T_t^{ACT}), which decreases the revenue.
2. A lower energy price (τ_t^{aFRR}) decreases the revenue per time step, however, results in a higher activation time (T_t^{ACT}), which increases the revenue.

Furthermore, for the correct selection of the τ_t^{aFRR} to optimize aFRR revenues one has to account for the costs of activation γ_t of the individual device. An energy price τ_t^{aFRR} below the actual cost of activation γ_t would cause losses for the operator for every aFRR call. To fully optimize the revenues from aFRR provision the operator would also have to forecast the activation time T_{ACT}. This is not an easy task, as the activation time depends on the position in the MOL and the state of the grid, i.e., the development of the grid frequency and imbalances of balancing groups.
Therefore, Lösch et al. [251] perform an analysis of historic aFRR auction and activation data to map energy price bids with the activation time. In that ex-post simulation, the authors quantify the share of aFRR bid activation given different energy prices and derive the profit potential for aFRR providers. Similar to [251] the analysis of this work consists of the following steps:

1. Gather aFRR call data from [379],
2. gather aFRR auction data from [398],
3. match aFRR call and auction data to calculate the call duration per auction bid, and
4. perform a long-term analysis to calculate call probability and revenue per energy price bid over the period 2015-2017. Yearly differences in the probability as in [250] were not taken into account.

While Lösch et al. [251] combine 4-second call data to 1-minute call data, this analysis stays with 4-second call data. This increases computation time but may lead to an increase in accuracy in the calculation of the call duration. The results of this analysis are shown in Figure 3.17. It was performed on auction and call data of the period 2015-2017. The resulting curves for all four available products ((NEG,POS)x(HT, NT)) are shown as dashed lines. A weighted average of the NT and HT curves was drawn to achieve one relation between energy price and call probability for each control reserve direction. These are shown in the solid lines.
The figure shows that a positive aFRR bid with an exemplary energy price of 50 EUR/MWh would have been activated 37% of the time, whereas a negative reserve bid with the same price would have been activated only 5% of the time. It is visible that around 56% of the time positive aFRR is called and negative aFRR is called almost all of the remaining 44% of the time. This is due to the fact that almost constantly a certain amount of either positive or negative aFRR is called.
Furthermore, it can be seen that negative aFRR is called with much lower energy prices than positive aFRR. Actually, the cheapest energy price bids are negative, i.e., the TSO receives money from the BSP. This is due to the fact

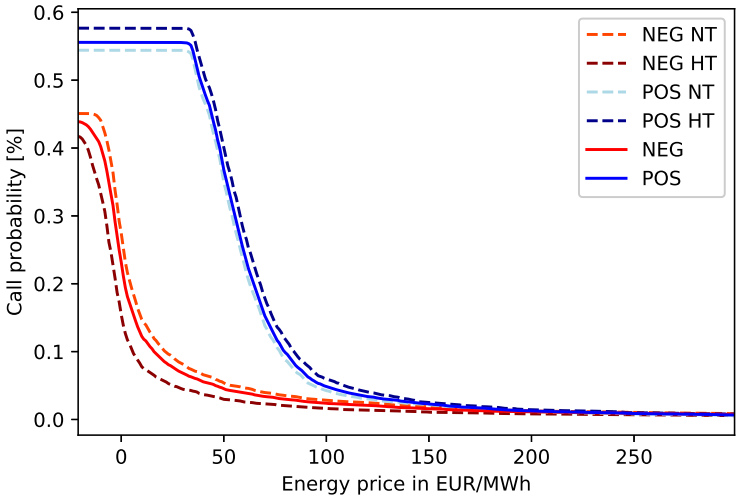

Figure 3.17: Results of modeling of aFRR energy price remuneration.
Call probability for aFRR bids (y-axis) depending on the energy price (x-axis) for four different aFRR products. NEG and POS products display the weighted average of HT and NT data. Data derived from FRR auction and call data for the years 2015-17.

that the majority of aFRR is still provided by conventional power plants, and negative reserve control corresponds to ramping down their generation which results in the avoidance of fuel costs. The curve for positive reserve does not contain any negative reserve prices as power plants providing positive reserve have to pay additional fuel costs to increase their power output [251].
In the dispatch model presented in Chapter 6, the resulting relationship between call probability and energy prices is used to determine the expected activation time and the expected revenues from aFRR provision of devices. The revenues are dependent upon a product of the energy price and the call probability; however, the call probability is again a function of the energy price as indicated in Equation 3.5. This results in a non-linear relationship.
The brute-force method is used to estimate an ideal energy price for each device: Depending on the activation cost γ_t, device specific aFRR call-related profits are calculated for a range of energy price and call probability combinations. The combination that leads to the maximum profit is selected. If necessary, a desired call probability is accounted for. This is explained in detail in Section 6.3.3.

3.6 Flexibility services for the balance responsible party

This section introduces the flexibility service *energy market optimization* (EMO), which profits from market transactions on electricity markets. The trading on electricity markets is generally done by the BRP. The BRP utilizes the flexibility of devices to gain profits on electricity markets. BRPs are responsible for matching the electricity generation and consumption with respective transactions to balance their balancing group. BRPs can further utilize the flexibility of the involved devices to minimize costs for their costumers on the energy markets.
In addition, one can see increasing trading activities on short-term energy markets, as a greater share of electricity is generated from intermittent RES such as wind or solar. Power companies and grid operators heavily rely on forecasts to know how much power is available by these sources and to correctly plan the dispatch of residual power sources. The quality of these forecasts increases in quality closer to the time of delivery. Consequently, the planning becomes more short-term and, hence, it becomes more profitable for BRPs owning flexible devices to participate in short-term power markets such as the German Intraday Continuous Market of the European Power Exchange (EPEX).

For the electrical energy system, the liquidity of electricity markets is of high importance. Offering flexibility on electricity markets, leads to less unbalanced balancing group and a more balanced electricity system. Consequently, the need for control reserve should decrease.
As this work implements a day-ahead optimization, the flexibility service EMO represents the potential for profits on the spot electricity markets that start a day before the actual delivery.

3.6.1 Energy market optimization

EMO realizes monetary profits using the flexibility of devices to benefit from price differences in electricity markets. The technology BSS is especially suited for trading activities, as it has no fixed fuel costs; instead, the costs of electricity at the time of discharge depend only on the costs of electricity at the time of charge.
In a simple two-period case, the battery represents a so-called spread option, i.e., the battery is used when the price gap between the periods is large enough to achieve a positive contribution margin despite efficiency losses.
The trading on continuous markets such as the Intraday continuous market offers the possibility to adjust the planned schedule of the energy device by continuously buying and selling electricity according to the restrictions defined by the model of the device.

3.6.2 Modeling approach of energy market optimization

This work analyzes the trading behavior on the Intraday continuous market and investigates the potential for two types of models of flexibility for the years 2015-2017. It performs a daily valuation of a BSS as an intraday option considering liquidity effects.
The methodology and results of this analysis are shown in Section 5.2. The results are then used in the scheduling optimization in Section 6.3.5. The utilization of the BSS at the case study industrial site for intraday trading on the continuous intraday market is modeled there.

3.7 Summary

This chapter introduces and describes the term *flexibility*. Possible services that can be provided with this electrical flexibility to stakeholders along the supply chain of the product electricity were introduced.Table 3.6 summarizes the analyzed flexibility services in this chapter. The colored flexibility services were selected to be modeled for the case study of the industrial site in Chapter 6 as they fit predefined criteria. Through the described methodology, the author answers research question 1.1.
These flexibility services were analyzed in detail in this chapter and partly combined into the following five flexibility services whose potential for lowering the energy costs is assessed by the optimization later in this work:

1. Frequency containment reserve (FCR) - load shaping to limit deviations of the grid frequency.
2. Automatic frequency restoration reserve (aFRR) - load shaping to restore the grid frequency.
3. Local peak optimization (LPO) - peak shaving or peak shifting to lower the maximum power consumption.
4. Energy market optimization (EMO) - continuous load shaping to maximize profits on the energy markets.
5. Local energy optimization (LEO) - load shaping, load shifting, and valley filling to reduce electricity procurement and commercialization costs.

The chapter described the modeling process for each flexibility service throughout Sections 3.3 - 3.6, thereby answering research question 1.2. The detailed mathematical model used in the developed scheduling model in Chapter 6 is introduced in Section 6.3.

Table 3.6: Selection of flexibility services to be modeled in the dispatch optimization of an industrial site

			Source of remuneration in the electricity supply chain						
			Generation	Trading	Transmission	Distribution	Retail	DER	Consumption
			Conventional PP	BRP	TSO	DSO	Supplier	Intermittent RES or BSS, etc.	Prosumer
Source of economic value	**Power quality**	Frequency			**FCR** **aFRR** mFRR				
		Voltage			Voltage control			RES smoothing	End-consumer power quality
	Power reliability	Operational planning			Redispatch & reserve				
		System restoration	Emergency power and islanding		Black start				Emergency power and islanding
	Portfolio or cost optimization	Bilateral Agreement or single price		BG self-balancing		**Peak shaving**		FCR charge balancing for BSSs	
		Market dynamics		**Energy market optimization**			**Real-time price optimization**	**RES buffering**	
	Hybrid use cases for enhanced utilization of existing assets	Fulfill legal specifications	Synthetic control reserve					RES firming	**Local self-balancing**
		Other	Improved load following			Load buffering			Increase in self-sufficiency
			External flexibility services in front of the meter ←				→ Local flexibility services behind the meter		

4 Related Work on Modeling and Optimization of Energy Systems

This chapter provides related work with respect to the research questions of this thesis. Section 4.1 describes related work that includes the scheduling of devices according to the objective of the dispatch problem and/or the aggregator problem. The identified literature is clustered according to the model class (Section 4.1.1). As a results of the revision of publications including different model class formulation, Section 4.1.2 selects the fitting model class to apply for the optimization problem described in Chapter 6. Furthermore, the applied objective functions (Section 4.1.3), works that include multi-objective optimization (Section 4.1.4), and publications that specifically show examples of multi-use dispatch models (Section 4.1.5) are described.
Section 4.2 describes modeling techniques of devices of energy technologies that have been introduced in Section 2.4. The literature review focuses on modeling approaches in MILP formulations of the dispatch or the aggregator problem. Furthermore, the use of these devices for the provision of flexibility services introduced in Table 3.1 is reviewed. The energy technologies include CHP plants (Section 4.2.1), BSSs (Section 4.2.2), EVs (Section 4.2.3), and controllable demand side power consumers (Section 4.2.4).
Particularly noteworthy is Section 4.2.2, which provides related work for the use case of a battery storage system providing frequency containment reserve. This literature review is done for the simulation of a BSS providing FCR in Section 5.1.

4.1 Device scheduling problem in energy systems

Scheduling problems in energy cells can be differentiated, for instance, by their model complexity or their objective function. The technical and contractual boundary conditions can be modeled in optimization problems of varying model classes. Section 4.1.1 gives an overview of applied problem class of scheduling problems found in literature. Based on the examples provided in this summary of related work, the adequate model class for the developed optimization problem in this work is selected subsequently in Section 4.1.2.
Concerning the objective function, most approaches follow the objective of cost minimization, other goals are also considered such as minimizing the environmental impact or increasing power quality and reliability [135]. Examples for different objective functions in scheduling problems of microgrids are given in Section 4.1.3.
Device deployment planning in energy systems is an essential energy management tool for the cost-effective provision of energy (the dispatch problem). The commercialization of flexibility provided by these plants as, for instance, ancillary services, can further increase the cost-effectiveness (the aggregator problem). Due to the fact that a combination of these problems can result in a multi-objective optimization problem (see Section 2.5.4), Section 4.1.4 provides related work concerning works that employ multi-objective optimization.
Furthermore, this work focuses on the use of the flexibility provided by DERs to provide multiple flexibility services as introduced in Chapter 3. The ability of an energy device to be used for different purposes is often referred to as a "multi-use" device. Section 4.1.5 gives examples of works that look into revenue streams provided by various flexibility services.

4.1.1 Optimization problem class

In the following, examples of works that implemented either LP, MILP, or MINLP models of scheduling problems are given. The applied optimization problem and the modeled devices are described briefly. Furthermore, the adequacy of the different model classes is discussed shortly.
Based on the knowledge of the authors, the earliest work to solve the economic dispatch problem goes back to Baldwin et al. [21]. The authors solved an economic dispatch problem for a group of turbines and boilers with hourly loads given for the metropolitan area of New York. The model includes start-up costs, non-linear fuel consumption, minimum down time and penalties for operating outside of the permissible pressure values of the technical units.

LP

LP formulations are rather rare, as the level of detail that can be modeled is comparably low. LP formulations are, consequently, employed for optimization problems that can be modeled through linear equations. According to [376], LPs are often applied simplified models of large-scale grid studies, such as a national energy system. In the following, a brief summary of LP applications for examples of scheduling devices within a microgrid is given.
Examples of LP formulations of the dispatch problem include Quiggin et al. [321], who modeled the dispatch of a mix of renewable generation technologies, energy storage and flexible demand in a linear program. The problem was solved using the simplex algorithm with a convergence criterion.
Majió [257] describes a dispatch of a CHP unit in two different LP models implemented in GAMS. The microgrid proposed in the first model consists of thermal and electrical loads and a CHP unit. The second model consists of the units considered in the first model with the addition of thermal and electrical storage. No information was provided on the solution algorithm employed.
Hawkes and Leach [172] provide an LP to model energy cost minimization of a microgrid including a set of DERs such as a CHP plant, wind turbines, a PV system, and thermal and electrical storage. The mathematical model includes typical conditions such as the electrical and thermal energy balance, power limits for DERs and ramp limits for generators. Monte Carlo simulations are performed with a range of probability functions with each set of input parameters.
Bracco et al. [53] model an energy system including CHP plants, a PV system, several concentrated solar power units coupled with Stirling engines, a micro-turbine, gas boilers, electrical and thermal storage, and EVs. No information was provided on the solution algorithm employed.
As visible from the brief summary, LP problems allow the modeling of a range of different devices and their interconnections; however, all of these works were neglecting start-up and shut-down processes of these devices. Moreover, none of the works consider the implementation of part-loads or of varying efficiencies in the model of energy devices, as this requires the use of binary variables. Especially for the modeling of CHPs, LP problems are generally not adequate as they ignore essential technical characteristics or costs such as the partial-load behavior. In the following, examples of such modeling approaches for microgrids using MILPs are introduced.

MILP

To the knowledge of the author, the first MILP formulation to solve the unit commitment problem of thermal units was presented in Dillon et al. [92]. The authors use a branch and bound method to solve the problem. Early works mainly focus on the scheduling of thermal units. These are introduced further in Section 4.2.1 which provides a literature review on MILP models for the dispatch problem of thermal units and CHP plants.
Progress in terms of application of MILP formulations for optimization problems in energy cells has been achieved by Yokoyama. Yokoyama et. al. formulate energy system design problems as MILPs and select the optimal device and technology configuration from a predefined superstructure [136,425] to solve the optimal design problem for a

microgrid. The authors were able to linearize, e.g., non-constant part-load efficiencies [425]. These achievements can also be used for operational energy scheduling problems. A summary of these energy system design methods is published in [427]. Yokoyama et al. solve the MILP implementation with a branch and bound algorithm.
Müller [289] models a building energy system by a MILP including a PV system, a CHP, a BSS, thermal and electric energy storage, and flexible electrical demand. A probabilistic prediction is included for the PV system. The MILP is solved using a rolling-horizon optimization that periodically updates input data information. The model has been implemented in MATLAB and solved with a commercial solver.
Hirsch [180] defines a MILP problem that optimizes the rescheduling process of several households in a grid planning approach. Constraints include line ratings, voltage, and power restrictions.
Concerning industrial microgrids, several studies exist: Misaghian et al. [277] perform a three step optimization of an industrial microgrid considering RES, CHPs and thermal and electrical storage. The optimal operation of the DERs of the industrial microgrid is solved firstly according to cost minimization, secondly, the upper grid is optimized according to security issues taking into account offered flexibility by DERs, and thirdly the redispatch of the DERs is performed according to the results of the second optimization. The problems were implemented in different modeling frameworks (MATLAB, GAMS) and solved sequentially; however, no detail was given concerning the solution algorithms of individual problems.
Liu et al. [246] model the energy system of an industrial microgrid with the objective to schedule the DERs for optimal participation in the Day-Ahead electricity market. The schedule takes into account uncertainties stemming from the power output of intermittent RES, load variation, and Day-Ahead and real-time market prices. Liu et al. implement the MILP in MATLAB and use the CPLEX solver to find a solution with an optimization gap of 0.1%.
Ding et al. [95] model an energy management system of an industrial facility including generation and storage systems in a MILP. The DERs are scheduled according to Day-Ahead electricity prices. A case study was performed based on oxygen generating industry. No information was given about the used modeling language and solver.
Chen et al. [74] determine an optimal operating strategy for a case study of a smart microgrid system in Taiwan based on a long-term analysis of an implemented dispatch problem. A MILP is implemented that models the operation of several different devices of energy technologies such as batteries, solar, wind, biomass and conventional power plants. The model is implemented in GAMS and solved using a CPLEX solver. The work tested the economic viability of the installation of a battery storage system.
Many works model the scheduling problem as a MILP because it allows the modeling of start-up and shut-down processes and other associated characteristics such as start-up costs, minimum up-time, minimum down-time, etc. of power plants. Depending on the adequacy, non-linearity can also be linearized and binary variables are often needed in scheduling problems. Examples of MILPs that model the provision and remuneration of selected flexibility services FCR [60, 355], aFRR [60, 287], LPO [260, 349], EMO [294], and LEO [246] have been found in literature. Further examples of MILP formulations are introduced in Section 4.2.

MINLP

Lösch et al. [249] model the optimized scheduling of controllable devices of an industrial microgrid to provide automatic frequency restoration reserve. Non-linearity results from the optimal choice of the energy price of the FRR bid as explained in Section 3.5.4. The author uses evolutionary algorithms to solve the non-linear problem.
Allerding and Mauser [10, 265] model a building energy system consisting of several hybrid devices optimizing the provision, conversion, distribution, storage, and utilization of all relevant energy carriers. The applied building energy management system (BEMS) is created with an Observer/Controller Architecture. Non-linearity stems from hybrid appliances that are able to change from one energy carrier to another. Again, evolutionary algorithms are used as a solution algorithm.

Hernandez-Aramburo et al. [178] include the provision of control reserve into a MINLP formulation of a microgrid consisting of two gas-fired engines, which can provide a reserve power of up to 5% of their rated power. A fourth-order polynomial was introduced to model the fuel consumption of the engines. The model was implemented in MATLAB. No information is given of the utilized solution algorithm.
Li et al. [242] form a MILP model to arrive at a day-ahead optimal dispatch for economic operation of an industrial microgrid. Non-linear constraints include, e.g., the quadratic cost function of generating units. The model is solved using the RegPSO (Regrouping particle swarm optimization) algorithm.
MINLP formulations enable the correct modeling of complex mathematical relations in microgrids. The problems are often solved with meta-heuristics or specialized solvers.

4.1.2 Selection of model class in this work

In this work, the energy system including various energy technologies is modeled as a MILP. A MILP formulation is chosen as it

1. enables the modeling of the energy system and flexibility services with sufficient technical detail, e.g., part-load operation of energy devices and non-constant co-generation efficiencies,
2. provides a flexible and comprehensible modeling framework of existing relations in an energy system,
3. provides plausibility of the results by the analysis of, e.g., the objective function and slack variables of constraints, i.e. the constraint that led to the decision is traceable, and
4. allows an application at the case study industrial site by the subsequent implementation in existing commercial software.

4.1.3 Objective Function

In dispatch problems and aggregator problems different factors are included in the objective function that generate costs or generate revenues. In the following, a summary of all terms of objective functions for a cost-minimizing dispatch in microgrids found in the literature is presented. Most works employ several different targets in a single objective, which is also the employed method in this work.
The objective function can include:

1. fuel costs ([3, 4, 19, 20, 27, 53, 70, 280, 357, 429]),
2. start-up and shutdown costs ([4, 27, 157, 280, 301, 357, 429]),
3. costs related to frequent schedule variations ([19, 323, 357]),
4. cost for externally procured energy, e.g., in the form of electricity from the public grid ([70, 269, 357, 428, 433]),
5. further charges such as grid fees ([70, 275]),
6. revenues from selling energy on energy markets or to customers ([70, 357, 429, 433]),
7. costs and revenues from the provision of balancing reserves ([251, 275, 323, 357, 428, 429]),
8. revenues and costs for DR measures from involved loads ([170, 428, 429]),
9. imbalance costs ([295, 429]),
10. pollutant related taxation, penalties, or emission charges such as CO_2 emission charges ([3, 19, 19, 20, 70, 428, 433]),
11. further contractual costs such as predefined bidirectional contracts ([281]),

12. capital cost of DERs including, e.g., amortization costs ([19, 20, 70, 183, 269]),
13. further operation and maintenance costs ([172, 269, 282]), and
14. degradation costs of DERs especially the BSS ([54, 284]).

The MILP model developed in this work in Chapter 6 employs cost factors 1, 2, 4, 5, 6, 7, 8, 9, 13 in the objective function applying cost functions of the used devices or possible cost saving or revenues generated from the provision of flexibility services. The selected costs and revenues were applicable at the industrial site to model site-related costs as well as revenues from flexibility services.

4.1.4 Multi-objective optimization

Multi-objective optimization (MOO) or multi-criteria analysis (MCA) is a frequently applied method for optimization problems in power systems. In MOO, conflicting objective functions are optimized, which leads to the case that a single solution cannot be an optimum for all objectives. A set of solutions exists that are Pareto-optimal - to improve the objective value for one objective function always leads to a decrease in the objective value of another objective function [55]. Algorithms to solve MOO problems include, for instance, evolutionary optimization algorithms and scalarized preferences.
Several MOO applications for the dispatch problem exist. Most include, on the one hand, monetary, and, on the other hand, environmental objectives. Inter alia [3, 283, 301, 332, 428, 431] follow the objectives of minimizing energy costs and minimizing emissions simultaneously. Other works look into the minimization of energy costs and maximizing the penetration of renewable energies [271, 308].
Next to environmental factors, concurrent optimization of energy costs and the minimization of energy losses [335], energy costs and reliability factors [281, 286, 332, 431], energy costs and deviations from a target profile [180], energy costs and degree of switching [73, 418], energy costs and public acceptance [38], and the minimization of energy costs and concurrent maximization of profits from flexibility services, can be found in the literature.
The schedule optimization of devices that provide several flexibility services generally leads to an MOO as several different competing objectives are followed. The provision of various flexibility services has recently been referred to as "multi-use" [137, 381, 405], "multitasking" [268, 430], "multi-purpose" [24] or "value stacking" [84, 228]. Examples from the literature is introduced in the following.

4.1.5 Multi-use optimization

Publications have mainly focused on the ability of a BSS to provide various services simultaneously or in a serial way. Furthermore, the literature differentiates between a split of the capacity and power of batteries to serve different flexibility services or the provision of various flexibility services simultaneously. Here, the literature further differentiates between a static and a dynamic split of capacity and power.
In the following, several publications will be introduced that deal with the combination of different flexibility services in a dispatch optimization. An extract of these are summarized in Table 4.1.
Megel [268] utilize a model predictive control method to schedule different applications on a set of storage units. Individual BSSs provide a single flexibility service such as RES buffering while the aggregation of all BSSs provides load-frequency control. The dynamic allocation of the capacity of the BSSs is optimized using a cost minimization target function for BSS operation. The author splits both capacity and power ranges of a BSS for the application of different use cases.
Wu et al. [422] model a BSS and the provision of various flexibility services in a linear program. The modeled battery can provide real-time price optimization, load-frequency control, load buffering for the distribution grid, and emergency power supply simultaneously. The objective function maximizes the sum of revenues from flexibility

services, thus implicitly defining a sequential order of the applications for each time step. Results for a case study find that load buffering for the distribution grid shows the highest revenues.
Tsagkou et al. [382] perform a simulation for the provision of real-time price optimization, load buffering in the distribution grid, and load-frequency control with a BSS. As in [422], the applications of flexibility services is done simultaneously without the reservation of capacity for the specific services, i.e. no conflicts between flexibility services exist.
Gantz et al. [137] model a BSS that can provide peak shaving, real-time price optimization and simultaneously provide back-up power. The services are fulfilled by dividing the capacity of the battery for the emergency back-up power application and the residual flexibility services for each individual time step. The authors use dynamic programming as a solution methodology. In a case study the authors indicate that even with the simultaneous provision of various flexibility services, the net present value is still negative.
Hu et al. [188] utilize a rolling-horizon approach to optimize the operation of the BSS to minimize operation costs and maximize revenues. The BSS can provide RES buffering, frequency regulation, spinning reserve, and real-time price optimization. The operation and flexibility service provision of the BSS is modeled as a mixed-integer quadratic program. The flexibility services can be provided simultaneously by dividing the capacity of the BSS for individual services dynamically. Results for a case-study including a PV-system with a peak power of 60% of the demand show that the highest profit can be achieved by RES buffering.
Zeh et al. [430] model a BSS that provides load balancing of the distribution grid, load-frequency control in the form of aFRR, and RES buffering of locally generated solar energy. The battery is modeled with strict separation of energy capacities for the flexibility services. Results show that the profitability of these flexibility services depends highly on the size of the installed PV system and the requests for battery usage for grid balancing.
Hollinger et al. [184] develop a method for a BSS in combination with a PV system used in residential energy systems to provide different flexibility services. The developed method allows for simultaneous provision of FCR and RES buffering and self-balancing if the battery's SOC lies in the permissible operation range defined for a BSS providing FCR. During this normal operation, the power range is split among the different flexibility services. Depending on the SOC of the battery, this power split is adjusted to assure the correct FCR provision. Furthermore, a CHP is used to provide charging of the battery if the BSS is exiting the lower bound of the permissible operation range. The authors find that it is profitable to employ flexibility services simultaneously as opposed to providing only single ones.
Metz and Saraiva [275] optimize the battery operation to provide multiple flexibility services using a BSS MILP model. The employed flexibility services are RES buffering, peak shifting, and provision of load-frequency control. The model is applied in a case study of a small-scale energy system of a residential consumer based on market data from Germany. The individual flexibility services are modeled to be provided simultaneously without splitting the capacity of the BSS. The authors find that revenues can be increased significantly when pursuing multiple applications simultaneously; however, revenues are not additive due to conflicting operations and conflicting regulation.
Bräuer et al. [54] describe the use of a BSS to provide the flexibility services RES buffering, load-frequency control in the form of FCR, peak shaving, and a light version of energy market optimization. The BSS and the individual flexibility services were modeled in a MILP. For every time step, the capacity of the BSS is divided into load-frequency control reserve provision and other services. Different combinations of flexibility services are tested for 50 different microgrid scenarios with varying loads. The energy market optimization used price data from the Day-Ahead and the Intraday Auction of the German short-term electricity market platform, the EPEX Spot. Results show that the application of the BSS can only be profitable for a combined provision for certain microgrids.
Stephan et al. [361] assessed the economic value of BSS that can provide a variety of flexibility services. They develop a techno-economic model and apply it to the case of BSS serving multiple stationary applications in the market model Germany. The authors find that combining applications can improve the investment attractiveness

substantially; however, political barriers exist that impede the combination of applications. The model employs two applications at a time, where the primary application is given priority, while the secondary application is served only if sufficient idle capacity is available. Primary flexibility services are real-time price optimization, RES buffering, and load buffering for the distribution grid. Secondary services are FCR, aFRR, and mFRR of the load frequency control.

Hao et al. [168] model BSSs and electric loads as storage applications that can provide energy arbitrage ($\approx$ electricity market optimization), frequency regulation, energy cost (= local energy optimization), and demand charge reduction (= local peak optimization). Two separate optimization problems for external and local flexibility services were designed. The authors showed that the multi-use approach increases revenues.

Konstantinov [228] performs an analysis of the profitability of a Redox-Flow BSS operation in Germany and Australia. A quantitative analysis and a simulation based on industrial load profiles from the respective countries is performed for serial provision of FCR, RES buffering, peak shaving, and real-time price optimization. For the simulation the MATLAB environment SimSES is employed. The author concludes that for both market areas, single revenue streams do not achieve profitability of the BSS and suggests that a multi-use approach is necessary to do so.

Kazempour et al. [216] develop a MINLP and a MILP to model the provision of FCR and real-time price optimization with a pumped-storage plant. The authors conclude that the provision of control reserve is responsible for the majority of revenues.

De Hoog et al. [84] calculate the optimal schedule of a BSS by the deployment of a local rule-based controller. The controller enables the battery to follow several value streams such as RES buffering, real-time price optimization, and energy market optimization. The flexibility services are employed serially and no sharing of capacity is done. Each flexibility service is assigned to a rule-based controller which maximizes the value of one flexibility service. A solution for all flexibility services is calculated from the individual solutions using a simplified version of dynamic programming.

He et al. [174] estimate the potential of compressed-air storage to deliver FCR and real-time price optimization in the French electricity and reserve markets. The authors use the subsequent gate closure time of individual market places to fully exploit the available capacity, i.e., if the full capacity is not utilized, another flexibility service is offered. The authors estimate that a positive net present value for investment of a BSS can be achieved. 00 Göbel and Jacobsen [147] develop an algorithm to aggregate small-scale, distributed storage systems and offer the flexibility on wholesale electricity and control reserve markets. Again it is concluded that the combination of flexibility services which is possible within the introduced framework increases profitability.

Market designs to commercialize the potential of a BSS among multiple stakeholders are, e.g., shown in [61, 173]. Both approaches describe auction-based marketing of capacity using a mathematical model. [173] propose a series of auctions for the right to utilize the energy storage to ensure non-conflicting usage of the energy storage by different stakeholders. The optimal composition of value stacking for a BSS relies on perfectly forecasted power demands or power profiles of related DERs.

Englberger et al. [102] differentiate between sequential, parallel, and dynamic multi-use. For sequential multi-use applications, the full potential of the BSS is allocated to a single application. Multi-use of different flexibility services is done by switching between different applications over time. This multi-use type is referred to as serial in this work. Parallel multi-use refers to a split in either capacity or power and simultaneous provision of services. The determined split is static. Dynamic multi-use refers to a non-static split of capacity or power to provide services simultaneously. In terms of use cases the authors investigate FCR, peak shaving (LPO), self-consumption of renewable energies (LEO), reactive power compensation, and arbitrage (EMO). Arbitrage, however, lacks the exploration of the intraday continuous market. In the simulation, FCR and LPO, are the predominantly used applications.

Table 4.1 summarizes the provision of at least two different flexibility services by a BSS. It is visible that the most prominent use case is the provision of load-frequency control as well as the buffering of energy produced by renewable energy technologies. Rarely, works look at the combined provision of flexibility services with other DERs.

Table 4.1: A literature review of modeled flexibility services in multi-use dispatch optimization of BSSs

Flexibility Services	References									
	[268]	[422]	[382]	[137]	[188]	[430]	[184]	[275]	[54]	This work
Spinning reserve	-	-	-	-	√	-	-	-	-	-
Load-frequency control	√	√	√	-	√	√	√	√	√	√
Emergency power	-	√	-	√	-	-	-	-	-	-
Peak Shaving	-	-	-	√	-	-	-	√	√	√
Energy market optimization	-	-	-	-	-	-	-	-	(√)	√
Real-time price optimization	-	√	√	√	√	-	-	-	-	√
RES buffering	√	-	-	-	√	√	√	√	-	√
Local self-balancing	-	-	-	-	-	-	√	-	-	√
Load balancing of the distribution grid	√	√	√	-	-	√	-	-	-	-

4.2 Modeling the flexibility of energy devices

In the following section, a literature review of the flexibility of devices of varying energy technologies has been created. The literature review focuses on the modeling of the flexibility applying appropriate constraints in a MILP model of the dispatch problem and the provision of flexibility services with individual devices of these technologies.
Table 4.2 provides an overview of modeled DERs in different works that look into a dispatch problem based scheduling of different devices in microgrids. A great difference among the works found in the literature lies in the modeling of different energy carriers. While some works only focus on the modeling of electricity [85, 210, 245, 324, 364, 368], others look into the modeling of heat and cooling [91, 265, 289, 433].

4.2.1 Combined Heat and Power Plant

A CHP plant has the flexibility to adjust its power generation in a part-load fashion. Due to the co-generation of electric and thermal power, it is further necessary to model the thermal energy system, as an adjustment of electric power generation has a direct influence on thermal power production. Many examples exist for the modeling of a CHP in a MILP model of the unit commitment problem.

Modeling the flexibility of a CHP in a MILP

The modeling of thermal power plants in a MILP has been widely investigated. The first MILP formulation to solve the unit commitment problem of an energy systems consisting of thermal units was presented in Dillon et al. [92]. The problem formulation was based on the definition of three sets of binary variables to model the startup, shutdown, and on/off states for every unit at every time step.

Table 4.2: A condensed literature review of modeled energy technologies in multi-DER dispatch optimization of microgrids based partly on [311]

DERs	References										
	[368]	[324]	[364]	[245]	[210]	[85]	[433]	[91]	[265]	[289]	This work
CHP	-	-	-	-	-	-	√	√	√	√	√
Micro-Turbine	√	√	-	√	√	√	-	-	-	-	-
EPS	-	-	-	√	-	-	-	-	-	-	√
Wind	√	√	√	√	√	√	-	-	-	-	√
PV	√	√	√	√	√	√	√	√	√	√	-
BSS	√	√	√	√	√	√	√	√	√	√	√
EV	-	-	√	-	√	√	-	-	-	-	√
Fuel cell	√	√	-	√	√	√	-	-	-	-	-
Gas-fired boiler	-	-	-	-	-	-	√	√	√	√	√
Heat Storage	-	-	-	-	-	-	√	√	√	√	-
Absorption chiller	-	-	-	-	-	-	-	√	-	-	√
Adsorption chiller	-	-	-	-	-	√	-	-	√	-	-
Heat pump or power to heat	-	-	-	-	-	-	-	√	√	-	√
Flexible consumers such as AHUs	-	-	-	-	-	-	-	-	√	√	√

Arroyo and Conejo [14] improved and extended the modeling performed in [92]. The authors present a MILP approach that allows modeling of i) non-convex and non-differentiable operating costs, ii) exponential start-up costs, iii) available spinning reserve taking into account ramp rate restrictions, and iv) minimum up and downtime constraints. The authors achieve to linearize an exponential start-up function and a quadratic variable cost function by a stepwise approximation with the use of several binary variables.

The work above is then further improved by Carrion and Arroyo [71]. The authors propose a MILP model that requires fewer binary variables and constraints than previous publications above. Instead of defining individual binary variables for start-up and shutdown and individual binary variables for linearization of, e.g., the variable cost, the authors manage to create the model with just one binary variable per device and time slot; thus, improving the computing time of, e.g., a branch and bound algorithm to solve the MILP.

For CHP plants or co-generation plant next to the electric power generation, the modeling of simultaneously produced thermal power is essential. In the works above, the conversion of an energy carrier like gas or another fossil fuel to electric power including the resulting efficiencies has not been taken into account.

Seeger and Verstege [345] were one of the first to model the electrical and thermal interactions in a single MILP without creating several sub problems.

Works of Yokoyama et al. [186,194,426] were able to implement linearized part-load efficiencies for co-generation plants. Their works focused mainly on cogeneration plant composed of a combination of gas or oil engine-driven

generators, electric and gas refrigerators, gas or oil engine- and electric-driven heat pumps, gas or oil boilers, single effect refrigerators, and heat exchangers.
A co-generation plant as it is commonly used in industrial sites is defined by the generation of electricity by a generator and production of usable heat by a heat exchanger (= combined heat and power plant). A heat engine or similar burns fuel to create steam, which is then used to generate mechanical energy by pistons or turbines. This mechanical energy is used to drive a generator.
The thermal and electrical efficiencies of a CHP are generally not constant within the power band, but instead, take up a non-linear form [276]. Electric efficiency in partial loads can degrade more than 20% compared to the full load efficiency according to [42, 215]; however, it can be linearized. While many works employ constant efficiencies [261], piece-wise linearization of efficiencies is another common method in MILP problems.
Kuhn [232] developed an elegant method to divide the fuel input into a power-independent (operation-dependent) portion and a power-related portion: As the electric power increases, the specific influence of the power-independent component diminishes, electric efficiency increases until the nominal load point is reached. The approach by Kuhn is applied in this work.
Mitra et al. [279] present a generalized model for the optimal scheduling of a CHP plant based on variable electricity prices. It models the states of individual components such as engine, generator, etc. in terms of operating modes and transitional behavior such as a differentiation between cold and warm startups.
Jochem et al. [202] use a MILP and a two-stage greedy algorithm to schedule a proton exchange membrane fuel cell micro-CHP and EVs in residential applications. Cost minimization is applied in the objective function and the optimization of the MILP is performed using a rolling window.
Constraints employed for CHP plants or similar thermal power plants generally include [2, 18, 44, 71, 87, 202, 221, 258, 279, 334, 357, 383, 419]:

1. availability of the units
2. part-load operation
3. minimum/ maximum up time and downtime
4. power limits
5. co-generation efficiencies
6. power gradient
7. ramp rate limit of generation units
8. decision for flexibility services
9. limits of offered power for flexibility services
10. maximum number of starts
11. must-run unit constraints
12. fuel limits
13. allowable emission limit
14. efficiency limits
15. connected thermal storage

This thesis uses a MILP model of the industrial CHP to represent the actual CHP in operation at the industrial site used as a case study by implemented constraints based on conditions 2-7, 9-10. Residual conditions were not applicable at the industrial site.

An alternative to MILP models are data-driven thermodynamic models that include balance equations for each individual component in the CHP plant. Thermodynamic models are generally non-linear such as the one in Jüdes et al. [206].

Flexibility services provided by a CHP

The participation of thermal units such as CHP plants on electricity and reserve markets is a common procedure as indicated by early publications such as Arroy and Conejo [14]. As most power plants produce steam that drives a generator via a steam turbine to produce electricity, electric power generation can be altered by an adjustment in the steam cycle or in the beforehand steam production process (e.g. combustion process). Fast reserves such as FCR can be provided by using the steam storage capacity of boilers and altering the steam flow to the turbine [80]. Slower reserves such as aFRR can be provided by adjusting the steam production process. Depending on the fuel used and the installed CHP technology, the speed of adjustment to control signals can vary greatly [411].
Industrial CHP plants operated with an engine can simply adjust the speed of the engine to react to power signals. The start-up times for a CHP greatly depend on if the CHP performs a warm or a cold start [279]. Through a warm start-up, a CHP can easily reach nominal power within a small number of minutes [291].
Although the commercializing of flexibility of CHPs as frequency control reserve might be a common use case, few works exist that describe this possibility. Haakana et al. [158, 159] show different possible flexibility services of CHP. They recommend the participation in electricity markets as well as control reserve markets. [351] provides work on a small-scale CHP participating in the German market for aFRR and the spot electricity markets. Wille-Hausmann et al. [419] model and aggregate the operation of a cluster of CHPs in a VPP to participate in energy markets.
As shown by Müller-Ruff et al. [291], a patent application resulting from the research project SmartFlex, industrial engine-driven CHP plants are able to provide both FCR as well as aFRR simultaneously. Tests at the target industrial site showed that around 17% of the rated power can be provided for FCR and around 50% of rated power for aFRR.
Furthermore, CHPs can adjust their power generation to assist wind power plants [351] or the charge management of a BSS to provide control reserve [331].
No research has been found that directly deals with CHP plants participating in the German aFRR and FCR market in combination with further energy technologies, while simultaneously delivering local flexibility services. The goal of this thesis is to fill this gap by modeling the participation in an optimization problem.

4.2.2 Battery storage systems

A BSS can temporarily store electricity. It has the flexibility to charge and discharge electric power subject to given SOC levels. Firstly, this section summarizes different modeling approaches of a BSS in a MILP formulation. Secondly, literature focusing on flexibility services provided by a BSS is summarized. Thirdly, related work concerning the flexibility service of a BSS providing FCR is introduced.

Modeling the flexibility of BSS in a MILP

Batteries are often modeled as simple storage types in MILP formulations [357, 433]: Capacity and storage limits, as well as charge and discharge efficiencies, are implemented. Furthermore, self-discharge is implemented occasionally as in Müller [289]. Variable, C-Rate- and SOC-dependent efficiencies are modeled in a MILP, e.g., as done in Sarker et al. [337].
Additionally, several works consider the degradation of batteries such as Bräuer et al. [54, 212, 213]. Degradation describes the process of loss of capacity due or the increase of inner resistance and can be differentiated into cyclical and calendar aging, i.e., natural or charging-related aging. The calendar aging occurs naturally during the

lifetime of the battery but is also dependent on battery technology, temperature, and SOC levels. For cyclical aging, energy throughput, equivalent full cycles, the average depth of discharge, the charge and discharge voltage, or the temperature are factors to determine the influence of charging and discharging activities on the aging of the battery. A lower SOC, for example, leads to slower calendar aging. A high cycle depth reduces the number of possible full cycles of the battery storage [23, 404]. Furthermore, the degradation of electronic equipment is important. It can affect charging through higher power losses, i.e., lower charging efficiencies, or failures of equipment. Typically, hours of operation and numbers of activations are taken as indicators of influence on the equipment aging [420]. To limit degradation some works consider cycle limits [213] that cannot be exceeded. As opposed to setting constraints on cycle limits or degradation, shadow costs can be included in the optimization function [171].
Rarely as in Kaschub [212] dynamic SOC-dependent dynamic power levels are modeled to replicate the constant-current and constant-voltage (CCCV) charging strategy implemented by battery management systems of most Li-ion batteries in MILPs (see Section 2.4.2). As this is generally a non-linear development, a discretization has to be done which causes the introduction of several integer variables and can elongate computation time [370]. Alternatively, the battery's capacity is limited to the levels of SOC that do not include constant-voltage charging as done in [213]; however, this limits the potential of the usage of the battery.
Constraints employed to model a BSS in a MILP formulation generally include [1,54,212,290,316,337,357,370], of which 1-6 and 8 were applied in this work. Residual constraints were not modeled due to the lack of data for the BSS at the target site.

1. availability of the units
2. power and energy/ SOC limits
3. energy/ SOC development
4. decision for flexibility services
5. limits of offered power for flexibility services
6. specifics concerning the provision of flexibility services
7. degradation
8. prevention of simultaneous charging and discharging
9. variable efficiencies, C-rates
10. cycling limits

Flexibility services provided by a BSS

Due to the apparent flexible control, a BSS can provide a majority of the flexibility services introduced in Table 3.1. A comparison of different multi-use approaches of a BSS is given above in Section 4.1.5. Especially due to the fast reaction speed, BSS are especially suited to provide FCR. The following section summarizes a literature review of works that focus on a BSS providing FCR. This literature review forms the basis for the battery model and methodology developed in Chapter 5.1.

Simulation of a BSS providing FCR

Traditionally, conventional power plants have provided FCR; however, only a small fraction of the rated power can be provided as fast response characteristics [411]. While intermittent RES already supply a great share of electricity supply, they hardly contribute to the provision of FCR. BSS have transient response characteristics well suitable for the provision of FCR: The process of converting chemical into electrical energy and vice versa entails fast response times and high accuracy towards power signal resulting in little overshoot [94].

First ideas for a BSS to provide control reserve were published by [235] for the insular power system of West Berlin. The successful operation of a test facility including a battery with a rated power of 14.4 kW by the local utility and transmission operator resulted in the operation of a lead-acid BSS with a rated power of 17 MW between 1987 and 1995 [99, 205, 369]. Due to high battery costs and short cycle lifetime, a limited number of mainly lead-acid BSS were built for the provision of FCR in the 1990s. Falling costs for lithium-ion BSS [303], high remuneration for the provision of FCR within Germany and specified operation criteria by the German TSOs [391, 392] have resulted in a strong increase in the number of battery projects providing FCR [160, 346].

This also led to an increase in publications concerning model-based approaches of a BSS providing FCR. The majority of these models intend to decrease necessary market-based (dis-)charge events of battery systems providing FCR, which result in higher operation costs [128, 185, 226, 240, 367].

Fleer et al. [128] compare different charge management strategies of FCR operation for a 2 MWh BSS in a simulation using grid frequency data of the year 2013-14. They compare the impact of different degrees of freedom (DOFs), different ratios between FCR power and capacity, and different triggers for DOF use. The work lacks the investigation of the 15-min. criterion as it has been done before the regulation was changed.

Thien et al. [377] extend the work by [128] and additionally investigate the use of the DOF gradient control and the lead time that triggers charge management events. Furthermore, the 15-min. criterion is applied.

Hollinger et al. [185] compare the impact of all available DOFs. Additionally to the degrees of freedom presented by [128] and [377], the authors look at response delay dynamic system time correction, which according to the knowledge of the author of this work is only allowed in the control area Switzerland. Current regulations on FCR also do not allow a delay of 15 seconds as the power is supposed to increase in a linear fashion upon frequency deviations. The authors identify that a delay of 15 seconds and dynamic system time correction yields a great reduction of charge management; however, the use of this DOF is questionable.

Therefore, [331] use the methodology of [128] and [377] to model BSS operation. [331] investigate the use of local flexible energy devices at the case study industrial site to substitute energy market based charging. The authors find out that flexible AHU operation, flexible CHP operation, and excess wind power generation can substitute a great amount of charge management; however, the authors further identify that due to the current scheme of grid charges (see Section 2.3.2), it is not worth using, for instance, the CHP for charge management. Additionally, excess wind power generation is not available for most of the time, leaving the AHU use as the only feasible option significantly reduce charge management.

As shown by the application in the example of the insular power system of West Berlin [235], the provision of control reserve is especially interesting for small and isolated power systems. Here several publications exist considering the economy, the technical specifications and the control of a BSS [5, 272, 350].

Furthermore, several model-based approaches exist that simulate a hybrid system to provide FCR. Johnston et al. [203] propose to integrate a BSS within a wind power park. Due to its high accuracy, the BSS would enable the correct provision of FCR by adjusting the power response and delivering power when the wind power park is not available. Henninger et al. [176], on the other hand, utilize wind power as well as solar power to charge and discharge the battery and therefore decrease the number of schedule-based transactions with the intraday market. In addition, the battery adjusts its power to avoid deviations from the forecasted output of renewable resources. A similar approach is chosen in Rominger et al. [331] who estimate the potential to substitute charge management by the control of flexible devices.

The provision of FCR by a BSS has been widely studied; however, none of the mentioned works included a correct cost calculation of the grid fees and balancing energy to assess the correct operating cost of a BSS providing FCR as done in this work. This has been done in Section 5.1, which provides a simulation of a BSS providing FCR according to the regulatory regime in Germany. The model of the BSS to provide FCR is taken from [331] and introduced in detail in Section 5.1.

In Chapter 6, this work models the provision of FCR, aFRR, energy market optimization and local flexibility services with a BSS at the industrial plant.
In Section 4.1.5 several multi-use models of a BSS have been introduced; however, none of the works has combined simultaneous and serial provision of flexibility services within a single model. Furthermore, the combination of flexibility services that is modeled in this work has not been found in another piece of literature. Especially the modeling of trading on short-term electricity markets using a BSS, is often not sufficiently adequate. Section 5.2 fills this literature gap by estimating the profits gained on the continuous Intraday market using the flexibility of a BSS.

4.2.3 Electric vehicles

Like a BSS, the battery of an EV can be used to provide services within energy systems. The main difference as opposed to stationary storage is given by 1) the availability of the storage unit, 2) the primary use of the storage for mobility, and 3) the dependency on the given charging infrastructure. These and further factors have to be taken into account when modeling an EV, as opposed to a stationary battery.
To provide flexibility services with an EV, one can adjust the standard uncontrolled power consumption of the EV charging session by charging with lower power consumption, stopping to charge, or discharging in the case of vehicle-to-grid capability of both the vehicle and the charger. The control of the charging event requires the availability of a power management solution installed either in the charging station or in the EV.
As explained in [329], this controlled charging, as opposed to uncontrolled charging, is only possible for the driver in case of the existence of

1. *charge flexibility* - the EV can make up for the missing energy at a later period during the plug time, i.e., the idle time of the EV at the charging station represents the flexibility, or
2. *range flexibility* - the driver permits to leave the charging station with a lower SOC than expected, e.g., if no full charge is necessary for the next drive.

This work focuses on the analysis of charge flexibility. As no information on the actual driving behavior of analyzed EVs was given within the data available at the case study industrial site, the estimation of range flexibility lies beyond this work.
Babrowski et al. [20] show load shifting potentials for charging events as with extra parking time, charging can be postponed or shifted. Another publication that covers the idea of the above-mentioned time-dependent charging flexibility is D'Hulst et al. [90]. Many works look into the utilization of charge flexibility of EVs; however, the data sources for the calculation vary greatly. Few papers use real charging data to calculate it. [77,78,198,248,387,421] all use predefined distributions for either arrival or departure times or charging power gained from conventional vehicles. Rominger and Csaba [327] derive vehicle movement from taxi fleet data while charging characteristics are taken from EV drivers in Japan or United States to model charging characteristics and estimate waiting times at charging stations. [247,338,342] use national mobility data derived from driving patterns to investigate the driving range and charging flexibility of EVs. In an extensive study accumulating charging data from three German mobility studies, Schäuble et al. generate empirical EV load profiles [339]. Flamini et al. [127] get charging data from the charging infrastructure and provide an extensive statistical analysis of EV behavior in the Netherlands. Another recent study analyzed one year of public charging station data, including the flexibility and its time-dependency [333]. To model charging flexibility, preferably, real charging data is used; however, due to the slow diffusion of the EV technology, publications have been sparse.

Modeling the flexibility of EVs in a MILP

In general, an EV is modeled with similar constraints as a BSS [146] in the case of bidirectional charging capability. The major difference is the availability of the EV, which is often taken from probability functions or actual charging data (see above). In the case of only unidirectional charging capability, EVs are often modeled as a movable load [150] within the plug-times. This work uses and extends the approach given in Gerritsma et al. [144] that defines the charge flexibility as defined above by the idle time, the time between the end of charging and the plug-out time as shown in Rominger et al. [330]. This flexibility can be utilized for many different flexibility services.

Seddig et al. [344] compare several methods to schedule the charging process of three different classes of electric vehicles fleets at a charging infrastructure belonging to a car park with installed PV under uncertainty. The methods include a heuristic, mixed-integer linear, and stochastic mixed-integer linear programming. A PV electricity generation is forecasted using different approaches while the data of charging events are modeled with a non-parametric probability density function. The scheduling objectives are the minimization of charging costs or the maximization of the utilization of generated electricity by the PV.

Wang et al. [412] develop a two-stage stochastic linear program for scheduling charging events subject to uncertainties of the availability of EVs and their electricity demand. A rolling-horizon optimization is performed that models real-time scheduling. Three different objectives (flattening EV charging demand, peak shaving and valley filling in combination with residential loads, and demand response for wind integration and aFRR-like control reserve calls) are investigated. Investigated options of EV charging forecasts include perfect foresight, a stochastic and a deterministic model. Results show that changing the charging schedules to fulfill the above mentioned objectives or flexibility services decreases the level fulfillment of charging events due to the given uncertainty.

Flexibility services provided by EVs

Many papers exist that look into the use of controlled charging based on either charging or range flexibility for different flexibility services. In the following some works are introduced ordered by the main flexibility service that they model.

Real-time price optimization

Vandael et al. [388] use a heuristic to schedule an EV fleet according to Day-Ahead prices based on a charge event forecast. The forecast is obtained from a forecasting model relying on batch mode reinforcement learning. The work does not model individual charging but instead schedules the aggregated fleet of EVs.

Jochem et al. suggest the use of dynamic electricity prices [201, 306] to save electricity costs for the drivers. Dynamic prices were optimized in a model-based environment and also tested in experiments at the Energy Smart Home Laboratory.

FCR provision

Arias et al. [13] display the results from a field test with a fleet of EVs with V2G capability able to provide FCR to stabilize the grid. Each charger with a maximum power of 10 kW was able to provide a maximum FCR power of 9.25 kW. It is visible that EVs were able to respond with a time delay of around 5 seconds, which equals the required reaction times by the German TSOs. Tests during the project SmartFlex support these reaction times for delay towards power signals; however, test results cannot be displayed in this work. Otherwise, the fleet of EVs complies with the requirements given by the German TSOs. The fleet of Nissan eNV200 is already providing FCR for the Danish TSO.

Pelzer et al. [313] use a dispatch model for EVs to provide frequency control, frequency containment, and contingency reserve in the National Electricity Market of Singapore. Based on market data for the year of 2012, the authors found out that charging costs can be completely absorbed by revenues generated from the flexibility services. Mobility data was taken from the mobility patterns of local residents.

Weerdt et al. [414] develop a stochastic MILP model to model the optimization of an EV fleet that purchases electricity day-ahead and real-time and offers power as control reserve. Here, authors show that charging costs can be completely absorbed by purchasing electricity on the Day-Ahead market, offering control reserve, and providing V2G services. The provision of reserve control is modeled according to the Electric Reliability Council of Texas and is slightly different from the reserve markets in Central Europe.
Schlund et al. [341] develop a stochastic model to show the potential of EVs providing FCR during home charging in Germany. Mobility data is taken from mobility patterns. Currently established regulations concerning the provision of FCR as described in Section 5.1 are partly resembled in the model; however, the work did not take into account the charge management for batteries providing FCR suggested by the TSOs but instead calculated the probability of EVs not being able to fulfill FCR signals using extensive simulations. Their results show that for an offered power of 1.5 kW per vehicle 25 kW of back-up power is necessary in order to provide FCR in a reliable way. 667 EVs are necessary to provide a joint offer of one MW and would have to drive an average annual mileage of 1573 miles to get to needed SOC values.

aFRR provision

Bessa et al. [41] use a fleet of EVs to bid on Day-Ahead and Intraday electricity markets and aFRR markets. The authors define three MILPs to serve the bidding on the Day-Ahead market (1), the Intraday spot and $aFRR^{-}$ market (2), the Intraday spot and $aFRR^{+}$ market (3). Data for EV power, SOC, and further characteristics are taken from truncated Gaussian probability density functions.
Göbel and Jacobsen [146] provide a MILP model of a fleet of EVs offering flexibility to provide aFRR and commercialize the flexibility on an intraday electricity market using an aggregator. The method used in this work builds on the concept of commercializing EV flexibility shown in Bessa and Matos [39, 40]. It is one of the only works found that considers the control market bid size constraints as also investigated in this thesis in Section 6.8. The applied MILP model by Göbel and Jacobsen, uses a tolerated difference to the Integer bid. Thus, the resulting it does not conform to the bid size and product length constraints of the target reserve and energy market. The authors denote that it is up to the aggregator to incur financial penalties or close this gap by dispatching additional resources. It is also mentioned that the bid size constraint leads to less commercialized capacity or not consideration of flexibility offers at all due to the market bid size constraints. Furthermore, a heuristic is presented that repairs the given schedule if the forecasted charging does not take place as planned.
Han et al. [164] developed an optimization problem using dynamic programming for optimally commercializing the flexibility of EVs as aFRR. Depending on the SOC given, a strategy is developed that limits the offered reserve power. The authors stress the dependence of earnings on given SOC values for the flexibility service aFRR.

Market-related flexibility services

In the work by Shafie-khah et al. [348] a control system for bidirectional charging is presented for optimized bidding on several market segments of the short-term electricity markets. In a multi-stage stochastic optimization, an EV fleet is optimized according to Day-Ahead energy and reserve, intraday energy, and intraday demand response markets. The optimization approach considers uncertainties regarding electricity prices and the charging behavior of the consumer. It is shown that the integration of intraday trading leads to higher revenues than the sole purchase from the day-ahead market.
In the work by Naharudinsyah and Limmer [294] the revenue potential of electricity market optimization via the participation of EVs in continuous intraday trading is investigated. Compared to the direct purchase of charging energy from the energy supplier, savings in unidirectional charging operation, as well as bidirectional charging operation were analyzed. The developed MILP formulation also complies with the bid size criteria of the continuous Intraday market.
Rominger et al. [330] calculate the profit for battery applications such as a BSS or EVs on the continuous intraday market. This paper is introduced in Section 5.2.

Sarker et al. [336] optimize a fleet of EVs that is managed by an aggregator to participate in electricity and reserve markets. Profits for both markets are maximized, thus compensating EV owners for additional degradation for the provision of flexibility services. Degradation takes into account the number of charging cycles.

RES buffering

Al-Awami and Sortomme [8] look at controlled charging of EVs for a VPP that includes thermal and wind plants. The implemented optimization intends to generate profits by selling electricity on the Day-Ahead market and avoid imbalance fees. The problem is formulated as a mixed-integer stochastic linear program.

Similarly, Zhang et al. [432] look at the use case of providing combined RES buffering and real-time price optimization by EVs at multiple charge points. The intermittent nature of electricity prices, RES, and EV availability is modeled using Markov processes. The objective function is defined as to minimize the waiting time of EVs at distributed charging stations. A framework of Markov decision process to investigate this constrained stochastic optimization problem.

In the work by Lee et al. [238], EV charging at a solar-powered car park is modeled using a LP with the objective, for instance, to maximize the utilization of solar energy to charge the EVs at the car park by changing the amount of PV installed and the size of the car park.

Grid-related flexibility services

Alonso et al. [11] use a genetic algorithm to find the optimal load pattern of EVs taking into account transformer, voltage limits, and parking availability patterns. Results show that a controlled charging schedule of EVs leads to a flattening of the load profile, peak load shaving, and less stress for power system elements such as lines and transformers.

Similarly, Mehta et al. [270] use statistically developed driving pattern; the authors try to maximize the EV penetration for a local car park without violating the local transformer power limit. A genetic algorithm is used to optimize charging schedules.

Neaimeh et al. [297] combines residential meter data of households and driving behavior data to perform Monte Carlo simulations in order to determine the effects of EV charging on the distribution grid.

Richardson et al. [325] and Sundstrom and Binding [366] use a linear program to compare controlled and uncontrolled charging in a low-voltage distribution system. Results of both works show that, by applying controlled charging, high penetrations of EVs can be accommodated on existing residential networks with little or no need for upgrading network infrastructure.

Peak Shaving

Rominger et al. [329] also analyze the charging behavior and develop different charging strategies to lower the peak power consumption of a charging cluster. Peak shaving and further demand response use cases are also suggested by Jochem et al. in [200].

In summary, many works cover the provision of flexibility services with EVs such as real-time price optimization [255,336,388], energy market optimization [8,41,294,330], control reserve markets [13,41,146,164,313,336,341, 414], the optimized scheduling in combination with renewable energies to achieve RES buffering [8,238,342,432], peak shaving [11,329], and load buffering at a transformer station for the DSO [144,325,366].

This works models the provision of FCR, peak shaving, and local flexibility services with EVs at the case study industrial site. While many studies look at the provision of individual flexibility services, few publications have been found that model flexibility services for EVs in a multi-use approach.

4.2.4 The flexibility of electric power demand

The utilization of demand side flexibility is indispensable for energy systems with a high penetration of intermittent renewable energy sources. This work identifies and simulates the flexibility of the electric power consumption of AHUs of HVAC systems, a power-to-heat plant, and a compression chiller.
Ventilation systems, or specifically AHUs, possess flexibility in their electricity consumption, as it can be temporarily adjusted without disrupting the feeling of comfort for the user. This is due to the flexibility in the given comfort conditions and the inertia of the air balance and the thermal balance of connected buildings. Building thermal dynamics allows demand flexibility to be introduced by temporarily changing indoor conditions without reducing occupant comfort. Thus, AHUs systems inherit significant potentials to provide flexibility services [9].
Several works suggest that the operation of a chiller can be rescheduled slightly if a storage tank is available. It must be ensured that the storage temperature - and thus the flow temperature to the cooling register - does not exceed a defined limit value in order to continue to meet the temperature requirements for product storage. Depending on the size of the storage tank and the temperature range to be maintained, the call-off time can be up to two hours and the call-off frequency once per day according to [154]; however, a case-by-case analysis is suggested.
A power-to-heat plant in the form of an electric boiler can convert electric power to thermal energy in the form of heat, which can then be used to satisfy the local heating demand. An electric boiler can be operated flexibly without part-load operation and can, for instance, be used when electricity prices are low or electricity generation is high to produce heat [45].

Modeling the flexibility of electric power consumers in MILP formulations

Not many MILP formulations for the dispatch or scheduling problem regarding the power consumption of demand-side devices exist. For AHUs, for instance, this can be related to the non-linear relationship between power consumption and volumetric airflow or temperature development in buildings [237].
Gottwalt et al. [150] model demand response by cooling devices, storage water heaters, and space heaters in a MILP model. The authors supply data such as the predefined cycle duration for individual electric power-consuming devices. From this information, the authors calculate the daily number of runs for each device.
Controllable devices are then grouped into two different groups: Group 1 describes sparsely controlled devices such as space heating while Group 2 describes frequently controlled devices such as cooling devices. Devices are modeled by fulfilling a certain consumption over a certain time step (modeled by the number of runs per day). For a refrigerator, daily run times of 32 x 15 min. are necessary to satisfy cooling demand. For sparsely controlled devices (Group 1) a further constraint is added: In their simulation with a horizon of 24h, devices have to consume 25% of their daily energy consumption over 25% of the day, i.e., devices can flexibly fulfill their electricity consumption for six hours subject to achievable power levels per time slot. A temperature-dependent usage for individual devices was only employed for storage space heating.
Ayón et al. [17] optimize the power consumption of the ventilation system according to Day-Ahead prices. The flexibility provided by the ventilation system is limited by a minimum and a maximum comfort level (flexibility bounds). The comfort levels are calculated from a forecast of consumer behavior. The problem is modeled as an LP.
Hartmann et al. [170] modeled demand side management as part of the scenario-based energy dispatch optimization in a distribution grid in a MILP model implemented in GAMS. DSM technologies, which are not further specified, were modeled as electric power devices that can be shifted by $+/-$ 4 h of the designated time-of-use.
Jindal et al. [199] propose a MILP model for intelligently scheduling the working of HVAC systems in university classrooms in an energy consumption minimization problem. The MILP is designed to guarantee thermal comfort depending on the occupancy of the given classrooms. To lower the total energy demand, this work also takes into account the rescheduling of classes. The authors also propose a heuristic-based algorithm to solve the given

problem. The developed algorithm uses the flexibility inherited by HVAC systems to reduce the energy demand and provide DR. Similar to this the authors of Chai et al. [72] schedule meetings in an office building for energy cost reduction in a similar MILP formulation.
Hao et. al. [166–168] present a virtual storage model to describe the flexibility of building loads and batteries.
To model compression chillers, Hakimi and Moghaddas-Tafreshi [162] model the power consumption of an air conditioning system. The power consumption depends on the difference in desired flow and return temperature, the distribution of the cooling using ventilation, the EER, and efficiency losses. In the study the seasonal energy efficiency ratio (SEER), which is defined different values of EER depending on the season, i.e., the cooling output of the summer season is divided by the electric energy input during the same season. Losses that are accounted for include radiation, conduction, convection, and internal load losses.
For the model of the power flexibility given by AHUs and the compression chiller, this work uses and extends the approach given in Gottwalt et al. [150], who define the flexibility by the electricity consumption of the ventilation system and chiller. The electricity consumption of such a consuming device is given by a baseline profile. The consumption of individual time slots can be altered, as long as, the consumption over a longer time frame remains the same. Losses in efficiencies account for the move away from the optimal operation point and added to the mathematical model. The model was chosen due to the availability of a baseline power consumption of the mentioned technologies at the case study site.
Böttger et al. [52] model the provision of control reserve with electric boiler power-to-heat applications in the German national energy system. Electric boilers are modeled in MILP with a constant thermal efficiency of 98%. Furthermore, limits are introduced to limit thermal power production to the maximum installed capacity. This work follows this modeling approach of an electric boiler, which can be controlled in a flexible manner without part-load efficiency and has a constant thermal efficiency.

Flexibility services with electric power consumers

The provision of flexibility services by HVAC systems and especially the ventilation system can be found in various research papers. As the authors of [256, 288, 304] point out, the type of balancing services to be offered varies among ventilation systems. The quick reaction speed of the electric motors driving the ventilation shaft enables the provision of fast-reacting FCR by AHUs. The following literature review has identified the provision of local flexibility and load-frequency control as key flexibility services provided by ventilation systems.
Lu and Zhang [252, 434] evaluate the performance of intra-hour load balancing service supplied by HVAC loads and air conditioning and find that an aggregate of devices can provide load-frequency control during operation.
Lee et al. [239] use a nonlinear autoregressive neural network combined with a MINLP to compute the optimal control of a building's HVAC system to reduce peak energy consumption (peak shifting), balance energy demand and supply (self-balancing), and reduce GHG emissions while satisfying the thermal comfort.
Khan et al. [219] use a MILP model to schedule HVAC systems to reduce energy costs, which are based on TOU tariffs. The authors achieve savings of up to 38%. The simulation was done in EnergyPlus.
Hartmann et al. [170] schedule the DSM potential according to given electricity prices and to avoid curtailments of wind power plants by applying local self-balancing activities.
Stadler [352] measures the different potentials for temporary increasing and decreasing the power consumption of a ventilation system of a lecture hall and refrigeration devices. The author intends to model the ventilation system and connected systems as an electric storage system. He provides a visualization of the load flexibilization potentials or power offered as positive and negative aFRR as a function of time. The author also points out that the flexibility depends on the current power consumption and consideration of times for regeneration.
The University of Colorado developed a grid frequency-based control of electric motors driving of ventilation fans for the TSO of the Pennsylvania-New Jersey-Maryland interconnection regional transmission grid published by

Zhao et al. [435]. Further configurations of the control system extended to the power control of electric heating and cooling devices of the HVAC system in [436]. The authors model the simulated buildings with the software EnergyPlus. In experiments at the University of Florida the frequency control was done with a ventilation system supplying a building on the university campus with fresh air [22, 165, 243]. It was shown that 5 kW of FCR can be achieved with electric motors with a rated power of 35 kW. The control was able to follow the target signals within 10 s, which easily qualifies for FCR in the German market. Furthermore, these experiments showed no significant increase or decrease in the temperature and noise of the buildings due to the frequency-based control.
Given the current state of the art, the provision of FRR with an aggregate of technical units [134,409], the provision of FCR by single technical units [224, 253] and the modeling of aggregates to deliver FCR is widely researched [253, 314, 408], while the combination of loads with devices of other energy technologies to deliver FCR lacks exploration and especially practical application.
Callaway and Hiskens show in [69] that loads can provide control reserve at low costs and with less environmental impact if properly controlled and aggregated. In [409], In Vrettos et al. propose a solution to deliver aFRR with an aggregate of HVAC systems and in [408] with an aggregate of water heaters.
Motegi et al. [288] gives an overview of demand response measures with HVAC and AHU systems. The implemented method limits the motor speed using VFDs.
A system architecture has been developed, implemented and employed in Rominger et al. [328]. It enables a provision of FCR by an aggregate of electric motors of AHU systems according to FCR standards defined by German TSO. The motor speed is adjusted by continuously updated VFD speed set points similar to the method in [288]. A power model is defined to estimate the amount of FCR to be offered by each individual electric motor and by the aggregate. A control algorithm utilizes information taken from these models to achieve a reliable FCR provision. This system architecture has been implemented at several industrial sites and is formulated in patents [33, 34].
[52, 125, 351, 424] underline that the provision of control reserve power is a commonly applied business model for P2H plants. While Feron and Monti and Jomaux et al. [125, 204] focus on the provision of FCR in combination with batteries, [52, 351] model the provision of aFRR with power-to-heat technologies.
[244, 264] stress the capability of P2H plants to balance the electrical energy system with a high penetration of RET. The installation of P2H plants can reduce the curtailment of intermittent power sources such as wind power by a great extent. P2H plants are therefore extremely valuable for balancing activities within a distribution system, balancing group, or local energy system.
In Hedegaard et al. [175] the placement of flexibility by electric heaters on the Danish spot market is investigated with a focus on the impact of intraday trading. They found that additional intraday trading of flexibility offered by the P2H technology could significantly reduce energy costs for heating in the winter months.
This work uses the models of Gottwalt et al. [150] and Böttger et al. [52] to model the electric power consumers. Furthermore, this work models the provision of FCR, aFRR, local peak optimization, and local energy optimization with the power consumption of AHUs and the electric boiler. Local peak optimization and local energy optimization is done with the chiller at the industrial plant. This combination of flexibility services for the AHUs and the P2H plant has not been found in the investigated literature.

4.3 Summary

The chapter provides related work for the simulations and optimizations performed throughout chapters 5 to 7.
First, related work on different problem classes LP, MILP, and MINLP, employed solution algorithms, and objective functions is introduced Section 4.1. Furthermore, examples of multi-objective optimizations in the form of multi-use optimization are presented.

Then, related work on the modeling approach of different energy technologies in the literature is reviewed in Section 4.2. The technologies include, for instance, CHP plants in Section 4.2.1. CHP plants have been modeled widely in the literature and a summary of employed constraints is given. The Section 4.2.2 provides a similar analysis for the energy technology BSS. A detailed literature review for a BSS providing FCR is presented that prepares the reader for the simulation model introduced in Section 5.1 of the following chapter. In addition, the modeling approach for electric vehicles in MILP formulations and the possibility to provide various flexibility services are introduced in Section 4.2.3. From the literature of electric power consumers in Section 4.2.4 modeling approaches for energy technologies AHUs, chillers, and power-to-heat plants are selected.
This chapter is used to answer part of research questions 2.1, 2.2, 3.1, and 3.2 as it provides modeling approaches for devices of used energy technologies and the multi-use provision of flexibility services by these devices. Thereby, it provides the fundamental knowledge for the actual modeling done in Chapter 6.

5 Provision of Flexibility Services by Battery Storage Systems

This chapter will provide two contributions which are essential as inputs for the main contribution in Chapter 6. The contributions assess the operation of a BSS for flexibility services FCR (frequency containment reserve) in Section 5.1 and EMO (energy market optimization) in Section 5.2.

5.1 Simulation of a BSS providing FCR

The following sections will introduce the model used for modeling the provision of FCR with a BSS. The model results from work done in the publication *Utilization of Local Flexibility for Charge Management of a Battery Energy Storage System Providing Frequency Containment Reserve* [331]. The publication investigates the influence of degrees of freedom in the FCR provision of a BSS on the charge management that is used to keep the BSS within permissible SOC ranges. Furthermore, the publication looks at the use of flexible local devices to provide this charge management which is normally done by energy market transactions.
This work will introduce the model of the publication and use it to estimate potential revenues of the flexibility service FCR provision for the BSS at the industrial site. The use of flexible local devices to perform charge management will not be covered in this work.
Firstly, the regulatory framework for FCR provision by a BSS will be presented in Section 5.1.1. The degrees of freedom, as well as the necessary charge management will be introduced. Secondly, the developed BSS model is introduced in Section 5.1.3. The results of a simulation with the presented model and grid frequency data of the year 2016 will be presented in Section 5.1.5.

5.1.1 Provision of FCR with a BSS: the regulatory framework

This section summarizes the regulatory framework set up by the German TSOs for BSSs providing FCR within Germany and describes DOFs that can be implemented in the battery management.
The German TSOs specified operation conditions for batteries that participate in the FCR markets within a regulatory framework [391, 392]. Here, the TSOs first defined a "30-minute-criterion", which was later substituted by the "15-minute-criterion" [67]. The "15-minute-criterion" assures that the BSS can provide fifteen minutes of FCR at any time if regular frequency conditions prevail. A permissible SOC range of the BSS is defined which is enveloped by a symmetric capacity that can only be entered in alert state (see Figure 5.1). The alert state are conditions defined by periods of time when extreme frequency conditions occur. This symmetric capacity depends on the ratio between prequalified FCR power ($\overline{P^{FCR}}$)[1] and available capacity ($\overline{E}$) of the BSS as indicated by Figure 5.1. For example, at a capacity/power ratio of 1 (x-axis), the SOC of the BSS should always remain between 25% and 75% during FCR operation (y-axis). The lower and upper limit of the permissible operation range (POR) are henceforward referred to as $SOC^{l,POR}$ and $SOC^{u,POR}$. In case of alert states these limits can be surpassed and buffer storage is left to provide the maximum FCR for a period of fifteen minutes [399].
To keep the BSS within these limits, a charge management that triggers charge and discharge events has to be implemented. Charge management is usually backed up by market transactions on the Continuous Intraday Market. This

[1] In this chapter it is always assumed that the offered FCR capacity at time step t, the FCR bid (P_t^{FCR}), equals the prequalified FCR power.

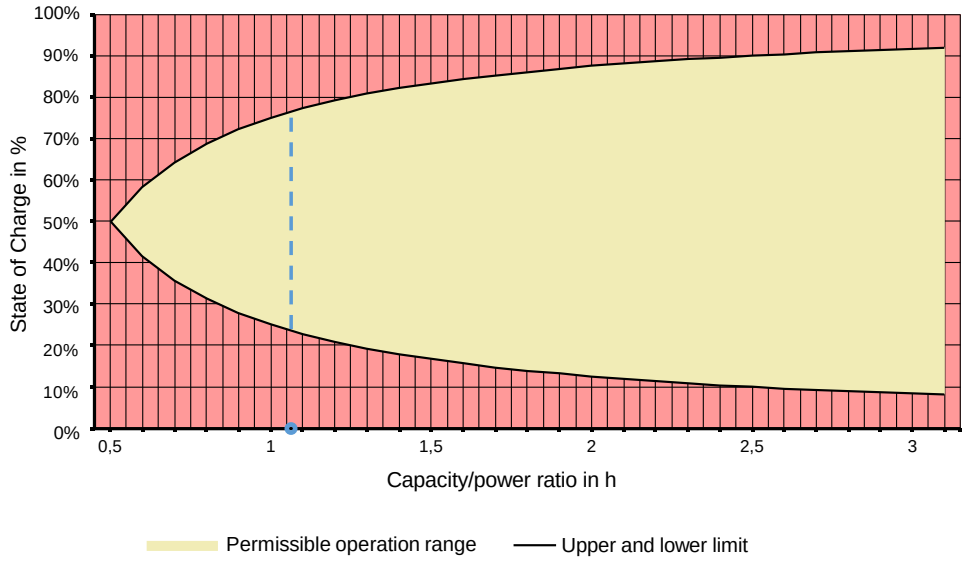

Figure 5.1: 15-minute-criterion for FCR-providing BSS
Permissible SOC operation range with the capacity/power ratio (x-axis) and the SOC plotted (y-axis); according to TSO regulations actively using the red area is forbidden in order to always be able to provide the maximum offered FCR for a period of 15 minutes during alert state. The blue dot and dashed line indicate the BSS configuration at the case study. Original diagram from [399]

market-based charging and discharging (MBC) has to satisfy lead-time criteria, must stick to 15-minutes trading time intervals and is carried out with a power of at least a quarter of the prequalified FCR power ($\overline{P^{FCR}}$). Consequently, the battery and the attached power electronics have to be able to deliver a power of at least $1.25 \cdot \overline{P^{FCR}}$. The simultaneous provision of FCR along the charge management has to be guaranteed.

5.1.2 Degrees of freedom of the FCR provision with a BSS

German TSOs additionally grant a number of DOFs that apply to all FCR-providing technical units. For a BSS, the DOFs enable the battery management system (BMS) to deviate from specific FCR signals. The degrees of freedom offered by the TSOs include:

1. **Dead band usage (DU)**: The range of 10 mHz around the nominal frequency of 50 Hz is referred to as the dead band. In this area, the provision of FCR is not obligatory. Therefore, unwanted FCR within the deadband can be omitted (see Figures 5.2).
2. **Overfulfillment (OF)**: Optional overfilling of up to 120% of FCR is permitted. This DOF can be used to accelerate the charging of the battery at low SOCs or to accelerate the discharging of the battery at high SOCs (see Figures 5.2).
3. **Gradient control (GC)**: Prequalified FCR power has to be provided after a maximum of 30 seconds at times of a frequency deviation of 0.2 Hz. As batteries can react even quicker, the BSS can use the gradient ($\Delta P/t$) as a DOF, i.e., it can slow down unwanted and accelerate suitable frequency responses for SOC management (see Figures 5.3).

The three DOFs presented above decouple the FCR provision to a limited extent from the mains frequency, thus offer the possibility to control SOC levels to remain within the permissible operation range and decrease charge and discharge events that cause costs. In the long term, however, DOFs do not prevent the SOC from exiting the permissible operation range.

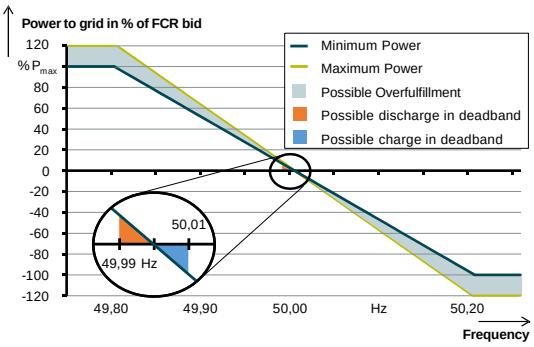

Figure 5.2: Utilization of degrees of freedom overfulfillment and dead band usage
Grid frequency is plotted on the x-axis, requested FCR power (dark blue) is plotted on the y-axis. Light blue (overfulfillment), orange, and blue (dead band usage) fields are permissible adjustments to the power.

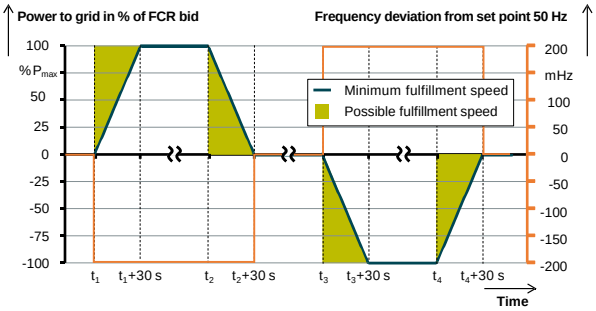

Figure 5.3: Utilization of degree of freedom gradient control
The x-axis shows time in seconds, requested FCR power (dark blue) is plotted on the primary y-axis and grid frequency deviation plotted on the secondary y-axis. Green areas are permissible adjustments to the power.

In the following, the application and model implementation of the three DOFs based on the given regulation is described. These models will then be implemented in a mathematical model that describes the BSS. For all DOFs, threshold SOC levels are defined. The DOFs are used to avoid charge events by moving the SOC to a desired level: Below the SOC threshold SOC^{DOF}, charging of the battery (negative FCR) is assisted; above the threshold SOC^{DOF}, discharging of the battery (positive FCR) is assisted. Furthermore, the same thresholds are selected for all DOFs.

Dead band usage:

Dead band usage can be applied if frequency values lie above 49.99 and below 50.01 Hz, the so-called *dead band*. For FCR within the dead band, it is up to the BMS to follow the FCR request or to eradicate the FCR request completely, leading to $P_t^{DU} \in [0, P_t^{FCR\_request}]$ as shown in Figure 5.2. In this work FCR requests within the dead band is omitted by default ($P_t^{DU} = P_t^{FCR\_request}$); however, if availed for SOC management, FCR requests can be used to stabilize SOC levels ($P_t^{DU} = 0$).

Figure 5.4 shows the use of the DOF dead band versus a reference scenario without the use of the DOF with frequency values of the first two hours of 2016 as implemented in the model. The predefined SOC threshold for dead band usage is set at SOC^{DU} = 50%. The upper part of the figure shows the development of the power signal. The lower part plots the resulting SOC development. As explained, in the reference scenario (no DOF use) requested FCR power within the dead band is by default set to 0. During the whole simulation run, the SOC level exceeds the limit, SOC^{DU}. Hence, the BSS is preferably discharged by providing positive FCR in the scenario "FCR w/ DU" depicted by the red line. Therefore, the DOF is used to increase the power within the dead band to trigger discharging. Power is increased within the dead band if frequency values are lower than 50 Hz. On the contrary, if the frequency rises above 50 Hz within the dead band and the battery is supposed to be charged, these requested FCR power signals continue to be omitted and the final power signal stays at 0.

Figure 5.4 additionally shows the SOC development of a reference scenario without the use of DU and the scenario, which applies DU. It is visible that the SOC can be guided towards the desired threshold of SOC^{DU}= 50%.

Overfulfillment:

As shown in Figure 5.2, overfulfillment can increase the charge ($P_t^{FCR\_request} < 0$) or discharge ($P_t^{FCR\_request} > 0$) using FCR requests by a maximum of 20% of $P_t^{FCR\_request}$. This leads to additional power signal corrections by overfulfillment in the range of $P_t^{OF} \in [0, 0.2 \cdot P_t^{FCR\_request}]$.

In contrast to dead band use, overfulfillment can be applied over the entire frequency range (see Figure 5.2).

Figure 5.5 shows the FCR provision with and without overfulfillment as a function of the SOC. Again limits that trigger DOF use are set at $SOC^{u,OF}$ = $SOC^{l,OF}$= 50%. In Figure 5.5, the SOC level lies above SOC^{OF}. The

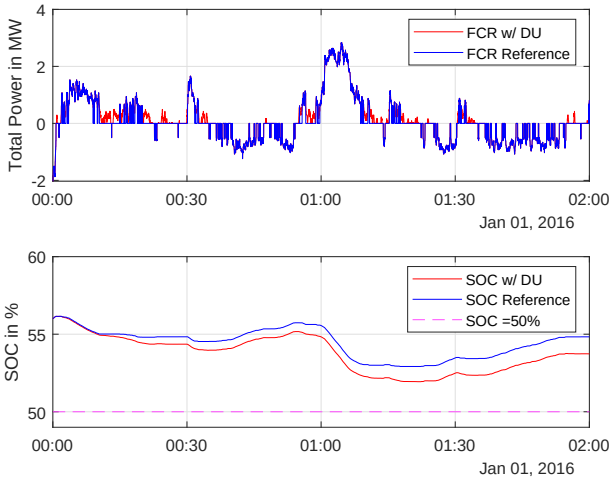

Figure 5.4: Example of the use of the dead band for FCR adjustment Example of the use of all DOFs for FCR adjustment. It shows on the y-axis of the top graph the original FCR target power $P_t^{FCR\_request}$ (FCR Reference), resulting BSS power P_t (FCR w/ DU), and simultaneous SOC development in the bottom graph for four minutes of FCR provision on the x-axis.

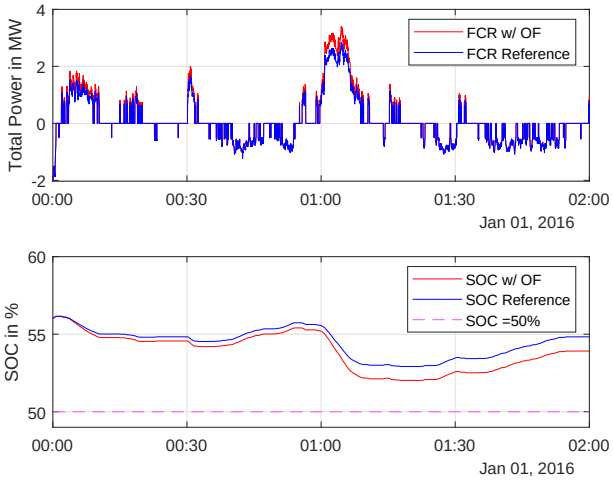

Figure 5.5: Example of the use of overfulfillment for FCR adjustment Example of the use of all DOFs for FCR adjustment. It shows on the y-axis of the top graph the original FCR target power $P_t^{FCR\_request}$ (FCR Reference), resulting BSS power P_t (FCR w/ OF), and simultaneous SOC development in the bottom graph for four minutes of FCR provision on the x-axis.

use of the degree of freedom is therefore taken to increase discharging (positive FCR requests) by 20% ($P_t^{OF} = 0.2 \cdot P_t^{FCR\_request}$). Vice versa, overfulfillment would increase charging if the SOC falls short of SOC^{OF}.

Figure 5.5 displays the SOC development of a reference scenario without the use of the DOF and the scenario, which applies the DOF *overfulfillment*. Similar to the use of DU, it is visible that the SOC can be guided towards the desired threshold of $SOC^{OF} = 50\%$ compared to the reference scenario.

Gradient control:

Gradient control (P_t^{GC}) uses the reaction speed of the BSS as the DOF. The minimum reaction speed requires the battery to provide the prequalified FCR power within 30 seconds; however, especially batteries are able to provide frequency response much faster. As a function of the SOC level, gradient control can be used to slow down unwanted FCR signals as shown in Figure 5.3. As a delay of the response to power levels can lead to an increase or decrease of the effective FCR provision, gradient control is defined all over the FCR range: $P_t^{GC} \in [-P_t^{FCR\_request}, P_t^{FCR\_request}]$; however, it has to fulfill the condition that it satisfies the minimum reaction speed of the requested FCR in the past 30 seconds. As the temporal resolution of the grid frequency values and corresponding FCR signals equals one second, gradient control has to satisfy the reaction speed of the past thirty signals. Only negative FCR leads to the condition $P_t^{GC} \leq \min_e(P_{t-e}^{FCR\_request} - \frac{e \cdot P_{t-e}^{FCR\_request}}{30}), e \in (1, ..., 30)$.

The implementation of gradient control was done by means of two gradients g_{max} and g_{min}. The gradient g_{max} stands for the maximum permissible rate of change of the FCR. The gradient g_{min} for the minimum permissible rate of change. By default, the fast reaction speed g_{max} is used. If convenient, the reaction speed can be slowed down to g_{min}. If the charge level of the BSS crosses the threshold of the threshold, SOC^{GC}, the negative FCR gradient can be limited by using g_{min}. Thus, the charging of the BSS is done slower, i.e., it is delayed, which in the long-term leads to a normalization of the charge level around the desired threshold. The positive gradient continues at normal speed by means of the gradient g_{max}.

In Figure 5.6, the FCR provision is shown for the first four minutes of the year 2016 at times of higher SOC values than SOC^{GC}, i.e., it is beneficial to discharge the battery or slow down charging. Thus, as visible in Figure 5.6, negative gradients (charge) are slowed down by the BSS, GC limits the positive gradient by g_{min}.

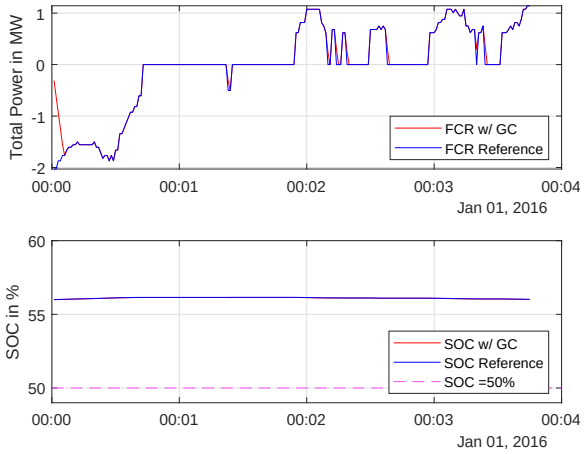

Figure 5.6: Example of the use of gradient control for FCR adjustment
It shows on the y-axis of the top graph the original FCR target power $P_t^{FCR\_request}$ (FCR Reference), resulting BSS power P_t (FCR w/ GC), and simultaneous SOC development in the bottom graph for four minutes of FCR provision on the x-axis.

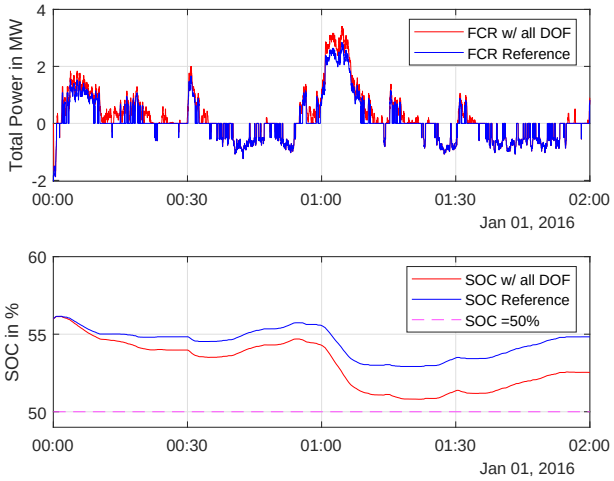

Figure 5.7: Example of the use of all DOFs for FCR adjustment
It shows on the y-axis of the top graph the original FCR target power $P_t^{FCR\_request}$ (FCR Reference), resulting BSS power P_t (FCR w/ all DOF), and simultaneous SOC development in the bottom graph for four minutes of FCR provision on the x-axis.

It is also visible in Figure 5.6 that GC has only a very limited effect on SOC development. This is on the one hand related to the small simulation time; however, results of longer simulations show that the influence of GC on SOC development is rather small compared to other DOFs.
Figure 5.7 shows the combined use of all DOFs for a time period of two hours. It is visible that the SOC development can be influenced significantly. The contribution of DOFs will be further examined below in Section 5.1.5.

5.1.3 Model overview of FCR provision with a BSS

In this section, the individual modules of the implemented model of the BSS are described. To investigate the amount of charge management and the potential to reduce external energy exchanges, a model has been developed that simulates the BSS operation during FCR provision. The time-discrete simulation is performed based on grid frequency values of the year of 2016 with a temporal resolution or time step of one second. The model was developed using MATLAB/Simulink.
The model used in this paper consists of six modules as depicted in Figure 5.8:

1. **Input**: The input data for the model includes the grid frequency time series of the year of 2016, as well as several parameters that define the battery behavior and the charge level management such as the prequalified FCR power and the available capacity.

   FCR is provided depending on the value of the grid frequency as explained in Equation 3.1. If the grid frequency rises above 50 Hz, an oversupply exists in the public grid ($P_t^{FCR\_request}$ takes on negative values) and the BSS is charged to balance the oversupply with negative FCR.

2. **Degrees of freedom**: DOFs are implemented as stated above in the regulatory framework of the FCR-providing BSS. Depending on predefined SOC thresholds, DOFs are utilized to perform SOC management by adjusting FCR requests with the target of minimizing costs of the FCR provision and related charge management. In this model, FCR requests are adjusted by reducing or increasing the power of FCR requests if DOFs are applicable. Applied DOFs are overfulfillment (P_t^{OF}), dead band usage (P_t^{DU}) and gradient

control (P_t^{GC}) as introduced above. Depending on the grid frequency (ν_t) which causes either positive of negative FCR, the effect of the DOF changes, leading to an inverted sign.

$$P_t^{DOFdisch} = P_t^{OF} + P_t^{DU} - P_t^{GC}, \text{ if } \nu_t < 50Hz \tag{5.1a}$$

$$P_t^{DOFch} = -P_t^{OF} - P_t^{DU} + P_t^{GC}, \text{ if } \nu_t > 50Hz \tag{5.1b}$$

3. **Energy exchange**: The energy exchange module receives the SOC at time step t (SOC_t) as an input from the BSS module. If predefined SOC limits are crossed, it triggers charge management using market-based charging or discharging. The predefined SOC limits are defined according to the boundaries of the permissible operation range ($SOC^{l,POR}$ and $SOC^{u,POR}$), the appropriate lead time for Intraday transactions, and the definition of alert states by the TSO.

   Charge management assures that SOC levels stay within the permissible operation range; however, MBC charge events can only be executed with a certain lead time. Due to the gate closure of the Continuous Intraday Market five minutes prior to delivery, a worst-case scenario of 20 minutes lead time for MBC charge events is assumed. That means that an energy buffer has to be created that lies at the edge of the permissible operation area. The buffer is able to provide 20 minutes of FCR without entering the non-permissible operation range. After a maximum duration, an MBC leads to a relaxation of SOC levels. Once the SOC level enters the buffer zone at either $SOC^{l,MBC}$ or $SOC^{u,MBC}$, MBC is triggered which is executed in the next possible 15-minute trading slot. The buffer is defined as to provide 20 minutes of FCR at a frequency deviation of 50 mHz or $\frac{1}{4}\overline{P^{FCR}}$ as defined in [392].

4. **Battery management system**: The BMS executes the introduced logic of modules 2 and 3. Firstly, it uses grid frequency data and battery parameters to calculate requested FCR signals. Requested FCR signals are calculated by the grid frequency (ν_t) as well as the FCR power bid for each product duration as shown in Equation 3.1. Then, the DOFs are added or subtracted from the requested FCR depending on SOC levels. If the battery is approaching the limits of the permissible operation range, energy exchanges are triggered. The final power signals per second for charging and discharging are calculated by the sum of individual power signals of the FCR requests ($P_t^{FCR\_request}$), DOF (P_t^{DOF}) and MBC-related (P_t^{MBC}) energy exchanges and assumed efficiency ratios (η^{ch}, η^{disch}=90%). The efficiencies include the efficiency of the battery and the power electronics.

$$P_t = \frac{1}{\eta^{disch}} \cdot (P_t^{FCR\_request} + P_t^{DOFdisch} + P_t^{MBC}), \text{ if } \nu_t < 50Hz \tag{5.2a}$$

$$P_t = \eta^{ch} \cdot (P_t^{FCR\_request} + P_t^{DOFch} + P_t^{MBC}), \text{ if } \nu_t > 50Hz \tag{5.2b}$$

5. **Battery module**: A physical battery model from the Simscape library was used to model the BSS. It is an SOC-dependent voltage source with resistors connected in series and is able to handle power inputs delivered by the BSS control.

6. **Output**: Charge management, DOF utilization, the SOC, and FCR provision recorded for every time step. Based on SOC and power output profiles, analyses are performed.

Figure 5.9 gives an example of the simulated FCR provision of the BSS including a charge event. The middle graph shows the final power P_t that is applied to the BSS resulting from values of the frequency, the applied DOFs, and charge management in blue. Furthermore, it displays the power level of a simulation without implemented charge management. Furthermore, the top graph displays the SOC level, the dashed red lines depict the threshold $SOC^{l,MBC}$ that triggers a charge management to stay within the permissible operation range. In Figure 5.9 it

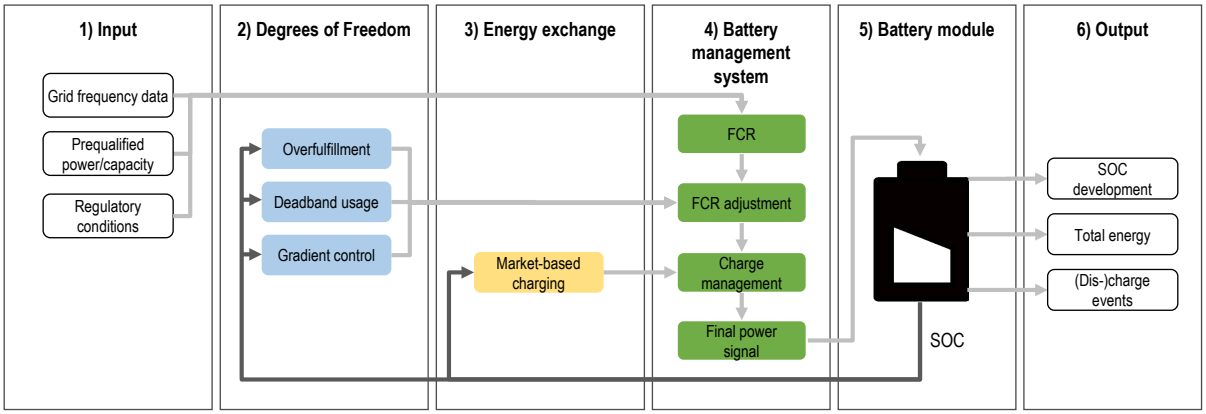

Figure 5.8: Simulation model of BSS providing FCR including individual modules used within the simulation

is visible that the threshold is crossed and, consequently, MBC is triggered in the following 15-minute trading interval shown in the bottom graph.
Due to the MBC a shift of the total power level applied to the BSS is visible (middle graph) while FCR is still provided. As can be seen in the top graph, this leads to a correction of the SOC, which is charged and exceeds the threshold.
The degrees of freedom are assessed according to the costs of the FCR operation of the BSS. Costs have four different sources:

1. Charged energy (any negative FCR) is penalized with fees and surcharges. According to [340, 375], a grid-connected BSS that only charges and discharges energy from the same grid is exempt from most of the grid fees and surcharges except of among others the grid concession fee and the offshore surcharge. These charges amount to a total surcharge of 7.21 EUR/MWh. Furthermore, grid fees with the value of 2.8 EUR/MWh arise for the energy losses of the power electronics which was calculated by the difference in energy charged and discharged.
2. Energy charged and discharged during MBC is bought and sold on the Intraday market. To assess the costs and revenues, Intraday Auction prices of the year 2016 for the 15-minute slots of charge events are used as costs/revenues.
3. Market transactions for MBC usually yield a transaction fee. In this work, a transaction fee of 3 EUR/MWh for both charge and discharge events is assumed. This transaction fee is accounted for both charge and discharge events of MBC.
4. Balance energy has to be paid for the difference between charged and discharged energy per 15 min. slots. The difference in energy charged and discharged has been multiplied with the average balance energy cost from the year 2016 taken from [66].

5.1.4 Simulation

Based on the described model, a simulation over 168 days (24 weeks) of the year 2016 has been performed that calculates SOC development, charge management activation, costs described above, and full-cycle equivalents (FCE). The simulation is performed with a BSS of a capacity $\overline{E}$ = 2.8 MWh and a power of $\overline{P^{FCR}}$ = 2.5 MW.
The investigated scenarios are shown in Table 5.1. The scenarios were selected as follows: Scenario 1 describes the reference scenario for the provision of FCR without the use of any DOFs. Scenario 2 uses DOFs around an SOC of 50%. Scenario 3 enables the comparison with a BSS with a lower prequalified FCR power. Scenario 4-6 show the impact of individual DOFs and Scenario 7 enables the impact of different SOC thresholds for DOF use.

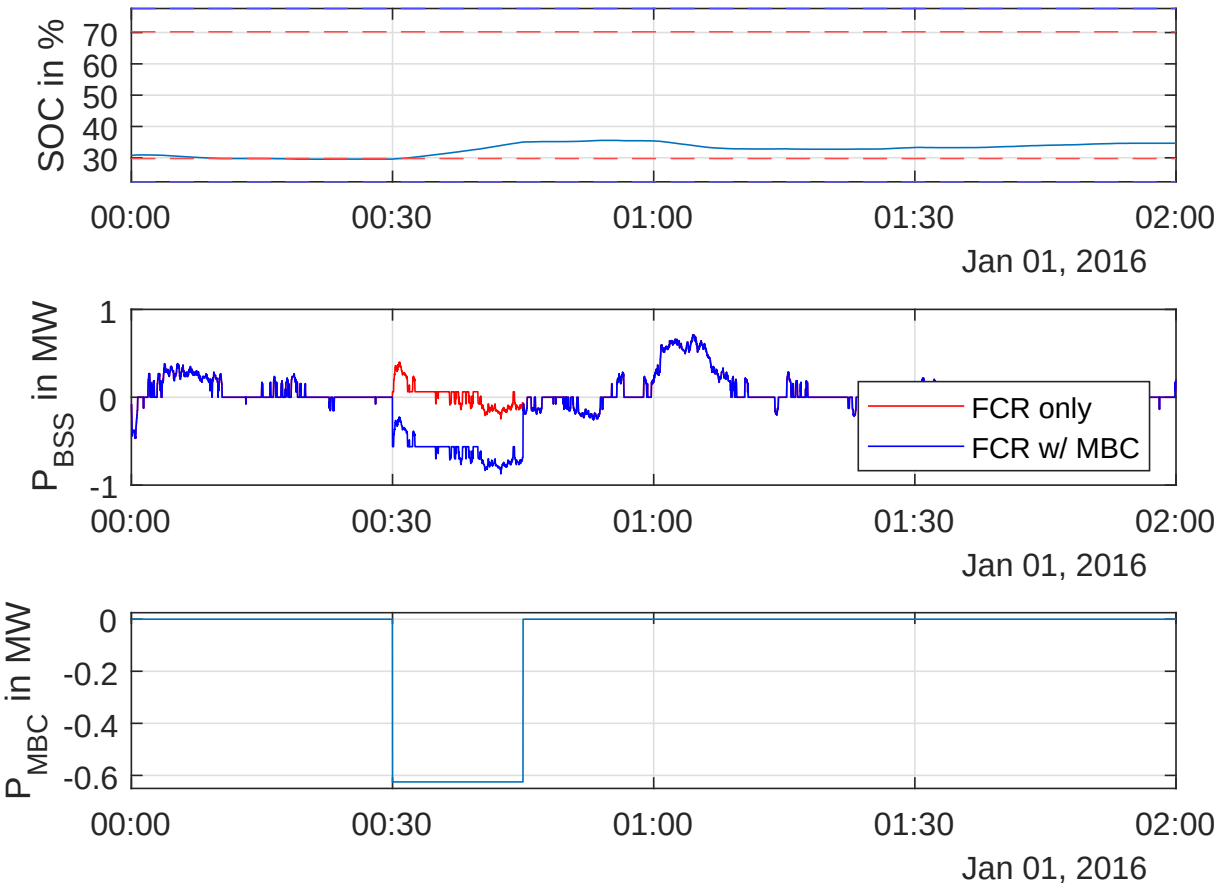

Figure 5.9: Example of charge management for charge of BSS while simultaneously providing FCR
The figure shows on the y-axis SOC development in the top graph, requested FCR power $P_t^{FCR\_request}$ (FCR only) and final power P_t (FCR w/ MBC) in the center graph, and MBC in the bottom graph for two hours of FCR provision on the x-axis

Table 5.1: Scenarios investigated for simulation of a BSS providing FCR

Scenario	P^{PQ_FCR}	$\overline{E}$	DU	GC	OF	SOC^{DOF}
1	2.5 MW	2.8 MWh	-	-	-	50%
2	2.5 MW	2.8 MWh	√	√	√	50%
3	2 MW	2.8 MWh	√	√	√	50%
4	2.5 MW	2.8 MWh	√	-	-	50%
5	2.5 MW	2.8 MWh	-	√	-	50%
6	2.5 MW	2.8 MWh	-	-	√	50%
7	2.5 MW	2.8 MWh	√	√	√	60%

5.1.5 Results

Figure 5.10 shows a contour plot for Scenario 1 of the resulting final charge and discharge power of the BSS (P_t) as a function of the SOC (SOC_t) and the given grid frequency (ν_t) of the simulation.
Generally, the final power applied to the BSS is a function of the grid frequency, which is visible by the mainly SOC independent colored lines that move up vertically; however, one can also identify the SOC dependent influence of the use of DOFs and execution of MBC on the final power within the figure:
MBC is visible in the bottom and top SOC areas. If lower SOC levels are reached, MBC is used to charge the battery with energy procured on the electricity markets. This leads to a decrease of the final BSS power and is visible by the shift of power levels on the bottom of the graph by a darker color. In a contrary manner, MBCs are used to discharge the BSS at high SOC levels, leading to an increase of the final BSS power level and a lighter coloring in the contour plot. Furthermore, at high grid frequency deviations, MBC seems to cause a strongly increased or strongly decreased power due to the use of MBC. This leads to a change of final BSS power by around 2.5 MW and is visible by the neutral coloring at the left and right side of the graph. As these extreme frequency levels rarely occur (see the histogram in Figure 3.6), the low number of data samples should be considered.
The SOC levels are further displayed in a histogram of Figure 5.11. The thresholds $SOC^{l,MBC}$ and $SOC^{u,MBC}$ that trigger MBC are shown in the red dashed line, while the limits of the permissible operation range $SOC^{l,POR}$ and $SOC^{u,POR}$ are shown in the dashed blue line. It is visible that normal FCR BSS operation as defined in Scenario 1 leads to a concentration of SOC levels close to the lower end of the permissible operation range. This is due to efficiency losses that cause an unbalanced amount of energy charged and discharged.
Figure 5.12 displays the same contour plot for Scenario 2. The use of DOFs is visible around at SOC levels of 50%. SOC levels higher than 50%, the defined threshold SOC^{DOF} causes a parallel shift of the final BSS power delivered: At higher SOCs, the power is increased by the DOFs, if possible, to cause a faster discharge. At lower SOCs, the power is decreased to cause charging of the battery.
In the histogram, Figure 5.13, it is visible that due to the placement of SOC^{DOF}, DOF use will guide the majority of SOC levels towards the region around $SOC = 50\% = SOC^{DOF}$.
Figures 5.14 and 5.15 display the same results for Scenario 7 with a threshold at the SOC of 60%. The described shift between FCR and frequency is visible at the new threshold SOC level. The histogram displays a peak around the level of 60%, thus also displaying the threshold. The skewness of the histogram to the left remains although it is slightly lower than in Figure 5.13.
Figure 5.16 indicates the energy charged to the battery for the provision of negative FCR and the necessary discharged energy for the provision of positive FCR for the predefined scenarios. Although the frequency is well balanced around the standard frequency of 50 Hz, it is visible that the energy needed for positive FCR is much larger than the energy needed for negative FCR. This is due to the efficiency losses during charge and discharge processes. Total FCR provides the difference between positive and negative FCR. Figure 5.16 shows that the use of DOFs actually increases the energy used for both positive and negative FCR provision; however, the difference between positive and negative energy decreases. It is visible that Scenario 7 depicts the lowest total FCR due to the provision of the highest amount of negative FCR.
Figure 5.17 shows the energy needed for MBC. It is visible that the energy used for market-based charging and discharging is reduced significantly using DOFs. The greatest impact of the implemented DOFs is given by the DOF dead band usage. Furthermore, a great reduction of energy needed for charge management is given by the reduction of prequalified and bid FCR power as shown by the comparison of Scenario 2 and Scenario 3.
The costs necessary for FCR operation are visible in Figure 5.18. While the discharge of energy using MBC mostly (in case of positive energy prices) yields revenues (red column), the charge of energy leads to costs (blue column) as this energy has to be procured on the electricity markets. Furthermore, grid fees have to be paid for the charged energy using the provision of negative FCR (green column) and balance energy costs arise from the

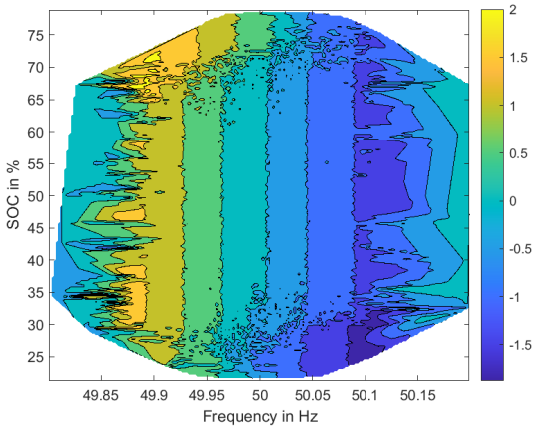

Figure 5.10: Contour plot of Scenario 1
Contour plot of final BSS power (color scale) in relation to the SOC of the BSS (y-axis) and the grid frequency (x-axis) without the use of DOFs

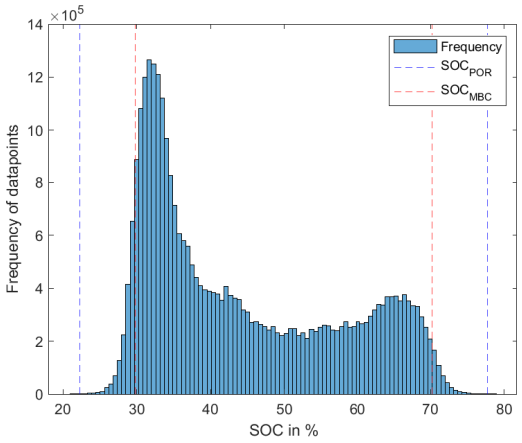

Figure 5.11: Histogram plot of SOC levels of Scenario 1
The dashed red line shows the thresholds SOC^{MBC} that trigger MBC, dashed blue line the limits of the POR SOC^{POR}

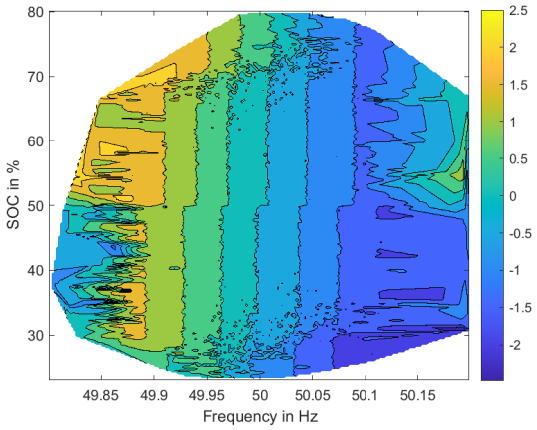

Figure 5.12: Contour plot of Scenario 2
Contour plot of final BSS power (color scale) in relation to the SOC of the BSS (y-axis) and the grid frequency (x-axis) with $SOC^{DOF} = 50\%$

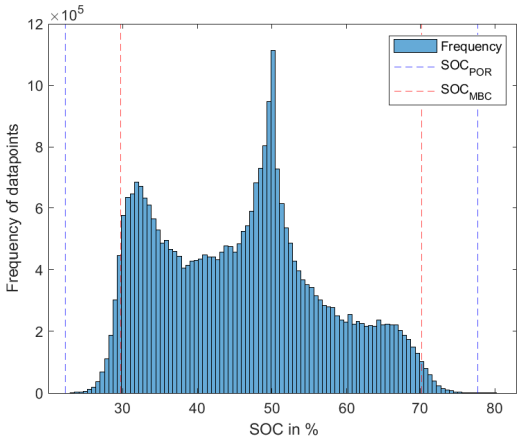

Figure 5.13: Histogram plot of SOC levels of Scenario 2
The dashed red line shows the thresholds SOC^{MBC} that trigger MBC, dashed blue line the limits of the POR SOC^{POR}

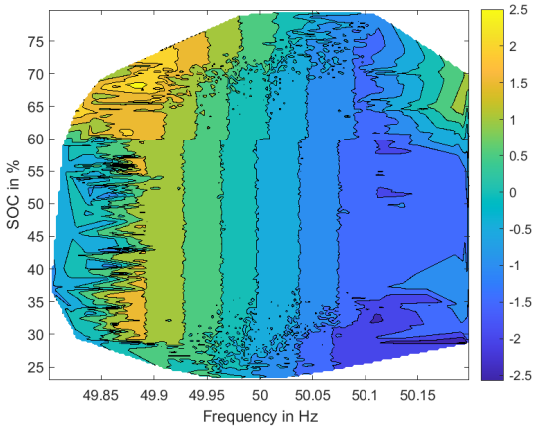

Figure 5.14: Contour plot of Scenario 7
Contour plot of final BSS power (color scale) in relation to the SOC of the BSS (y-axis) and the grid frequency (x-axis) with $SOC^{DOF} = 60\%$

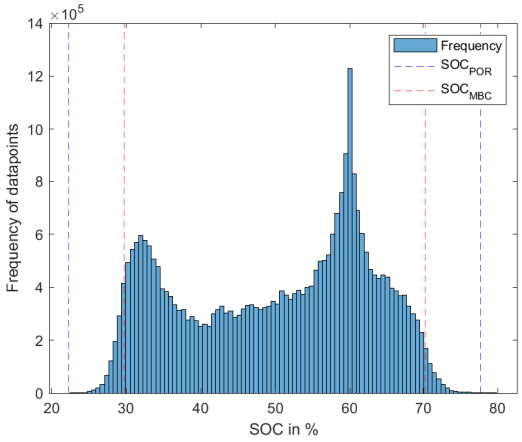

Figure 5.15: Histogram plot of SOC levels of Scenario 7
The dashed red line shows the thresholds SOC^{MBC} that trigger MBC, dashed blue line the limits of the POR SOC^{POR}

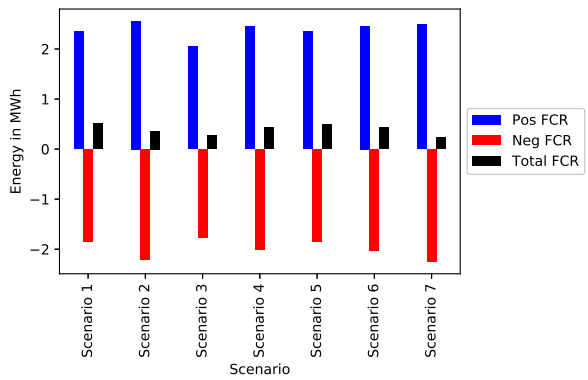

Figure 5.16: Average daily FCR in MWh provided by the BSS for individual scenarios
FCR is divided into positive (blue bars) and negative (red bars) FCR

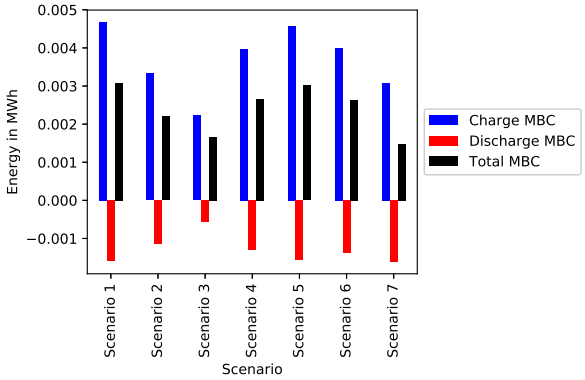

Figure 5.17: Average daily MBC in MWh of the BSS for individual scenarios
MBC is divided into charge (blue bars) and discharge (red bars)

electricity balance between positive and negative electricity (yellow column). For MBC related costs, it is visible that the costs for charging greatly exceed the revenues for discharging for all scenarios because of the higher necessary energy amounts as shown in Figure 5.17. Scenario 2 can reduce greatly the cost of MBC charging as opposed to Scenario 1 by applying DOFs; however, the revenues from MBC discharging also decrease as less market based charging is done. Scenario 3 can further decrease the total costs; however, this is done at the expense of lowering the total prequalified FCR power. Scenario 7, on the other hand, which shifts SOC values towards the value of 60%, can slightly decrease costs related to charging and increase revenues from discharging concerning MBC. Furthermore, Scenario 7 greatly decreases the costs for balance energy as energy amounts for charging and discharging are more balanced out (see Figures 5.16 and 5.17). This is done at the expense of higher grid fees due to more charging by providing more negative FCR; however, the savings clearly compensate for the extra cost. Looking at the graph, future work can look at the impact of an even greater value for the threshold (SOC^{DOF}) to further lower costs.

Figure 5.19 sets the costs of the individual scenarios into perspective with the revenues of FCR commercialization assuming the average FCR price (2870.42 EUR/MW per week) for the years of 2015-2017. It is visible that it is not valuable to pursue Scenario 3 with a much lower prequalified FCR power. Although the operational costs are the lowest, the reduction in FCR remuneration of this scenario does not justify the reduction of the prequalified FCR power. Scenario 7 yields the highest total revenue: The operational costs only take up 3.92% of the FCR income as opposed to 5.67% in Scenario 1. This results in a reduction of the operational cost by 31%. Scenario 7 is used as the basis for the cost estimate of FCR provision by a BSS in Chapter 6.

Figures 5.20 and 5.21 show the average SOC that the battery operates on, the SOC standard deviation, and the full cycle equivalent (FCE) associated with every single scenario. Results show, that the use of the DOFs lead to higher FCEs (7%) as more energy is charged and discharged and a higher mean SOC (3%) as the DOFs are mostly used to lift the SOC. An increase in FCE can lead to faster degradation of the battery capacity, which is not accounted for in this work. Scenario 7 further increases the mean SOC to slightly above 50%, which can be explained by the strategy of trying to push SOC levels to elevated levels using DOFs. This can also be seen in Figure 5.15.

5.2 Potential of a BSS participating in Intraday trading

Next to the provision of control reserve as described in the previous section, buying and selling electricity on Intraday markets proves to be an interesting use case for a BSS. This section, therefore, describes the methodology to assess the potential of a BSS trading on the Intraday Continuous Market of the European Power Exchange

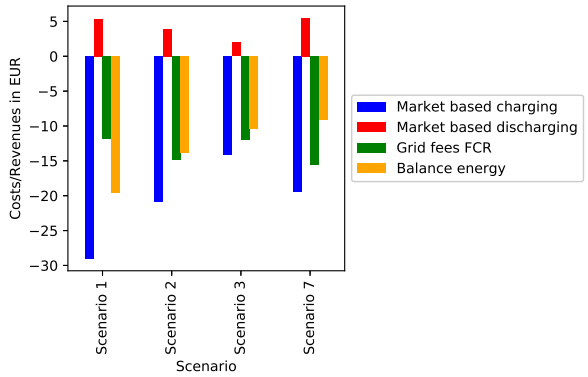

Figure 5.18: Average daily costs and revenues associated with MBC, grid fees, and surcharges for individual scenarios

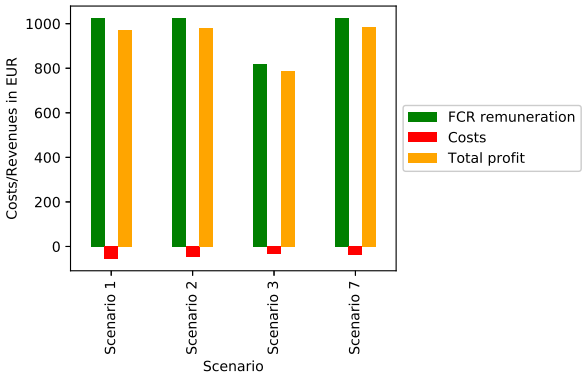

Figure 5.19: Operational costs compared to revenues of FCR provision for individual scenarios

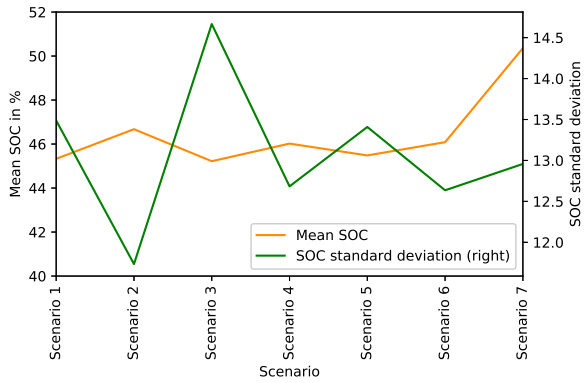

Figure 5.20: Mean and standard deviation of SOC for individual scenarios

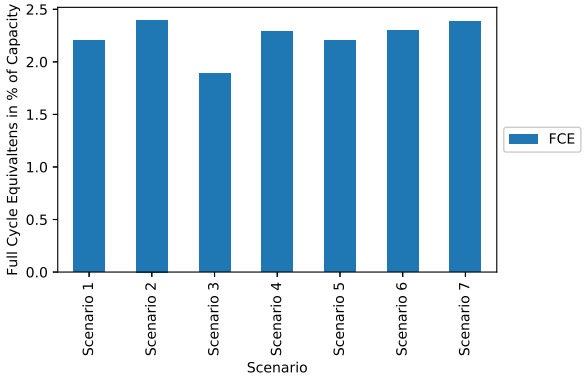

Figure 5.21: Average daily full cycle equivalents of the BSS for individual scenarios

(EPEX) spot market. The section aims to provide the daily revenue potential for the flexibility service *energy market operation* to be used in the dispatch optimization in Chapter 6. The model results from work published in the publication *Analysis of the German Continuous Intraday Market and the Revenue Potential for Flexibility Options* [330].

The contribution is organized as follows: Section 5.2.1 introduces the market design of the Intraday Continuous Market, Section 5.2.2 gives an overview of existing literature on the optimization of flexible energy devices participating in this power market, and Section 5.2.3 presents the methodology and condensed results of the performed analysis of intraday trading transactions. Section 5.2.4 introduces the proposed methodology for the optimization of flexibility options, and Section 5.2.8 shows the corresponding results.

5.2.1 Market Characteristics of the German Intraday Continuous Market of the European Power Exchange (EPEX)

As shortly described in Section 2.2.3, short-term power trading for the German power region is done on three different markets: (1) the Day-Ahead Auction, (2) the Intraday Auction, and (3) the Intraday Continuous Market. As opposed to the auctions, energy delivered within the same day can be traded on the Intraday Continuous Market. Although the majority of energy among those three markets is still traded on the Day-Ahead Auction, the volume traded on the Intraday Continuous Market steadily increased over the last years (see Table 5.2).

In addition to hourly products of the Day-Ahead Auction, the Intraday Continuous Market of the German market region allows trading 15-minute products and 30-minute products (since March 2017). Trading begins every day

Table 5.2: Traded yearly energy and average daily number of transactions on the German Intraday Continuous market

		2015	2016	2017
Traded yearly energy (TWh)	**Total**	**35.4**	**38.1**	**44.1**
	1h	27.7	30.6	36.5
	1/2h	–	–	0.1
	1/4h	4.0	3.8	4.9
	Block	3.6	3.7	2.6
Average daily number of transactions (thousands)	**Total**	**13.03**	**18.26**	**27.76**
	1h	6.31	9.45	12.62
	1/2h	–	–	0.06
	1/4h	6.71	8.85	15.09
	Block	0.02	0.02	0.01

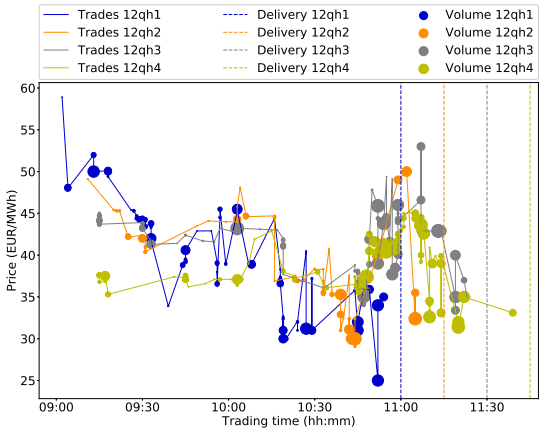

Figure 5.22: Price development at the Intraday Continuous Market prior to delivery
Single trades with their prices (y-axis) and volumes (marker size) for four subsequent products on an exemplary day (24th Oct. 2017)

at 15:00 h with the continuous trading of hourly products and an opening auction for the quarter-hour products (Intraday Auction). The opening auction results in a reference price signal for the continuous trading of quarter-hour products, which then opens at 16:00.
Market participants enter their bids in an electronic trading system known as the order book. If a buy bid and a sell bid match, they are merged into one transaction or trade. It is also possible to accept a bid in the order book directly instead of entering a counter bid. Accordingly, continuous intraday trading follows the "pay-as-bid" principle, i.e., the bid price is realized. Within the same control area, transactions are possible up to five minutes before the start of the delivery period. For transactions between different control areas, this lead time is 30 minutes.

Figure 5.22 gives an example of the price development of the continuous intraday trading of four neighboring quarter-hour products over the indicated trading time. Prices and volumes are changing for almost every transaction. Especially close to the delivery time, an increase of liquidity in the market can be recognized.
Short lead times, quarter-hour products, and high transparency in the form of an open order book characterize continuous intraday trading. Consequently, intraday trading is well suited for market participants that act flexibly and spontaneously. In particular, unplanned power plant outages, changed weather conditions in the generation of renewable energies and other spontaneous and unforeseen changes in generation and consumption require a marketplace in which these can be compensated by balancing responsible parties.

5.2.2 Related work concerning modeling of Intraday trading

An in-depth analysis of the German quarter-hourly Intraday Auction is provided in [58]. As main drivers for trading volume and price formation in the quarter-hourly auction, the authors identified solar power production as well as gradients of demand and the ramps of thermal power plants. On the other hand, [6, 211, 310] show that, above all, Intraday Continuous trading, as opposed to the Intraday Auction is used to correct forecast errors from wind power generation.
Braun et al. also published several works on the scheduling of hydro power storage on the Intraday Continuous market [56, 57, 59]. The authors identified high monetary potential for storage limited flexibility options.
[161] construct a fundamental model and use 2010-11 continuous Intraday data and analyze the difference of day-ahead and volume-weighted Intraday. They show that ex-post forecast error wind, ex-post forecast error PV, and

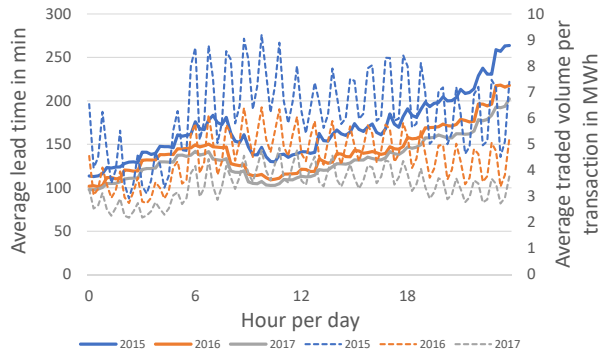

Figure 5.23: Lead time and volume of trades for years 2015-17
Average time spans between trading time and product delivery (left y-axis, solid lines) and average traded volumes per transaction (right y-axis, dotted lines) per 1/4h product for three years

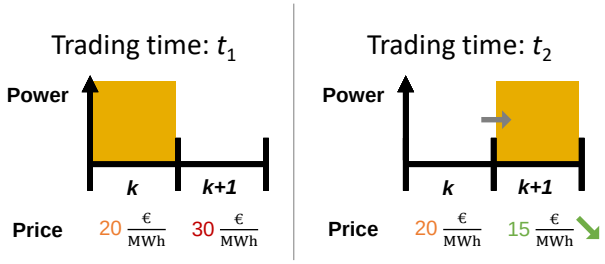

Figure 5.24: A simplified example illustrating the flexibility potential of an electric vehicle
It shows prices and optimized schedules consisting of two time slots k and $k+1$ at the trading time t_1 and the later trading time t_2

unplanned outages of power plants significantly change the Intraday prices in a regression analysis. Nevertheless, it is questionable whether Intraday trading today is comparable to data from a decade before.
In [267] the scheduling of industrial processes based on the German Day-Ahead and Intraday Continuous Market has been investigated using a mixed-integer linear program. In line with the previous reference, the authors confirm that additional intraday trading allows to significantly lower the energy costs.
In [262] a market model of the German Continuous Intraday Market is presented based on the EPEX Spot M7 order book data, which contains all orders submitted to the market, i.e., also orders that have not been executed. While the paper at hand is based on EPEX transaction data, i.e., orders that have been executed, such a market model could be used for evaluating trading strategies and flexibility potentials in a more detailed way.

5.2.3 Analysis of Intraday Trading

Based on all EPEX Intraday Continuous Market transactions from 2015 to 2017 [109], an analysis to identify characteristics of and structural changes within the market is performed.
An increase in both the volume and the number of transactions, as well as the increasing trading frequency, point out the increasing importance of the intraday market. Table 5.2 in the Appendix displays the total traded volume and the number of transactions from 2015 to 2017. The share of traded volume and number of transactions among the different product duration (1h, 1/2h, 1/4h or block products for several hours) did not change significantly in the investigated time interval. It can be seen that 1h products account for the majority of energy traded.
Figure 5.23 shows the average lead time and the average traded volume per transaction for all 96 1/4h products. The lead time, as well as the traded volume per transaction, decreased from 2015 to 2017. This indicates that trading has moved closer to the actual delivery and supports the idea that the traded volume per transaction for 1/4h products has decreased (as seen in Table 5.2). The positive gradient of the lead time curve is given by the fact that later products can be traded longer than earlier products as trading begins at the same market opening time. The lead time plot takes a dip around noon, which could be linked to increased trading during normal office hours. Another explanation could be the higher trading demand for PV generation regarding the continuous changes in weather forecasts. The high trading volumes of the first and the last quarter-hour of each hour of the day reflect the compensation of load and generation ramps after hour-wise trading of the Day-Ahead auction.
While trading structures remain constant regarding product shares, price development within single trading periods and trading times, our analysis shows that absolute volumes and the number of transactions have increased. In

recent times the Intraday Continuous Market has been used more flexibly and closer to delivery. Hence, this raises the question if, and to what extent, flexibility options bear revenue potential in this environment.

5.2.4 Methodology for Analyzing Revenue Potentials of a BSS

One option to realize monetary profits using flexibility options is to benefit from price differences among products in the power market and temporal price differences of a single product.
Figure 5.24 gives a simplified example of the potential for a flexibility option on the Intraday Continuous Market. Imagine an EV including a battery, which could be charged either at time slot k or time slot $k+1$ to fulfill its energy requirements for the next trip. If prices for both time slots differ, the required energy would thus be purchased for the time slot with the lowest electricity price, for example, time slot k at trading time t_1. After a while, at trading time t_2, a sudden drop in the price for power in time slot $k+1$ allows to sell the purchased energy amount for time slot k, and to buy the same amount for time slot $k+1$ instead. In the simplified example, the cost for the charge is therefore reduced from 20 EUR/MWh to 15 EUR/MWh.
Contrary to power plants, batteries are not dependent on fuel costs but are dependent on electricity prices for different time slots. According to [413] batteries are regarded as so-called spread option in the described example above as batteries are being used as long as the spread between two prices is high enough to cover efficiency losses for charge and discharge.
Once electricity prices (i.e., respective buy or sell bids that will be matched) for different charging time slots (i.e., power products) change over time, a price-optimized charging control can continuously change the charging schedule in order to profit from price volatility. With quickly changing prices over time on continuous markets, automatic real option trading on continuous markets can thereby accumulate profits using the same flexibility of devices multiple times.
A minimum trading duration of 7.9 hours for the power product with the earliest delivery time at 00:00 and a maximum duration of 31.7 hours for the power product with the latest delivery at 23:45 is given in the continuous Intraday market. The methodology to quantify the revenue potential of the BSS on the Intraday Continuous Market follows three steps that are subsequently explained in detail:

1. Development of a model for the German Intraday Continuous Market based on historical market data.
2. Definition of the flexibility models based on the approach of [315].
3. Implementation of a simulation based on the market model and the flexibility models.

5.2.5 Market Model

The Intraday Continuous Market is modeled using transaction data of the quarter-hour products. Each transaction is marked by the trading time, the traded power product (time of delivery), the product price, and the volume (energy amount). Firstly, all transactions are sorted by trading time.
The transaction data is prepared in two data frames, one for price related data and one for volume related data. The columns are given by individual transactions, the lines represent the 96 traded products. As a very first column, the results of the Intraday Auction are used, which contain the market clearing prices and the traded volumes per quarter-hour product of each day for an initial optimization. The consecutive columns are filled using information from the sorted list of transactions. For every registered trade, a new column is created. The values of the previous column are copied and only the prices and volumes of the new transactions are updated. This creates a total data frame with 96 x (I+1) dimensions.
Therefore, the price related data frame shows a price column for the market state after each transaction. Thus, it is assumed that the price of the last transaction of a product represents the current price level and that these prices can be realized again regardless of the elapsed time since the previous transaction of this product.

This modeling approach allows the price level of the market to be mapped without any knowledge of order book data or forecasts of future market developments. The price dynamics can alternatively be mapped by calculating the current price level as the average of the previous and subsequent transactions. The aim, however, is to derive the revenue potential of flexibility options independently of the prices expected in the future.
In addition, the current price level can be defined as the volume-weighted average of all transactions already concluded. In this case, the variance decreases as the number of transactions within the trading interval increases. Extreme prices are mitigated under this assumption, which is why price dynamics are not fully exploited in this modeling approach.
Furthermore, the following assumptions are taken:

1. Market conditions from 2017 are used: A lead time of five minutes is uniformly assumed and reflected in the transactions.
2. All contract sizes are regarded as tradable, whereas EPEX Spot specifies a minimum product size of 100 kW and a minimum increment of 100 kW.

5.2.6 Flexibility Models

For the modeling of power and energy-constrained flexibility options that function like a BSS, this work refers to one of three flexibility models presented by Petersen et al. [315]. This abstract device class *bucket* is modeled as a linear program using power and capacity restrictions. This work adjusted the objective function and constraints of the presented model in [315] to model the flexibility service EMO for a BSS.

Flexibility Model Bucket

The *bucket* model represents storage applications that can be actively charged and discharged by optimization decisions in Equations 5.3. It is modeled as an LP with constraints describing mainly power and energy levels.
Index t represents the time of charge. The time of charge is given by the quarter-hour time interval traded on the Intraday markets. The time step Δt of this simulation, thereby, equals 15 minutes.
Energy input/output e_t is restricted by $\underline{P}\Delta t < 0$ (generation) resp. $\overline{P}\Delta t > 0$ (consumption). Regarding limited storage capacity, the charge level E_t is restricted to the physical limits $\underline{E} = 0$ and $\overline{E}$, and it is recursively defined by the previous time slot. The duration of one single time slot is given by $\Delta t = 15\text{min}$. For this kind of abstract flexibility, this work assumes boundary values $E^{start} = 0.5 \cdot \overline{E}$ at the beginning of the optimization horizon ($T = \{1,...,t_{\max}\}$), and $E^{end} = 0.5 \cdot \overline{E}$ at the end of the optimization horizon.

$$\underline{P}\Delta t \leq e_t \leq \overline{P}\Delta t, \forall t \in T \tag{5.3a}$$

$$E_t = E_{t-1} + e_t, \forall t \in T \tag{5.3b}$$

$$0 \leq E_t \leq \overline{E}, \forall t \in T \tag{5.3c}$$

$$E^{start} = 0.5 \cdot \overline{E}, E^{end} = 0.5 \cdot \overline{E} \tag{5.3d}$$

For batteries with higher power levels than the minimum order size of 100 kW, the constraint 5.4 is added to include a limit to the latest registered volume of an Intraday power product (V_t) of a single trade similar to the log of prices of transactions as described in Section 5.2.5:

$$-V_t \leq (e_t - e_t^{plan}) \leq V_t, \forall t \in T \tag{5.4}$$

The currently traded volume is given by the difference between the resulted schedule of the previous optimization, e_t^{plan}, which is provided as a parameter time series, and the updated schedule, e_t. This constraint prevents to trade

more than the latest registered volume to account for market liquidity. It is important to add that e_t^{plan} is provided as a known parameter and is not a decision variable.
Using the following objective function, trading revenues resulting from price differences of products for different delivery time slots t are maximized:

$$\max \sum_{t=1}^{t_{\max}} (\tau_t \cdot (e_t^{plan} - e_t)) \tag{5.5}$$

Further assumptions and possible shortcomings

Grid fees of a grid-connected BSS amount to 7.21 EUR/MWh for the energy taken from the grid as explained in Section 5.1.3. These were accounted for the charged energy of the final schedule of the BSS after all transactions are completed. Due to the consequent charging and discharging in the bucket model, the amount of energy charged can take off a high share of revenues.
In practice, additional transaction fees and energy losses due to efficiencies have to be considered; however, the implementation of these additional cost components requires charged and discharged electricity to be modeled individually. A MILP implementation of this altered problem can be found in the Appendix (Equations A1).
The optimization problem including transaction fees (0.09 EUR/MWh) and charging and discharging efficiencies (both at 90%) was run for individual days to compare the results with the simplified LP bucket model described above. This was done for 20 days of trading. Results showed that the introduction of efficiencies and transaction fees led to 11.1% ($= \phi$) less results. As the second model has higher adequacy to model a real BSS, results from the bucket model were multiplied with the factor $(1 - \phi)$.
Furthermore, the performed simulation does not account for degradation effects due to cyclical aging caused, for example, by a high depth of discharge. The participation in electricity markets with a BSS generally leads to the utilization of maximum power levels and the whole capacity range. To avoid high degradation of the BSS a similar approach as in [212] is taken which accounts for these different aging effects by oversizing the BSS capacity. To avoid extreme SOC ranges, this work limits the battery capacity to the permissible operation range for FCR provision indicated in 5.1. At the case study, this equals a resulting capacity of the BSS of 1.4 MWh. This approach permits to not model the constant voltage charging levels as no storage levels at extreme ends are accessed. Although extreme SOC ranges are not touched, rough estimates that the FCE of the flexibility service EMO are 6-7 times higher than the FCEs for FCR displayed in Figure 5.21.
In Equations 5.3a it is visible that start and end storage levels are set at 50% of the energy capacity. Instead of setting strict limits at the end of the day, a rolling window could have been employed as in [289] to allow different start and end storage levels.

5.2.7 Simulation

The aim of the simulation is to quantify the daily revenue potential of flexibility. Revenues are generated by optimizing the device's schedule according to the current market condition and the device model. The simulation consists of the following steps:

1. The schedule (e_t for all quarter-hours t) of the device is first optimized on the Intraday Auction defining the first schedule by using the first column of the data frame from the presented market model and its prices $\tau_{t,0}$. The given schedule (e_t^{plan}) is set to 0 for all values of t. Costs or revenues of this first optimization are not considered to identify the revenue potential of exclusively continuous trading.
2. Market prices τ_t are retrieved from the next column of the data frame. A new optimization run is performed to get a new schedule e_t. The value of the objective function reflecting the trading revenues is summed up.
3. Step 2 is repeated until the data frame is completely processed.

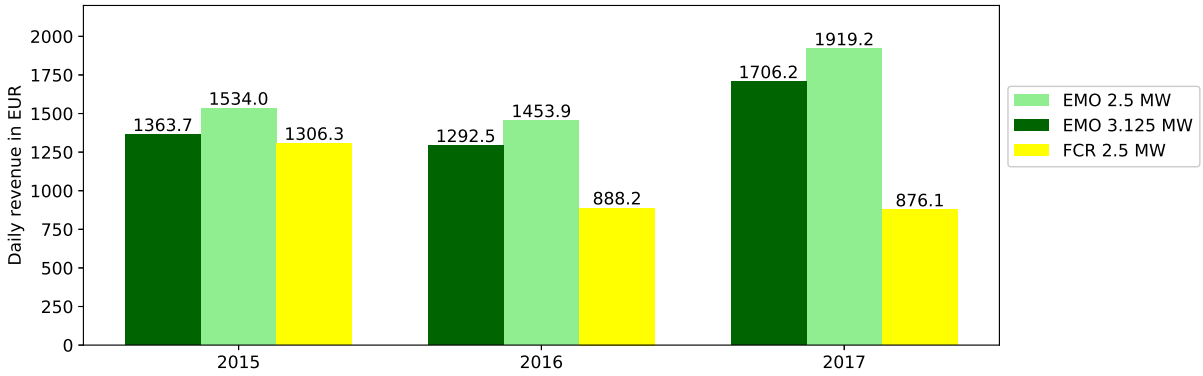

Figure 5.25: Average daily revenue for flexibility services EMO and FCR with indicated maximum power levels

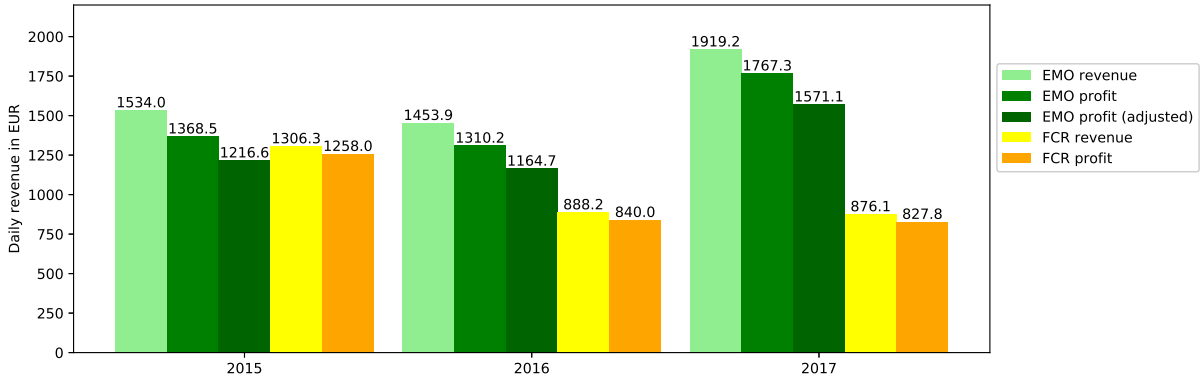

Figure 5.26: Average daily profit comparison of flexibility services FCR and EMO with a BSS with 3.125 MW EMO and 2.5 MW FCR

4. Fees for grid services are accounted for all charged energy of the resulting schedule.

The optimization is carried out for all days in the years 2015–2017. The trading interval begins at 16:00 on the previous day and ends at 23:40 on the delivery day. At this time, the minimum lead time for the 96th quarter-hour, 23:45–24:00, ends. The optimization horizon is adjusted once products reached their gate closure time. For example, for transactions completed at 13:02, the schedule is only optimized for the period from 13:15 to 24:00. In this example, the already implemented and realized schedule for the quarter-hour products 00:00 to 13:00, is fixed.

The simulation including the optimization model has been implemented in R and the optimization problem has been solved with the commercial solver Gurobi.

The simulation was carried out with the parameters of a $\overline{E} = 1.4$ MWh and maximum power levels $\overline{P} = \{2.5\,\text{MW}, 3.125\,\text{MW}\}$. The set capacity equals the capacity of a partition of the BSS at the target industrial site. The power levels are set to equal the prequalified FCR Power ($\overline{P^{FCR}}$) and the maximum power possible with installed power electronics ($1.25 \cdot \overline{P^{FCR}}$) of the individual partitions of the BSS at the target site. The results are used to assess the revenue potential of the flexibility service *energy market optimization* for the dispatch model in Chapter 6.

5.2.8 Results

Figure 5.25 shows the average daily revenue for the simulation performed with a BSS of 1.4 MWh with the same parameters as the BSS at the target industrial site. The maximum power is set at two levels: 1) the maximum

power of the BSS including power electronics (3.125 MW), and 2) the power commercialized as FCR (2.5 MW). Furthermore, revenues for the same BSS commercializing its flexibility as FCR is displayed.

For the flexibility service EMO, similar revenues over the years 2015–2016 for both power levels are visible. The year 2017, however, showed 28% higher revenues. This could be explained by the higher number of transactions of quarter-hour products in 2017 shown in Table 5.2, which would lead to a higher number of possible optimization runs per day in the market model.

For the higher power level, slightly higher daily revenues are visible. With higher power the battery can increase the traded power. The increase in revenue from the low power scenario (EMO 2.5 MW) to the high power scenario (EMO 3.125 MW) is lower than the actual increase in power. This can be related to the constraint on capacity and tradable volume. Some trades cannot be executed with higher power, as the battery reaches storage limits or the tradable volume is not sufficient.

Figure 5.25 also gives a comparison of the average daily revenue of the flexibility options EMO, investigated in this section, and FCR, investigated in the previous section. The flexibility service FCR shows decreasing revenues over the years 2015–2017. It is also visible that both flexibility services are quite competitive in terms of revenues as average daily revenues show similarity in the year 2015. In years 2016 and especially 2017, however, the flexibility service EMO shows much higher revenues.

As mentioned above, the revenues gained for the flexibility services EMO and FCR yield costs such as grid fees under the current regulatory framework. Furthermore, the results of the flexibility service EMO has been adjusted due to shortcomings in the applied model. The final results for the actual operating profits[2] of these flexibility services is shown in Figure 5.26. Results for the flexibility service EMO are displayed for the maximum power level 3.125 MW.

For EMO, the light green column displays the actual revenues, the green column shows the revenues minus the grid fees. These profits are then adjusted by the factor $= \phi$ to display the final estimated profits. For FCR, the yellow column displays the actual revenues and the orange column shows the revenues minus the costs for grid fees, balance energy, and charge management.

It is visible that the operating cost of the flexibility service EMO has a much higher share of costs relative to the revenues as opposed to the flexibility service FCR. Due to this development, EMO is on average less profitable than FCR in 2015; however, in 2017, profits still amount to almost double the value of the flexibility service FCR.

Figure 5.27 displays the revenues for a partition of the BSS at the case study for both FCR and EMO in the months of February and March of 2017. Revenues for FCR were calculated on a 4h-basis and from the capacity prices displayed in Figure 3.9 minus the costs of the charge management and grid fees calculated in Section 5.1. Revenues of EMO (commercializing the flexibility on the Intraday market) show the results of this section on a daily basis after the subtraction of grid fees. It is visible that the commercialization of the BSS for flexibility service EMO shows occasionally higher and occasionally lower earnings.

One can recognize in Figure 5.27 that a multi-use concept, in which a device is used for the optimal flexibility service at the correct time, leads to advantages in comparison with a constant provision of a single flexibility service. Therefore, a multi-use model of energy technologies found at the case study industrial site is developed in Chapter 6.

It is worth noting that relying on transaction data, i.e., executed trades, results in a lower bound for the revenue potential, compared to relying on the order book. This is because unmatched buy or sell bids are present in the order book that could have been realized given a respective trading partner. An increase in the revenue potential can be reached by modeling the full order book as done in [262]. Additionally, an extension of the model to 1h, 1/2h and block products would yield additional opportunities to achieve higher revenues.

[2] This does not equal OPEX as it does not include salaries, license fees, etc.

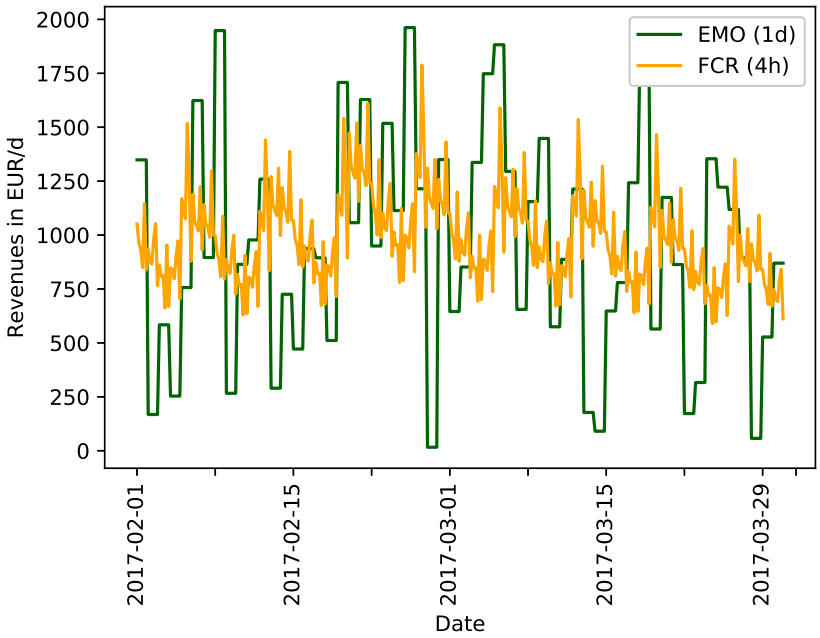

Figure 5.27: Revenues of FCR provision and EMO for the period of February and March of 2017 for a BSS at the case study

5.3 Summary

This chapter assesses revenue potentials of two flexibility services, the provision of frequency containment reserve (FCR) and energy market optimization (EMO), for a battery storage system.

For the flexibility service FCR, a simulation model of a battery is developed along Section 5.1 with the configuration of a BSS used in Chapter 6. The model is created according to the regulatory framework provided by the German transmission system operators using the available degrees of freedom (DOFs) for FCR provision.

The impact of the application of DOFs on the operational cost of FCR provision is assessed in different simulations and the optimal configuration selected for Chapter 6. Results show that an intelligent application of the DOFs can lower the operational costs by 31%.

Section 5.2 assesses the flexibility services EMO using a market model based on Intraday transactions of the EPEX Spot Intraday Continuous market and a model of a bidirectionally charging battery based on the publication of Petersen et al. [315].

The schedule of these battery types has been optimized for all trading days in the years 2015 to 2017. Results show that EMO can achieve high earnings that exceed earnings of the provision of FCR. The results point to the potential of a multi-use optimization of the BSS, which will be tested by the model in Chapter 6.

The chapter thereby answers part of research question 2.2 for the energy technology BSS, as it provides simulation models that assess the value of a BSS for those flexibility services. It, therefore, lays the ground for correct modeling of a BSS that provides these flexibility services. The work, therefore, improves the work done, for example, by Bräuer et al. [54] that use a much more simplified model for FCR provision and EMO.

6 Multi-Use Model of Energy Technologies in Industrial Sites

This chapter presents the main contribution of this thesis: A day-ahead optimization of the energy device operation of an industrial site that includes the provision of various flexibility services as introduced in Chapter 3 and is based on the related work given in Chapter 4. Chapter 5 provides relevant input for the modeling of flexibility services provided by the BSS applied in this chapter.
First, Section 6.1 describes the methodology employed to identify, model, and simulate the energy system at an industrial plant. The notation, terminology, and basic modeling approach are introduced in Section 6.2. Section 6.3 describes the modeling approach used for the flexibility services selected in Chapter 3. Section 6.4 introduces the implemented objective function, which includes the revenue and cost functions of the flexibility services. Section 6.5 displays the energy system that has been investigated, Section 6.6 describes local energy demands, and Section 6.7 shows the modeling of energy technologies.
Section 6.8 shows different levels for aggregation that can be employed in the commercialization of control reserve. Finally, Section 6.9 gives an overview of the performed simulations that are evaluated in the following Chapter 7 and Section 6.10 provides a summary of the chapter.
The chapter thereby answers part of RQ2 as the mathematical model used to describe the selected flexibility services is introduced in Section 6.3. Furthermore, the different aggregation levels for control reserve commercialization, the answer to RQ3, are given in Section 6.8. The chapter, as a whole, describes the linear model to be optimized to answer RQ4.

6.1 Methodogy

The developed model in this work results from work done in the research project *SmartFlex* during the employment of the author at the FZI Research Center for Information Technology. During this project, the energy system of a manufacturing plant of an automotive OEM has been investigated and modeled. This plant has been taken as a case study for the model developed in this chapter.
The following steps were taken during the research project *SmartFlex*:

1. **The identification, analysis, and selection of local energy technologies and description of flexibility potential** - in cooperation with energy managers responsible at the case study, devices of local energy technologies were analyzed with the help of historic load profiles, the control scheme implemented in the local SCADA system, specification sheets, tests performed at the industrial site, publicly available energy reports, and interviews with local energy managers. This resulted in a description of the flexibility model of relevant technologies and devices. These descriptions were converted into mathematical models introduced in Section 6.7.
2. **Identification of target scenario for local energy management** - the target scenario was defined in close consultation with managers from related departments (energy operation, commodity purchasing, et cetera) as well as local energy managers. Next to the conventional cost minimization of the device operation, the objective function should also incorporate flexibility services described in Chapter 3. This target was transferred into an objective function, which is presented in Section 6.4.

3. **Modeling of the local energy management** - a mathematical modeling technique has been selected after the consultation of related work and requirements set out by local energy managers. Each energy technology identified and selected in step 1 is modeled individually in Section 6.7. Furthermore, technical and economic dependencies among the devices of the technologies were implemented in the mathematical model.
4. **Validation of the model** - in joint meetings with local energy managers at the industrial plant, the model described in this chapter has been validated.
5. **Implementation of the model** - together with external partners part of the model of the energy system has been implemented into the processes of the operational energy management at the case study. As a result, the energy manager receives day-ahead schedules for devices of a share of identified technologies on a daily basis and controls the devices accordingly.

During the research project, the author identified devices of the following technologies to possess flexibility relevant for energy management at the case study manufacturing plant:

1. Combined heat and power plant (CHP)
2. Dry cooler (DCO)
3. Gas driven boilers (BOI)
4. Emergency power system (EPS)
5. Battery storage system (BSS)
6. Electric vehicles (EV) and charging infrastructure
7. Air handling unit (AHU)
8. Chiller (CHI)
9. Power-to-heat plant (P2H)

For each energy technology a, a number of devices b are available at the case study and have been modeled in this work. The energy system with the selected system boundaries of the case study is introduced in Section 6.5 including the selected energy technologies and the number of devices for each technology.

6.2 Variables and parameters

This section introduces crucial decision variables and parameters used in the optimization problem in this chapter and explains the reason for introducing them. Variables and parameters generally describe variable or constant values necessary to describe, e.g., energy technologies. Variables generally refer to decision variables of the optimization problem. Parameters are predefined values provided as input to the optimization. An overview about the variables and parameters used in the optimization model is provided in the Appendix in Table A2.

6.2.1 Notation and Terminology

To facilitate the reading process, firstly, the notation of variables and parameters applied in this chapter is introduced. In general, a variable or parameter can be described by the following notation:

$$v^{d}_{a,b,t} \tag{6.1}$$

v is a letter describing the variable. In this model v can take up the form of P (power), Q (heat), E (energy), F (flexibility), π (price), c (costs), θ (temperature), T (duration), η (efficiency), and x (binary variable or parameter). Partly, a diacritic such as a bar is added to the parameter to show, e.g., peak power ($\overline{P}$).

Subscripts give information about the modeled device and the time step. a describes the energy technology that the variable or parameter v is defined for. b indicates which device number of the energy technology a is described by v. t indicates the time step of the variable within the optimization horizon. Not time-related parameters are defined without the subscript t. The superscript d gives a further description to characterize the variable.

6.2.2 Device operation

A unit commitment problem such as the one introduced in this chapter selects different units to operate at certain time steps. The binary variable that decides to operate or not operate a unit is defined as $x^{op}_{a,b,t}$. The operating electric power at time t is defined as $P_{a,b,t}$ and resembles the effective power generation or consumption of the device.
Three types of operation regimes of energy technologies are modeled in this work:

1. **Continuous operation** - the entire power range between minimum power and nominal power can be used.
2. **Partial load operation** - only a share of the difference between minimum and maximum power allows for stable operation. If the device is on, a certain power level is at all times generated or consumed.
3. **On/Off operation** - only two states, either no operation or the nominal power operation, permit stable operation.

6.2.3 Device operation model

The three mentioned models of operation are modeled using three different power levels ($\underline{P}_{a,b}, \check{P}_{a,b}, \overline{P}_{a,b}$). While for every device $b \in \mathbb{B}$ of energy technology $a \in \mathbb{A}$, $\underline{P}_{a,b}$ and $\overline{P}_{a,b}$ define the minimum and maximum power level in general, stable operation is only allowed in the range between partial load or generation ($\check{P}_{a,b}$) and maximum power ($\overline{P}_{a,b}$). The window between $\underline{P}_{a,b}$ and $\check{P}_{a,b}$ cannot be accessed by the variable $P_{a,b,t}$. Partial power $\check{P}_{a,b}$, thereby represents a minimum power required for operation.
The model describes only the power levels that can be accessed during operation. To not operate the device is assured by the binary variable $x^{op}_{a,b,t}$.

Continuous operation

Devices with continuous operation can be modeled by setting the minimum power equal to the partial power. Therefore, all devices can be characterized by the constraint in Equation 6.2:

$$\underline{P}_{a,b} = \check{P}_{a,b} < \overline{P}_{a,b} \tag{6.2}$$

Partial load operation

Many energy technologies operate only in partial load ranges. An industrial CHP plant, for example, often allows for stable operation from 50% of the rated electric power and cannot operate below this threshold. This partial-load operation can be found with various energy technologies that employ engines, steam turbines, motors, et cetera. In mathematical terms, a partial-load operation represents a discontinuity in the relationship between fuel consumption and power output. Partial-load operation is modeled in the following way: For devices that employ partial-load operation, partial power ($\check{P}_{a,b}$) is greater than the absolute minimum power ($\underline{P}_{a,b}$). The resulting relationship is depicted in Equation 6.3:

$$\underline{P}_{a,b} < \check{P}_{a,b} < \overline{P}_{a,b} \tag{6.3}$$

Table 6.1: Assignment of the operation model to modeled energy technologies

	continuous	partial-load	on/off operation
CHP	-	√	-
DCO	√	-	-
BOI	-	√	-
EPS	-	-	√
BSS	√	-	-
EV	√	-	-
HVAC	-	√	-
CHI	√	-	-
P2H	√	-	-

On/Off operation

On/off devices can be modeled by the relationship that partial power equals maximum power in Equation 6.4:

$$\underline{P}_{a,b} < \check{P}_{a,b} = \overline{P}_{a,b} \tag{6.4}$$

These models are used to define a universal cost function for all three types of devices. This cost function considers costs that are related to the state of operation and costs that develop with a gradual power increase.
Table 6.1 shows how individual devices were modeled according to the three device operation models. The models are further explained in Section 6.7.

6.3 Mathematical model of flexibility services

This section extends the assessment of flexibility services given in Chapter 3 by adding the mathematical model for possible cost savings or earnings of the flexibility services.
Firstly, this thesis introduces modeling approaches applied in this work - load profile commitment and load profile adjustment. The introduced flexibility services are matched with these modeling approaches. Furthermore, two different types of load profile adjustment models - simultaneous multi-use and serial multi-use - are defined. Then, devices of each energy technology are matched with the potential flexibility services summarized in Table 6.2.
Next, each flexibility service is explained by the choice of the employed decision variables and parameters. Each model describes the expected revenues or costs associated with each flexibility service l (r_t^l, c_t^l). This is generally a product of power value and a parameter given as revenue or cost per power.

6.3.1 Flexibility service modeling

This work distinguishes between two types of models of flexibility services in the dispatch optimization:

1. **Load profile commitment using local flexibility services** - the optimization problem determines the expected energy exchanged with the public grid (= the load profile of the industrial site) by scheduling all energy devices in a cost-efficient manner. The load profile equals the planned power exchanged with the public grid ($P_{GRID,t}$) of the day-ahead schedule. By determining the optimal load profile local flexibility services can be provided. In this case, flexibility is used locally behind the meter of the local energy system.

   This modeling approach describes flexibility close to the definition in Mauser et al. [266].

2. **Load profile adjustment using external flexibility service** - the optimization problem determines an electric power (the flexibility) that the load profile can be adjusted. This potential adjustment can be offered to external stakeholders. It is done by calculating the technically feasible variation of the load profile of each controllable energy device at the industrial site. The optional load profile adjustment is offered to stakeholders as external flexibility services.

   This modeling approach describes the flexibility close to the definition in Eurelectric [110].

While load profile commitment represents a commitment to deliver a certain power output in the day-ahead schedule, load profile adjustment reserves a power range that can be adjusted by external stakeholders. Both, load profile commitment and load profile adjustment are closely intertwined. Load profile commitment determines the load profile of the industrial site - the electric power exchanged with the public grid ($P_{GRID,t}$), load profile adjustment calculates the potential of each individual device to alter its power consumption or generation and, consequently, the load profile of the industrial site.
At times, the external offer of the flexibility of individual devices can be worth more than the use of flexibility in the local energy management. This multi-objective trade-off is solved in this work by establishing a weighted sum of objective functions resulting in different revenue or cost components of a single objective function.
It is worth noting that for the selected flexibility services modeled by load profile commitment, an actual adjustment of the load profile by external stakeholders does not influence the earnings or costs of local flexibility services. This is due to the common practice of schedule exchanges of load profile adjustment measures between relevant stakeholders.
Load profile adjustment is modeled as follows: Depending on the decision variables power level ($P_{a,b,t}$) and state of operation ($x^{op}_{a,b,t}$), energy devices can offer flexibility to adjust their power consumption or generation to provide load profile adjustment flexibility services. This flexibility is split into positive ($F^{+}_{a,b,t}$) and negative ($F^{-}_{a,b,t}$) flexibility. For a consumer in the electricity system such as an industrial site, negative flexibility describes the possibility to increase the overall power consumption or decrease local generation, while positive flexibility describes the possibility to decrease overall power consumption or increase local generation as shown in Equations 6.5.

$$F^{-}_{a,b,t} = P_{a,b,t} - \check{P}_{a,b} \cdot x^{op}_{a,b,t}, \forall a \in \mathbb{A}, \forall b \in \mathbb{B}, \forall t \in \{1,...,t^{hor}\} \tag{6.5a}$$

$$F^{+}_{a,b,t} = \overline{P}_{a,b} \cdot x^{op}_{a,b,t} - P_{a,b,t}, \forall a \in \mathbb{A}, \forall b \in \mathbb{B}, \forall t \in \{1,...,t^{hor}\} \tag{6.5b}$$

Naturally, for most devices the offered flexibility depends on more factors than the power level; for example, for a storage restricted device such as a battery the SOC has to be modeled as well. Therefore, the individual modeling for each energy technology is elaborated further in Section 6.7.

6.3.2 Multi-use modeling

As shown in Chapter 5, it makes sense to offer several different flexibility services with an individual device - the concept of a multi-use or multi-purpose device.
For the provision of local flexibility services using load profile commitment, a device can simultaneously deliver various flexibility services without any additional modeling required: A high peak load may concur with high electricity prices. Thus, decreasing the electricity feed-in from the public grid would address the flexibility services LPO and LEO at the same time.
For the provision of external flexibility services using load profile adjustment, this work differentiates between simultaneous and serial multi-use as done in the literature introduced in Section 4.1.5:

Simultaneous multi-use

Generally, load profile adjustment permits to deliver several flexibility services simultaneously, e.g., an individual device can provide FCR and aFRR at the same time. This means that the available flexibility can be split into power values for different load profile adjustment flexibility services as shown in Equation 6.6. Therefore, four decision variables are created to estimate the power of FCR or aFRR provided by each individual device at time step t. The third and fourth equation ensure that FCR provision is done in a symmetric way on a device level (see Table 3.5).

$$\forall a \in \mathbb{A}, \forall b \in \mathbb{B}, \forall t \in \{1, ..., t^{hor}\}:$$

$$P_{a,b,t}^{FCR^+} + P_{a,b,t}^{aFRR^+} \leq F_{a,b,t}^{+} \tag{6.6a}$$

$$P_{a,b,t}^{FCR^-} + P_{a,b,t}^{aFRR^-} \leq F_{a,b,t}^{-} \tag{6.6b}$$

$$P_{a,b,t}^{FCR} = P_{a,b,t}^{FCR^+} \tag{6.6c}$$

$$P_{a,b,t}^{FCR} = P_{a,b,t}^{FCR^-} \tag{6.6d}$$

Serial multi-use

As an exception, for storage applications, the provision of flexibility services has been modeled in a serial manner due to regulatory conditions. Currently, depending on the provided flexibility service, different rules apply for storage applications that greatly influence the profitability of this application [375].
As a consequence, serial provision of flexibility services by the individual partitions of the BSS and the EVs is modeled. This is realized by using binary variables for each flexibility service as shown in Equation 6.7. Hereby, $x_{a,b,t}^{LFS}$ defines, for instance, the decision to use the respective device for local flexibility services or peak shaving.

$$x_{a,b,t}^{LFS} + x_{a,b,t}^{FCR} + x_{a,b,t}^{EMO} \leq 1, \forall a \in \mathbb{A}, \forall b \in \mathbb{B}, \forall t \in \{1, ..., t^{hor}\} \tag{6.7}$$

Application of flexibility services at the case study

The selected flexibility services from Chapter 3 are modeled with the devices at the industrial plant. As explained before these flexibility services include

1. Frequency containment reserve (FCR),
2. Automatic frequency restoration reserve (aFRR),
3. Local peak optimization (LPO),
4. Energy market optimization (EMO), and
5. Local energy optimization (LEO).

For the local flexibility services LPO and LEO, flexibility costs or revenues are modeled as load profile commitment. External flexibility services FCR, aFRR, and EMO are modeled as load profile adjustment. The reasons for this modeling approach lie within the market design and the regulatory framework of the German electricity system as described in Chapter 3.
Furthermore, not all energy technologies are capable to deliver each modeled flexibility service. Based on analyses and tests pursued during the research project *SmartFlex* with individual devices, each individual energy technology has been assigned with possible flexibility services and modeled appropriately. Tests showed that some devices lack the ability to control power generation or consumption, while others cannot achieve the required technical

Table 6.2: Assignment of local and external flexibility services to modeled energy technologies

	Local		External			Multi-use model
	LPO	LEO	FCR	aFRR	EMO	
CHP	√	√	√	√	-	simultaneous
DCO	-	-	-	-	-	-
BOI	-	-	-	-	-	-
EPS	√	√	-	√	-	simultaneous
BSS	√	√	√	-	√	serial
EV	√	√	√	-	-	serial
HVAC	√	√	√	√	-	simultaneous
CHI	√	√	-	-	-	simultaneous
P2H	√	√	√	√	-	simultaneous

parameters such as the required reaction speed or ramp-up time for specific flexibility service. A summary of the modeled ability to provide flexibility services by the energy technologies is given in Table 6.2.

6.3.3 Model of control reserve provision - flexibility services FCR and aFRR

As opposed to the model developed in Section 5.1 where actual provision of FCR based on frequency data is modeled, this chapter focuses on the modeling of the reservation of power for different control reserve products. Due to objective of creating a day-ahead optimization, the actual provision is unknown and can only be estimated based on historical values.

FCR and aFRR are procured in auctions run by the TSOs as described in Section 3.5. FCR (υ_t^{FCR}) and aFRR ($\upsilon_t^{aFRR^-}, \upsilon_t^{aFRR^+}$) are remunerated by a capacity price for the reserved commercialized power ($P_{a,b,t}^{FCR}, P_{a,b,t}^{aFRR^+}, P_{a,b,t}^{aFRR^-}$). As shown in Figures 3.9 and 3.10 to 3.14, historic FCR and aFRR power prices are used to account for the remuneration of reserved power, specifically, the weekly weighted capacity price is used. This weekly capacity price is adjusted to 4-hour power prices by the methodology shown in Section 3.5.4. The capacity prices ($\upsilon_t^{FCR}, \upsilon_t^{aFRR^-}, \upsilon_t^{aFRR^+}$) are provided as parameters to the optimization. The revenues of each flexibility service ($r_t^{FCR}, r_t^{aFRR^+}, r_t^{aFRR^-}$) depend on the reserved power and are shown in Equations 6.8 below:

$$r_t^{FCR} = \sum_{a\in\mathbb{A}}\sum_{b\in\mathbb{B}} \left(P_{a,b,t}^{FCR}\cdot \upsilon_t^{FCR}\right), \forall t \in \{1,...,t^{hor}\} \tag{6.8a}$$

$$r_t^{aFRR^+} = \sum_{a\in\mathbb{A}}\sum_{b\in\mathbb{B}} \left(P_{a,b,t}^{aFRR^+}\cdot \upsilon_t^{aFRR^+} + P_{a,b,t}^{aFRR^+}\cdot p_{a,b}^{aFRR^+}\cdot(\tau_{a,b}^{aFRR^+} - \gamma_{a,b}^{aFRR^+})\cdot\Delta_t\right), \forall t \in \{1,...,t^{hor}\} \tag{6.8b}$$

$$r_t^{aFRR^-} = \sum_{a\in\mathbb{A}}\sum_{b\in\mathbb{B}} \left(P_{a,b,t}^{aFRR^-}\cdot \upsilon_t^{aFRR^-} + P_{a,b,t}^{aFRR^-}\cdot p_{a,b}^{aFRR^-}\cdot(\tau_{a,b}^{aFRR^-} - \gamma_{a,b}^{aFRR^-})\cdot\Delta_t\right), \forall t \in \{1,...,t^{hor}\} \tag{6.8c}$$

As visible in Equations 6.8b and 6.8c, aFRR provision includes revenues for the actual energy delivered in time step t. This depends on the aFRR call duration during this time step. Here, the methodology of Section 3.5.3 is employed: Based on a long-term analysis, a call probability p^{aFRR} per energy price is estimated that defines the expected call rate for certain energy price bids based on an analysis of aFRR auctions in the period 2015-17. Based on this relationship an energy price bid ($\tau_{a,b}^{aFRR^+}, \tau_{a,b}^{aFRR^-}$) is derived on a device level either based on the

1. **cost of reserve calls** ($\gamma_{a,b}^{aFRR}$), or
2. the desired **call probability** ($p_{a,b}^{aFRR^+}$) of the device required in the local energy system.

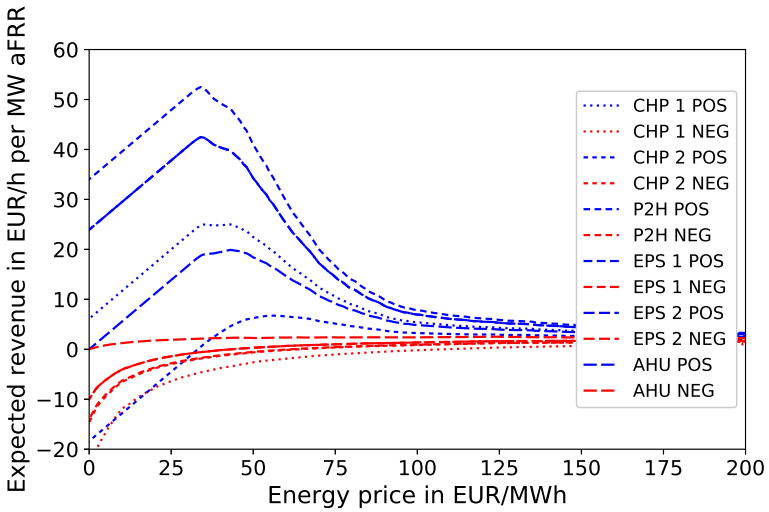

Figure 6.1: Revenue analysis of aFRR calls for devices at case study industrial plant
Expected revenue in EUR/MWh for positive and negative aFRR bids for each device b at the case study taking into account the cost of reserve calls for the device b and the corresponding call probability for each energy price

In addition, an analysis is done using the relationship of the Figure 3.17 to choose the optimal energy price for a long-term aFRR provision. The analysis calculates the energy price related revenues for every probability and energy price combination taking into account the individual costs of reserve calls of each device at the case study. Results are shown in Figure 6.1 for energy prices in the range of -50 to 1000 EUR/MWh.
From the figure the energy price resulting in the maximum revenues is used for each individual device. For devices that are limited by a given call probability requirement, the energy price is selected subject to the call probability. The analysis therefore identifies the energy price that maximizes aFRR call related earnings. The energy price and the appropriate call probability ($p_{a,b}^{aFRR^+}, p_{a,b}^{aFRR^-}$) are provided jointly as parameters to the optimization model of the industrial site.

Expected value of control reserve calls based on the determination of reserve control probability for FCR and aFRR provision

Next to the model of the expected remuneration of control reserve, modeled by a reserved amount of power, the actual provision of FCR and aFRR shoudl be anticipated in a day-ahead schedule, as the actual electric power level has effects on other processes. Looking at devices in the field of integrated energy, for example in the case of a CHP plant, the heat production is stronlgy dependent on the electric power generation.
The provision of control reserve influences the intended electric power levels ($P_{a,b,t}$) depending on the actual FCR and aFRR provision (depending on FCR signals and aFRR calls). This influence is modeled by implementing a net power ($\dot{P}_{a,b,t}$) that represents the expected power level after control reserve provision for an electricity generator (Equation 6.9a) and electricity consumer (Equation 6.9b). The expected control reserve provision is modeled by probabilities ($p^{FCR^+}, p^{FCR^-}, p_{a,b}^{aFRR^+}, p_{a,b}^{aFRR^-}$) that are explained below:

$$\dot{P}_{a,b,t} = P_{a,b,t} + p^{FCR^+} \cdot P_{a,b,t}^{FCR^+} - p^{FCR^-} \cdot P_{a,b,t}^{FCR^-} + p_{a,b}^{aFRR^+} \cdot P_{a,b,t}^{aFRR^+} - p_{a,b}^{aFRR^-} \cdot P_{a,b,t}^{aFRR^-}, \forall a \in \mathbb{A} \text{if } a \text{ is an electricity generator}, \forall b \in \mathbb{B}, \forall t \in \{1,...,t^{hor}\} \tag{6.9a}$$

$$\dot{P}_{a,b,t} = P_{a,b,t} - p_{a,b}^{FCR^+} \cdot P_{a,b,t}^{FCR^+} + p_{a,b}^{FCR^-} \cdot P_{a,b,t}^{FCR^-} - p_{a,b}^{aFRR^+} \cdot P_{a,b,t}^{aFRR^+} + p_{a,b}^{aFRR^-} \cdot P_{a,b,t}^{aFRR^-}, \forall a \in \mathbb{A} \text{if } a \text{ is an electricity consumer}, \forall b \in \mathbb{B}, \forall t \in \{1,...,t^{hor}\} \tag{6.9b}$$

Symmetric FCR provision

As described in Equation 3.1, requested FCR power levels are directly dependent on the frequency deviation from the nominal value. Frequency values are symmetrically distributed around the nominal value of 50 Hz as shown in Figure 3.6. Therefore, for symmetric provision of FCR, equal amounts of positive and negative FCR and, consequently, no effect on the intended power level ($P_{a,b,t}$) is expected.

Asymmetric FCR provision

The effect of asymmetric control reserve provision, however, has to be modeled in the optimization problem. The expected value of control reserve calls is added with the probabilities (p^{FCR^-}, p^{FCR^+}). For FCR provision, historic frequency values from Table 3.3 are taken to estimate the probability of FCR provision. As visible, these probabilities are not device-dependent.

Asymmetric aFRR provision

In the case of aFRR, the call probability ($p_{a,b}^{aFRR^-}, p_{a,b}^{aFRR^+}$) calculated from the long-term analysis in Figure 3.17 is taken as the expected value of aFRR calls. This is done on a device level, as different energy prices are used for different devices.

Lösch [251] simulates the actual operation with historic aFRR call values instead of solely calculating expected aFRR call values; however, as the contribution of this work is a day-ahead dispatch, the actual control reserve calls or the state of the grid cannot be forecasted the day before. Therefore, only expected values are used in this work. Furthermore, approaches of stochastic programming, could be applied to deal with these uncertainties as done in Müller [289].

Product duration

The product duration of control reserve provision is four hours. This means that the offered power has to be provided for the whole duration of pre-defined 4-hour timeslots. This is modeled in Equation 6.10 for the control reserve products FCR and aFRR: At the beginning of each 4h slot, for a given time step Δ_t in minutes, $\frac{4 \cdot 60}{\Delta_t} - 1$ equations are set up that guarantee the offered capacity for FCR and aFRR provision to be equal over all following time steps within the 4h slot. The modulo operator is used to identify the start of a 4h slot.

$$\begin{aligned} \forall a \in \mathbb{A}, \forall b \in \mathbb{B}, \forall t \bmod \frac{4 \cdot 60}{\Delta_t} \equiv 0 \in \{1, ..., t^{hor}\}, \forall s \in \{1, ... \frac{4 \cdot 60}{\Delta_t} - 1\} : \\ P_{a,b,t}^{FCR} = P_{a,b,t+s}^{FCR} \\ P_{a,b,t}^{aFRR^-} = P_{a,b,t+s}^{aFRR^-} \\ P_{a,b,t}^{aFRR^+} = P_{a,b,t+s}^{aFRR^+} \end{aligned} \tag{6.10}$$

Section 6.8 investigates different scenarios of aggregation of individual energy devices given by the market conditions of the control reserve market in terms.

6.3.4 Model of local peak optimization

The flexibility service local peak optimization (LPO) describes the lowering of the maximum peak electricity feed from the public grid: The costs related to the peak power (c^{LPO}) sum up grid fees that arise from the maximum power externally procured over a period T ($\max_t P_{GRID,t}^+$). In an agreement with local DSOs in Germany, the customer can generally select the period T to be either a calendar month or a calendar year. Generally, the customer selects the latter, as it mostly yields lower peak costs. This is also done in this work.

Modeling the problem to lower the maximum power level of a load profile results in minimax formulation, maximum value of the load profile is to be minimized.

Minimax problems can be linearized by introducing a universal (not time step dependent) upper bound (P^{peak}) to the desired variable. This upper bound is defined as a decision variable that is minimized in the objective function.

It is important to note that this upper bound variable is not dependent on the time step t but it is minimized over the entire optimization horizon.
Furthermore, this modeling approach has been adjusted to only consider peaks above the previously given peak threshold: Once a certain peak of electricity procurement exists, it is not necessary to lower the peak electricity consumption lower than this peak. Therefore, a parameter defining a peak power threshold ($\overline{P}^{+}_{GRID}$) is implemented. Only if exceeded, the difference between the new peak and this threshold incurs costs with the price of the peak tariff of the local DSO (υ^{peak}). The power threshold represents the peak power level thus far in the accounting period, one year. An initial peak power threshold for the first optimization at the beginning of the year is set at $\overline{P}^{+init}_{GRID}$. The value can be taken from a peak power targets set at the beginning of the year or empirical values from previous year. The described mathematical model is shown in Equations 6.11. Equation 6.11b represents the objective that is minimized and Equation 6.11a represents the constraint.

$$P^{+}_{GRID,t} \leq \overline{P}^{+}_{GRID} + P^{peak}, \forall t \in \{1,...,t^{hor}\} \tag{6.11a}$$

$$c^{LPO} = P^{peak} \cdot \upsilon^{peak} \tag{6.11b}$$

6.3.5 Model of energy market optimization

The revenues for the flexibility service *EMO* are taken from results of Section 5.2. The revenues are provided based on a daily simulation for storage-limited energy devices such as a BSS. As only results on a 24h-basis are available, a product duration of one day is implemented as also shown in Figure 6.2. The 24-h horizon of the simulation has been chosen as the product of one individual day can be traded together. This is assured by Equation 6.12.

$$\begin{gathered}\forall a \in \mathbb{A}, \forall b \in \mathbb{B}, \forall t \bmod \frac{24 \cdot 60}{\Delta_t} \equiv 0 \in \{1,...,t^{hor}\}, \forall s \in \{1,..., \frac{24 \cdot 60}{d} - 1\} : \\ x^{EMO}_{a,b,t} = x^{EMO}_{a,b,t+s}\end{gathered} \tag{6.12}$$

The simulation in Section 5.2 results in a value of EMO profits of a storage-limited energy device with a given power and given capacity. As no capacity sharing of flexibility services is assured by Equation 6.7, the revenue is defined as a daily capacity price (υ^{EMO}_{t}) for the maximum power of a BSS. The revenue of the flexibility service EMO is therefore defined in Equation 6.13 as:

$$r^{EMO}_{t} = \sum_{a \in \mathbb{A}} \sum_{b \in \mathbb{B}} \left(x^{EMO}_{a,b,t} \cdot \upsilon^{EMO}_{t} \right), \forall t \in \{1,...,t^{hor}\} \tag{6.13}$$

At the case study, this flexibility service is only provided by four devices of the energy technology $a = BSS$. The daily capacity price (υ^{EMO}_{t}) is taken from the results of Section 5.2 that calculate daily profits in the period 2015–2017 for the configuration of the BSSs at the case study.

6.3.6 Model of local energy optimization

Local energy optimization includes the costs or revenues for real-time price optimization, RES buffering, and self-balancing. These are all modeled as load profile commitment.
The total costs of LEO (c^{LEO}_{t}) include inter alia costs for the power externally procured ($P^{+}_{GRID,t}$) in timeslot t at the current electricity price ($\tau^{DA}_{GRID,t}$) to model *real-time price optimization*. For the case study, real-time pricing with market prices of the German Day-Ahead market of the EPEX Spot was assumed. Furthermore, additional costs for grid fees, surcharges for subsidy programs, and taxes as elaborated in Section 2.3.2 are modeled (τ^{fees}_{GRID}). These, however, do not take on a dynamic shape.

Further revenues or costs are incurred by the export of electricity to the public grid to model *self-balancing*. It was assumed that this amount of electricity ($P^{-}_{GRID,t}$) can be sold on the electricity markets for a price ($\tau^{DA}_{GRID,t}$). As the sale of electricity leads to transaction fees, a penalty term (ϕ^{SB}) is added that reflects the transaction costs related to a negative grid balance.
To model *RES buffering*, the sale of electricity is penalized further by the penalty term ϕ^{RES} if local energy generated from renewable energies is fed to the public grid. To model this, all energy injected into the public grid is to be smaller than the energy generated by non-renewable sources. If otherwise, renewable energy is not used locally, but sold to the public grid. This amount of energy is measured by the variable $P^{RES\_PEN}_{t}$ and penalized by the constant penalty ϕ^{RES}.

$$P^{RES}_{t} = \sum_{a\in\mathbb{A}}\sum_{b\in\mathbb{B}} P_{a,b,t}, \forall t \in \{1,...,t^{hor}\}, \text{if } a \text{ is renewable.} \tag{6.14a}$$

$$P^{CONV}_{t} = \sum_{a\in\mathbb{A}}\sum_{b\in\mathbb{B}} P_{a,b,t}, \forall t \in \{1,...,t^{hor}\}, \text{if } a \text{ is non-renewable.} \tag{6.14b}$$

$$P^{-}_{GRID,t} - P^{CONV}_{t} = P^{RES\_PEN}_{t}, \forall t \in \{1,...,t^{hor}\} \tag{6.14c}$$

The total revenues or costs related to the flexibility service *LEO* are summarized in Equation 6.15. All prices and fees in this equation are provided as parameters prior to the optimization.

$$c^{LEO}_{t} = P^{+}_{GRID,t}\cdot(\tau^{DA}_{GRID,t} + \tau^{fees}_{GRID}) - P^{-}_{GRID,t}\cdot(\tau^{DA}_{GRID,t} - \phi^{SB}) + P^{RES\_PEN}_{t}\cdot\phi^{RES}, \forall t \in \{1,...,t^{hor}\} \tag{6.15}$$

In Equation 6.16, a reference cost function in the objective function is defined to estimate the value of the flexibility service LEO. The equation uses the average energy price ($\tau^{DA_{AVG}}_{GRID}$) for im- and export of electricity and disregards costs for a negative grid balance and a self-balancing. Applying the change from a flexible electricity price to a flat price, the assessment of *real-time price optimization* is possible. The penalty terms related to *self-balancing* and *RES buffering* are set to 0 in the reference scenario.

$$c^{LEO_{REF}}_{t} = P^{+}_{GRID,t}\cdot(\tau^{DA_{AVG}}_{GRID} + \tau^{fees}_{GRID}) - P^{-}_{GRID,t}\cdot(\tau^{DA_{AVG}}_{GRID}), \forall t \in \{1,...,t^{hor}\} \tag{6.16a}$$

$$\tau^{DA_{AVG}}_{GRID} = \frac{1}{t^{hor}}\cdot\sum_{t=1}^{t^{hor}} \tau^{DA}_{GRID,t} \tag{6.16b}$$

6.3.7 Data for flexibility services in case study simulation

To estimate the remuneration of provided flexibility services, market data from the years 2015-2017 has been used. For FCR and aFRR, auction results for the years 2015 to 2017 have been included. It has been assumed that the participation in the markets is guaranteed, i.e., no bid has been rejected, and that the average power price is remunerated. Furthermore, for market access using an aggregator a commercialization fee, which is paid to the VPP of the aggregator, is accounted for. For this commercialization fee, standard market data as shown in Rominger et al. [328] is taken. Usually, it amounts to a share of the capacity-related revenues gained from the control reserve commercialization. Thus, the revenues related to the capacity price in Equations 6.8 are multiplied by a factor ϕ^{VPP} if commercialized by a VPP. Costs to account for the charge management for storage constrained devices result from the model developed in Section 5.1.
For the flexibility service LPO, grid fees of the DSO of the case study from the years 2015 to 2017 were taken to constitute the grid fee paid for the annual maximum consumption of electricity from the public grid.

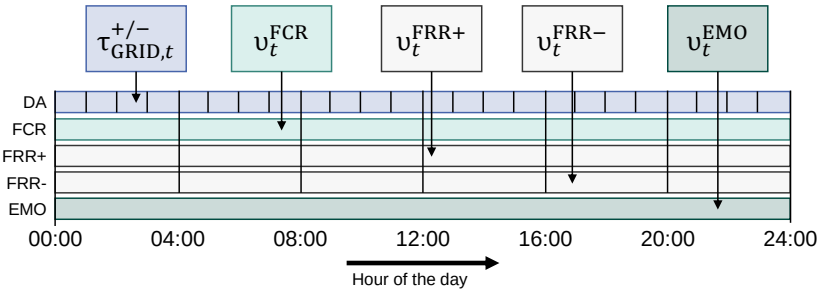

Figure 6.2: Modeled duration of validity belonging to employed capacity and energy prices of individual flexibility services

The remuneration of EMO is calculated from results of Section 5.2. Daily revenues for a BSS with the parameters of a single partition of the BSS at the case study have been calculated. Again a share of the revenues is deducted for market access using an external partner by multiplication with a factor ϕ^{VPP}.
Concerning electric power sourcing, most industrial sites procure electricity on long-term electricity markets as shown in Section 2.3.2. In this work, the electricity price taken from the public grid is valued with the EPEX Spot Day-Ahead auction price for hourly products as long-term OTC contracts at the industrial site are generally not disclosed and the share of the power price is valued at the price of the Day-Ahead auction. Similar to electricity, gas is generally procured on long-term markets. In this work, a one-year constant gas price has been assumed for the simulation period. The relevant surcharges for individual devices (e.g., the cogeneration bonus for CHP plants) and grid fees have been implemented as well.
Market data for FCR, aFRR, and short-term electricity prices were gained from the market data crawler provided by Wagner [410].
The different product duration and price validity for flexibility services are summarized in Figure 6.2. While real-time energy prices for LEO taken from the day-ahead market are changing on an hourly basis, control reserve bids of FCR and aFRR provision are placed for 4h-products. Furthermore, this work modeled the optimization of the BSS on the short-term electricity markets as a 24h block product for the flexibility service EMO.

6.3.8 Assessment of the contribution from flexibility services

Due to the differing revenue or cost structure of the individual flexibility services, varying assessments of these flexibility services have been used.

Load profile adjustment - revenue-based assessment

Flexibility services for load profile adjustment earn revenues from the provision of flexibility services. This facilitates the process of assessing the value of the flexibility service. The revenues earned from the flexibility services FCR and aFRR are displayed in Equations 6.8: FCR revenues are taken from Equation 6.8a and aFRR revenues sum up the result of Equations 6.8b and 6.8c. Revenues earned from energy market optimization are taken from Equation 6.13.

Load profile commitment - cost-based assessment

The flexibility services LPO and LEO employ cost functions according to Equations 6.11b and 6.15. These are implemented in the global objective function and avoid energy costs by penalizing, for instance, the feed-back of energy to the grid in the case of LEO. To assess the effect of these cost functions, reference scenarios with slightly different objective functions are created. For the flexibility service LPO, the peak power of a reference scenario that uses Equation 6.21 as its objective function is used. For the flexibility service LEO, a reference scenario is created that uses the cost function $c_t^{LEO_{REF}}$ instead of c_t^{LEO} in the objective function. This reference scenario is referred to as REF_LEO.

The reference scenarios simulate the neglection of costs related to these flexibility services. Therefore, the resulting schedules of the optimization of the reference scenarios are priced with the correct cost function. These costs are compared to the costs of resulting schedules using the correct objective function.
In other words, the reference scenario for LPO ignores peak shaving in its objective function. The costs related to the resulting peak are then compared to the costs of the optimization problem with the correct objective function. For flexibility service LEO, the same methodology is applied.

6.4 Objective function

The described flexibility services are included in the objective function and represent the part that addresses the aggregator problem described in Chapter 2.
As described, the energy devices at an industrial site are generally run according to the objective function of the dispatch problem. In the dispatch problem, the main target is to lower the energy costs necessary for satisfying the energy demands of the industrial site. In this work, costs include operation, gradient, and ramp costs. These costs are minimized and combined with the previously introduced cost functions of the flexibility services.

$$min \sum_{t=1}^{t^{hor}} \left(\sum_{a \in \mathbb{A}} \sum_{b \in \mathbb{B}} \left(c^{op}_{a,b,t} + c^{grad}_{a,b,t} + c^{ramp}_{a,b,t} \right) - r^{FCR}_t - r^{aFRR}_t - r^{INT}_t + c^{LEO}_t \right) + c^{LPO} \tag{6.17}$$

Costs arise per device b of energy technology a and time slot t. The applied cost model is based on Arroyo and Conejo [14], who were among the first to introduce a linear approximation of variable cost functions suitable for partial-load devices. The device operation model from Section 6.2.3 it is possible to model the cost function of all relevant devices.
The costs include

1. **Operation costs** ($c^{op}_{a,b,t}$) are costs that occur for the sole operation of the devices. It is important to notice that these costs depend on the sole state of operation not on the actual power level ($P_{a,b,t}$). This includes maintenance costs ($c^{mt}_{a,b,t}$), which are often paid per hour of use, and partial-load costs. These include variable costs ($\check{c}^{var}_{a,b}$) at the minimum operation point (partial load or partial generation) ($\check{P}_{a,b}$) such as fuel costs ($\check{c}^{fuel}_{a,b}$) and surcharges ($\check{c}^{sur}_{a,b}$) paid for the minimum power operation. If partial-load conditions are not applicable for a, $\check{P}_{a,b}$ and $\check{c}^{var}_{a,b}$ equal 0. Consequently the operation costs only include maintenance costs ($c^{mt}_{a,b,t}$). It is important to add that total operation cost ($c^{op}_{a,b,t}$) takes up the unit *EUR* while the variable cost factor ($\check{c}^{var}_{a,b}$) takes up *EUR/MWh*.

$$c^{op}_{a,b,t} = (c^{mt}_{a,b} + \check{P}_{a,b} \cdot \check{c}^{var}_{a,b}) \cdot x^{op}_{a,b,t} \cdot \Delta_t, \forall a \in \mathbb{A}, \forall b \in \mathbb{B}, \forall t \in \{1, ..., t^{hor}\} \tag{6.18a}$$

$$\check{c}^{var}_{a,b} = \check{c}^{fuel}_{a,b} + \check{c}^{sur}_{a,b}, \forall a \in \mathbb{A}, \forall b \in \mathbb{B} \tag{6.18b}$$

2. **Gradient costs** ($c^{grad}_{a,b,t}$) are costs dependent on the actual power level, not the state of operation. This mainly includes fuel costs for power generation or consumption and relates to the change of the power level during the operation of the device. In case of partial-load operation, gradient costs amount only to the additional fuel costs above the partial-load power. As explained in Section 6.2.3, energy technologies with partial-load conditions were modeled with three checkpoints - no operation, operation at minimum load and at nominal load. A stair-wise approximation of the cost is modeled in this work which allows the representation of

different costs at and above partial load. Again, total gradient cost ($c^{grad}_{a,b,t}$) takes up the unit *EUR* while the cost factor at nominal load ($\bar{c}^{var}_{a,b}$) takes up *EUR/MWh*.

$$c^{grad}_{a,b,t} = \bar{c}^{var}_{a,b} \cdot (P_{a,b,t} - \check{P}_{a,b} \cdot x_{a,b,t}) \cdot \Delta_t, \forall a \in \mathbb{A}, \forall b \in \mathbb{B}, \forall t \in \{1,...,t^{hor}\} \tag{6.19a}$$

$$\bar{c}^{var}_{a,b} = \bar{c}^{fuel}_{a,b} + \bar{c}^{sur}_{a,b}, \forall a \in \mathbb{A}, \forall b \in \mathbb{B} \tag{6.19b}$$

3. **Ramp costs** ($c^{ramp}_{a,b,t}$) sum up the costs necessary for the cold start and the shut down of devices. $c^{on}_{a,b}$ are costs incurred for the start of the operation. These start-up costs only exist if the energy device changes the operation state from off to on, which is defined by the binary variable $x^{on}_{a,b,t}$. It is irrelevant if the ramp up of the device is a complete ramp up to nominal power as the gradient-related costs are covered above. Accordingly, costs are incurred for the shut down of a device: $c^{off}_{a,b}$.

$$c^{ramp}_{a,b,t} = c^{on}_{a,b} \cdot x^{on}_{a,b,t} + c^{off}_{a,b} \cdot x^{off}_{a,b,t}, \forall a \in \mathbb{A}, \forall b \in \mathbb{B}, \forall t \in \{1,...,t^{hor}\} \tag{6.20}$$

Furthermore, **flexibility services** are provided applying load profile commitment and load profile adjustment. The flexibility services and appropriate price modeling have been described in Section 6.3. The revenues generated include revenues for the offer of FCR (r^{FCR}_t), aFRR (r^{aFRR}_t) and EMO (r^{EMO}_t), as well as avoided costs related to LEO (c^{LEO}_t) and LPO (c^{LPO}).
Costs and revenues of flexibility services implicitly define a sequential order of the flexibility services as, e.g., in [422].

Reference Scenario

In addition, a reference scenario REF is created with the objective function in Equation 6.21 that does not take into account any flexibility services, i.e., it only solves the classic dispatch problem. The objective function only takes into account operation costs, gradient costs, and ramp costs of energy devices. Furthermore, the im- and export of electricity is remunerated with a flat electricity price in Equations 6.16. The aggregator problem is disregarded in this objective function. As described, the resulting schedules of the total reference scenario are weighted with the correct cost functions for local flexibility services LEO and LPO. This means that although not part of the objective function, for instance, the peak load is still priced with the peak tariff.

$$min \sum_{t=1}^{t^{hor}} \left(\sum_{a \in \mathbb{A}} \sum_{b \in \mathbb{B}} \left(c^{op}_{a,b,t} + c^{grad}_{a,b,t} + c^{ramp}_{a,b,t} \right) + c^{LEO_{REF}}_t \right) \tag{6.21}$$

6.5 Energy system

A model of an energy system consists of sources, conversion processes, and sinks of different forms of energy.
The thermal and electrical balances combine all electric and thermal feeds and withdrawals. These balances are fed by generators, discharges by storage applications, and external sources. Withdrawals include the consumption and the conversion of the energy carrier (e.g., the power-to-heat plant).

6.5.1 The local energy system of the case study

The case study is one of the most modern and sustainable car plants in the world according to the OEM [47]. The construction of the manufacturing plant finished in 2005. More than 1000 vehicles are produced on a daily basis. The majority of these vehicles have conventional internal combustion engines; however, also two vehicles types with alternative drive systems are produced. Energy is needed for the production of these automobiles as well as

for the numerous supporting plants and facilities. The majority of electricity and natural gas at the case study plant is purchased directly from the energy supplier and distributed to the relevant devices [47].
Electricity is, for instance, generated from a wind power plant (WPP) directly on the site. Four wind turbines have a rated output of 2.5 MW each. In 2017, 28.3 GWh of electricity were generated from wind energy.
Additional electricity is generated by burning natural gas in CHP units. According to the principle of combined heat and power generation, the resulting engine and exhaust heat are used and fed into the local heating network. Thanks to the simultaneous use of electricity and heat, generation efficiency higher than 80 percent are achieved - more than with a conventional power plant. Two CHPs exist at the manufacturing plant with a total electric power of 6.4 MW and were installed in the years 2009 and 2016. The CHP plant design includes a dry cooler that can be used to discard needless heat. Due to regulatory and energy management issues, it is desired that the plant uses all generated power by the CHP and wind power plant locally.
Heating demand is also satisfied by heat production in four gas-fired boilers with a total thermal power of 58.7 MW and an electrode boiler that uses the concept of P2H with a total thermal power output of 0.5 MW. The CHPs, as well as the gas boiler and the electrode boiler, are heating water for the local heating network, which has a total length of around 5 km.
Fuel oil is only required for emergency power supply. Two emergency power stations (EPS) with a total electric power output of 5.3 MW are available at the plant. As their primary purpose is to establish minimum power services in times of a blackout, they are limited by the number of hours they can run per year but have to be operated occasionally to test the functionality.
Furthermore, a second-life battery storage system exists since 2017, which contains several hundred batteries of electric vehicles produced at the site. This adds up to a total capacity of 11.2 MWh. Power electronics were installed to manage power flows up to 12.5 MW. The batteries are separated into four different partitions each connected to an individual transformer. Hence, the plant has four individual batteries with a capacity of around 2.8 MWh and a power of 3.125 MW [46].
On the demand side, measures to reduce energy consumption have been implemented over the past years. Energy efficiency measures were able to reduce consumption by 10 GWh in the year of 2017 [47]. Demand response measures with electric power devices have been investigated in the research project *SmartFlex*. These devices do not directly influence the automotive production but provide accompanying services such as ventilation, cooling, or air compression.
AHUs have a peak electric demand of around 10 MW and can temporarily adjust their power profile for demand-side measures. A chiller provides cooling power to the production plant with a peak power of 7.2 MW and can be turned off for short periods depending on the outside temperature level.
Air compression plants amount to a total power of 3 MW; however, no flexibility has been identified in the power consumption. Therefore, air compression has been left out of the modeled energy system.

6.5.2 The model of the local energy system of the case study

Figure 6.3 describes the modeled energy system at the case study. The system boundaries of the energy system were set to include all identified flexible devices. Energy procured from external sources includes electricity drawn from the public grid and gas from the public gas network.
Electricity generators include the WPP, the EPS generators, and the CHP plants. While generated power from the WPP is forecasted and given by parameter $P_{WIND,t}$, the generated power of the EPSs and the CHPs is decided by the optimization problem in decision variables $P_{EPS,k,t}$ and $P_{CHP,i,t}$.
Storage applications include, on the one hand, electrical storage in the form of batteries in the constantly available BSS or in the temporarily available EVs. Charge ($P^{ch}_{BSS,l,t}$) and discharge ($P^{disch}_{BSS,l,t}$) are modeled for the BSSs. EVs need electricity to satisfy the demand for mobility; however, they also often possess idle time where vehicles are

connected to the charger but do not actually charge their batteries. During these times vehicles can be used like a battery if bidirectional charging is available. The energy consumption during charging events has been given but can be changed. A reduction ($P^{-}_{EV,m,t}$) or an increase ($P^{+}_{EV,m,t}$) of the given power profile are modeled for EVs. Moreover, storage levels ($E_{BSS,l,t}, E_{EV,m,t}$) of the BSSs and EVs are modeled.

Furthermore, storage is available in the form of thermal system inertia in both the ventilation and the cooling balance, which allows flexible operation of the chiller and the AHUs. The electricity consumption of devices of both energy technologies is included in the total electrical energy demand. Adjustment to this consumption can be done using the local demand response modeled with variables $P^{+}_{AHU,n,t}, P^{-}_{AHU,n,t}, P^{+}_{CHI,n,t}, P^{-}_{CHI,n,t}$. Moreover, electricity is used on the demand side to produce heat in a power-to-heat plant ($P_{P2H,p,t}$). The residual demand for, e.g., production processes is modeled as uncontrollable electricity demand.

Heat can be produced either by the CHP plants ($Q_{CHP,i,t}$), the power-to-heat plant ($Q_{P2H,p,t}$), or gas boilers ($Q_{BOI,j,t}$) that are also available at the site. The heat is then transported using a heating network to individual buildings of the industrial site to serve their thermal demands for production-related (direct) and not production-related processes (indirect). Indirect heating in the actual buildings is done by radiators and the AHU. The heat produced by the CHP plants can further be discarded by the installed dry cooler. As no heat storage has been installed at the industrial site, the flexibility of heat production lies in the substitution of different devices.

Forecasted parameters include energy demands at the target industrial site, and the electricity generation of the wind power plant. Examples for methods to forecast energy demands include among others autoregressive, linear methods, or artificial neural networks [180].

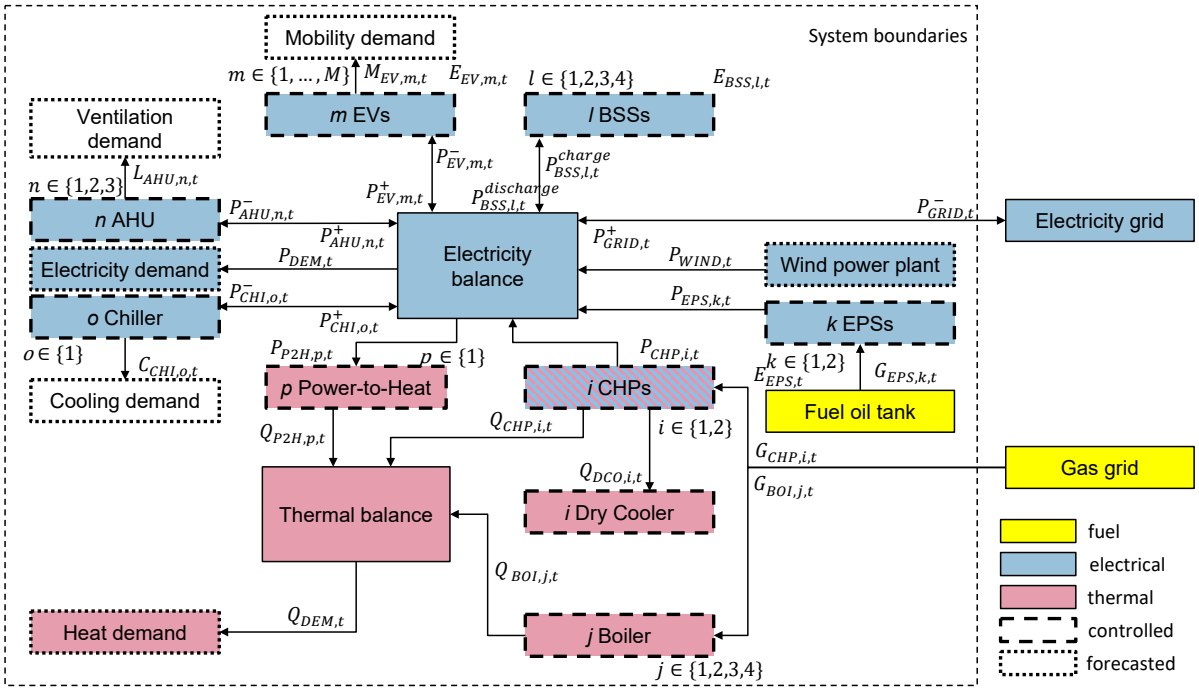

Figure 6.3: Overview of the modeled energy systems
Arrows indicate power flows while labels show the corresponding symbols used in the definition of the model. Colors indicate the different energy carriers

Based on the relationship between individual devices of the energy system, constraints are included in the MILP model. The individual energy demands are introduced in Section 6.6.

6.6 Energy demands

Energy is needed in various locations in an automotive production site. Machines and vehicles need energy to run and employees need correct ambient temperatures and fresh air to work.
This work investigates the demand for:

1. **Electricity** to power machines such as robots, motors, lighting, et cetera for production processes and offices. This demand can be satisfied by various local sources of electrical energy but also external sources such as the distribution grid. As the electricity grid does not have any storage capability, for every time step the amount of electricity generated has to equal the electricity consumed. This is assured in the electricity balance.
2. **Heating** demand is either caused as direct energy by production processes and as indirect energy by the heating of buildings. Direct energy in production processes in the automotive industry includes, for example, the heating of the paint and dip baths for coating processes in the paint shop as these processes require specific temperature ranges to guarantee high-quality production [7].

   The heating demand can be satisfied by local production, external procurement, or storage discharge. This relationship is given in the thermal heat balance.
3. **Cooling** of production processes and buildings is mandatory to assure comfortable working conditions in the summer and assure the function of special machines, for instance, computer servers. Generally, the desired flow temperature of the cooling medium is controlled; however, often the flow temperature does not have to equal a certain value, instead, a range of temperatures is often sufficient to ensure the functionality of the cooling. Thus, depending on the cooling demand and the thermometric conditions, flexible control of the power consumption is modeled.
4. The **ventilation** of buildings is needed to provide fresh air, lower the pollution by pollutants such as carbon dioxide, and transfer heating and cooling to respective buildings. The demand for ventilation can be explained by the volumetric airflow, which is dependent on the electricity consumption of the motor of the air handling units. The amount of energy used for heating and cooling of buildings is in this work already covered in the heating and cooling demand mentioned above. The influence on changing electricity consumption on the provided heating and cooling is existent but much smaller than on the amount of airflow for ventilation. Therefore, this influence is disregarded in this work.
5. **Mobility** is needed to move people or necessary parts for production. It describes the energy to power EVs that are used at the production site. For EVs, mobility is generally expressed in a driving range or an electricity demand. EVs possess flexibility as they often sojourn longer at the charging station than necessary to charge the energy required for their mobility.

Electricity demand

The annual electrical energy needed for production adds up to around 200 GWh and is mainly connected to the production activities at the plant. In the automotive production, the paint shop is the biggest electricity consumer and responsible for around a fourth of the thermal and electrical energy demand at the plant as shown in Figures 6.5 and 6.8. Figure 6.4 shows the average weekly electrical load at the case study production facilities. It is visible that the load on working days Monday to Friday is higher than on Saturday and much higher than on Sunday. This results from shift schedules for individual production processes and can be seen in Figure 6.6, which provides a heat plot of the daily electrical energy consumption. It is visible that electricity consumption on single holidays, on Saturday and especially Sundays is low. On Sunday the plant only produces a base load of around 10 GW (see Figure 6.5), as production is only done in exceptional cases. Furthermore, night shifts are only performed for

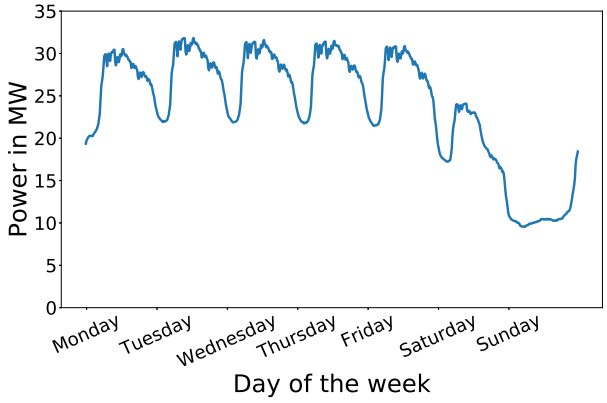

Figure 6.4: Average weekly electric power demand of the case study over the years 2015- 2017

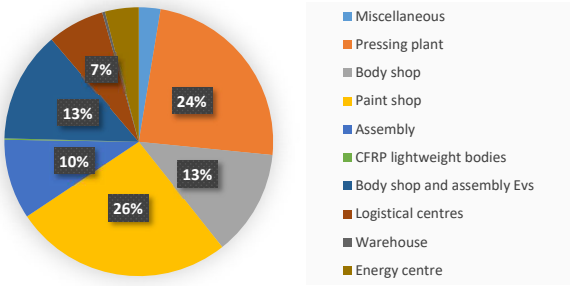

Figure 6.5: Pie chart of contribution of production processes to the electricity demand of 2016
The share of the six highest consuming buildings is displayed

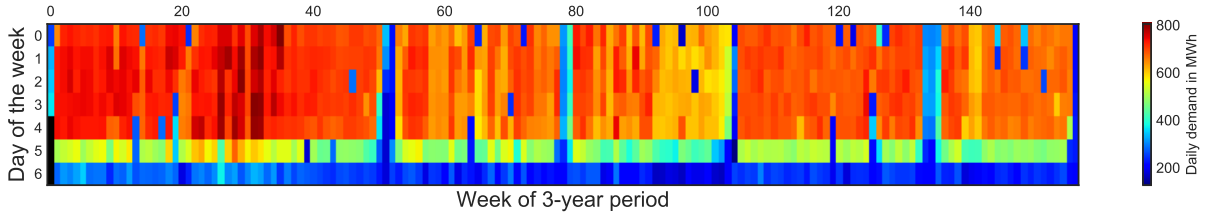

Figure 6.6: Heat plot of daily energy demand over the years 2015-2017

individual production processes. This can be seen by the lower load at night as compared to the load throughout the day. Strong exceptions to this weekly power profile are weeks with holidays or production shutdown periods. The electricity balance of the case study production plant is defined in Equation 6.22 according to the energy system presented in Figure 6.3. The required electric power ($P_{DEM,t}$) can be generated locally by the wind power plant ($P_{WIND,t}$), CHP plants ($P_{CHP,i,t}$), emergency power stations ($P_{EPS,k,t}$), retrieved externally from the public grid ($P^{+}_{GRID,t}$), or provided by positive local DR measures by AHUs ($P^{+}_{AHU,n,t}$) or chillers ($P^{+}_{CHI,o,t}$), or discharged from electric vehicles ($P^{+}_{EV,m,t}$) or battery storage systems ($P^{disch}_{BSS,l,t}$). Negative local DR measures ($P^{-}_{AHU,n,t}, P^{-}_{CHI,o,t}, P^{-}_{EV,m,t}$), the feed-back of electricity to the grid ($P^{-}_{GRID,t}$), the charge of the battery storage systems ($P^{ch}_{BSS,l,t}$), or the use of electricity to produce heat by the power-to-heat plants ($P_{P2H,p,t}$) lead to an increase in electric power demand.

$$\begin{aligned} P_{DEM,t} = {} & P^{+}_{GRID,t} - P^{-}_{GRID,t} + P_{WIND,t} + \sum_{i \in I} P_{CHP,i,t} + \sum_{k \in K} P_{EPS,k,t} \\ & + \sum_{l \in L} \left(P^{disch}_{BSS,l,t} - P^{ch}_{BSS,l,t} \right) + \sum_{m \in M} \left(P^{+}_{EV,m,t} - P^{-}_{EV,m,t} \right) \\ & + \sum_{n \in N} \left(P^{+}_{AHU,n,t} - P^{-}_{AHU,n,t} \right) + \sum_{o \in O} \left(P^{+}_{CHI,o,t} - P^{-}_{CHI,o,t} \right) - \sum_{p \in P} P_{P2H,p,t}, \forall t \in \{1, \ldots, t^{hor}\} \end{aligned} \tag{6.22}$$

Heating demand

Thermal power demand amounts to around 70 GWh per year and is needed for the heating of buildings as well as for production purposes. No data for the case study was found; however, similar production plants show a higher direct portion (60%) than indirect portion (40%) of the heating demand [48]. The average annual thermal energy demand for the years 2015-17 is visible in Fig. 6.7. It is visible that thermal power demand is much higher during winter months than in the summer and seasonality has a great influence on the demand.

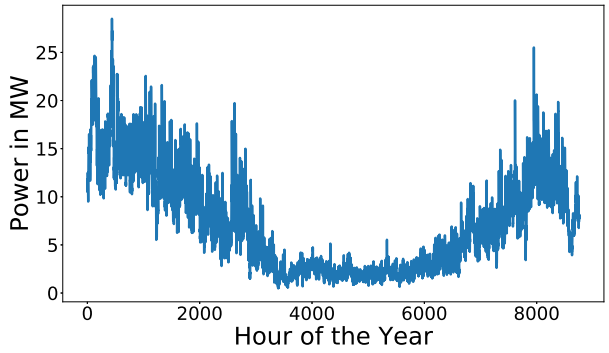

Figure 6.7: Average annual thermal power demand of the case study over the years 2015- 2017

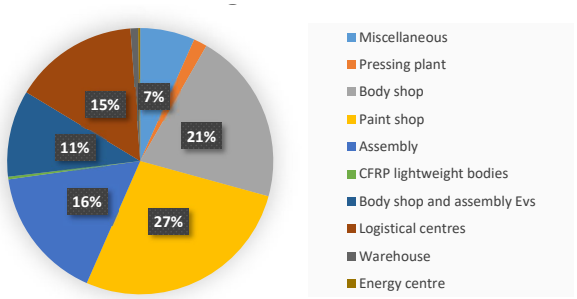

Figure 6.8: Pie chart of contribution of production processes to the heating demand of 2016
The share of the six highest consuming buildings is displayed

The production and consumption of heat in the energy system of the case study is defined in the thermal heat balance in Equation 6.23.
As the energy system of the case study does not show any connection to an external heating grid (see Figure 6.3), the required heat ($Q_{DEM,t}$) is only produced locally by CHP plants ($Q_{CHP,i,t}$), gas boiler ($Q_{BOI,j,t}$) and the P2H plant ($Q_{P2H,p,t}$). Moreover, thermal losses caused by the process of distributing heat using the heating network have to be accounted for. Therefore, the heating demand is divided by a distribution efficiency (η_{HN}) analyzed from the difference between heat production and demand in historical data. Additionally, a dry cooler can be utilized to discharge dispensable heat from CHP i using a stack ($Q_{DCO,t}$). This process artificially decreases the heat production of the CHP as shown in Figure 6.10.

$$\frac{Q_{DEM,t}}{\eta_{HN}} = \sum_{i \in I} Q_{CHP,i,t} - Q_{DCO,i,t} + \sum_{j \in J} Q_{BOI,j,t} + \sum_{p \in P} Q_{P2H,p,t}, \forall t \in \{1,...,t^{hor}\} \tag{6.23}$$

Cooling demand

For the case study a load profile of the chiller is given as a time series ($P_{CHI,o,t}$). This load profile is included in the total electricity demand of the plant and is adjusted by decision variables $P^{+}_{CHI,o,t}$ and $P^{-}_{CHI,o,t}$ according to the model in [150].

Ventilation demand

Tests at office buildings and manufacturing sites [33] showed that a temporary flexible operation of the electric motors of the ventilation system still satisfies the allowed limits at the production plant. This allows to alter the electricity consumption of the ventilation system up to certain time limits.
Therefore, as with the chiller, a modeling approach according to [150] has been applied. The electricity consumption of the ventilation system ($P_{AHU,n,t}$) is also included in the general electricity demand and is adjusted by decision variables $P^{+}_{AHU,n,t}$ and $P^{-}_{AHU,n,t}$.

Mobility demand

At the case study, information of charging events of EVs has been provided. It includes time and SOC values at plug-in, charge end, and plug-out. Furthermore, the capacity of the battery of the vehicle is given. From this data, the charged energy ($E_{EV,m,t}$) is calculated as the given mobility demand of an EV. The electricity consumption ($P^{plan}_{EV,m,t}$) per time step is calculated from this mobility demand and can be adjusted if the vehicle possesses charge flexibility. The EV is modeled as a temporarily available battery during the charging event.

Data for energy demands at the case study

Data sources of energy demands include metered values for electricity, heating, and cooling demand. Data was gathered both from official meters used for the electricity billing and internal meters. Data preparation of the respective time series in terms of missing values, infeasible outliers, et cetera has been done by the author. Electricity demands for the ventilation has been taken from power profiles and the control mechanism programmed in the SCADA system. The mobility demand was taken from GPS-dependent telematic data of charging electric vehicles at the case study.

6.7 Model of energy technologies

This Section introduces the mixed-integer linear model of devices of individual energy technologies that can be found at the case study. Depending on the complexity of the model, for each energy technology, individual constraints are introduced. The models for each energy technology are based on work introduced in Chapter 4 and enhanced if necessary.
These constraints model the operation, the dependencies on other devices, and the available power for local and external flexibility services.
Local flexibility services by devices of each energy technology are modeled by the change in the power exchange with the public grid in the electricity balance in Equation 6.22.
Here a distinction between two modeling approaches of energy technologies is made. This distinction is mainly done due to the given data at the case study. For some devices, a load profile was available and facilitated a realistic model of the device. Thus, this work distinguishes between

1. **a baseline power profile** - in this case, a load profile of the device is given or can be constructed from a related time series, the programmed control of the device in the SCADA system, et cetera. The load profile is given as a parameter time series, which can be adjusted by implemented variables. This modeling approach is used for the energy technologies EV, AHU, and CHI. Each device can provide local flexibility by altered power consumption from the given load profiles.
2. **a free power profile** - in this case, no predefined load profile is given and the device can freely select the optimal power generation or consumption within the given constraints. The provision of local flexibility is done directly using the power generation or power consumption variable. This approach is taken for residual technologies.

In terms of the number of constraints, the most complex model of the energy technologies is the one of the CHP plants. It possesses constraints concerning the co-generation process, part-load operation, ramping, minimum operation time, minimum downtime, dry cooler operation and flexibility modeling.

6.7.1 Combined heat and power plant

A CHP plant burns fuel to generate heat and power. This cogeneration process generally offers higher energy efficiencies than processes where only power is generated and heat is discarded by, e.g., cooling towers as is done in many conventional power plants.

Part-load characteristic of operation

CHP plants generally only allow part-load operation, i.e., they offer an exploitable power range, which starts higher than minimum possible power $\underline{P}_{CHP,i}$. The only feasible operation to generate power happens between $\check{P}_{CHP,i}$ and $\overline{P}_{CHP,i}$; nevertheless, the power plant can still be turned off resulting in no generation ($\underline{P}_{CHP,i,t} = 0$). To model this

a binary variable $x^{op}_{CHP,i,t}$ is introduced that defines limits in the case of operation ($x^{op}_{CHP,i,t} = 1$) and no operation ($x^{op}_{CHP,i,t} = 0$). This is shown in Equation 6.24.

$$\check{P}_{CHP,i} \cdot x^{op}_{CHP,i,t} \leq P_{CHP,i,t} \leq \overline{P}_{CHP,i} \cdot x^{op}_{CHP,i,t}, \forall i \in I, \forall t \in \{1,...,t^{hor}\} \tag{6.24}$$

Ramping

The start and shutdown of the power plant are crucial events as they often incur costs. To model the change in the operation, two binary variables are introduced that reveal the start ($x^{on}_{CHP,i,t} = 1$) and the end of the operation ($x^{off}_{CHP,i,t} = 1$). Ramping up and ramping down are identified by the change in the binary variable used for operation ($x^{op}_{CHP,i,t}$). This is shown in equation 6.25.

$$x^{on,t}_{CHP,i} \leq x^{op}_{CHP,i,t} - x^{op}_{CHP,i,t-1}, \forall i \in I, \forall t \in \{2,...,t^{hor}\} \tag{6.25a}$$

$$x^{off,t}_{CHP,i} \leq x^{op}_{CHP,i,t-1} - x^{op}_{CHP,i,t}, \forall i \in I, \forall t \in \{2,...,t^{hor}\} \tag{6.25b}$$

It is visible that both $x^{off}_{CHP,i,t}$ and $x^{on}_{CHP,i,t}$ are forced to take up the value 1 when the appropriate switch in operation occurs. In all other cases, the variables opt to take up the value 0 as ramping is accounted for with ramping costs.

Minimum operation and downtime

The inert reaction of complex power plants leads to the necessity of modeling minimum operation times ($\overline{T}_{CHP,i}$) and minimum down times ($\underline{T}_{CHP,i}$).
Minimum operation time is modeled as follows: For a minimum operation time of $\overline{T}_{CHP,i}$ time slots, the plant has to be in operation ($x^{op}_{CHP,i,t} = 1$) for $\overline{T}_{CHP,i}$ consecutive time slots after the start of operation ($x^{on}_{CHP,i,t} = 1$).
Minimum downtime is modeled similarly: The plant has to be off ($x^{op}_{CHP,i,t} = 0$) for $\underline{T}_{CHP,i}$ time slots after it has been turned off ($x^{off}_{CHP,i,t} = 1$). The modeling in shown in equations 6.26.

$$\sum_{s=0}^{\overline{T}_{CHP,i}} x^{op}_{CHP,i,t+s} \geq x^{on}_{CHP,i,t} \cdot \overline{T}_{CHP,i}, \forall i \in I, \forall t \in \{1,...,t^{hor} - \overline{T}_{CHP,i}\} \tag{6.26a}$$

$$\sum_{s=0}^{\underline{T}_{CHP,i}} x^{op}_{CHP,i,t+s} \leq (1 - x^{off}_{CHP,i,t}) \cdot \underline{T}_{CHP,i}, \forall i \in I, \forall t \in \{1,...,t^{hor} - \underline{T}_{CHP,i}\} \tag{6.26b}$$

Power-to-heat ratio

CHP plants generate power at the same time as they produce heat. Depending on the operation condition, the energy efficiencies, as well as the thermal and electric efficiencies are changing. The power-to-heat ratio is defined as the ratio between the electric energy output and the thermal energy output. In many modeling approaches the power-to-heat ratio ($\mu_{CHP,i}$) is assumed to be a constant value per plant as in Equation 6.27.

$$P_{CHP,i,t} = Q_{CHP,i,t} \cdot \mu_{CHP,i}, \forall i \in I, \forall t \in \{1,...,t^{hor}\} \tag{6.27}$$

Data from the CHP plant at the target industrial plant showed different power-to-heat ratios for partial-load operation than for operation at nominal power. Therefore, an approach was adopted from [233], which assigns two different power-to-heat ratios at nominal power ($\overline{P}_{CHP,i}$) and minimum power level ($\check{P}_{CHP,i}$). Efficiencies for power levels are calculated using linear regression with coefficients a and b. Therefore, a linear relationship in the development of the power-to-heat ratio between the two fix points $\check{P}_{CHP,i}$ and $\overline{P}_{CHP,i}$ is applied, as small differences between the actual power generation and the linear model exist (see Figure 6.9). Coefficients are calculated with

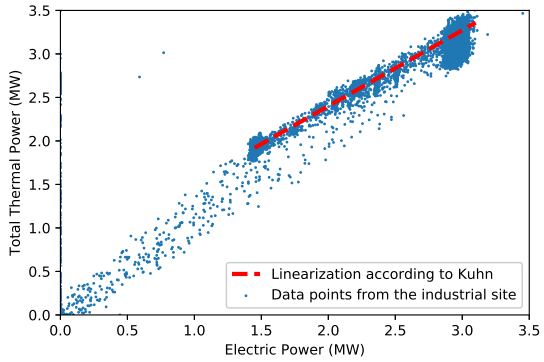

Figure 6.9: Scatter plot of data points from CHP 1 from the years 2014-17 at the case study and implemented linearization according to [233]

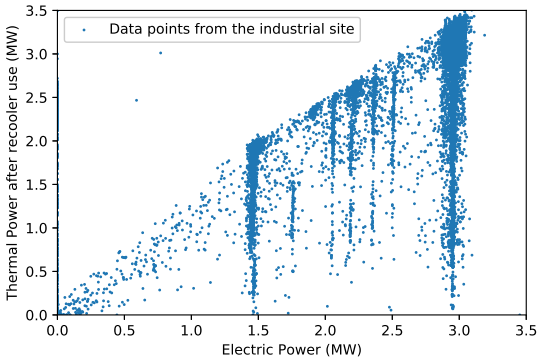

Figure 6.10: Scatter plot of data points from CHP 1 from the years 2014-17 with thermal power delivered to heating network at the case study

the total energy efficiency $\eta^{tot}_{CHP,i}$ as well as electric efficiencies and power levels of the CHP plant at nominal power $\overline{\eta}^{el}_{CHP,i}$ and at partial-load $\check{\eta}^{el}_{CHP,i}$ as shown in Equations 6.28.

$$Q_{CHP,i,t} = c_i \cdot x^{op}_{CHP,i,t} + d_i \cdot \dot{P}_{CHP,i,t}, \forall i \in I, \forall t \in \{1,...,t^{hor}\} \tag{6.28a}$$

$$c_i = \eta^{tot}_{CHP,i} \cdot \frac{\frac{1}{\overline{\eta}^{el}_{CHP,i}} - \frac{1}{\check{\eta}^{el}_{CHP,i}}}{\frac{1}{\overline{P}_{CHP,i}} - \frac{1}{\check{P}_{CHP,i}}}, \forall i \in I \tag{6.28b}$$

$$d_i = \eta^{tot}_{CHP,i} \cdot \left(\frac{1}{\check{\eta}^{el}_{CHP,i}} - \frac{\frac{1}{\overline{\eta}^{el}_{CHP,i}} - \frac{1}{\check{\eta}^{el}_{CHP,i}}}{\frac{\check{P}_{CHP,i}}{\overline{P}_{CHP,i}} - 1} \right) - 1, \forall i \in I \tag{6.28c}$$

It is important that the net power generation after control reserve provision ($\dot{P}_{CHP,i,t}$) is used as the planned electric power generation can vary from the actual power generation due to reserve calls.
Figure 6.9 shows a scatter plot of the operation of a CHP at the case study from the years 2014-2017. The data points of the scatter plot depict the electric power generation on the x-axis and the thermal power production on the y-axis. The implemented linearization as described in Equation 6.28 is also shown in the plot by the dashed line in red. The majority of data points lies in the exploitable power range. The data points outside of it can be explained by the ramping activities of the CHP. As the data is taken on an hourly basis from the CHP, data taken during the ramping process of the CHP is shown outside the allowed power range. The implemented linearization shows that the actual CHP operation was modeled in a suitable manner as most data points from actual operation lie close to the linearized model. For the depicted linearization, the power-to-heat ratio changes develop linear from 0.85 at partial load and 1.07 at nominal power.

Dry cooler

A dry cooler can dump waste heat of a CHP plant. This allows operation of a CHP even at times of low heating demand such as the summer. If a dry cooler is installed for a single CHP plant, one must link the operation of the dry cooler to the operation of the CHP plant, i.e., the dry cooler can only dump as much heat as the CHP is producing. This is done in Equation 6.29.

$$Q_{DCO,i,t} \leq \overline{Q}_{DCO,i} \cdot x^{op}_{CHP,i,t}, \forall i \in I, \forall t \in \{1,...,t^{hor}\} \tag{6.29}$$

Figure 6.10 shows data points of the actual thermal power that was transmitted to the heating network (y-axis) for the simultaneous electric power generation (x-axis) of the CHP. The main difference between Figure 6.9 and Figure 6.10 lies in the use of the dry cooler, which can lower the use of the thermal energy by discarding heat. The plot shows that dry cooler use is mainly done at partial load or nominal power levels. A maximum difference of around 3 MW is visible between total thermal power production Figure 6.9 and thermal power after dry cooler use in Figure 6.10.

Electrical Flexibility

The operation of the CHP plant permits adjustments of the power level between $\check{P}_{CHP,i}$ and $\overline{P}_{CHP,i}$ that are suitable, e.g., for the provision of ancillary service. Therefore, the flexibility of the CHP is defined by Equations 6.30.

$$F^{-}_{CHP,i,t} = P_{CHP,i,t} - \check{P}_{CHP,i} \cdot x^{op}_{CHP,i,t}, \forall i \in I, \forall t \in \{1,...,t^{hor}\} \tag{6.30a}$$

$$F^{+}_{CHP,i,t} = \overline{P}_{CHP,i} \cdot x^{op}_{CHP,i,t} - P_{CHP,i,t}, \forall i \in I, \forall t \in \{1,...,t^{hor}\} \tag{6.30b}$$

The additional heat production has to be used at the industrial site either using higher demand or substitute heat production of another producer. As no flexible heat demand or storage is modeled, it is subtracted from the heat production of other heat producing devices assuring that the additional heat production due to flexibility services can be carried out, even in a situation where the operation of the CHP is heat-led.
In this case, the additional heat production can either substitute heat sources that do not generate electricity such as gas boilers or be discarded by the dry cooler. This relationship is depicted in Equation 6.31. To avoid making the optimization problem non-linear, a power-to-heat ratio ($\mu_{CHP,i}$) of 1 is used in this constraint for the CHPs. As suggested by [273,356], the use of a dry cooler is a standard tool to assure the technical feasibility of the provision of positive control reserve for CHPs.

$$\sum_{i \in I} F^{+}_{CHP,i,t} \cdot \mu_{CHP,i} + \sum_{p \in P} F^{+}_{P2H,p,t} \cdot \mu_{P2H,p} \leq \sum_{j \in J} Q_{BOI,j,t} + \sum_{i \in I} \left(\overline{Q}_{DCO,i} - Q_{DCO,i,t} \right), \forall t \in \{1,...,t^{hor}\} \tag{6.31}$$

External flexibility services

The resulting flexibility can then be used for the provision of ancillary services, more precisely aFRR and FCR. While FCR, generally, has to be provided in a symmetrical fashion (see Section 6.8), aFRR can be provided in positive and negative direction individually. The modeling approach is shown in Equations 6.32. The offered capacity for symmetric FCR ($P^{FCR}_{CHP,i,t}$) is limited by both negative ($F^{-}_{CHP,i,t}$) and positive ($F^{+}_{CHP,i,t}$) flexibility, while positive (negative) aFRR provision is only limited by positive (negative) flexibility. The provision of reserve control is limited by prequalified powers $\overline{P^{aFRR}}_{CHP,i}$ and $\overline{P^{FCR}}_{CHP,i}$. Prequalified power relies on tests and actual official prequalifications done throughout the research project *SmartFlex*.

$$F^{-}_{CHP,i,t} \geq P^{aFRR^{-}}_{CHP,i,t} + P^{FCR}_{CHP,i,t}, \forall i \in I, \forall t \in \{1,...,t^{hor}\} \tag{6.32a}$$

$$F^{+}_{CHP,i,t} \geq P^{aFRR^{+}}_{CHP,i,t} + P^{FCR}_{CHP,i,t}, \forall i \in I, \forall t \in \{1,...,t^{hor}\} \tag{6.32b}$$

$$P^{aFRR^{-}}_{CHP,i,t}, P^{aFRR^{+}}_{CHP,i,t} \in [0, \overline{P^{aFRR}}_{CHP,i}], P^{FCR}_{CHP,i,t} \in [0, \overline{P^{FCR}}_{CHP,i}], \forall i \in I$$

Cost components for the objective function

Equations 6.33 and 6.34 show the cost calculations for fuel costs and the surcharges at partial and nominal power. The cost of electricity generation is calculated from the costs for gas c^{gas}_{CHP} and the electric efficiency at partial and nominal load ($\check{\eta}^{el}_{CHP,i}, \overline{\eta}^{el}_{CHP,i}$). This includes the cost of simultaneous heat production. The cost of gas for CHP plant differs slightly from the cost of gas for, e.g., gas boilers as CHP receive a premium. Surcharges for electricity

generation by CHPs currently amount to the EEG-surcharge c^{EEG}; however, the amount of EEG-surcharge depends on the year the CHP was installed, the size and further parameters, expressed by $f^{EEG}_{CHP,i}$, according to the EEG. In addition, CHP plants receive a premium on the electricity generated for the first 30,000 full load hours ($r^{CHP\_sur}_{CHP,i}$) according to the KWKG.

$$\check{c}^{fuel}_{CHP,i} = \frac{c^{gas}_{CHP}}{\check{\eta}^{el}_{CHP,i}}, \forall i \in I \tag{6.33a}$$

$$\check{c}^{sur}_{CHP,i} = (\gamma^{EEG} \cdot f^{EEG}_{CHP,i} - r^{CHP\_sur}_{CHP,i}), \forall i \in I \tag{6.33b}$$

$$\overline{c}^{fuel}_{CHP,i} = \frac{c^{gas}_{CHP}}{\overline{\eta}^{el}_{CHP,i}}, \forall i \in I \tag{6.34a}$$

$$\overline{c}^{sur}_{CHP,i} = (\gamma^{EEG} \cdot f^{EEG}_{CHP,i} - r^{sur}_{CHP,i}), \forall i \in I \tag{6.34b}$$

aFRR call energy cost

Due to the partial-load operation, the CHP devices can operate freely between $\overline{P}_{CHP,i}$ and $\check{P}_{CHP,i}$. The difference between these two operation points is the possible power that CHP plants at the target site can prequalify for both negative and positive aFRR ($\overline{P^{aFRR}}_{CHP,i}$). In the following costs of positive and negative aFRR calls are estimated to select the correct energy price for the commercialization of the CHP:
In order to assess the corresponding energy costs for $aFRR^{-}$ and $aFRR^{+}$, the difference in operation cost between $\overline{P}_{CHP,i}$ and $\check{P}_{CHP,i}$ is calculated in Equation 6.35 for negative aFRR and in Equation 6.36c for positive aFRR. This cost difference is defined in Section 6.4 by the gradient cost ($c^{grad}_{CHP,i,t}$).
$\underline{aFRR^{-}}$: A decrease in electricity generation leads to a consecutive increase in power consumption by the industrial plant. Concurrently, the heat production of the CHP decreases. This heat production has to be substituted by the production of heat of another device such as a gas boiler. Boiler 1 was chosen as the substituting device. Furthermore, with the increase of external power consumption by the industrial site, additional surcharges, taxes, and fees for the increased procurement of electricity have to be paid.

$$\gamma^{aFRR^{-}}_{CHP,i} = \frac{(\overline{P}_{CHP,i} - \check{P}_{CHP,i}) \cdot (-\overline{c}_{CHP,i} + \tau^{fees}_{GRID}) + (\overline{Q}_{CHP,i} - \check{Q}_{CHP,i}) \cdot \overline{c}^{th}_{BOI,1}}{(\overline{P}_{CHP,i} - \check{P}_{CHP,i})}, \forall i \in I \tag{6.35}$$

$\underline{aFRR^{+}}$: An increase in power generation generally leads to an opposite marginal energy price; however, the CHP is generally not run at full power, if there is either not enough heat (heat-led operation) or power demand (power-led operation). The marginal energy is expressed for heat-led operation in Equation 6.36a and for power-led operation in Equation 6.36b. This work chose to take the maximum of both values for the energy cost of a reserve call to assure that no additional costs were caused by aFRR provision as shown in Equation 6.36c.

$$\tau^{aFRR^{+}_{heat}}_{CHP,i} = \overline{c}_{CHP,i} - \tau^{fees}_{GRID}, \forall i \in I \tag{6.36a}$$

$$\tau^{aFRR^{+}_{power}}_{CHP,i} = \frac{(\overline{P}_{CHP,i} - \check{P}_{CHP,i}) \cdot \overline{c}_{CHP,i} - (\overline{Q}_{CHP,i} - \check{Q}_{CHP,i}) \cdot \overline{c}^{th}_{BOI,1}}{(\overline{P}_{CHP,i} - \check{P}_{CHP,i})}, \forall i \in I \tag{6.36b}$$

$$\gamma^{aFRR^{+}}_{CHP,i} = \max\{\tau^{aFRR^{+}\_margin_{heat}}_{CHP,i}, \tau^{aFRR^{+}\_margin_{power}}_{CHP,i}\}, \forall i \in I \tag{6.36c}$$

Table 6.3: Parameters of CHP plants at the case study

CHP	1	2
Nominal electric power $\overline{P}_{CHP,i}$ in MW	3.138	3.356
Partial electric power $\check{P}_{CHP,i}$ in MW	1.524	1.66
Nominal thermal power $\overline{Q}_{CHP,i}$ in MW	2.934	3.227
Partial thermal power $\check{Q}_{CHP,i}$ in MW	1.79	1.92
Nominal gas consumption $\overline{G}_{CHP,i}$ (LHV) in MW	6.809	8.246
Partial gas consumption $\check{G}_{CHP,i}$ (LHV) in MW	3.809	4.466
Ramp up cost $c^{on}_{CHP,i}$ in EUR	1	
Ramp down cost $c^{off}_{CHP,i}$ in EUR	1	
Maintenance cost $c^{mt}_{CHP,i}$ in EUR/h	16	
Minimum operation time $\overline{T}_{CHP,i}$ in h	1	
Minimum downtime $\underline{T}_{CHP,i}$ in h	1	
Nominal thermal power dry cooler $\overline{Q}_{DCO,i,t}$ in MW	3	-
Prequalified FCR power $\overline{P^{FCR}}_{CHP,i}$ in MW	0.538	0.565
Prequalified $aFRR^{+}$ power $P^{PQ\_aFRR^{+}}_{CHP,i}$ in MW	1.614	1.696
Prequalified $aFRR^{-}$ power $P^{PQ\_aFRR^{-}}_{CHP,i}$ in MW	1.614	1.696
Energy cost of $aFRR^{+}$ call $\gamma^{aFRR^{+}}_{CHP,i}$ in EUR/MWh	-11.02	33.06
Energy cost of $aFRR^{-}$ call $\gamma^{aFRR^{-}}_{CHP,i}$ in EUR/MWh	107.58	63.50
Selected energy price of $aFRR^{+}$ call $\tau^{aFRR^{+}}_{CHP,i}$ in EUR/MWh	43	56
Selected energy price of $aFRR^{-}$ call $\tau^{aFRR^{-}}_{CHP,i}$ in EUR/MWh	340	340
Resulting probability for positive aFRR reserve call $p^{aFRR^{+}}_{CHP,i}$ in %	54.2	21.4
Resulting probability for negative aFRR reserve call $p^{aFRR^{-}}_{CHP,i}$ in %	1.7	2.4
Cost of gas used for CHPs c^{gas}_{CHP} in EUR/MWh	26	
EEG factor $f^{EEG}_{CHP,i}$ in %	0	60
CHP subsidy $r^{sur}_{CHP,i}$ in EUR/MWh	0	23.2
Cost of electricity generation at nominal power operation in EUR/MWh	61.5	86.2

Installation at the case study

At the industrial plant $|I| = 2$ CHP plants are operated and modeled using the constraints above. These CHPs have the following parameters. Parameters concerning surcharges vary mainly due to the year each CHP has been installed. It is visible that CHP 1 is cheaper to operate.

Efficiencies and gas power values are related to the lower heating value (LHV) of the gas. The cost of gas of the CHPs is slightly lower than the cost of gas of the boilers due to subsidies provided for CHPs.

The electricity price includes all listed CHP-related costs. The value of the usable heat could have been further subtracted from the price for electricity generation. This would result in an even lower electricity price.

Table 6.4: Parameters of gas boilers at the case study

Boiler	1	2	3	4	5
Nominal thermal power $\overline{Q}_{BOI,j}$ in MW	9.726	14.435	16.577	18.093	2
Partial thermal power $\check{Q}_{BOI,j}$ in MW	1.086	1.879	2.362	2.522	0.5
Nominal gas consumption $\overline{G}_{BOI,j}$ (LHV) in MW	11.610	16.564	18.962	20.443	4
Partial gas consumption $\check{G}_{BOI,j}$ (LHV) in MW	1.227	2.111	2.663	2.829	1
Maintenance cost $c^{mt}_{BOI,j}$ in EUR/h	12				
Cost of gas used for boilers c^{gas}_{BOI} in EUR/MWh	31.5				

6.7.2 Gas boilers

Partial-Load Operation

Residual heat production at the industrial plant is done by gas-powered boilers (BOI) $j \in J$. Each boiler has a nominal ($\overline{Q}_{BOI,j}$) and a partial load ($\check{Q}_{BOI,j}$) as with the CHP plant.

$$Q_{BOI,j,t} \leq \overline{Q}_{BOI,j} \cdot x^{op}_{BOI,j,t}, \forall j \in J, \forall t \in \{1,...,t^{hor}\} \tag{6.37a}$$

$$Q_{BOI,j,t} \geq \check{Q}_{BOI,j} \cdot x^{op}_{BOI,j,t}, \forall j \in J, \forall t \in \{1,...,t^{hor}\} \tag{6.37b}$$

Cost components for the objective function

As with CHPs a linearized cost function between partial and nominal load was defined for each individual boiler. The efficiencies refer to the thermal efficiencies at partial load ($\check{\eta}_{BOI,j}$) and nominal load ($\overline{\eta}_{BOI,j}$). Furthermore, maintenance costs ($c^{mt}_{CHP,i}$) were accounted for.

$$\check{c}^{fuel}_{BOI,j} = \frac{c^{gas}_{BOI}}{\check{\eta}_{BOI,j}} \cdot \Delta_t, \forall j \in J \tag{6.38a}$$

$$\overline{c}^{fuel}_{BOI,j} = \frac{c^{gas}_{BOI}}{\overline{\eta}_{BOI,j}} \cdot \Delta_t, \forall j \in J \tag{6.38b}$$

Installation at the case study

Table 6.4 summarizes the values of the mentioned required parameters to model the operation of the gas boilers at the case study. The values for partial and nominal heat production and gas consumption were adjusted to ascertain a solvable optimization problem for all possible thermal loads.

6.7.3 Emergency power station

At the investigated industrial plant, each EPS system contains an oil-driven engine and a generator.

Operation

The EPS works like a power source that can be switched either on or off. When it is switched on, it delivers maximum power ($\overline{P}_{EPS,k}$). Thus, depending on the operation of the EPS, the power generation ($P_{EPS,k,t}$) either takes up the value 0 or maximum power. To achieve this, a binary variable ($x^{op}_{EPS,k,t}$) is added.

$$P_{EPS,k,t} = \overline{P}_{EPS,k} \cdot x^{op}_{EPS,k,t}, \forall k \in K, \forall t \in \{1,...,t^{hor}\} \tag{6.39}$$

Flexibility

The flexibility of the EPS is given by the scheduled power level ($P_{EPS,k,t}$). This is due to the binary operation only two power levels are allowed.

$$F^{-}_{EPS,k,t} = P_{EPS,k,t}, \forall k \in K, \forall t \in \{1,...,t^{hor}\} \tag{6.40a}$$

$$F^{+}_{EPS,k,t} = \overline{P}_{EPS,k} - P_{EPS,k,t}, \forall k \in K, \forall t \in \{1,...,t^{hor}\} \tag{6.40b}$$

External flexibility services

Due to its step wise operation and a rather long reaction time the EPS can only deliver aFRR as an external flexibility service. Due to the step wise operation only full power corrections can be offered as aFRR. Thus, the Equations 6.41 are equality constraints as opposed to other technologies such as the CHP. Additionally, a binary variable ($x^{aFRR}_{EPS,k,t}$) is added to allow not to deliver control reserve. Depending on the call probabilities ($p^{aFRR^{+}}_{EPS,k}, p^{aFRR^{-}}_{EPS,k}$) the normal power level is adjusted, leading to a net power level after reserve calls $\dot{P}_{EPS,k,t}$.

$$F^{-}_{EPS,k,t} = P^{aFRR^{-}}_{EPS,k,t} \cdot x^{aFRR}_{EPS,k,t}, \forall k \in K, \forall t \in \{1,...,t^{hor}\} \tag{6.41a}$$

$$F^{+}_{EPS,k,t} = P^{aFRR^{+}}_{EPS,k,t} \cdot x^{aFRR}_{EPS,k,t}, \forall k \in K, \forall t \in \{1,...,t^{hor}\} \tag{6.41b}$$

$$P^{aFRR^{-}}_{EPS,k,t}, P^{aFRR^{+}}_{EPS,k,t} \in [0, \overline{P^{aFRR}}_{EPS,k}], \forall k \in K$$

Minimum operation time

A further condition is the minimum operation time of the EPS. The generator has to run for the minimum operation time $\overline{T}_{EPS,k}$ once it started operation. The modeling of the minimum operation time is done following the example of the CHP plant in Equation 6.26.

$$\sum_{s=0}^{\overline{T}_{EPS,k}} x^{op}_{EPS,k,t+s} \geq (x^{op}_{EPS,k,t} - x^{op}_{EPS,k,t}) \cdot s, \forall k \in K, \forall t \in \{1,...,t^{hor} - \overline{T}_{EPS,k}\} \tag{6.42}$$

Maximum hours of operation

Additionally, due to conditions of service warranty generally valid for emergency power stations, the number of operating hours per year is limited by T^{IFS}_{EPS}. This work splits the allowed duration of operation for local flexibility services T^{LFS}_{EPS} and external flexibility services T^{EFS}_{EPS}. While T^{EFS}_{EPS} is used to define the desired call probability, T^{LFS}_{EPS} is defined as a constraint of the operation problem:

$$T^{LFS}_{EPS} + T^{EFS}_{EPS} = T^{IFS}_{EPS} \tag{6.43a}$$

$$\sum_{k \in K} \sum_{t=0} t^{hor} x^{op}_{EPS,k,t} \leq \Delta_t \cdot T^{LFS}_{EPS} \tag{6.43b}$$

aFRR call energy costs

As emergency power systems are in general not run, the standard use case for control reserve is the provision of positive reserve power. The cost of a positive reserve call is determined by fuel costs; however, it generally leads to a reduction in electric power procurement from the public grid as shown in Equation 6.44.

$$\gamma^{aFRR^{+}}_{EPS,k} = \tau^{fees}_{GRID} - \overline{c}^{fuel}_{EPS,k}, \forall k \in K \tag{6.44}$$

Table 6.5: Parameters of EPSs at the case study

EPS generator	1	2
Nominal electric power consumption $\overline{P}_{EPS,k}$ in MW	3.3	
Fuel efficiency at nominal power $\overline{\eta}_{EPS,k}$ (LPV) in %	0.4	
Fuel cost at nominal power $\overline{c}^{oil}_{EPS}$ (LPV) in EUR/MWh	66	
Maintenance cost $c^{mt}_{EPS,k}$ in EUR	40	
Minimum operation time $\overline{T}_{EPS,k}$ in h	1	
Maximum hours of operation for external flexibility services T^{EFS}_{EPS} in h per day	1	
Maximum hours of operation for local flexibility services T^{LFS}_{EPS} in h per day	1	
Prequalified $aFRR^{+}$ power $P^{PQ\_aFRR^{+}}_{EPS,k}$ in MW	3.3	
Prequalified $aFRR^{-}$ power $P^{PQ\_aFRR^{-}}_{EPS,k}$ in MW	3.3	
Energy cost of $aFRR^{+}$ call $\gamma^{aFRR^{+}}_{EPS,k}$ in EUR/MWh	-43.06	
Energy cost of $aFRR^{-}$ call $\gamma^{aFRR^{-}}_{EPS,k}$ in EUR/MWh	43.06	
Selected probability for positive aFRR reserve call $p^{aFRR^{+}}_{EPS,k}$ in %	1.14	
Selected energy price of $aFRR^{+}$ call $\gamma^{aFRR^{+}}_{EPS,k}$ in EUR/MWh	214	
Selected energy price of $aFRR^{-}$ call $\gamma^{aFRR^{-}}_{EPS,k}$ in EUR/MWh	285	
Resulting probability for positive aFRR reserve call $p^{aFRR^{+}}_{EPS,k}$ in %	5.3	
Electricity price for nominal power operation in EUR/MWh	165	

For negative aFRR, opposite costs are used in the optimization model.

Operation cost components for the objective function

Due to the on/off-operation, the EPS has equal partial and full power cost factors. To calculate total operational costs, the maintenance cost $c^{mt}_{EPS,k}$ has to be added.

$$\check{c}^{fuel}_{EPS,k} = \overline{c}^{fuel}_{EPS,k} = \frac{c^{oil}_{EPS}}{\overline{\eta}_{EPS,k}}, \forall k \in K \tag{6.45}$$

Installation at the case study

The sizing of the EPSs can be found in Table 6.5. The fuel cost is derived from the calorific value (lower heating value) of the fuel and an assumed price per volume of the fuel. The selected probability for negative aFRR reserve calls ($p^{aFRR^{-}}$) is derived from the operating hours for external flexibility services (T^{EFS}_{EPS} = 100 h per year). Total annual operation of 450 h is guaranteed. Therefore, the use of local flexibility services (T^{LFS}_{EPS}) is set to 350 h per year, which is rounded up to 1 hour per day.

6.7.4 Battery storage system

The BSS represents a storage systems that can temporarily store electric power and release it at a later time. As shown in Table 6.2 the BSS is modeled as serial flexibility service provision, i.e., binary variables are introduced to cover the different flexibility services that the BSS can provide (see Equation 6.7). The exact charge and discharge operation is modeled for the provision of local flexibility services. External flexibility services, such as FCR and EMO, rely on the simulation results of Chapter 5.

Flexibility Services

The binary variable $x^{LFS}_{BSS,l,t}$ defines the use of the BSS for local flexibility services LPO or LEO. The flexibility service FCR provision is defined by the binary variable $x^{FCR}_{BSS,l,t}$ and the flexibility service electricity market optimization is committed to by the variable $x^{EMO}_{BSS,l,t}$. The constraint 6.46 declares that only one flexibility service (LPO/LEO, FCR, EMO) can be provided for a single time step (serial provision).

$$x^{LFS}_{BSS,l,t} + x^{FCR}_{BSS,l,t} + x^{EMO}_{BSS,l,t} \leq 1, \forall l \in L, \forall t \in \{1,...,t^{hor}\} \tag{6.46}$$

Power restriction

The allowed charging levels lie between the minimum charging level $\underline{P}_{BSS,l}$ and the maximum charging power $\overline{P}_{BSS,l}$. Binary variables assure that the charge and discharge power variables ($P^{disch}_{BSS,l,t}, P^{ch}_{BSS,l,t}$) only take on values when power is used for local flexibility services.

$$P^{disch}_{BSS,l,t} \leq x^{LFS}_{BSS,l,t} \cdot \overline{P}_{BSS,l}, \forall l \in L, \forall t \in \{1,...,t^{hor}\} \tag{6.47a}$$

$$P^{-}_{BSS,k,t} \geq x^{LFS}_{BSS,l,t} \cdot \underline{P}_{BSS,l}, \forall l \in L, \forall t \in \{1,...,t^{hor}\} \tag{6.47b}$$

Energy restriction

For local flexibility services, the storage balance determines that the stored energy quantity in time step t ($E_{BSS,l,t}$) is equal to the energy quantity of the preceding time step ($E_{BSS,l,t-1}$) plus the charged energy ($P^{ch}_{BSS,l,t} \cdot \Delta_t$) and minus the discharged energy ($P^{disch}_{BSS,l,t} \cdot \Delta_t$). Both temporal storage losses ($\eta^{temp}_{BSS,l}$) from the transition of one time step to the next and charging ($\eta^{-}_{BSS,l}$) and discharging efficiencies ($\eta^{+}_{BSS,l}$) must be taken into account. These efficiencies have already been included in the simulations done in Chapter 5. Thus, these have to be modeled only in case of the local flexibility services.
Due to the serial provision of the flexibility service, no dynamic capacity split of the BSS is modeled.
The SOC is modeled as a variable that is constrained by equations. This means, that SOC levels are not provided as parameters but are actually determined by other decision variables (in this case the charge and discharge powers) by equality constraints.
For FCR provision and energy market operation, no influence on the SOC is modeled as in the case of FCR this is assured by the FCR charge management described in Section 5.1 and in the case of EMO the results of the simulation done in Section 5.2 have excluded the influence of a SOC change.

$$E_{BSS,l,t} = E_{BSS,l,t-1} - E_{BSS,l,t-1} \cdot \eta^{temp}_{BSS,l} \cdot x^{LFS}_{BSS,l,t} + (P^{ch}_{BSS,l,t} \cdot \eta^{-}_{BSS,l} - \frac{P^{disch}_{BSS,l,t}}{\eta^{+}_{BSS,l}}) \cdot \Delta_t, \forall l \in L, \forall t \in \{2,...,t^{hor}\} \tag{6.48}$$

FCR provision with a BSS

The parameters used to model FCR operation are based on the results of the simulation in Section 5.1.
This includes

1. the possible power to commercialize as FCR,
2. energy levels necessary to satisfy the 15-minute-criterion,
3. the actual FCR provision including charge management, and
4. the resulting cost of the charge management.

Power restriction

The prequalified power ($\overline{P^{FCR}}_{BSS,l}$) is an upper limit to the possible FCR power. For serial provision of flexibility services, this relationship is used to introduce the binary variable ($x^{FCR}_{BSS,l,t}$) that commits the battery to provide FCR shown in Equation 6.49. FCR is provided by setting $x^{FCR}_{BSS,l,t} = 1$.

The 15-minute-criterion defines a capacity-to-power ($\psi_{BSS,l}$) relationship. It defines the relation between FCR power and available energy and also defines the permissible operation range during FCR provision as shown in Figure 5.1. It is chosen as 1.5 at the target site.

$$P^{FCR}_{BSS,l,t} = \frac{\overline{E}_{BSS,l}}{\psi_{BSS,l}} \tag{6.49a}$$

$$P^{FCR}_{BSS,l,t} \leq x^{FCR}_{BSS,l,t} \cdot \overline{P^{FCR}}_{BSS,l}, \forall l \in L, \forall t \in \{1,...,t^{hor}\} \tag{6.49b}$$

SOC restriction

To model the permissible operation range, Δ^{FCR}_t is introduced which determines the duration of FCR provision during alert state. In this case it is 15 minutes. The model has to assure that during the time of FCR provision, the SOC levels remain within this range. Thus, the lower and upper level of the permissible operation range are defined in the following constraints as required by the TSOs [392]:

$$E_{BSS,l,t} \geq x^{FCR}_{BSS,l,t} \cdot \overline{P^{FCR}}_{BSS,l} \cdot \Delta^{FCR}_t, \forall l \in L, \forall t \in \{1,...,t^{hor}\} \tag{6.50a}$$

$$E_{BSS,l,t} \leq x^{FCR}_{BSS,l,t} \cdot \overline{E}_{BSS,l} - \overline{P^{FCR}}_{BSS,l} \cdot \Delta^{FCR}_t + (1 - x^{FCR}_{BSS,l,t}) \cdot \overline{E}_{BSS,l}, \forall l \in L, \forall t \in \{1,...,t^{hor}\} \tag{6.50b}$$

Equation 6.50a shows the minimum level, which is 0 for non-FCR operation and a quarter of the prequalified power for FCR operation (15-min criterion). The maximum level in Equation 6.50b provides a maximum level of $\overline{E}_{BSS,l}$ for non-FCR operation and a maximum level of $\overline{E}_{BSS,l} - \frac{\overline{P^{FCR}}_{BSS,l}}{4}$ for FCR operation. These conditions ascertain that, upon FCR provision, the SOC of the battery is within the permissible operation range.

Actual FCR provision including charge management

As this chapter describes a day-ahead dispatch and the actual FCR provision depends on the development of the grid frequency, a prediction of the actual grid frequency values beforehand is not possible. Furthermore, the installed charge management assures that the SOC is kept within the permissible operation range. Thus, it is assumed in this model that the SOC levels do not change during FCR provision and an average cost of charge management is taken for times the BSS provides FCR.

The standard defining the provision of FCR with storage-limited devices such as batteries only enables the symmetric provision of FCR. This is modeled in Equation 6.51.

$$P^{FCR}_{BSS,l,t} = P^{FCR^+}_{BSS,l,t} = P^{FCR^-}_{BSS,l,t}, \forall l \in L, \forall t \in \{1,...,t^{hor}\} \tag{6.51}$$

The resulting cost of the charge management

The resulting costs of the charge management are included in the objective function. The amount of charge management per time step depends on if and to what extent the BSS provides FCR. The costs are taken from Scenario 7 of the simulation done in Section 5.1.

Table 6.6: Parameters of battery storage systems at the case study

BSS	1	2	3	4
Nominal electric power $\overline{P}_{BSS,l}$ in MW	3.125			
Nominal electrical storage $\overline{E}_{BSS,l}$ in MWh	3.75			
Discharge efficiency $\eta^{+}_{BSS,l}$ in %	90			
Charge efficiency $\eta^{-}_{BSS,l}$ in %	90			
Self-discharge efficiency $\eta^{temp}_{BSS,l}$ in % per month	2			
Electrical storage level $E_{BSS,l,1}$ at optimization start	$\frac{\overline{E}_{BSS,l}}{2}$			
Electrical storage level $E_{BSS,l,t^{hor}}$ at optimization start	$\frac{\overline{E}_{BSS,l}}{2}$			
Prequalified FCR power $\overline{P^{FCR}}_{BSS,l}$ in MW	2.5			

Energy market operation with a BSS

The model for the energy market operation by a BSS is modeled according to Equations 6.12 and 6.13 shown in Section 6.3.6. The BSS commits to energy market operation by setting $x^{EMO}_{BSS,l,t} = 1$. Revenues acquired by energy market operation are taken from the simulation in Section 5.2.
It is assumed that for the flexibility service EMO, the configuration with a maximum power of $\overline{P}^{EMO}_{BSS,b,t}$ used in Section 5.2 is commercialized on the Intraday market for each battery storage system.

Operation cost components for the objective function

The cost of charging and discharging of energy for individual flexibility services is covered by the costs and revenues of the flexibility services.
The charged and discharged amount influences the exchange of electricity with the public grid ($P^{disch}_{BSS,l,t}, P^{ch}_{BSS,l,t}$) by the power balance in Equation 6.22 leads to revenues or costs for the flexibility services LPO and LEO.
As shown in Section 5.1, the provision of FCR incurs costs related to the charge management and grid fees as shown in Equation 5.18. These are broken down into the length of a time step and dependent on the amount of power commercialized as FCR. This relationship is modeled as a linear cost ($c^{FCR}_{BSS,l}$) per MW of FCR power commercialized by the BSS in Equation 6.52:

$$c^{grad}_{BSS,l,t} = P^{FCR}_{BSS,l,t} \cdot c^{FCR}_{BSS,l}, \forall l \in L, \forall t \in \{1, ..., t^{hor}\} \tag{6.52}$$

EMO generates revenues by trading power on electricity markets. Fees and surcharges apply as described in Section 5.2 are included in the revenues given for the flexibility service. Costs for the cost of the operation of the metering points and maintenance are disregarded in this work.

Installation at the case study

At the case study a BSS with four identical partitions with a capacity of 3.75 MWh and a power of 3.125 MW is available. The parameters are shown in Table 6.6.

6.7.5 Electric Vehicles

This work models the existence of EVs that possess *charge flexibility* as described in Section 4.2.3 and by Rominger et al. [329]:
Figure 6.11 depicts an exemplary power profile of an EV charging at an AC charging station derived from actual metering data at an office facility taken from [329]. With non-controlled charging, the EV normally charges with

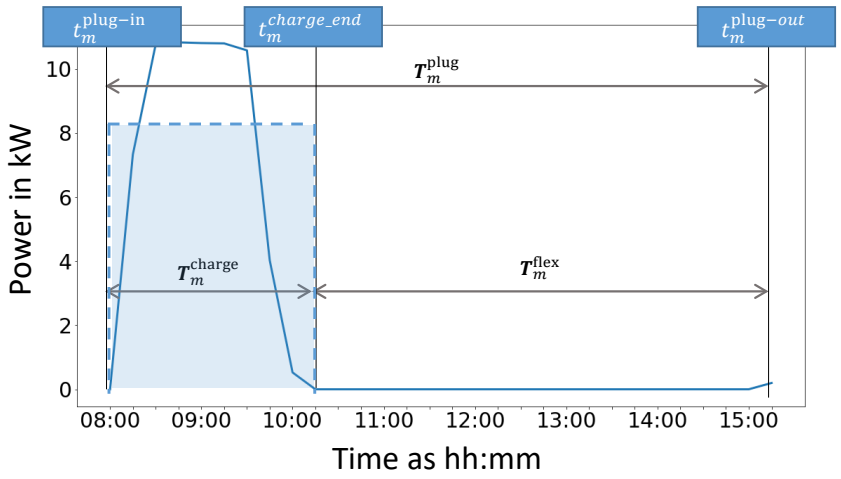

Figure 6.11: EV charging flexibility model
Plot of exemplary power profile of charging event with 15-minute granularity (blue line) and implemented a simplified model of the charging event (dashed blue line).

the highest possible charging power as soon as it plugs in. This charging power is limited either by the BMS of the EV or by the charging infrastructure. The charging either stops when the battery is full or when it is plugged-out from the charging station. In the case of the first, flexibility exists to either decrease the power or postpone the charging event while still guaranteeing the expected full charge of the vehicle. The existence of the flexibility is also visible in Figure 6.11.

Charge flexibility

To describe charge flexibility, the following equations from [144] are introduced that are depicted in Figure 6.11:

$$T_{EV,m}^{ch} = t_{EV,m}^{charge\_end} - t_{EV,m}^{plug-in}, \forall m \in M \tag{6.53a}$$
$$T_{EV,m}^{plug} = t_{EV,m}^{plug-out} - t_{EV,m}^{plug-in}, \forall m \in M \tag{6.53b}$$
$$T_{EV,m}^{flex} = t_{EV,m}^{plug-out} - t_{EV,m}^{charge\_end}, \forall m \in M \tag{6.53c}$$

Equation 6.53a describes the time that the EV is actually charging. Equation 6.53b describes the time that the vehicle is connected to the charging station and can, therefore, alter its power consumption. The difference of $T_{EV,m}^{plug}$ and $T_{EV,m}^{ch}$ determines the charging flexibility $T_{EV,m}^{flex}$ as described in Equation 6.53c.
One can use this available flexibility $T_{EV,m}^{flex}$ for the provision of flexibility services, e.g., by delaying the power consumption to move the procurement from the public grid to a cheaper period (LEO).

Modeling of EVs

The selected modeling technique in this work is based on the constructed load profiles of individual charging events visible by the dashed line in Figure 6.53c.
Figure 6.11 shows the modeled load profile of a charging event m by the dashed blue line. The baseline load profile is modeled by the average power ($P_{EV,m,t}^{plan}$) between plug-in time $t_{EV,m}^{plug-in}$ and charge-end time $t_{EV,m}^{charge\_end}$. With the condition that the energy consumed by the EV is the same as in the metered profile, the artificial baseline power profile is derived as shown in Equation 6.54a.

This modeling technique is used due to the lack of actual metered data at the case study. Instead, only the time of plug-in, the time of charge end, the time of plug-out, the appropriate SOC values at these timestamps, and the capacity of the battery of the vehicle were available.

$$E^{ch}_{EV,m} = (SOC^{charge\_end}_{EV,m} - SOC^{plug-in}_{EV,m}) \cdot \overline{E}_{EV,m}, \forall m \in M \tag{6.54a}$$

$$P^{plan}_{EV,m,t} = \frac{E^{ch}_{EV,m}}{\eta^{ch}_{EV,m} \cdot (t^{plug-in}_{EV,m} - t^{charge\_end}_{EV,m})}, \forall m \in M \tag{6.54b}$$

The given power consumption (baseline power profile) in the load profile was defined as $P^{plan}_{EV,m,t}$. The power was calculated from the battery capacity and SOC values at charge start (= plug-in) and charge end. This modeling approach omits the CCCV behavior generally encountered in the last part of an unidirectional charging session. It is omitted as the energy charged between the modeled approach and the normal charge profile does not vary greatly and further binary variables would have been necessary that lead to longer run times.
The EVs were modeled as batteries that can be charged and discharged (V2G capability) and whose given load profiles can be adjusted. These adjustments can influence the local electricity balance to provide local flexibility services. Therefore, variables are defined as $P^{-}_{EV,m,t}$ modeling an increase in power and $P^{+}_{EV,m,t}$ modeling a decrease in power consumption from the baseline power profile ($P^{plan}_{EV,m}$).
In other words, the model of charging events in this work models every individual charging event as a temporarily available battery with a given load profile. The load profile can be adjusted under the condition that the energy charged in this load profile still has to be fulfilled.
Furthermore, the EV can provide the external flexibility service FCR during $T^{flex}_{EV,m}$.

Baseline power profile

The final power is split into power that is charged ($P^{ch}_{EV,m,t}$) and discharged ($P^{disch}_{EV,m,t}$) in order to account for different charging or discharging efficiencies in Equation 6.56. All variables are defined as non-negative variables, to assure that they serve the above-described purpose.

$$P^{ch}_{EV,m,t} - P^{disch}_{EV,m,t} = P^{plan}_{EV,m,t} + P^{-}_{EV,k,t} - P^{+}_{EV,k,t}, \forall m \in M, \forall t \in \{1,...,t^{hor}\} \tag{6.55}$$

Energy restriction

The battery of the EV is modeled like the battery of the BSS, which is either charged or discharged. This means that EVs were modeled to possess the ability to perform bidirectional charging.

$$\begin{gathered} E_{EV,m,t} = E_{EV,m,t-1} + P^{ch}_{EV,m,t-1} \cdot \eta^{ch}_{EV,m} \cdot \Delta_t - \frac{P^{disch}_{EV,m,t-1} \cdot \Delta_t}{\eta^{disch}_{EV,m}}, \forall m \in M, \forall t \in \{2,...,t^{hor}\} \\ E_{EV,m,t} \in \{0, \overline{E}_{EV,m}\}, \forall m \in M, \forall t \in \{1,...,t^{hor}\} \end{gathered} \tag{6.56}$$

Availability and power restrictions

Furthermore, charge and discharge is only limited to the periods at which the EV is plugged in. This is assured by the binary parameter $x^{plug}_{EV,k,t}$, which equals one during the plug time between $t^{plug-in}_{EV}$ and $t^{plug-out}_{EV}$. The parameter

values are set prior to the optimization based on the available charging data. Furthermore, the equations assure that charging and discharging power remain between minimum and maximum power levels.

$$P^{ch}_{EV,m,t} \leq x^{plug}_{EV,m,t} \cdot \overline{P}_{EV,m}, \forall m \in M, \forall t \in \{1,...,t^{hor}\} \tag{6.57a}$$
$$P^{disch}_{EV,m,t} \leq x^{plug}_{EV,m,t} \cdot \underline{P}_{EV,m}, \forall m \in M, \forall t \in \{1,...,t^{hor}\} \tag{6.57b}$$

To assure that the energy charged remains the same as given by the baseline power profile, the SOC at the beginning and at the end of the charging event is set in the model. This is done by implementing the following two constraints that only count until plug in time $t^{plug-in}_{EV,m}$ and before plug-out time $t^{plug-out}_{EV,m}$.

$$E_{EV,m,t} = E^{plug-in}_{EV,m} \text{ , if } t \leq t^{plug-in}_{EV,m}, \forall m \in M \tag{6.58a}$$
$$E_{EV,m,t} = E^{plug-out}_{EV,m} \text{ , if } t > t^{plug-out}_{EV,m}, \forall m \in M \tag{6.58b}$$

Flexibility services

In order to avoid the simultaneous provision of flexibility services, binary variables for the influence of the power balance using local flexibility services ($x^{+}_{EV,t}, x^{-}_{EV,t}$) and the external flexibility service FCR ($x^{FCR}_{EV,m,t}$) are implemented.

$$x^{+}_{EV,m,t} + x^{-}_{EV,m,t} + x^{FCR}_{EV,m,t} \leq 1, \forall m \in M, \forall t \in \{1,...,t^{hor}\} \tag{6.59}$$

Local flexibility services

The allowed levels for load profile adjustments for local flexibility services are between the minimum charging level $\underline{P}_{EV,m}$ and the maximum charging power $\overline{P}_{EV,m}$ and equally discharging limits are between $\underline{P}_{EV,m}$ and $\overline{P}_{EV,m}$.

$$P^{+}_{EV,m,t} \leq x^{+}_{EV,m,t} \cdot (\overline{P}_{EV,m} - \underline{P}_{EV,m}), \forall m \in M, \forall t \in \{1,...,t^{hor}\} \tag{6.60a}$$
$$P^{-}_{EV,m,t} \geq x^{-}_{EV,m,t} \cdot (\overline{P}_{EV,m} - \underline{P}_{EV,m}), \forall m \in M, \forall t \in \{1,...,t^{hor}\} \tag{6.60b}$$

FCR provision with an EV

As indicated by Table 6.2, EVs are modeled to be able to provide FCR at the charging stations at the industrial plant like a stationary battery. Similar to the modeling approach of the BSS, restrictions exist concerning the power that can be commercialized, energy range, and assumptions concerning charge management.

Power restriction

In comparison with the BSS, an EV is only available during the plug-in time. This is again assured by the binary parameter $x^{plug}_{EV,m,t}$, which defines the plug time. It is modeled that the EV can provide FCR at the respective charging station and that no the required technical specifications are fulfilled. It is assumed that the regulations for FCR provision of batteries as introduced in Section 6.7.4 apply to batteries of EVs as well. A capacity/power ratio ($\psi_{EV,m}$) of 1.5 is assumed. At times the maximum prequalified power cannot be called due to limitations by the possible maximum power of the charging infrastructure. Therefore, the maximum FCR possible for the charging event m is given by the minimum of the prequalified power depending on the capacity of the vehicle and the baseline power profile, which represents the power constraint of the charging station. Thus, the power that can be commercialized depends on the vehicle and the charging station at hand.

Table 6.7: Exemplary parameters of EV charging event at the case study.

EV charging event	m
Nominal electrical storage $\overline{E}_{EV,m}$ in kWh	33.2
SOC at plug in $SOC_{EV,m}^{plug-in}$ in %	12.3
SOC at charge end $SOC_{EV,m}^{charge\_end}$ in %	100
Time of plug-in $t_{EV,m}^{plug-in}$	2017-01-03 04:30
Time of charge end $t_{EV,m}^{charge\_end}$	2017-01-03 07:45
Time of plug-out $t_{EV,m}^{plug-out}$	2017-01-03 14:00
Resulting modeled power $P_{EV,m}^{plan}$ in kW	9.95
Discharge efficiency $\eta_{EV,m}^{disch}$ in %	90
Charge efficiency $\eta_{EV,m}^{ch}$ in %	90
Prequalified FCR power $\overline{P^{FCR}}_{EV,m}$ in kW	9.95

$$\overline{P^{FCR}}_{EV,m} = \frac{\overline{E}_{EV,m}}{\psi_{EV,m}}, \forall m \in M \tag{6.61a}$$

$$\overline{P}_{EV,m}^{FCR} = \min(\overline{P^{FCR}}_{EV,m}, P_{EV,m}^{plan}), \forall m \in M \tag{6.61b}$$

$$P_{EV,m,t}^{FCR} \leq x_{EV,m,t}^{FCR} \cdot \overline{P}_{EV,m}^{FCR} \cdot x_{EV,m,t}^{plug}, \forall m \in M, \forall t \in \{1, ..., t^{hor}\} \tag{6.61c}$$

SOC restriction

SOC restrictions describe the 15-min. criterion, which defines SOC levels of the permissible operation range during FCR provision. The equation is only defined for the time steps that the vehicle is plugged in to model availability.

$$\forall m \in M, \forall t \in \{t_{EV,m}^{plug-in}, ..., (t_{EV,m}^{plug-out} - 1)\}:$$

$$E_{EV,m,t} \geq x_{EV,m,t}^{FCR} \cdot \overline{P^{FCR}}_{EV,m} \cdot \Delta_t^{FCR} \tag{6.62a}$$

$$E_{EV,m,t} \leq x_{EV,m,t}^{FCR} \cdot \overline{E}_{EV,m} - \overline{P^{FCR}}_{EV,m} \cdot \Delta_t^{FCR} + (1 - x_{EV,m,t}^{FCR}) \cdot \overline{E}_{EV,m} \tag{6.62b}$$

FCR provision and charge management costs are modeled as with the BSS (see, for instance, Equation 6.51).

Installation at the case study

EVs are used at the industrial production plant to commute from one building to another. These vehicles are charged at private charging stations within the premises. Furthermore, workers or visitors use semi-public charging stations on the public parking spaces of the industrial production plant.

For the case study, vehicle telematics data has been received from the OEM, which runs the production plant. Data was given for all charging events that took place within the premises of the case study. The data contains information on the timestamp for plug-in time (charge start), charge end, and plug-out time, as well as the SOC level at these times were given. To adjust this data to the time step of the implemented optimization, the timestamps were rounded to the time step frequency. The data only includes vehicles manufactured by the OEM. Therefore, not all charging events at semi-public charging stations is included. A perfect forecast of the contained data has been assumed for the optimization.

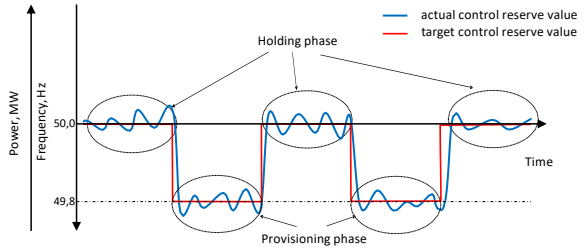

Figure 6.12: FCR prequalification protocol of German TSOs
Control reserve provision is tested for a period of usually two 15-minute time slots in negative and positive direction

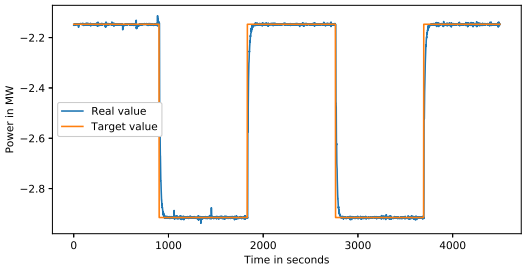

Figure 6.13: Prequalification of 675 kW of FCR power with an aggregate of AHU of building 1
Negative power values are applied due to the role of an electric power consumer

6.7.6 Air handling units

At the industrial site AHUs were aggregated per building. The baseline aggregated AHU power output per building was estimated from the control parameters for AHU control at the target site. As opposed to the modeling approach of, e.g., the CHP but similarly to the model of the EV, the power level in time step t ($P_{AHU,n,t}$) is given as a parameter by a baseline load profile as defined in Equation 6.63. This modeling approach was chosen due to the fact that a time series of the power consumption of individual AHUs was retrievable from the implemented control logic of the electric motors of the AHUs in the SCADA system.
The following subsections provide the modeling approach for

1. the standard operation,
2. the flexibility,
3. the local DR, and
4. the provision of control reserve

of each AHU m.

Operation

At the investigated industrial site the power consumption of the AHU is mainly controlled by the outside temperature. Higher temperatures cause the electric motors to run at higher power levels as more air is needed to cool the connected buildings. Therefore, the power consumption of the AHU increases in a linear fashion between a winter (at $\theta_t < \underline{\theta}$) and a summer (at $\overline{\theta} \geq \theta_t$) operation point depending on the outside temperature. This is shown in equation 6.63.

$$P_{AHU,n,t} = \begin{cases} \check{P}_{AHU,n} \cdot x^{op}_{AHU,n,t} & \text{for } \theta_t < \underline{\theta} \\ \frac{(\theta_t - \underline{\theta})}{(\overline{\theta} - \underline{\theta})} \cdot (\overline{P}_{AHU,n} - \check{P}_{AHU,n}) \cdot x^{op}_{AHU,n,t} & \text{for } \underline{\theta} \geq \theta_t < \overline{\theta}\ , \forall n \in N, \forall t \in \{1,...,t^{hor}\} \\ \overline{P}_{AHU,n} \cdot x^{op}_{AHU,n,t} & \text{for } \overline{\theta} \geq \theta_t \end{cases} \tag{6.63}$$

Electrical Flexibility

The negative flexibility of each AHU can be defined by the difference of the maximum power $\overline{P}_{AHU,n}$ and the operation point $P_{AHU,n,t}$ and the positive flexibility by the difference of the operation point $P_{AHU,n,t}$ and the partial power $\check{P}_{AHU,n}$ respectively as shown in equation 6.64.

$$F^{-}_{AHU,n,t} = \overline{P}_{AHU,n} - P_{AHU,n,t}, \forall n \in N, \forall t \in \{1,...,t^{hor}\} \tag{6.64a}$$

$$F^{+}_{AHU,n,t} = P_{AHU,n,t} - \check{P}_{AHU,n}, \forall n \in N, \forall t \in \{1,...,t^{hor}\} \tag{6.64b}$$

Local and external flexibility services

The flexibility services provided by the AHUs include LEO, LPO, FCR and aFRR. Due to the different modeling approach, the use of load profile commitment and load profile adjustment are modeled in the following Equation 6.65. While power for local flexibility services $P^{-}_{AHU,n,t}, P^{+}_{AHU,n,t}$ changes the power level from the normal operation, power reserved for external flexibility services $P^{FCR}_{AHU,n,t}, P^{aFRR}_{AHU,n,t}$ reserves a power range that can be called if required.

$$F^{-}_{AHU,n,t} = P^{FCR^{-}}_{AHU,n,t} + P^{aFRR^{-}}_{AHU,n,t} + P^{-}_{AHU,n,t}, \forall n \in N, \forall t \in \{1,...,t^{hor}\} \tag{6.65a}$$

$$F^{+}_{AHU,n,t} = P^{FCR^{+}}_{AHU,n,t} + P^{aFRR^{+}}_{AHU,n,t} + P^{+}_{AHU,n,t}, \forall n \in N, \forall t \in \{1,...,t^{hor}\} \tag{6.65b}$$

$$P^{aFRR^{-}}_{AHU,n,t}, P^{aFRR^{+}}_{AHU,n,t} \in [0, \overline{P^{aFRR}}_{AHU,n}], P^{FCR}_{AHU,n,t} \in [0, \overline{P^{FCR}}_{AHU,n}], \forall n \in N$$

Local flexibility services

AHUs can influence the power consumption of the industrial site using local DR. Positive local DR ($P^{+}_{AHU,n,t}$) implies the reduction of the power consumption of the electric motor, which would result in a lower ventilation speed and less airflow and negative local DR ($P^{-}_{AHU,n,t}$) vice versa.
To prohibit the simultaneous use of positive as well as negative local DR, the binary variables $x^{+}_{AHU,n,t}$ and $x^{-}_{AHU,n,t}$ were introduced and the following relationships were defined:

$$P^{+}_{AHU,n,t} \leq (\overline{P}_{AHU,n,t} - \check{P}_{AHU,n,t}) \cdot x^{+}_{AHU,n,t}, \forall n \in N, \forall t \in \{1,...,t^{hor}\} \tag{6.66a}$$

$$P^{-}_{AHU,n,t} \leq (\overline{P}_{AHU,n,t} - \check{P}_{AHU,n,t}) \cdot x^{-}_{AHU,n,t}, \forall n \in N, \forall t \in \{1,...,t^{hor}\} \tag{6.66b}$$

$$x^{+}_{AHU,n,t} + x^{-}_{AHU,n,t} \leq 1, \forall n \in N, \forall t \in \{1,...,t^{hor}\} \tag{6.66c}$$

The relationships prevent the case that $x^{+}_{AHU,n,t}$ and $x^{-}_{AHU,n,t}$ take up the value 1 and consequently set either $P^{+}_{AHU,n,t}$ or $P^{-}_{AHU,n,t}$ to 0.
The use of local DR is modeled similarly to [150]: Under the condition of

1. operation between $\check{P}_{AHU,n,t}$ and $\overline{P}_{AHU,n,t}$ and
2. the same electricity consumption over the periods of a duration of T^{LDR}_{AHU},

The model of the provision of flexibility services is based on the model of automatically controlled appliances in Gottwalt et. al [150]. The inertia of the air balance as described in Section 4.2.4 suggests that a decrease of power consumption of the ventilators is justified if it is increased at a later time. One can imagine this model like a virtual storage. This idea has also been introduced by, e.g., [168, 352]. Equation 6.67 models exactly this condition in which positive local DR in timeslot t has to equal the average of negative local DR over the next T^{LDR}_{AHU} periods. This period T^{LDR}_{AHU} is defined by [150] as the flexibility interval and accounts for the modeling of the rebound effect. Furthermore, it was assumed that the AHUs normally run on the most efficient operation point in terms of output per power consumption. A temporary change of the operation point leads to losses in efficiency. Thus, an efficiency for local DR measures ($\eta^{-}_{AHU,n} = 0.95$ %) was included in the equation to make up for the loss in output efficiency

Table 6.8: Parameters of HVACs at the case study.

AHU	1	2	3
Nominal electric power consumption in summer $\overline{P}_{AHU,n}$ in MW	3.375	4.671	2.187
Nominal electric power consumption in winter $\check{P}_{AHU,n}$ in MW	1.728	2.392	1.120
Prequalified FCR power $\overline{P^{FCR}}_{AHU,n}$ in MW	0.675	0.9342	0.4374
Prequalified aFRR power $\overline{P^{aFRR}}_{AHU,n}$ in MW	1.647	2.279	1.067
Selected probability for positive aFRR reserve call $p^{aFRR^+}_{AHU,n}$ in %		1.2	
Selected probability for negative aFRR reserve call $p^{aFRR^-}_{AHU,n}$ in %		1.2	
Resulting energy price of $aFRR^+$ call $\gamma^{aFRR^+}_{AHU,n}$ in EUR/MWh		210	
Resulting energy price of $aFRR^-$ call $\gamma^{aFRR^-}_{AHU,n}$ in EUR/MWh		272	
Efficiency of negative local demand response $\eta^-_{AHU,n}$ in %		95	
Flexibility interval T^{LDR}_{AHU} in h		4	

of the fan. The definition of efficiencies to model the inequalities in positive and negative DR measures has also been used by Hao et. al [168].

$$\sum_{i=0}^{T^{LDR}_{AHU}} P^+_{AHU,n,t+1} = \sum_{i=0}^{T^{LDR}_{AHU}} \eta^-_{AHU,n} \cdot P^-_{AHU,n,t+i}, \forall n \in N, \forall t \bmod T^{LDR}_{AHU} \equiv 0 \in \{1,...,t^{hor}\} \tag{6.67}$$

aFRR model

For the commercialization of the AHU as aFRR, a call probability of 2h per week and a balanced call ratio between positive and negative call probability was desired by the local energy management. Thus, both positive and negative energy prices were selected upon the desired call probability. This leads to the following conditions:

$$p^{aFRR^+}_{AHU,n} = p^{aFRR^-}_{AHU,n}, \forall n \in N \tag{6.68a}$$

$$p^{aFRR^+}_{AHU,n} \leq \frac{2}{(24 \cdot 7)}, \forall n \in N \tag{6.68b}$$

Installation at the case study

At the case study the AHU of three buildings has been modeled (see Table 6.8). Figure 6.13 shows a prequalification run of the aggregated AHUs of building 1.

6.7.7 Chiller

For the chiller, a baseline load profile is given that shows the power consumption $P_{CHI,o,t}$ (see Figure 6.14). This power profile can be adjusted to provide local flexibility services. Due to the lack of the ability to control, the chiller is not able to provide external flexibility services such as FCR or aFRR.
The power consumption of the chiller can be controlled by an adjustment of the desired flow temperature, leading to a start and stop of the operation of individual compressors of the chiller.

Electrical flexibility

The flexibility of the chiller is defined similarly to the flexibility of the AHUs. As shown in Table 6.1, continuous operation between a minimum and a maximum power has been modeled. Although the chiller consists of a number

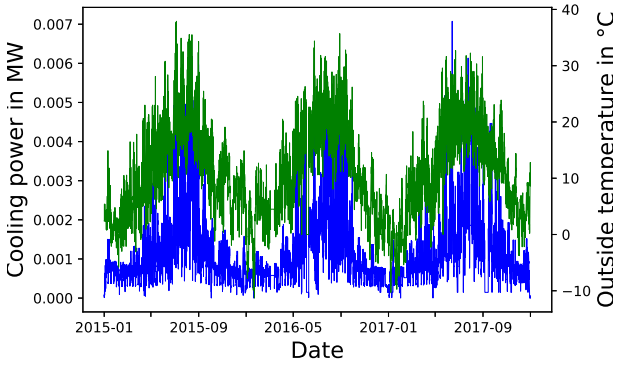

Figure 6.14: Electric power consumption of Chiller and outside temperature
Power consumption(in blue) and outside temperature (in green) displayed for years 2015-17 at the case study

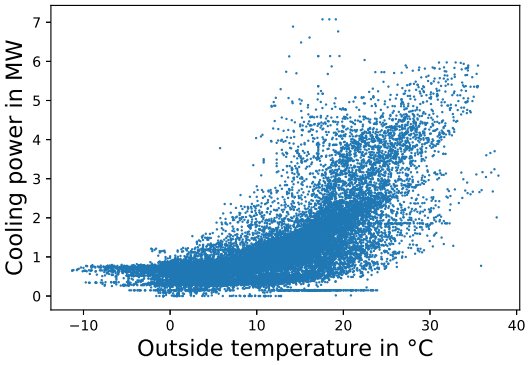

Figure 6.15: Scatter plot of electric power consumption of Chiller
Electric power consumption(y-axis) and outside temperature (x-axis) displayed for the years 2015-17 at the case study

of compressors that are switched on or off, the power profile with metered data of a frequency of 15 min. still resembles a continuous power profile. Thus a continuous operation of the chiller can be achieved by the switching and the length of operation of individual compressors.

$$F^{-}_{CHI,o,t} = (\overline{P}_{CHI,o} - P_{CHI,o,t}) \cdot x^{op}_{CHI,o,t}, \forall o \in O, \forall t \in \{1,...,t^{hor}\} \tag{6.69a}$$

$$F^{+}_{CHI,o,t} = (P_{CHI,o,t} - \underline{P}_{CHI,o}) \cdot x^{op}_{CHI,o,t}, \forall o \in O, \forall t \in \{1,...,t^{hor}\} \tag{6.69b}$$

Flexibility services

The resulting flexibility can be used to provide local flexibility services such as peak shaving; however, the adjustment of the power level should not influence the actual purpose of satisfying the cooling demand. To model the cooling demand, the relationship with the outside temperature and the power consumption is used. In Figure 6.14 a clear correlation between these two time series is visible. Figure 6.15 provides a scatter plot of temperature levels and power of the chiller. It is visible that below a temperature of around 10 °C, the temperature hardly has influence on the power level. Generally, this indicates that at this temperature the base load for cooling is operated which can be provided with the power output of an individual compressor. Above this threshold, the outside temperature has a strong influence on the cooling power. This is due to the higher difference in the ambient temperature and the desired flow temperature. Losses due to convection increase and the EER decreases.
Therefore, a temperature-dependent factor was added to limit the offered flexibility. Thus, in warm days, when cooling demand is high, a smaller share of the power consumption is provided as flexibility. A drawback of this methodology is that it is solely temperature driven and does not take into account other influences on cooling demand such as production activity. This can be partly justified, as during times of less production activity the need for flexibility services is also generally lower, as no peak in electricity consumption occurs. The factor is shown in Equation 6.70. It limits the flexibility in a linear fashion above a temperature of 10 °C.

$$P^{-}_{CHI,o,t} \leq F^{-}_{CHI,o,t} \cdot \frac{10}{\max(\theta_t, 10)}, \forall o \in O, \forall t \in \{1,...,t^{hor}\} \tag{6.70a}$$

$$P^{+}_{CHI,o,t} \leq F^{+}_{CHI,o,t} \cdot \frac{10}{\max(\theta_t, 10)}, \forall o \in O, \forall t \in \{1,...,t^{hor}\} \tag{6.70b}$$

Table 6.9: Parameters of the chiller at the case study.

Chiller	1
Nominal electric power consumption $\overline{P}_{CHI,o}$ in MW	7.2
Efficiency of negative local demand response $\eta^{-}_{CHI,o}$ in %	90
Flexibility interval T^{LDR}_{CHI} in h	2

Local flexibility services

For the provision of local flexibility services, the same model as for AHU plants is used. A flexibility interval of the chiller T^{LDR}_{CHI} is defined that allows to temporarily adjust the power consumption.

$$\sum_{i=0}^{T^{LDR}_{CHI}} P^{+}_{CHI,o,t+i} = \sum_{i=0}^{T^{LDR}_{CHI}} \eta^{-}_{CHI,o} \cdot P^{-}_{CHI,o,t+i}, \forall o \in O, \forall t \bmod T^{LDR}_{CHI} \equiv 0 \in \{1,...,t^{hor}\} \tag{6.71}$$

Installation at the case study

One chiller is available at the case study with characteristics displayed in Table 6.9.

6.7.8 Power-to-heat plant

Energy conversion

P2H plants convert electric energy ($P_{P2H,p,t}$) to thermal energy in the form of heat ($Q_{P2H,p,t}$). The P2H technology at the case study is an electric boiler, which carries out the power to heat conversion with an efficiency of $\mu_{P2H,p}$ as defined in equations 6.72. To account for aFRR calls the net power ($\dot{P}_{P2H,p,t}$) is used in the equation.

$$\dot{P}_{P2H,p,t} \cdot \mu_{P2H,p} = Q_{P2H,p,t}, \forall p \in P, \forall t \in \{1,...,t^{hor}\} \tag{6.72}$$

Electrical Flexibility

The available flexibility of power-to-heat plants in time step t is defined by the difference of the P2H power level $P_{P2H,p,t}$ to the minimum power level ($\underline{P}_{P2H,p} = 0$) and the nominal power level ($\overline{P}_{P2H,p}$).

$$F^{-}_{P2H,p,t} = \overline{P}_{P2H} - P_{P2H,p,t}, \forall p \in P, \forall t \in \{1,...,t^{hor}\} \tag{6.73a}$$

$$F^{+}_{P2H,p,t} = P_{P2H,p,t}, \forall p \in P, \forall t \in \{1,...,t^{hor}\} \tag{6.73b}$$

External flexibility services

The P2H plant can deliver external flexibility services in the form of FCR and aFRR. Due to the high reaction speed, the P2H can provide the full power range as FCR and aFRR.

$$F^{-}_{P2H,p,t} \geq P^{aFRR-}_{P2H,p,t} + P^{FCR}_{P2H,p,t}, \forall p \in P, \forall t \in \{1,...,t^{hor}\} \tag{6.74a}$$

$$F^{+}_{P2H,p,t} \geq P^{aFRR+}_{P2H,p,t} + P^{FCR}_{P2H,p,t}, \forall p \in P, \forall t \in \{1,...,t^{hor}\} \tag{6.74b}$$

$$P^{aFRR-}_{P2H,p,t}, P^{aFRR+}_{P2H,p,t} \in [0, \overline{P^{aFRR}}_{P2H,p}], P^{FCR}_{P2H,p,t} \in [0, \overline{P^{FCR}}_{P2H,p}], \forall p \in P$$

Table 6.10: Parameters of P2H plant at the case study

P2H plant	1
Nominal electric power consumption $\overline{P}_{P2H,p}$ in MW	0.5
Power-to-heat efficiency $\mu_{P2H,p}$ in %	0.9
Prequalified FCR power $\overline{P^{FCR}}_{P2H,p}$ in MW	0.5
Prequalified aFRR power $\overline{P^{aFRR}}_{P2H,p}$ in MW	0.5
Energy cost of $aFRR^{+}$ call $\gamma^{aFRR^{+}}_{P2H,p}$ in EUR/MWh	-61.23
Energy cost of $aFRR^{-}$ call $\gamma^{aFRR^{-}}_{P2H,p}$ in EUR/MWh	61.23
Selected energy price of $aFRR^{+}$ call $\gamma^{aFRR^{+}}_{P2H,p}$ in EUR/MWh	34
Selected energy price of $aFRR^{-}$ call $\tau^{aFRR^{-}\_margin}_{P2H,p}$ in EUR/MWh	340
Resulting probability for positive aFRR reserve call $p^{aFRR^{+}}_{P2H,p}$ in %	54.2
Resulting probability for negative aFRR reserve call $p^{aFRR^{-}}_{P2H,p}$ in %	2.6

aFRR call energy costs

The energy costs for providing negative control reserve, which is the standard case for P2H plants, is determined by costs of additional surcharges and grid fees as well as savings due to the value of the resulting heat production. In Equation 6.75 it is assumed that the heat production, which is replaced by the power-to-heat plant, is done by a gas boiler. Here, the gradient cost is assumed.

$$\gamma^{aFRR^{-}}_{P2H,p} = \tau^{fees}_{GRID} - \frac{\overline{c}^{var}_{BOI,1}}{\mu_{P2H,p}}, \forall p \in P \tag{6.75}$$

For positive aFRR, opposite costs are used in the optimization model assuming that the plant is procuring energy from the grid at the time of the reserve call.

Cost components for the objective function

The P2H plant converts electric power into thermal power. The cost of additional power consumption leading to increased procurement of electricity from the public grid is registered by the local flexibility service LEO (c^{LEO}_{t}).

Installation at the case study

At the case study, one small P2H plant exits. Parameter values are summarized in Table 6.10

6.8 Aggregation of flexibility for control reserve provision

The regulatory framework for FCR and aFRR grants the possibility to aggregate individual devices. Final bids for FCR and aFRR auctions have to satisfy the criteria in Table 3.5; however, these conditions can also be fulfilled by multiple devices together. Various devices can combine their flexibility offers to form bids specified according to the conditions set by the TSOs.
Furthermore, the TSOs define four kinds of level of aggregation according to [399]:

1. a technical unit (TU) - power generating modules and demand units that deliver control reserve
2. a reserve providing unit (RPU) - a single or an aggregation of TUs connected to a common grid connection point (GCP)

Table 6.11: Conditions for reserve control bids of products FCR and FRR that offer degrees of freedom for aggregation.

	FCR	**aFRR**
Product duration	4 hours	
Minimum bid size	1 MW	
Minimum bid increment	1 MW	
Product symmetry	Symmetric bids	Asymmetric bids

3. a reserve providing group (RPG) - any aggregation of technical units connected to more than one grid connection point
4. a pool - single or multiple aggregated RPUs and/or RPGs that fulfill(s) the requirements of control reserve products. A pool is required for placing bids for control reserve products.

As introduced in Section 2.2.3, external aggregators or VPPs exist that form pools to commercialize different RPGs or RPUs. Specifically, they bundle flexibility offers by DERs and commercialize them on the control reserve markets; however, to do so they generally demand a fee.
With an industrial site as large as the case study, the potential of local aggregation and commercialization can be increased by aggregating local TUs within an RPU, instead of commercializing TUs individually. Furthermore, depending on the number, timing, and size of flexibility offers, it might make sense to form an own local pool instead of commercializing the flexibility using an external aggregator. To answer these research questions, different scenarios are defined that model these scenarios by exploring the degrees of freedom of control reserve provision. Table 6.11 summarizes the relevant conditions that allow degrees of freedoms relevant for the aggregation of devices. For both FCR and aFRR control reserve products, the product duration equals 4h, the minimum bid size is 1 MW and can be increased by 1 MW increments.

6.8.1 Degrees of freedom in control reserve provision

Still, most providers use individual devices b or TUs to provide FCR. As FCR has to be provided symmetrically for a product duration of 4h, this entails that positive and negative reserve power for each device providing FCR have to match each other for the entire product duration.

Individual vs. aggregated control reserve provision

This symmetric provision of FCR by an individual TU can be modeled as follows:

$$P_{a,b,t}^{FCR} = P_{a,b,t}^{FCR-} = P_{a,b,t}^{FCR+}, \forall a \in \mathbb{A}, \forall b \in \mathbb{B}, \forall t \in \{1, ..., t^{hor}\} \tag{6.76}$$

Devices exist, however, that can only supply either positive or negative FCR. As no symmetric FCR can be offered by these TUs individually, this can result in forfeited revenues.
A solution to this problem is the introduction of an aggregated FCR power (P_t^{FCR}) over an aggregate of TUs that aggregates both positive and negative FCR over all devices. The aggregated FCR provision can be achieved by equating the FCR power to the sum of all possible positive and negative FCR powers of individual devices for each t thereby replacing Equation 6.76 with the following constraint:

$$P_t^{FCR} = \sum_{a \in \mathbb{A}} \sum_{b \in \mathbb{B}} P_{a,b,t}^{FCR^-} = \sum_{a \in \mathbb{A}} \sum_{b \in \mathbb{B}} P_{a,b,t}^{FCR^+}, \forall t \in \{1, ..., t^{hor}\} \tag{6.77}$$

Equation 6.78 provides the mathematical relation to sum up all aFRR offers of individual devices. Symmetry is not required for aFRR bids; however, an aggregation can help to achieve the required bid size or bid size increment as shown in Table 6.11.

$$P_t^{aFRR^-} = \sum_{a\in\mathbb{A}} \sum_{b\in\mathbb{B}} P_{a,b,t}^{aFRR^-}, \forall t \in \{1,...,t^{hor}\} \tag{6.78a}$$

$$P_t^{aFRR^+} = \sum_{a\in\mathbb{A}} \sum_{b\in\mathbb{B}} P_{a,b,t}^{aFRR^+}, \forall t \in \{1,...,t^{hor}\} \tag{6.78b}$$

Product duration

Furthermore, for both FCR and FRR provision, the power (resp. capacity) for the declared control reserve product has to be reserved for the entire product duration. This has been modeled for individual provision already in Equation 6.10.

Nevertheless, often devices can only provide FRR or FCR for a time interval shorter than the actual product duration. When combining devices locally as an RPU, one can use this opportunity and increase the reserve power that can be offered, while at the same time assuring the safe provision of flexibility services. This allows different devices to contribute to the control reserve provision at a different time slot of the product duration. For example, for a 4h product duration, the first two hours can be provided by device x, while the second two hours can be provided by device y.

For aggregated control reserve of an RPU, it is required to respect the product duration of the reserve products:

$$\begin{aligned} \forall a \in \mathbb{A}, \forall b \in \mathbb{B}, \forall t \in \{1,...,t^{hor}\}, t \bmod \frac{4\cdot 60}{\Delta_t} \equiv 0, \forall s \in \{1,...\frac{4\cdot 60}{\Delta_t} - 1\} : \\ P_t^{FCR} = P_{t+s}^{FCR} \\ P_t^{aFRR^-} = P_{t+s}^{aFRR^-} \\ P_t^{aFRR^+} = P_{t+s}^{aFRR^+}, \end{aligned} \tag{6.79}$$

A decentralized aggregation of devices to provide control reserve is already done by a VPP; however, current virtual power plants often lack the possibility to provide flexibility offers over shorter periods than the 4h-time slots of control reserve products defined by the TSOs. Furthermore, there seems to exist an abundance of negative flexibility, while positive flexibility is scarce. Therefore, it is often difficult to find a device that can provide positive FCR to match a negative FCR plant.

Bid size

In the case of aggregation by an external aggregator, the flexibility offers do not have to comply with the bid sizes defined in Table 6.11 as the aggregator can combine the flexibility offers with flexibility offers from different BSPs. Thus, for the commercialization using a VPP, the following condition holds true concerning the bid size:

$$P_{a,b,t}^{FCR}, P_{a,b,t}^{FRR-}, P_{a,b,t}^{FRR+} \in \mathbb{R}_{\geq 0}, \forall a \in \mathbb{A}, \forall b \in \mathbb{B}, \forall t \in \{1,...,t^{hor}\} \tag{6.80a}$$

$$P_t^{FCR}, P_t^{FRR-}, P_t^{FRR+} \in \mathbb{R}_{\geq 0}, \forall a \in \mathbb{A}, \forall b \in \mathbb{B}, \forall t \in \{1,...,t^{hor}\} \tag{6.80b}$$

Equation 6.80a describes the bid size for control reserve provision by individual devices and Equation 6.80b for an aggregated control reserve power.

For the provision of control reserve without the further aggregation of an external VPP, it is necessary to comply with the defined bid sizes given for control reserve products. As shown in Table 6.11 minimum bid sizes for FCR,

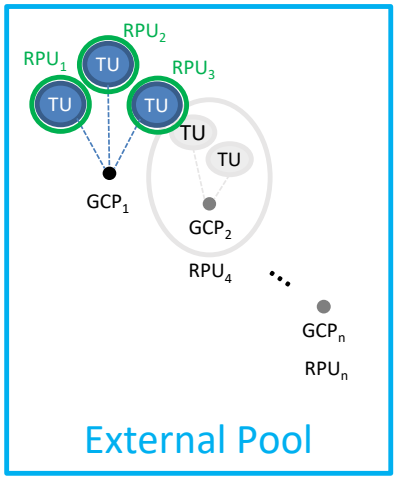

Figure 6.16: Aggregation model of Scenario 1
The industrial site provides control reserve commercializing each TU individually and is part of an external pool run by an external aggregator.

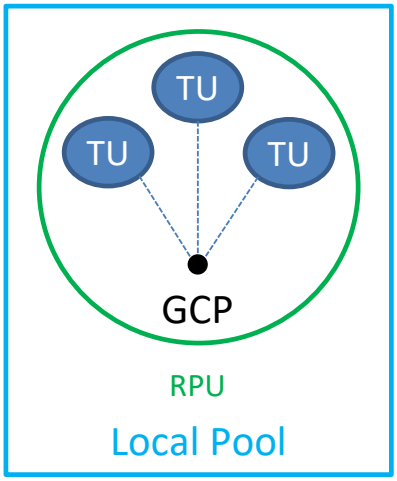

Figure 6.17: Aggregation model of Scenario 2
The industrial site provides control reserve commercializing an aggregate using all TUs and forms a local pool not run by an external aggregator.

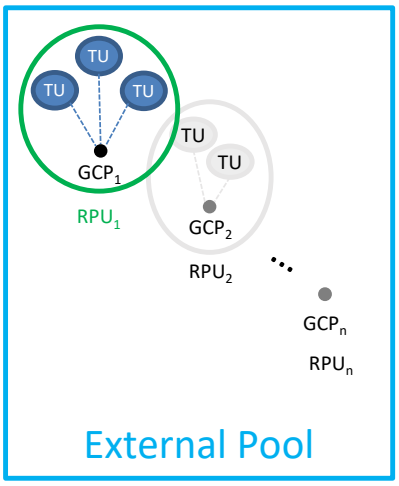

Figure 6.18: Aggregation model of Scenario 3
The industrial site provides control reserve commercializing an aggregate using all TUs. This aggregate is part of an external pool run by an external aggregator.

as well as FRR are 1 MW with bid increments of 1 MW. This can be modeled by changing the variables of control reserve power from positive real numbers to integer numbers.

$$P^{FCR}_{a,b,t}, P^{FRR-}_{a,b,t}, P^{FRR+}_{a,b,t} \in \mathbb{N}, \text{ for individual control reserve provision} \tag{6.81a}$$

$$P^{FCR}_{t}, P^{FRR-}_{t}, P^{FRR+}_{t} \in \mathbb{N}, \text{ for aggregated control reserve provision} \tag{6.81b}$$

Again, Equation 6.81a describes the bid size for control reserve provision by individual devices and Equation 6.81b for an aggregated control reserve power.

Investigated scenarios

To evaluate the effect of the degrees of freedom concerning aggregation, three scenarios have been defined:

1. **Scenario 1** - individual commercialization on a device-by-device basis by an external aggregator.
   This scenario uses the equations set in 6.76 and 6.10. Furthermore, the offer of flexibility to an external aggregator allows for a flexible bid size defined in Equation 6.80a. By the definition of the TSOs, each TU is commercialized individually as an RPU as shown in Figure 6.16. These are coupled in a pool run by an external aggregator. The aggregator can combine the flexibility offers of the individual RPUs with other flexibility offers. It was assumed that the flexibility offers in this scenario can be provided to the aggregator. The flexibility offers are reimbursed with the actual control reserve price minus an aggregator fee.
2. **Scenario 2** - Local aggregation and direct commercialization without an external aggregator.
   This scenario uses equations 6.77, 6.78, and 6.79 for the modeling of control reserve aggregation and relies on direct commercialization without an aggregator as shown in Equation 6.81b.In this scenario, TUs are connected to one grid connection point (of the industrial site) and aggregated as a single RPU. This RPU forms a local pool as shown in Figure 6.17. The flexibility offers are offered without the assistance of an external aggregator. Thus, direct commercialization rules apply, such as the integer-value bid size of reserved power.

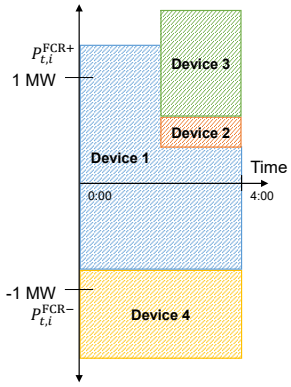

Figure 6.19: Example of FCR offers
Exemplary positive and negative FCR offers for a time slot by four devices

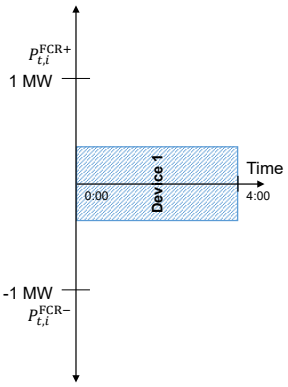

Figure 6.20: Illustration of Scenario 1
Only device 1 shows a symmetric FCR offer over the entire time slot

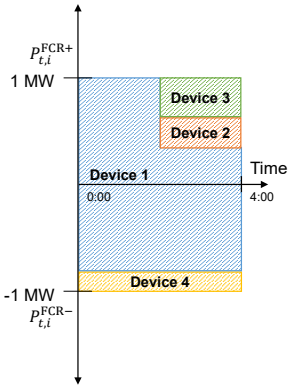

Figure 6.21: Illustration of Scenario 2
Devices 1-4 form a symmetric, Integer value FCR offer over the entire time slot

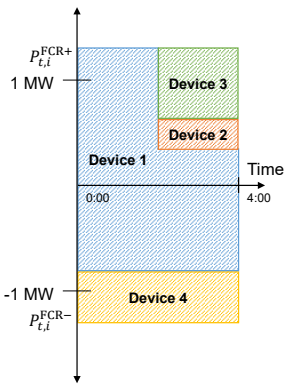

Figure 6.22: Illustration of Scenario 3
Devices 1-4 jointly form a symmetric FCR offer over the entire time slot

3. **Scenario 3** - Local aggregation and indirect commercialization by an aggregator.
   This scenario relies on the control reserve modeling of equations 6.77, 6.78, 6.79, and the commercialization using an aggregator as shown in Equation 6.80b. In terms of aggregation, TUs are again aggregated as a single RPU. In contrast to Scenario 2, this RPU is commercialized by an external pool (aggregator) as shown in Figure 6.17. The aggregated flex offers of the industrial site participate within a virtual power plant and can, thus, be combined with flex offers of external TUs. The remuneration is calculated as in Scenario 1; however, this time each TU is not commercialized individually but all TUs are commercialized in an aggregated manner.

To illustrate the three selected scenarios, Figures 6.19 depicts a scenario of different FCR flex offers concerning symmetry, duration, and size. Based on these flex offers, Figures 6.20 to 6.22 show how much reserved FCR power the industrial site would be able to commercialize for the scenarios defined above.
Figure 6.19 shows the example of FCR power offers. Device 1 can offer to provide positive as well as negative FCR; however, the positive FCR power flexibility offer cannot be provided to the full extent for the whole displayed product duration of 4 hours. Devices 2-4 can provide either only positive or only negative FCR power, Devices 2-3 also not for the whole product duration.
Figure 6.20 shows the possible FCR power to be commercialized in **Scenario 1**. FCR power has to be provided symmetrically on a device-by-device basis for the whole product duration. Thus, only part of the flexibility offer of Device 1 can be used, as the other devices can only offer to provide FCR on an asymmetrical basis.
Figure 6.21 shows the possible FCR power to be commercialized in **Scenario 2**. FCR power does not have to be provided symmetrically on a device-by-device basis but is tied to the bid size of 1 MW (integer value). Therefore, FCR offers of Devices 1, 3-4 can not be used to the full extent.
Figure 6.22 shows the possible FCR power to be commercialized in **Scenario 3**. Reserved FCR power is not tied to the bid size of 1 MW as further aggregation is done by an external VPP. Only the FCR offers of Devices 3, 4 are not used to the full extent as the FCR power is reserved in a symmetric fashion over the entire product duration.
Naturally, each scenario has a strong influence on the possible solution space. While the solution space for Scenario 1 is very limited due to strong restrictions on control reserve offers, the solution space of Scenario 3 is much greater due to the less constrained problem formulation. From the solution space in Scenario 3, Scenario 2 has to identify

all the solutions, which results in an integer value for control reserve offers. Therefore, the solution space of Scenario 1 and 2 is a subset of the solution space of Scenario 3.
For the case study, each scenario is evaluated according to the possible reserve control for products aFRR and FCR. A commercialization fee taken by the external aggregator is accounted for in Scenarios 1 and 3.

6.9 Optimization parameters

6.9.1 Selection of time step

In this thesis, time-discrete values are employed and Δ_t is used to denote the discretization step (e.g., Δ_t = 15 minutes), and t to index the t-th time step. A length of the time step of 15 minutes was chosen for the simulation of the modeled energy system. The selected time step for the optimization was chosen due to the following reasons:

1. Market design of the German electric power system: Trading of electrical energy happens for 15-minute intervals. Companies trading electricity have to forecast quantities of injection to and withdrawal from the electric power grid. Therefore, generation and consumption have to be forecasted on a 15-minute basis, which was also adopted in this simulation.
2. Available data: Various heterogeneous data sources from the industrial production site were used in the modeling process. Especially data relating to the energy system showed a minimum time step of 15 minutes. Data of the CHP plant, the thermal power balance, and local temperature measurement were only recorded in 1-hour intervals. Therefore, it was chosen to interpolate this data.

6.9.2 Optimization horizon

For visualization purposes of the results, the optimization has firstly been performed with an optimization horizon of seven days as a repeating pattern of energy demands due to weekly shift schedules is given at the case study (see Section 6.6). Thus, t^{hor} equals 672. This weekly pattern is also visible in the electrical power consumption in Figure 6.6. The corresponding figures and results are displayed in Section 7.1.
For the analysis of the contribution of flexibility services, an optimization horizon of one day (t^{hor} = 96) was selected. Results are given in Sections 7.2 and 7.3.

6.9.3 Simulation environment

The environment of the simulation has been built in the open-source optimization modeling language Pyomo of the programming language Python. During one simulation run the following steps are taken:

1. Parameter values are read from input data files.
2. Parameter values are pre-processed for the use in the simulation. During pre-processing the data is converted into a uniform format that fits the selected time step and optimization horizon.
3. The optimization problem is constructed including the predefined constraints and objective function.
4. The optimization problem is solved using the commercial solver Gurobi with given solution tolerances.
5. Results are visualized and interpreted.

6.9.4 Input data

Input data in Pyomo is stored in the form of parameters. The parameter values are given as either time series values or constant values describing plant or flexibility service parameters.
These parameters can be grouped into the following groups:

Table 6.12: Parameters relevant for energy demands and flexibility services for the case study

Parameter	Value
Heat loss efficiency in thermal distribution system η_{HN} in % (Eq. 6.23)	24.9
Share of FCR and EMO capacity-related revenues (ϕ^{VPP}) that is paid to the aggregator in %	20
Peak tariff υ^{peak} in EUR/MW (Eq. 6.11)	91.9
Grid fees and surcharges τ^{fees}_{GRID} in EUR/MWh (Eq. 6.15)	96.56
Penalty for the feed out of electricity ϕ^{SB} in EUR/MWh (Eq. 6.15)	10
Penalty for the sale of locally generated renewable electricity ϕ^{RES} in EUR/MWh (Eq. 6.15)	40

1. Constant plant parameters (e.g., nominal electrical power of a device) and constant schedule specifications (e.g., storage level at the beginning or end of the optimization horizon): These parameters are provided in the Tables for each energy technology in Section 2.4.
2. Constant energy demand and flexibility service parameters (e.g., the cost of feed-back into the grid or product duration) are displayed in Table 6.12.
3. Time series parameters including forecasted prices or energy demands (e.g., electrical energy demand or FCR power prices): The majority of the relevant market-based time series are introduced in Chapters 3, and 5. The most important energy demands are displayed in Chapter 6.

6.9.5 Assumptions

Regulatory conditions such as the taxation and subsidy of devices of certain energy technology were modeled according to the current legal German framework as to the knowledge of the authors and as explained in Sections 2.2 and 2.3.2.
Furthermore, assumptions were taken for the availability of forecasts. It is assumed that energy demands, energy prices, and energy generation by intermittent energy technologies such as the wind power plant can be forecasted. Final papers on forecasts supervised by the author can be found for instance in [180, 285].

6.9.6 Performed Simulation

The optimization was performed for 365 days of the year 2017 for all scenarios given in Section 6.8 and appropriate reference scenarios. A MIPGap of 10^{-7} and a time limit of 10 minutes were set per optimization. The time limit was assumed as adequate for sufficient time necessary for a day-ahead optimization.
The Gurobi MIPGap describes the relative gap between a lower bound l and an upper bound u. A solver continuously narrows down the search space of possible solutions by using the branch-and-cut method. In a minimization problem the lower bound is the best objective value an integer solution could potentially have in the current search space. This lower bound is identified by a relaxed problem (non-integer problem). The upper bound is the currently best objective value for the actual optimization problem. If the relative gap between the lower and the upper gap ($\frac{|l-u|}{|u|}$) is below the defined MIPGap the solver stops optimizing.
The respective code and the used data of the simulation can be found in the following GitHub repository [326].
The simulation was performed on a hardware provided by the FZI Research Center for Information Technology. The simulation uses 28 cores of an Intel Xeon E5-2697 processor with 2.60 GHz and 62 GB of RAM.
A total of eleven calculations are run to measure the impact of

1. the flexibility services and
2. the level of aggregation of control reserve offers

on the total energy cost. Thus, simulations are run with defined scenarios 1-3 and reference scenarios REF and LEO. The same input data such as wind power generation, control reserve market prices, and energy market prices from the year 2017 was used for the all calculations. Continuous availability of the individual energy devices is assumed. For the flexibility services FCR, aFRR, and energy market optimization, continuous bid acceptance has been assumed. Results are presented in the following Chapter 7.

6.10 Summary

In this chapter, a model of the dispatch and the aggregator problem for an industrial site with devices of a diverse set of energy technologies is developed and applied to a case study of the automotive industry. Additionally, the model is extended to reflect multiple scenarios of device aggregation for the provision of control reserve.
For the modeling of individual devices, the notation and generalized models are defined in Section 6.2; for example, a generalized device operation model is developed that is able to model three types of devices present at the case study. Based on this model, a generalized cost function for the objective function is implemented.
Furthermore, flexibility services identified in Chapter 3 are modeled in Section 6.3. The work classifies the flexibility services in two groups based on the way these services are provided and remunerated - load profile commitment and load profile adjustment. Reflecting regulatory conditions, simultaneous and serial provision of flexibility services by these devices are modeled. Depending on the identified group, the flexibility services vary greatly in terms of their cost or revenue function.
These cost and revenue functions are included in the objective function in Section 6.4. Next to the avoided costs or earnings from the flexibility services, the objective function includes the cost structure of the dispatch problem. Sections 6.5 and 6.6 describe the energy system and the energy demands at the case study. In addition, devices of eight different energy technologies found at the case study are modeled in Section 6.7. Depending on the data available, devices of the technologies are modeled based on a baseline or a free power profile. The implemented constraints reflect technological modeling of the devices and conditions of flexibility service provision.
Section 6.8 provides the mathematical modeling for degrees of freedom concerning the provision of control reserve. Flexibility offers can either be commercialized on a device level, or on an aggregated site level. Scenarios are defined concerning the level of aggregation of flexibility offers for the flexibility services FCR and aFRR, which is evaluated in Chapter 7.
The chapter thereby answers part of research questions 2 to 4: The chapter provides

1. the mathematical model of energy technologies and their capability to provide flexibility services (RQ 2),
2. the mathematical model for a joint optimization of the dispatch and the aggregator problem implementing also the multi-use functionality of energy technologies (RQ 3.1 and 3.2), and
3. a description and the mathematical model of the degrees of freedom in terms of aggregation of control reserve provision (RQ 4.1).

7 Evaluation

This chapter evaluates the results of the optimization performed with the model developed in Chapter 6. In Section 7.1, results of the optimization model introduced in Sections 6.2 to 6.7 are graphically illustrated. The optimization runs are performed with a horizon of one week and constraints of Scenario 1 of the aggregation levels of Section 6.8 are shown. The model of energy balances and individual energy technologies will be described along the results of the optimization runs.
Section 7.2 shows the results from an optimization over the entire year 2017 with an optimization horizon of a single day. This section displays the contribution of individual flexibility services to lower the total energy cost using Scenario 1 of the different scenarios displayed in Section 6.8.
Section 7.3 introduces results of Scenarios 2 and 3, and points out the differences to Scenario 1. Furthermore, it provides a comparison between the scenarios in terms of the optimal value of the objective function and the contribution of individual flexibility services.
Section 7.4 puts the results in perspective and discuss limitations to the optimization model and future research that is suggested by the author.

7.1 Results

This section illustrates the modeling done in Chapter 6 using figures that visualize the implemented constraints of the mathematical model. The section focuses on the model of flexibility services, energy demands, and energy technologies. The figures display the results from optimization runs with an optimization horizon of one week and a slightly adapted time limit[1] and parameters[2].
Firstly, energy demands for electrical and thermal energy are introduced. As the model of local flexibility services is determined by the load profile, the influence of local flexibility services will primarily be discussed along with the power balance in Section 7.1.1. The power balance determines the exchange of electricity with the public grid - the load profile. Secondly, illustrations of the models of energy technologies CHP, BSS, EV, AHU, and chiller in Section 7.1.2 are presented. External flexibility services are modeled on a device-level as defined in Scenario 1 and are, consequently, explained alongside the technologies.
The results rely on the configuration of energy technologies at the case study described in Chapter 6.

7.1.1 Energy demands

The fulfillment of energy demands modeled in the electrical and thermal power balance will be discussed in this chapter. The displayed figures illustrate the composition of the energy supply of an optimized schedule with the constraints introduced in Chapter 6. Furthermore, it is depicted how changes in production activities influence the energy supply.

Electrical power balance

Figure 7.1 shows the electric power balance as a result of the optimization in calendar week 20 of the year 2017.

[1] Instead of a time limit of 10 minutes, a time limit of 30 minutes has been chosen.
[2] Parameters such as the maximum run time of the EPS were adjusted according to the optimization horizon.

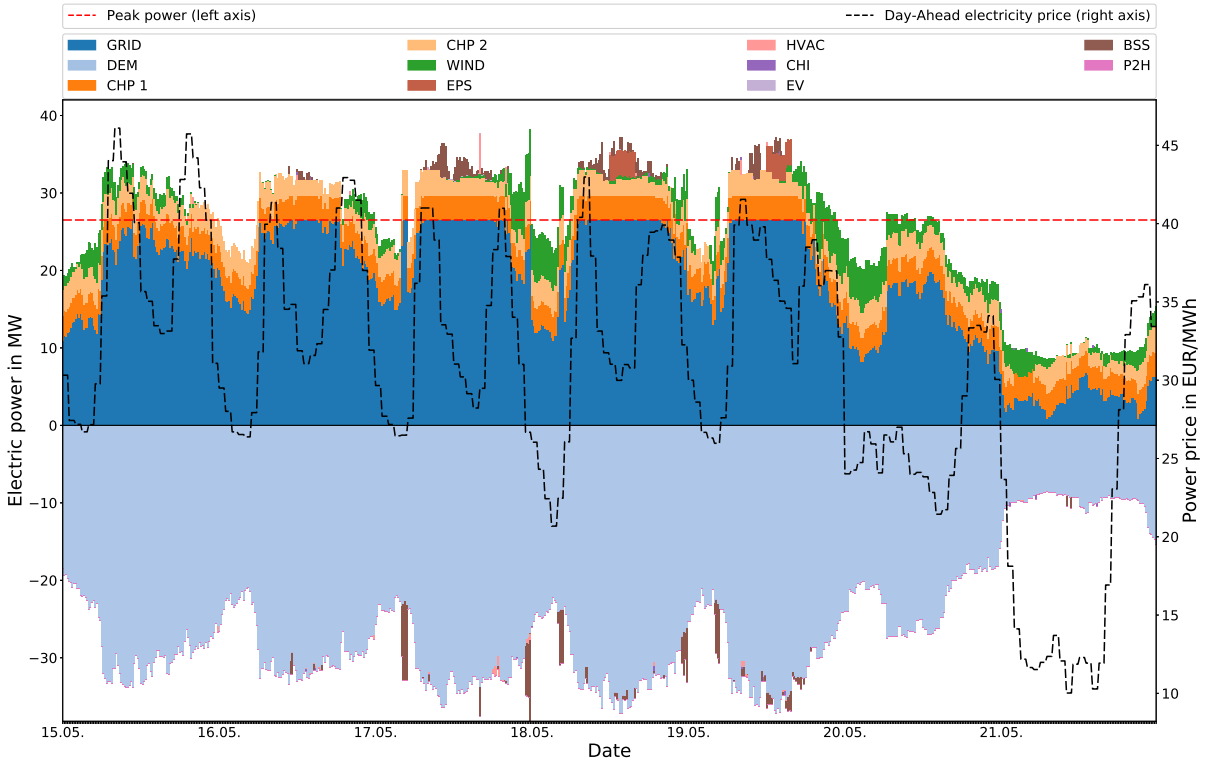

Figure 7.1: Electric power balance of calendar week 20 of 2017 optimized with constraints of Scenario 1
The primary y-axis displays electricity demand (light blue) or device-related consumption on the negative and external sourcing (dark blue) or device-related electricity generation on the positive axis. The dashed red line indicates the peak threshold of externally sourced electricity. The secondary y-axis displays electricity prices of the Day-Ahead market relevant for flexibility service LEO.

The primary y-axis shows the electric power: Negative values display the demand of electricity (DEM: $P_{DEM,t}$) in light blue and the use of energy technologies, which leads to an increase in electric power demand such as the charge of a BSS. Positive values show how this electricity demand is covered, e.g., by the import of electricity from the public grid in dark blue (GRID: $P^{+}_{GRID,t} - P^{-}_{GRID,t}$) or the discharge of a BSS in brown (BSS: $\sum_{l \in L} P^{+}_{BSS,l,t} - \sum_{l \in L} P^{-}_{BSS,l,t}$).

Other colors show the local electricity generation by generators or the adjustment of the power consumption of demand-side energy technologies. The orange shades, for instance, indicate the electricity generation of the two CHP plants ($\sum_{i \in I} P_{CHP,i,t}$).

The displayed power level of controllable energy technologies also influences the ability to provide external flexibility services. These will primarily be introduced on a device level, local flexibility services will be introduced in the following:

The red dashed line indicates the parameter of the peak threshold ($\overline{P}^{peak}$) for this optimization run set at 26.5 MW. It is visible that the final schedule of the load profile (*GRID*) is kept below this level although a maximum energy demand of 37.5 MW on May 19th was present.

This peak reduction is done utilizing different energy technologies: Especially visible is the use of the EPSs ($\sum_{k \in K} P_{EPS,k,t}$) and the BSSs. Additionally, small amounts of energy are buffered by the change in power consumption of the AHUs ($\sum_{n \in N} P^{+}_{AHU,n,t} - \sum_{n \in N} P^{-}_{AHU,n,t}$) and the chiller ($\sum_{o \in O} P^{+}_{CHI,o,t} - \sum_{o \in O} P^{-}_{CHI,o,t}$)). The BSSs, AHUs, and the chiller, represent electric storage flexibility. While the BSS represents an actual electricity storage, the AHUs and chiller represent a virtual storage: The storage capacity is defined by the flexibility of the demand for ventilation and cooling. The use of these storage technologies leads to an increase of electricity demand in the negative part of the y-axis at times where no peak reduction is necessary. The BSS, for instance, is charged in

the night before days with use for peak shaving, which leads to an increased electric power demand. This is also shown in Figures 7.9 and 7.8.

The black dashed line shows varying power prices from the Day-Ahead auction ($\tau^{DA}_{GRID,t}$) that are used for the flexibility service LEO. Values are shown on the secondary y-axis. Most weekdays display the "duck curve" form hinting at a high generation of solar energy in Germany during these days.

Energy technologies can be utilized for the flexibility service LEO, e.g., by moving the electricity import to periods with cheaper prices. The employment of this flexibility service, however, is not visible during the displayed week. Actually, electricity import is often reduced during times of comparably low energy prices around noon instead of reducing power procurement during the highly priced times in the morning and evening. This reduction can be attributed to the flexibility service LPO, as high demands of electric energy exist at noon. The primary use of flexibility for the flexibility service LPO instead of LEO can be explained by the much higher cost (higher coefficient in the objective function) of energy above the peak threshold, which is, consequently, prioritized in the displayed week.

Figure 7.2 shows the power balance as a result of the optimization in calendar week 18 of the year 2017. This week included a public holiday on Monday, the 1st of May. Naturally, this resulted in no production activities on this day at the industrial site, visible by the low electrical load required on this day.

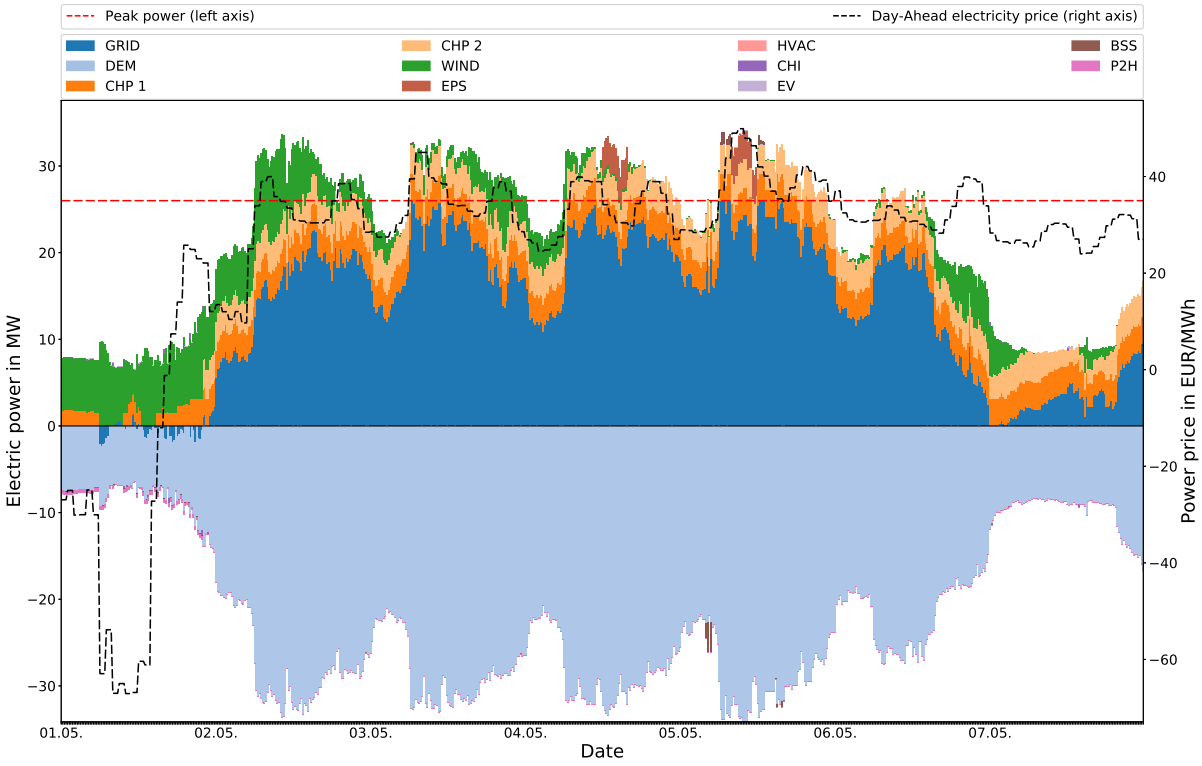

Figure 7.2: Electric power balance of calendar week 18 of 2017 optimized with constraints of Scenario 1
The primary y-axis displays electricity demand (light blue) or device-related consumption on the negative and external sourcing (dark blue) or device-related electricity generation on the positive axis. The dashed red line indicates the peak threshold of externally sourced electricity. The secondary y-axis displays electricity prices of the Day-Ahead market relevant for flexibility service LEO.

Furthermore, this low electricity demand coincided with strong wind power production ($P_{WIND,t}$) on this day shown in green[3]. These two parallel developments led to a load profile that partly includes an electricity export to the

[3] A sharp increase in wind power production is shown in the morning of May 1st. This is due to curtailment of wind power during night hours due to noise.

public grid, which contradicts local flexibility services *self-balancing* and *RES buffering* that are penalized in the cost function of LEO.
As the wind power production is sufficient to cover the demand, high wind power generation leads to a shut-down of both CHP 2 and CHP 1. Nevertheless, CHP 1 is operated in some instances, which leads to an export of electricity in the night between Monday, 1st of May, and Tuesday, the 2nd of May.
This leads to the conclusion that respective penalties ϕ^{SB} and ϕ^{RES} in the cost function of LEO are apparently chosen too small to fully avoid electricity exports: It is more economic to pay these penalties, operate the CHP at partial power, and export small amounts of electricity than to produce heat with gas boilers and import electricity. Still, the schedule abstained from the operation of the more expensive CHP 2, although this would have been technically feasible - the resulting heat could have been covered by the heating demand and the use of the dry cooler. The operation of the CHPs on this day is further explained in the respective heat balance in Figure 7.4.
Furthermore, the negative prices on May 1st would offer the possibility to charge the battery in a very inexpensive way; however, instead all BSSs are employed for EMO during this day, as it posed exceptionally high earnings. These were four times higher than the average daily EMO earnings.
Furthermore, on May 5th, the operation of the EPS is visible at peak electricity prices in Figure 7.2. This leads to a reduction of the load profile far below the given peak threshold, which is an example for the use of local flexibility with respect to *real-time price optimization* (flexibility service LEO).
The two examples of electric power balances have provided an overview of decisions that are taken into account for scheduling the controllable devices.

Thermal power balance

In the following, the balance of the thermal power production of heat is illustrated. To show the dependency on climatic conditions, the heat balance of the different seasons is introduced - winter, summer, and the transition period between winter and summer. The effects on the operation of individual devices is shown.

Winter

Figure 7.3 shows the heat balance during a winter week in mid February of 2017. The primary y-axis displays the thermal power balance from Equation 6.23. As with the electric power balance, the negative values show the heating demand and positive values indicate which devices are employed to satisfy this heating demand. Losses indicate the additional heat production necessary to cover the losses that occur during the transport of heat through the heating system.
The secondary y-axis shows temperature levels during the week. The negative correlation between the temperature level and the actual heating demand can be spotted in this week: On days with very low temperatures (Monday, 13th, and Tuesday, 14th of February), the heating demand is higher than on days with higher temperatures (Thursday, 16th, and Friday, 17th of February), although these days show similar production activities.
The base load of the heating demand is covered by CHP plants shown in orange colors. The peak load is served by the boilers that vary in minimum power levels and efficiencies at minimum and maximum power. Depending on these parameters, it is more economic to operate different boilers for different load levels, i.e., different ranges of load levels exist that favor the operation of certain boilers. Figure 7.3 shows boilers switching with a frequency as low as one hour. To avoid a high-frequent switching behavior, a minimum operation time or start-up costs could be added to the boiler model.
The lowest heating demand is visible on Sundays, although temperature levels are lower than on other days. This shows the effect of production on the heating demand, as no production occurs on Sundays.
Although the demand for heating is low on Sunday, it is sufficient to run both CHPs at nominal power. Nevertheless, the power levels of CHP 1 and 2 are slightly reduced. This can be explained by the electricity-led operation of the

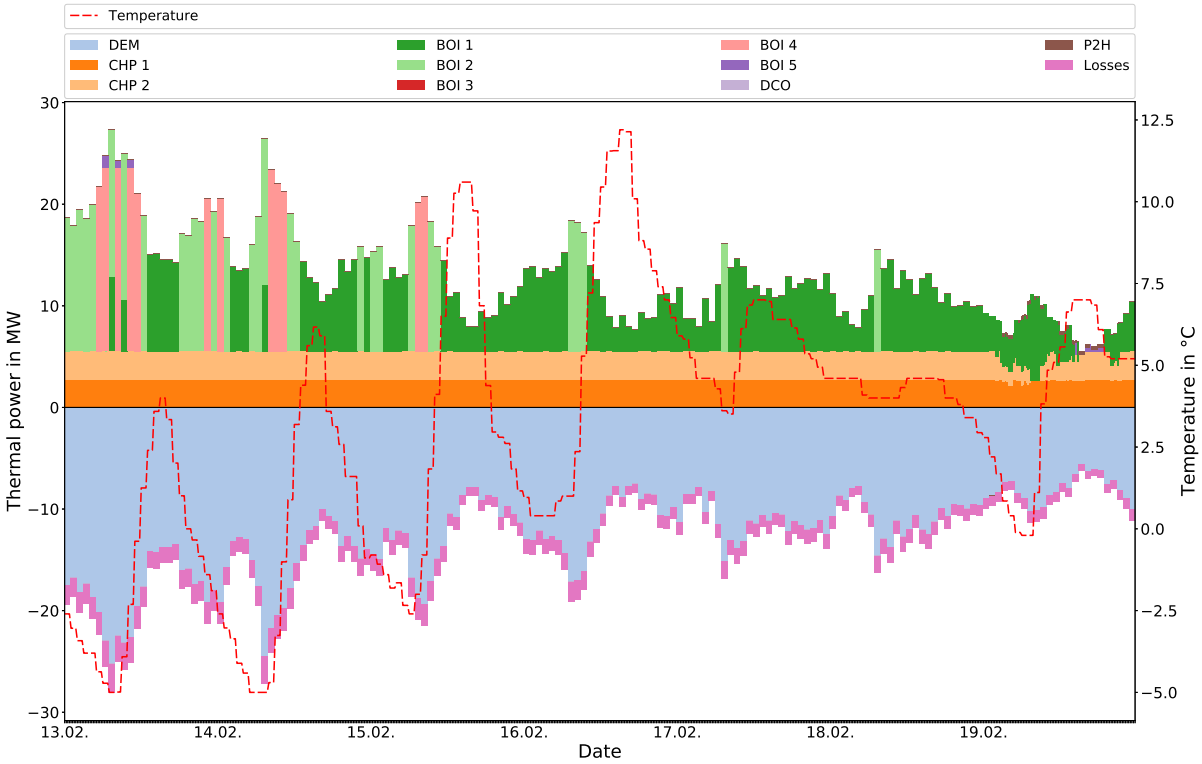

Figure 7.3: Heat balance of calendar week 7 of 2017 optimized with constraints of Scenario 1
The primary y-axis displays heating demand (light blue) or device-related consumption on the negative and device-related heat production on the positive axis. The secondary y-axis displays outside temperatures measured at the case study.

CHPs during this time, which often appears on days with low electricity demand and high wind production: The power of the CHPs is reduced to avoid electricity exports and resulting penalties.
The winter period generally includes high participation of the gas boilers in the heat production as the sole CHP operation is not sufficient to satisfy the heating demand.

Transition period

The transition period describes the period in spring or fall. To display the heat load during this time and further explain the circumstances of Figure 7.2, the heat balance of calendar week 18 is displayed below in Figure 7.4.
Calendar week 18 is the same week as depicted in Figure 7.2, which includes the public holiday on the 1st of May. The public holiday leads to a comparably low heating demand on this day. As explained above, due to the simultaneously low electrical power demand, this leads to a stop of operation of CHP 2. Additionally, the heating demand is very low in the night partially requiring the use of the dry cooler displayed in brown (DCO: $Q_{DCO,1,t}$), which leads to an additional heating demand and allows the operation of CHP 1. Furthermore, the heat production of the power-to-heat plant (P2H: $Q_{P2H,1,t}$) is visible on this day in pink colors. The P2H is used to convert abundant electricity generation by wind power plants (see Figure 7.2) to produce heat.
The rest of the week shows the typical situation during the transition period: Gas boilers are used occasionally to buffer peak demands, the dry cooler helps to fill the times of low demand to make it possible to run the CHPs (at nominal power). Running the CHPs at nominal power even with the dry cooler is more economical as electricity generation substitutes electricity imports.

Summer

Figure 7.5 shows the heat balance for a summer week. It is visible that the heat load is very low. The heat load varies around an average heat load of 2 MW for most of the week. Exceptions are visible after colder mornings (3rd of July) or due to the start-up of machinery for the start of the production on Sunday evening (9th of July).

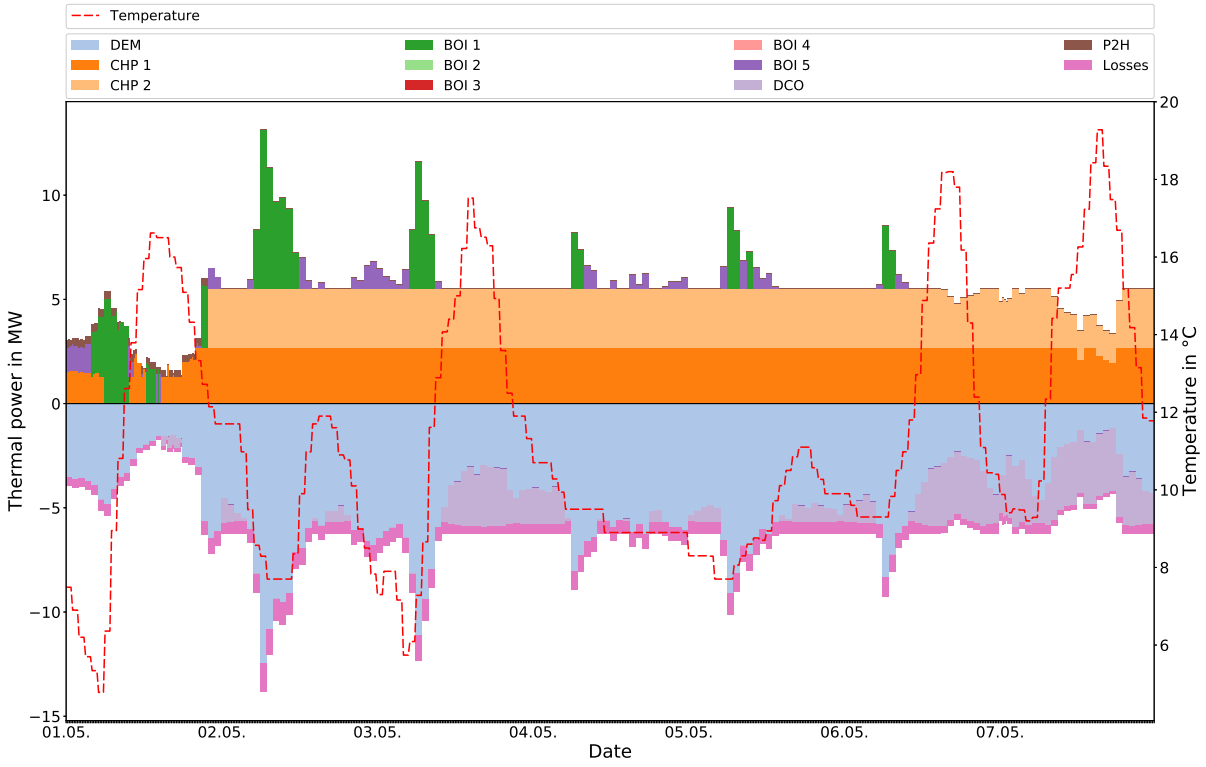

Figure 7.4: Heat balance of calendar week 18 of 2017 optimized with constraints of Scenario 1
The primary y-axis displays heating demand (light blue) or device-related consumption on the negative and device-related heat production on the positive axis. The secondary y-axis displays outside temperatures measured at the case study.

The low heat load would prevent the operation of both CHP plants; as a consequence, the schedule suggests the continuous use of the dry cooler to create artificial heating demand. This operation proves to be more economic than to renounce the cost savings achieved by the electricity generation of the CHP plants. On Sunday, the 9th of July, heating demand reaches such low values that the operation of the more expensive CHP 2 is stopped almost exclusively with the exception of a single hour of operation.
It is visible that heat production in the summer can be supplied by the sole operation of the CHP plants. The operation of both CHP plants requires almost continuous operation of the dry cooler during this period.

7.1.2 Energy technologies

In the following, the operation of different energy technologies and their contribution to external flexibility services are illustrated.

CHP

Figures 7.6 and 7.7 display the load profile of the CHPs during parts of the calendar week 18. Grey lines show the partial ($\underline{P}_{CHP,i}$) and black lines indicate the maximum possible ($\overline{P}_{CHP,i}$) power generation modeling partial load behavior. The dashed blue line indicates the resulting electric power output ($P_{CHP,i}$) of the CHPs and the color-shaded areas show the resulting flexibility and its commercialization as control reserve. All power levels below the partial power mean that the CHP is shut down.
The power reserved for load-frequency control is displayed around the power profile. While red shades indicate aFRR commercialization ($P^{aFRR^-}_{CHP,i,t}$, $P^{aFRR^+}_{CHP,i,t}$), FCR commercialization ($P^{FCR}_{CHP,i,t}$) is shown in yellow or golden colors.
It is from Figure 7.4 visible that both CHPs are in operation for most of the week and run mainly on nominal power. CHP 1, however, shows partial power behavior on the first day of the week displayed in Figure 7.6. If running for a

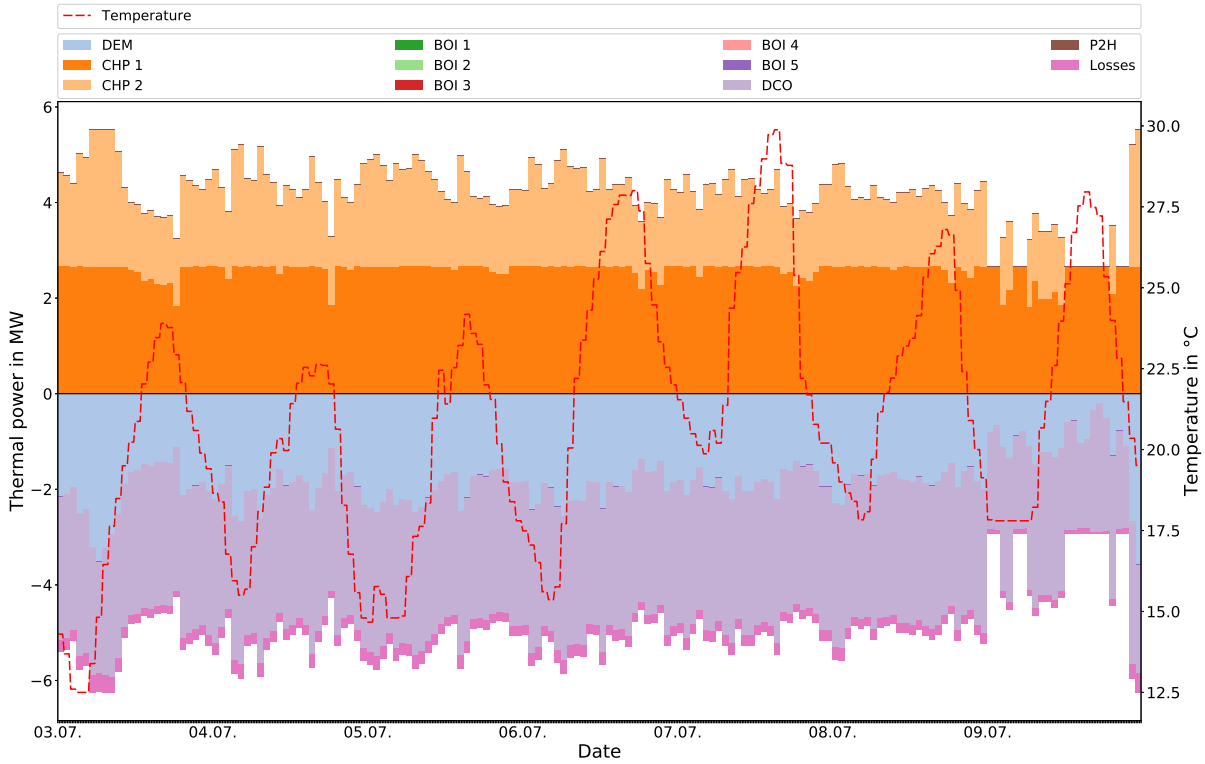

Figure 7.5: Heat balance of calendar week 27 of 2017 optimized with constraints of Scenario 1
The primary y-axis displays heating demand (light blue) or device-related consumption on the negative and device-related heat production on the positive axis. The secondary y-axis displays outside temperatures measured at the case study.

full 4-hour slot (separated by vertical black lines), it is visible that the resulting flexibility is commercialized fully as aFRR+ and/or aFRR-.

CHP 2 also runs on nominal power for the majority of the week and flexibility is commercialized as aFRR-; however, it shows loads between partial and nominal power on Sunday seen in Figure 7.7. It is visible that partial load is commercialized as FCR if symmetric flexibility exists over an entire 4-hour slot. Synchronous commercialization of both FCR and aFRR- is also visible for CHP 2 by the simultaneous provision of FCR and aFRR- on the 6th of May.

An interesting observation is that CHP 1 commercializes symmetric flexibility as aFRR+ and aFRR-, while CHP 2 commercializes symmetric flexibility as FCR. This might be due to the fact that CHP 1 and CHP 2 show different reserve call costs and consequently different energy prices for aFRR commercialization as shown in Figure 6.1 and Table 6.3.

It is visible that the flexibility of the CHPs in partial load is tied to 4-hour slots for Scenario 1. This creates idle flex displayed in gray - flexibility that cannot be commercialized. Scenarios 2 and 3 offer the possibility to commercialize flexibility as it is not tied to the 4-hour slots. This would offer the possibility for the CHP to offer more control reserve especially during times that show high partial load behavior such as the summer period.

BSS

Figure 7.8 shows the operation of a BSS during calendar week 20. The displayed period correlates with the electric power balance in Figure 7.1. The figure shows the development of the SOC by the energy level ($E_{BSS,l,t}$) of the BSS in the blue dashed line. Furthermore, charges (BSS-: $P^{+}_{BSS,l,t}$) and discharges (BSS+: $P^{-}_{BSS,l,t}$) are displayed during operation for local flexibility services. The use of the BSS for external flexibility services is done by the

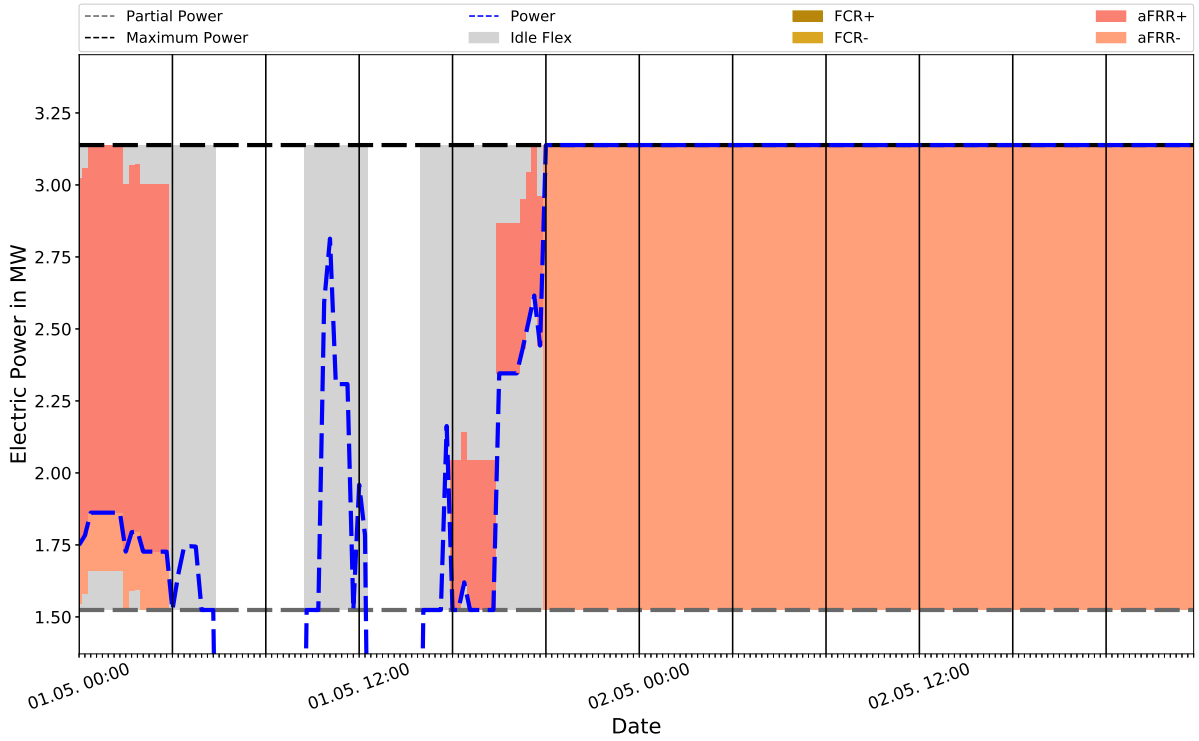

Figure 7.6: Load profile and flexibility services of CHP 1 in calendar week 18 of 2017 optimized with constraints of Scenario 1
The y-axis displays load levels of the CHP. The dark gray line shows partial power level, the black line maximum power level, and the blue line actual power level. Shaded colors indicate the use of resulting flexibility for FCR and aFRR provision.

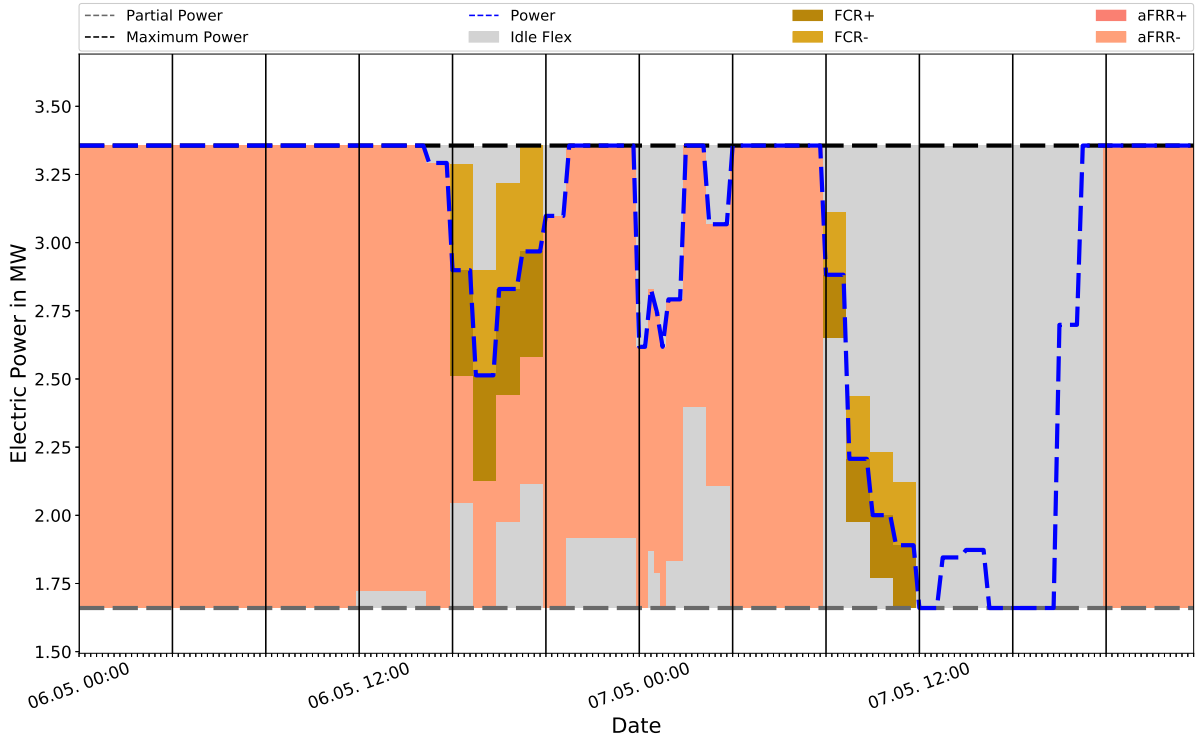

Figure 7.7: Load profile and flexibility services of CHP 2 in calendar week 18 of 2017 optimized with constraints of Scenario 1
The y-axis displays load levels of the CHP. The dark gray line shows partial power level, the black line maximum power level, and the blue line actual power level. Shaded colors indicate the use of resulting flexibility for FCR and aFRR provision.

provision of FCR (yellow) and EMO (green). As with CHPs, FCR refers to the reservation of power and capacity for FCR provision ($P^{FCR}_{BSS,l,t}$).
For the BSS, serial provision of flexibility services has been modeled as shown in Table 6.2. This results in periods, in which the BSS is reserved for different flexibility services. In Figure 7.8, the BSS is employed for local flexibility services (BSS+/BSS-), FCR provision, and EMO. As shown in the power balance in Figure 7.1, most peak shaving activities occur on May 17th, 18th, and 19th. It is visible that the displayed BSS is used for these peak shaving activities on these days, while almost all residual slots are commercialized as FCR power. Solely the 20th of May is commercialized as EMO, as it offers more earnings than FCR provision. Prior to the use for local peak shaving the BSS is charged at low electricity prices generally during the night before.
FCR is traded in 4h-slots which can be recognized by the vertical black lines that separate each slot. Furthermore, the 15-minute-criterion shown in Figure 5.1 provides strict boundaries for the permissible operation range (POR) that SOC levels have to be in during FCR provision. It is visible that SOC levels are within POR limits at each start of a FCR-providing slot. As explained in the BSS model, the SOC is not modeled to change during FCR provision, as frequency values cannot be forecasted precisely and the implemented charge management assures SOC to be kept within POR limits.
Figure 7.9 displays the utilization of the flexibility of the BSS 3 during calendar week 20.
It is visible that BSS3 is employed less for the flexibility service LPO. Instead, the BSS has been used predominantly for the flexibility service EMO on these days. As described in Section 6.3, the battery is commercialized for entire days for the flexibility service EMO.

EV

Figure 7.10 shows the total power profile of all EVs during calendar week 8. The original uncontrolled power profile (in dark blue) and the optimized final power profile (in brown) of the EVs are displayed. Changes to the original power profile are done by EV+ ($P^{+}_{EV,k,t}$) in blue and EV- ($P^{-}_{EV,k,t}$) in orange. Additionally, FCR provision by the EVs is displayed in shades of yellow.
Furthermore, the figure displays the electricity price at the Day-Ahead market during that week on the secondary y-axis. This is relevant for the flexibility service LEO. It is visible that changes to power profiles done in the optimization during this week are partly done with regard to price differences of electricity prices. This can be especially seen at the peak time of charging in the morning hours. This peak occurs at high electricity prices and is reduced slightly. The charged energy is moved from more expensive periods, generally occurring during the day, to less expensive periods. This is visible by the orange (EV+: reduction in charged energy) and blue (EV-: increase of charged energy) shaded areas. In rare cases at the end of the week, this even results in a final power profile with periods of discharged energy (bidirectional charging).
FCR provision is visible by the shaded yellow areas and depends on EVs that inhibit high charge flexibility, i.e., are connected to the charging station longer than they need to. It is visible that FCR power is often higher than the actual power charged and in this week can achieve values of around 50 kW. At the industrial energy system, high FCR power provision is visible on weekdays, while weekends show little potential. Results show 14 times higher potential for FCR provision on weekends than on weekdays. This finding is supported by an analysis of charging stations done by the author at an office site of the OEM [330]. The author has to add; however, that for weekly optimization runs only charging events were included that started and stopped within the week, which underestimates the potential of the start and the end of the week.
One of the EV power profiles that includes bidirectional charging is shown in Figure 7.11. The vehicle showed an extraordinarily long plug-in time with a total of 2 days and 4 hours. The plug-in and plug-out time are indicated by the black vertical lines. Furthermore, the vehicle was fully charged during a fraction of the total plug time ($T^{plug}_{EV,m}$),

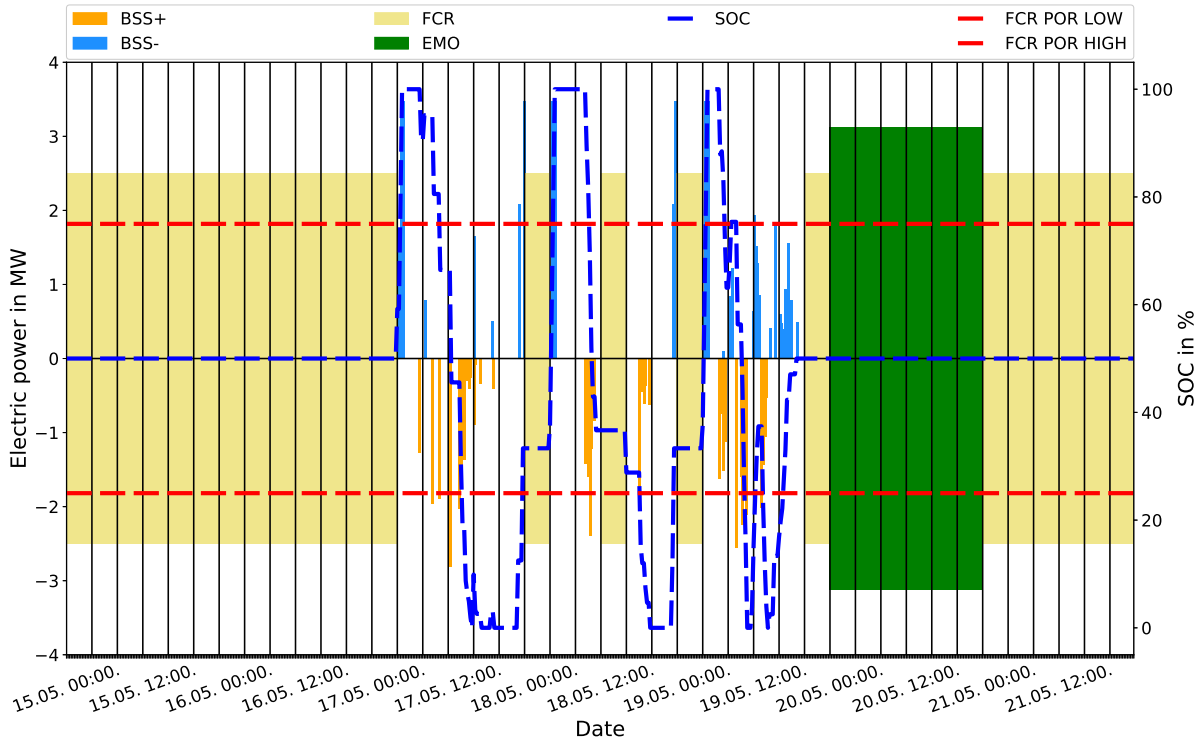

Figure 7.8: Load profile and flexibility services of BSS 1 in calendar week 20 of 2017 optimized with constraints of Scenario 1
The y-axis shows power charged and discharged for local flexibility services and power reserved for external flexibility services (FCR, EMO). On the secondary y-axis the SOC of the BSS is displayed in the blue dashed line. The red dashed lines indicate the SOC limits when providing FCR.

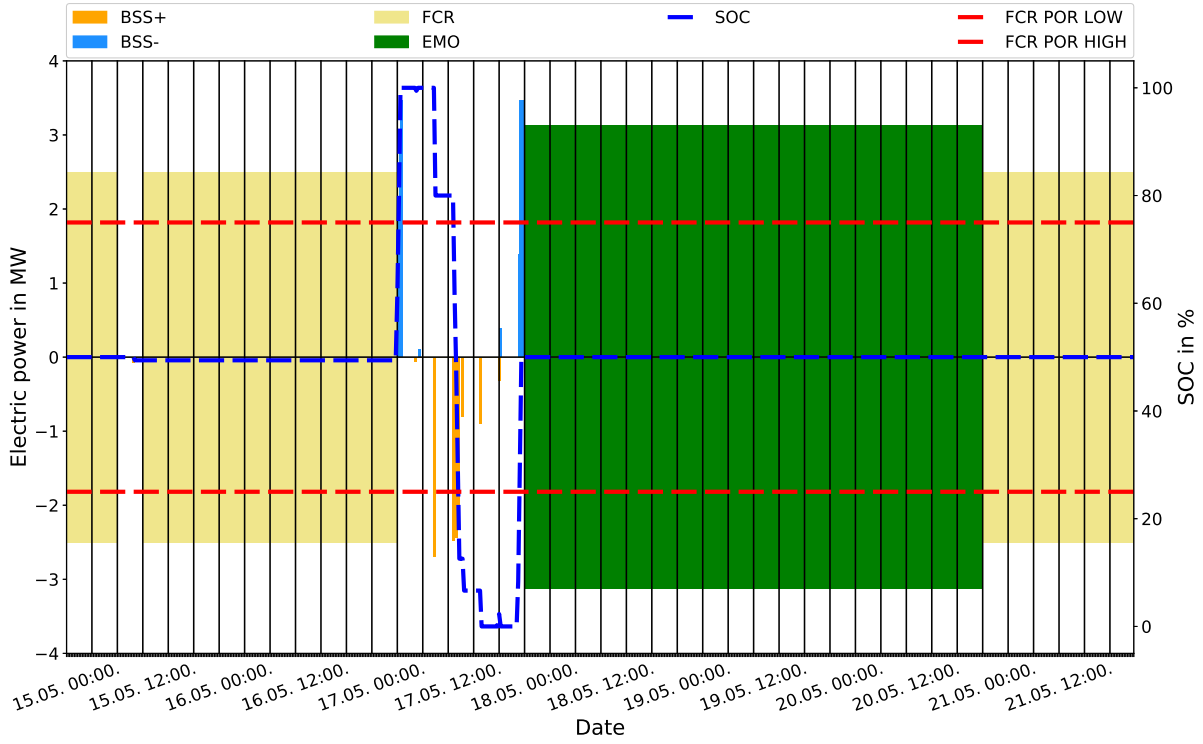

Figure 7.9: Load profile and flexibility services of BSS 3 in calendar week 20 of 2017 optimized with constraints of Scenario 1
The y-axis shows power charged and discharged for local flexibility services and power reserved for external flexibility services (FCR, EMO). On the secondary y-axis the SOC of the BSS is displayed in the blue dashed line. The red dashed lines indicate the SOC limits when providing FCR.

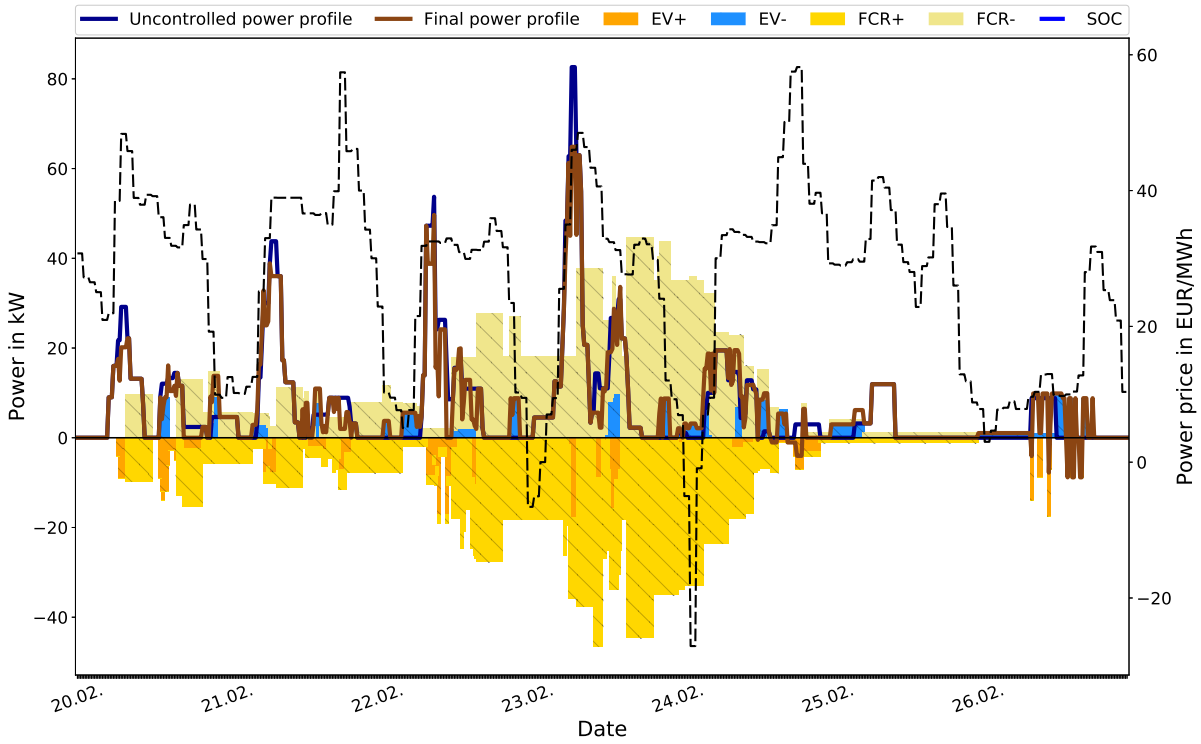

Figure 7.10: Load profile and flexibility services of all EVs for calendar week 8 of 2017 optimized with constraints of Scenario 1
The primary y-axis displays the uncontrolled power profile before and the final power profile after the optimization. Changes to the power profile are indicated by EV+ and EV-. Power reserved for FCR is displayed by FCR+ and FCR-. The black dashed line indicates electricity prices on the secondary y-axis.

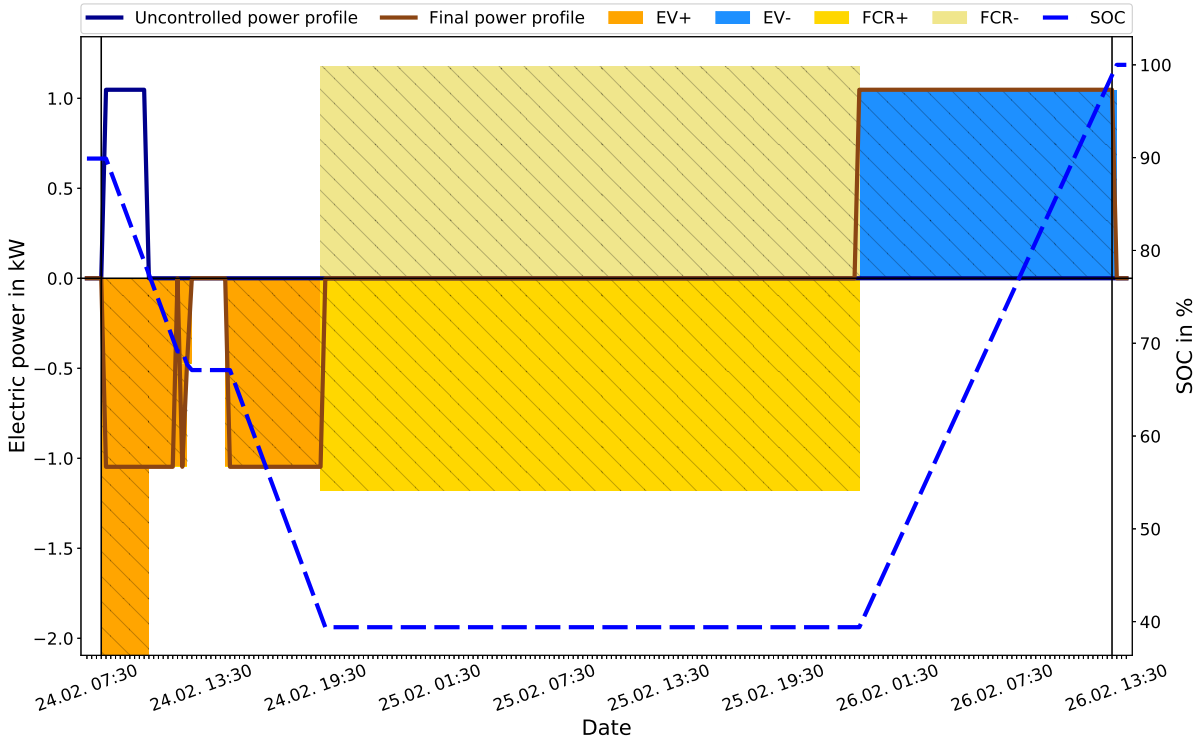

Figure 7.11: Load profile and flexibility services of vehicle 44 in calendar week 8 of 2017 optimized with constraints of Scenario 1
The primary y-axis displays the uncontrolled power profile before and the final power profile after the optimization for a single EV. Changes to the power profile are indicated by EV+ and EV-. Power reserved for FCR is displayed by FCR+ and FCR-. The blue dashed line indicates the SOC of the EV on the secondary y-axis.

thus, offering a high charging flexibility ($T^{flex}_{EV,m}$). This enabled discharging the vehicle for several hours down to an SOC of around 40% and charging the vehicle for the final hours of the plug-in time to reach the desired full charge. FCR is provided by the vehicle in Figure 7.11 for the majority of the time (28h or seven 4h-slots), as it proves more profitable than local flexibility services. To provide FCR, the SOC of EVs has to be lowered to satisfy the criteria given by the TSOs for batteries (see Equation 6.50). Partly, it is difficult for EVs to provide FCR in Scenario 1 as not all vehicles possesses a charge flexibility that includes the 4h-slots of the control reserve market slots.
The figure also shows possible shortcomings of the implemented EV model: As explained in Section 6.7.5, the average charging power of the EV from the given data has been used as the maximum power. As this EV started charging with a very high SOC (90%), the BMS of the vehicle charged with a very low current to not damage the battery (constant voltage phase in the CCCV charging strategy). This resulted in a very low average power level. The vehicle can presumably discharge and charge with higher power levels; nevertheless, this has not been modeled in this thesis. Therefore, an SOC-dependent preprocessing to model the power levels is suggested for future work.

AHU

Figure 7.12 shows the power balance of the energy technology AHU of building 3 in calendar week 18. The operation of AHUs is closely tied to the working hours of the production shifts that are pursued in this building. Due to continuous production in building 3 except for production-free days, the AHUs generally run from Monday to Sunday. Due to the public holiday on Monday, May 1st, AHUs only operated from Tuesday to Saturday during that week. The power profile is displayed by the blue dashed line ($P_{AHU,n}$) while gray dashed lines show partial ($\underline{P}_{AHU,n}$) and maximum ($\overline{P}_{AHU,n}$) power. Due to changes in temperature (see Figure 7.4), the AHU increases its normal operation point, which leads to a higher symmetric flexibility.
Given the input parameters for the AHUs, the results show the commercialization of symmetric FCR around the operation point for all available 4h-slots. The increase in the operation point slightly increases the FCR commercialization. aFRR is only offered for individual 4-hour slots; however, idle flex exists that could be commercialized as aFRR-. This is not done due to the low expected income from this flexibility service, which falls short of the MIPGap limit proposed for the optimization: The average capacity price for aFRR- is only 4.2 EUR/MW for the 4h-slots during the displayed period and energy price earnings are low due to the low call probability set for AHU devices, which leads to low energy prices.
Hardly any change of the planned power profile is seen in calendar week 18.
Figure 7.13 displays the AHU operation during calendar week 20. Higher temperatures lead to much higher operation points, which increases positive and symmetric flexibility. Very high temperatures, on the other hand, lead to the non-existence of negative flexibility. During the displayed week, positive flexibility is commercialized as aFRR+ and symmetric flexibility as FCR. These two control reserve products offer higher capacity prices than aFRR- and thus show higher power values in the displayed solution. Furthermore, small changes in the power profile are visible by AHU+ and AHU- calls, in blue and in orange colors. The balanced alterations of the load profile are based on the Equation 6.67. During the displayed week, these flexibility calls mainly contribute to peak shaving as depicted in Figure 7.1. Often the power is lowered at around 4 p.m. and increased within the four-hour slot before 8 p.m., as loads are higher during the day than in the evening.

Chiller

The operation of the chiller during parts of calendar week 20 is shown in Figure 7.14. The top graph shows the planned and final power consumption after the optimization. The bottom graph depicts the changes made to the planned power profile.

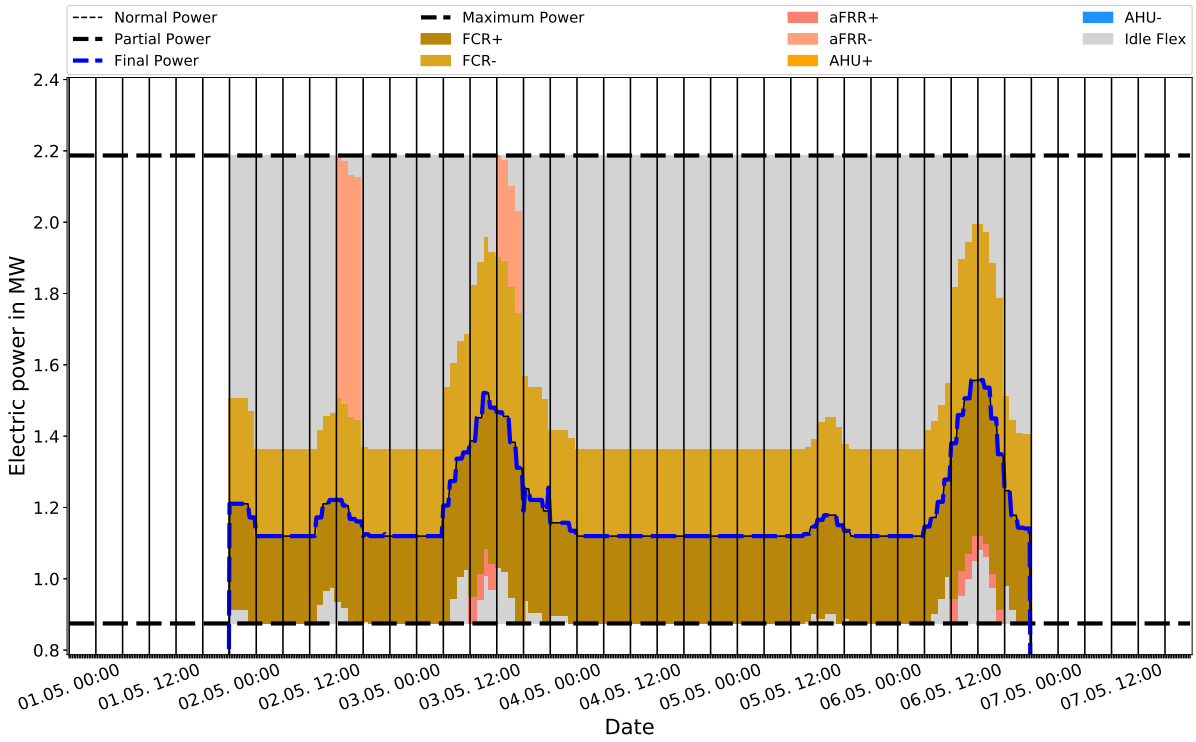

Figure 7.12: Load profile and flexibility services of AHUs of building 3 in calendar week 18 of 2017 optimized with constraints of Scenario 1 The dashed lines indicate power level. Black lines indicate maximum and partial power. The thin black line shows the power consumption before and the dark blue dashed line after the optimization. Power used for local flexibility services is shown by the variable AHU. Power reserved for control reserve provision is indicated by FCR and aFRR.

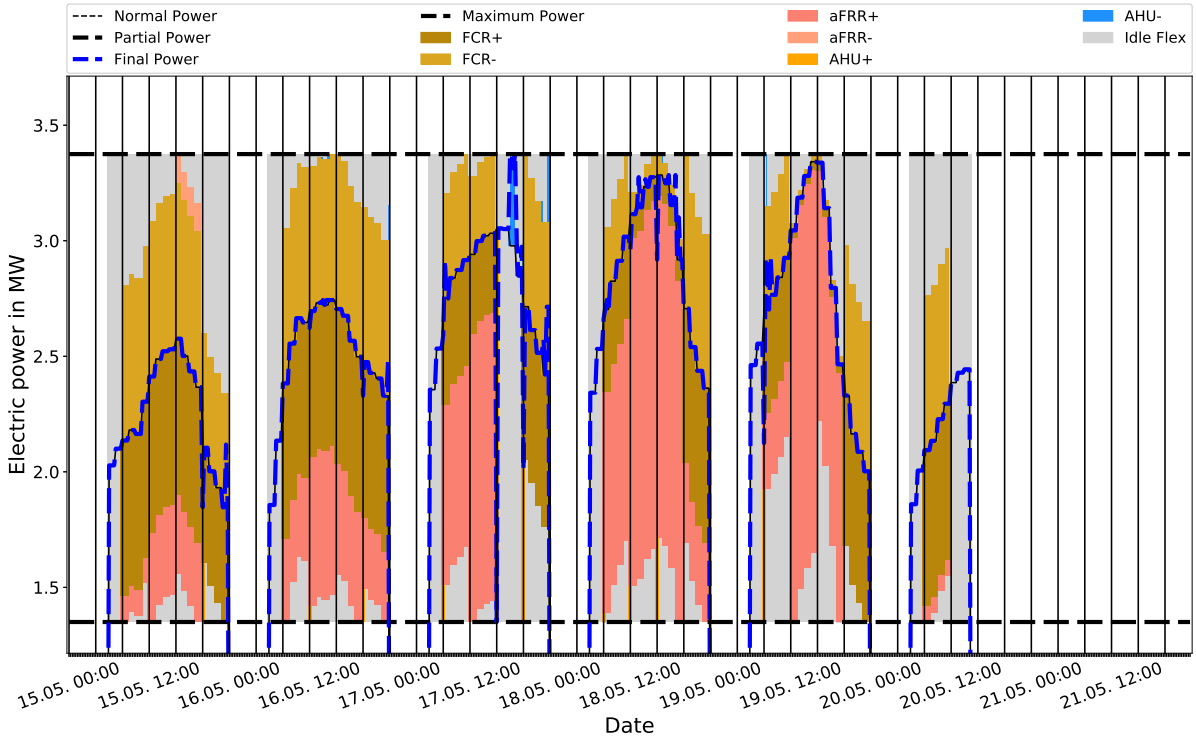

Figure 7.13: Load profile and flexibility services of AHUs of building 1 in calendar week 20 of 2017 optimized with constraints of Scenario 1 The dashed lines indicate power level. Black lines indicate maximum and partial power. The thin black line shows the power consumption before and the dark blue dashed line after the optimization. Power used for local flexibility services is shown by the variable AHU. Power reserved for control reserve provision is indicated by FCR and aFRR.

It is visible that the cooling demand generally increases in the afternoon similarly to the temperature development during the day. Equation 6.71 allows the balanced change of the planned power consumption within a period of two hours. Changes to the power profile of the chiller in this week are used to contribute to the flexibility service LPO and move planned power consumption to a later period of the day.

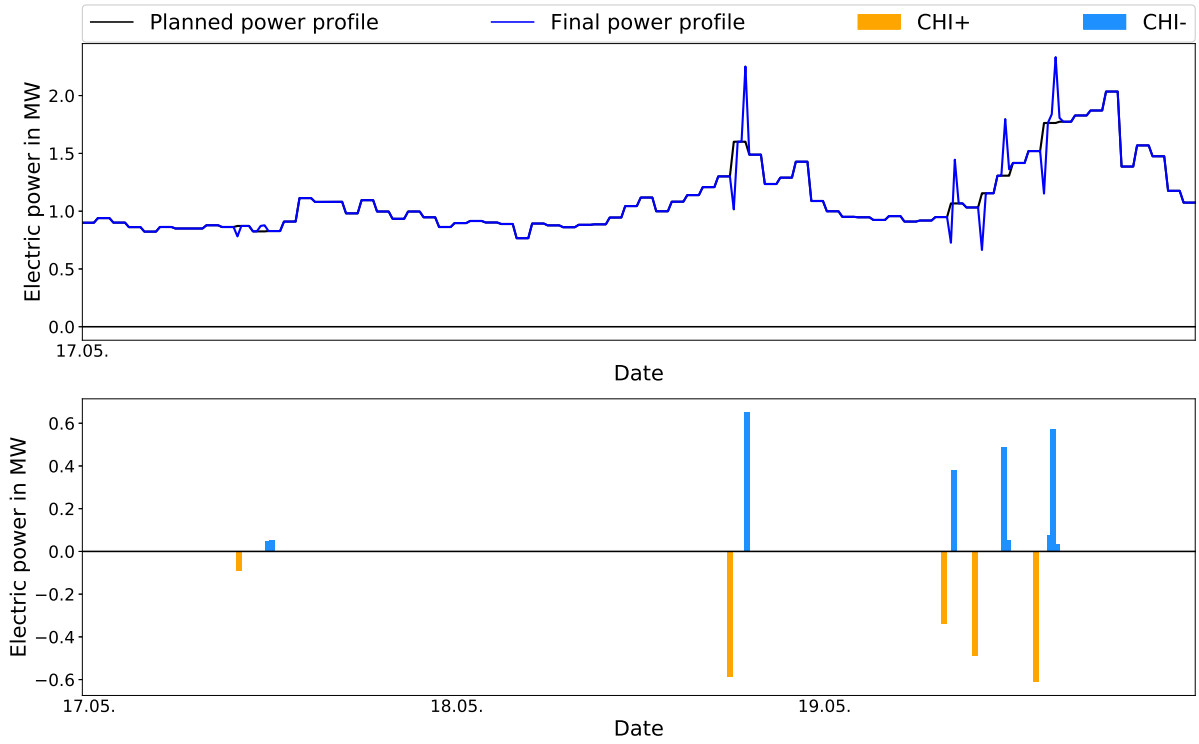

Figure 7.14: Load profile and flexibility services of the chiller in calendar week 20 of 2017 optimized with constraints of Scenario 1
Top graph indicates the planned power profile before and final power profile after the optimization. Changes to the power profile used for local flexibility services are shown in the bottom graph.

The modeling approach of balanced demand response chosen in Equation 6.71 is visible in this figure. The approach allows the chiller to adjust the power consumption within the period T_{CHI}^{LDR} of two hours. This leads to frequently alternating positive and negative demand response activities.

7.1.3 Control reserve provision

FCR control reserve provision in calendar week 20 is shown in Figure 7.15. It is visible that FCR is provided by the BSS, the AHUs, and the CHP in this week. P2H and EV commercialize very small power levels that are hardly visible during the week due to the requirements of symmetric FCR provision and the requirement to provide FCR over entire 4-hour slots. The device-by-device symmetric provision of FCR required in Scenario 1 can be seen as every energy technology provides the same amount of positive and negative FCR power per 4-hour slot.
It is visible that the majority of FCR is provided by the BSS for almost the entire week. This is due to the high prequalified FCR power (10 MW). As shown in Figures 7.1 and 7.8, the energy technology BSS is used for flexibility services LPO and EMO during most of the 17th to 20th of May. Due to the serial provision of flexibility services, FCR power is reduced during these days. BSSs only provide FCR for single 4h slots during the night when no LPO is necessary.
FCR is also provided by AHUs. The main factors influencing the FCR power of AHUs are the operation hours and the outside temperature, which influence the power consumption and consequently the availability of symmetric flexibility. This is visible in Figure 7.13.

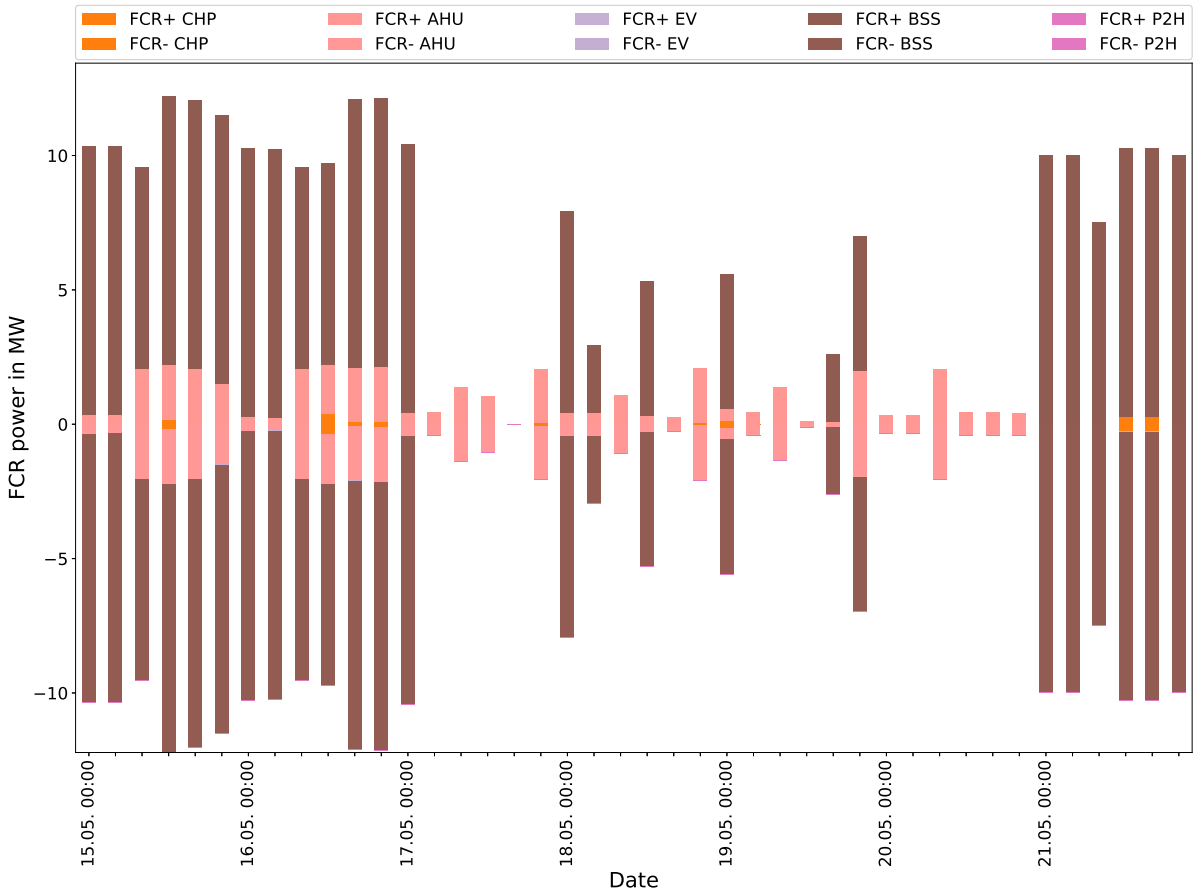

Figure 7.15: FCR provision in calendar week 20 of 2017 optimized with constraints of Scenario 1
Positive and negative FCR bids from individual devices are shown by stacked bars for all 4h time slots during calendar week 20.

In Scenario 1, CHPs can only provide FCR during partial load operation. As this occurs rarely, only small amounts of FCR power are provided by CHPs.

7.2 Impact of flexibility services on total energy cost

In the following, results are displayed for the entire year 2017 with an altered optimization horizon of one day. Figure 7.16 shows results from the 365 optimization runs over the year 2017. It displays the reduction of the energy costs as opposed to the reference scenario REF and the contribution by individual flexibility services.
Net energy costs display the objective value from each daily optimization run (operational energy costs) plus the capacity-related grid fees for the initial peak threshold (20 MW), which were not accounted for in the objective function.
The displayed savings of the flexibility services LPO and LEO represent the savings of this simulation run as opposed to the corresponding reference scenarios REF and REF_LEO. The values for FCR, aFRR, and EMO show the revenues gained from these flexibility services. The revenues are added onto the net energy costs and compared to the total energy costs (sum of all objective values) of the scenario REF. The remaining difference in energy costs between the reference scenario and the investigated scenario is displayed in "Difference with REF". Figures 7.17 to 7.19 show the contribution of energy technologies to the provision of FCR and aFRR.
In Figure 7.16, it is visible that the total energy cost of the reference scenario is reduced by around 2.66 million EUR, which equals an energy cost reduction of around 12.1%.

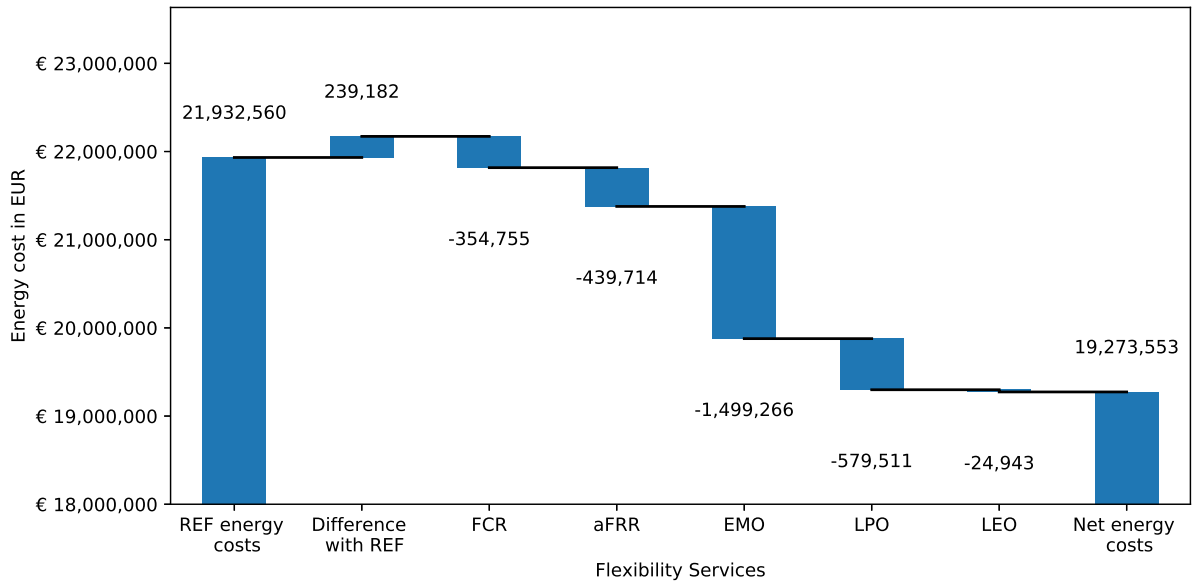

Figure 7.16: Energy cost and contribution of individual flexibility services for year 2017 with the optimization problem defined for Scenario 1

The highest contribution to these savings lies in the provision of EMO (1.5 million EUR). These can be fully attributed to the BSS, which is the only energy technology that can provide EMO. To achieve these revenues the battery was used 69% of the simulated time for this flexibility service.
The second highest contribution of flexibility services is achieved by LPO, which is able to lower the peak power procurement from a level of 32.03 MW for uncontrolled power procurement to a value of 26.7 MW. This resulted in a reduction of operational energy costs by 579k EUR. The main contributors to achieve peak shaving are the technologies CHP, EPS, and BSS; however, an individual BSS has been used on average only 0.6 h per day to contribute to this local flexibility service.
aFRR provision achieved revenues of 440k EUR. 237k EUR (53.9%) can be attributed to the earnings from capacity prices - the reservation of the capacity[4]. Furthermore, 203k EUR (46.1%) of energy price profits can be achieved by actual reserve calls. The costs of reserve calls (18 k EUR) are included in the total energy costs and partly explain the additional costs compared to the scenario REF. The selection of the correct energy price elaborated in Section 3.5.4 is crucial for this part of the revenues. As visible in Figures 7.18 and 7.19, the majority of aFRR+ is provided by the energy technology EPS with an average power of 5.5 MW, while the majority of aFRR- is provided by the CHPs with an average power of 2.6 MW. Due to the higher offered power and the higher capacity prices for positive aFRR, the EPSs are the strongest contributors to the aFRR revenues.
FCR revenues contribute 354.7k EUR to the reduction of energy cost. Around two thirds of these FCR revenues can be attributed to the energy technology BSS with an average FCR power of 2.6 MW as visible in Figure 7.17; however, only 26% of the time does the BSS actually provide FCR. Furthermore, big FCR providers are the AHUs with a power of 1.4 MW.
For the flexibility service LEO, results were compared to the reference scenario LEO_REF. The results show that a controlled scheduling of Scenario 1 can decrease costs associated with dynamic electricity prices and the export of electricity to the public grid by 25k EUR.
The additional value of flexibility services entails operation costs displayed in the column "Difference with REF". This includes increased operation costs of the devices and further procurement of electricity to generate additional value by flexibility services.

[4] The aggregator fee (ϕ^{VPP}) has been deducted in Scenario 1 from these earnings.

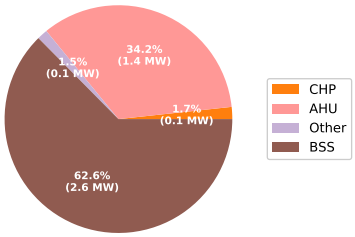

Figure 7.17: FCR provision in Scenario 1
Pie chart showing relative and average FCR power.

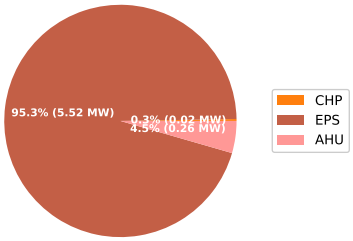

Figure 7.18: Positive aFRR provision in Scenario 1
Pie chart showing relative and average $aFRR^{+}$ power.

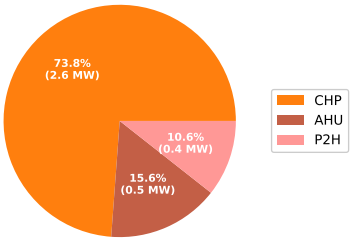

Figure 7.19: Negative aFRR provision in Scenario 1
Pie chart showing relative and average $aFRR^{-}$ power.

7.3 Impact of control reserve aggregation on total energy cost

In the following, results of Scenario 1 will be compared with results from Scenarios 2 and 3 that were described in Section 6.8. By this comparison it is intended to measure the impact that internal aggregation of control reserve flexibility offers have on the total energy costs for the case study scenario. First, the differences between the scenarios will be illustrated. Then, results of Scenario 2 and 3 will be introduced and compared to Scenario 1.

7.3.1 Differences between scenarios

To illustrate the differences in modeling between the selected scenarios, results of a randomly selected day are shown. Figures 7.20 to 7.22 illustrate the differences of the FCR commercialization for a single day.
Scenario 1 allows the commercialization of symmetric flexibility on a device level over the 4-hour slot period. On the simulated day, this condition can be satisfied by the BSSs, the CHPs, and the HVACs; however, it is visible that only small amounts of FCR can be provided by the CHPs and the HVACs.
Scenario 2, on the other hand, allows internal aggregation of asymmetric flexibility; however, it requires to commercialize integer values of the FCR power. It is visible that this scenario is able to slightly increase the commercialized FCR power of the later 4-hour slots by integrating more flexibility of the CHP, AHU, and P2H devices. CHPs and AHUs offer FCR power that is not uniformly distributed over 4-hour slots and is often asymmetric, and P2H plants only offer negative flexibility. Nevertheless, for the first two 4-hour slots a decrease in commercialized power is visible for Scenario 2: While Scenario 1 can provide 10.74 MW and 10.37 MW, Scenario 2 can only offer 10 MW of FCR as commercialization is done without an external aggregator.
The average FCR power for both scenarios over the whole day is very similar (11.45 MW for Scenario 1 and 11.3 MW for Scenario 2); however, Scenario 2 can achieve much higher revenues as the cost of aggregation (ϕ^{VPP}) paid to the aggregator is not applied in this scenario. By the direct commercialization, Scenario 2 increases the revenues of FCR commercialization by 23.7%. The total operational energy cost (75,247 EUR) on this specific day is decreased by around 2.9% (2,287 EUR) by Scenario 2.
Scenario 3 uses an aggregator to commercialize FCR, thus, the solver is not concerned that the value of the FCR power needs to be an integer value. The results for the specified day are visible in Figure 7.22. The results show that FCR power can be increased further for certain FCR time slots. The average FCR power slightly increases to 11.56 MW and this scenario performs better than Scenario 1 in terms of FCR revenues (increase by 1.3%); however, this scenario does not reach the savings made by Scenario 2 as the aggregator has to be reimbursed. The total energy costs (75,882 EUR), however, are close to the value of Scenario 2. To satisfy the integer condition for FCR and aFRR commercialization, Scenario 2 adjusts the load profile of individual devices, which can result

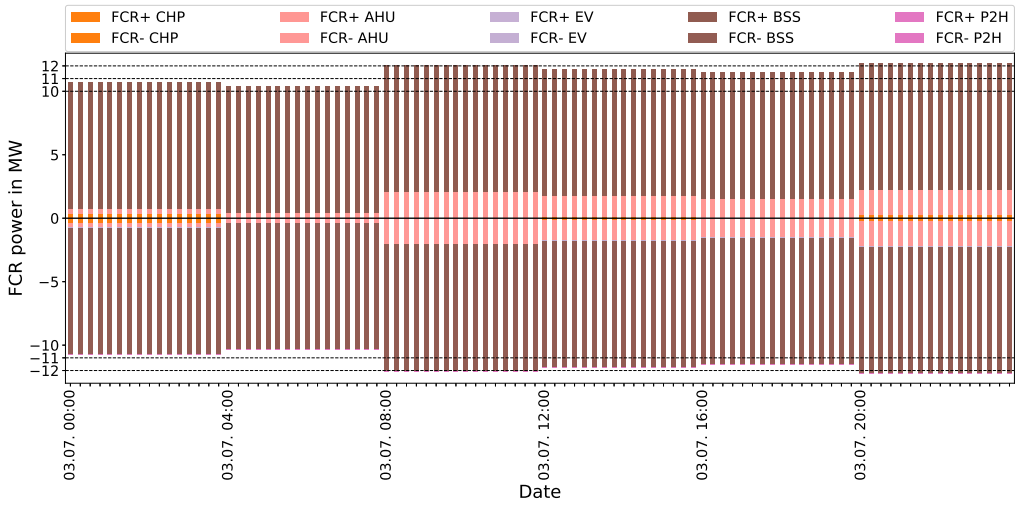

Figure 7.20: FCR provision on 3rd of July 2017 with constraints of Scenario 1

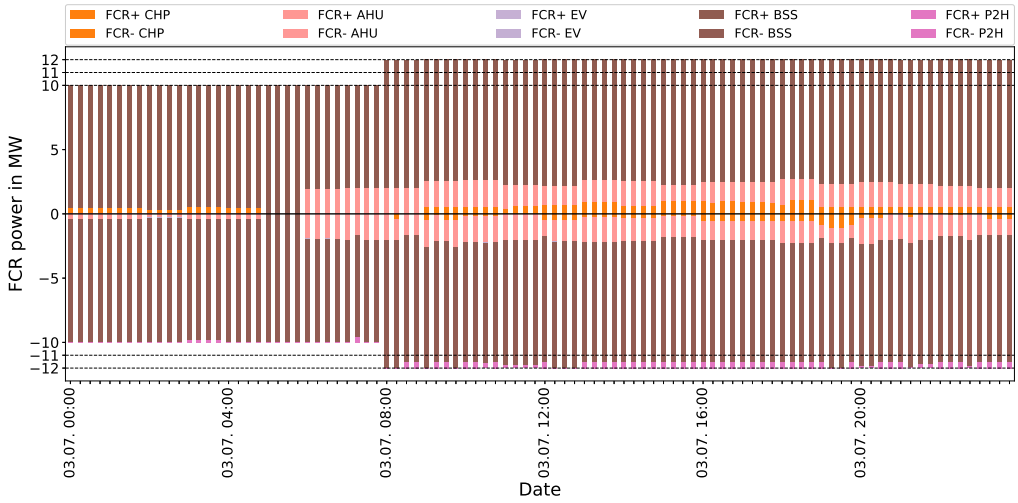

Figure 7.21: FCR provision on 3rd of July 2017 with constraints of Scenario 2

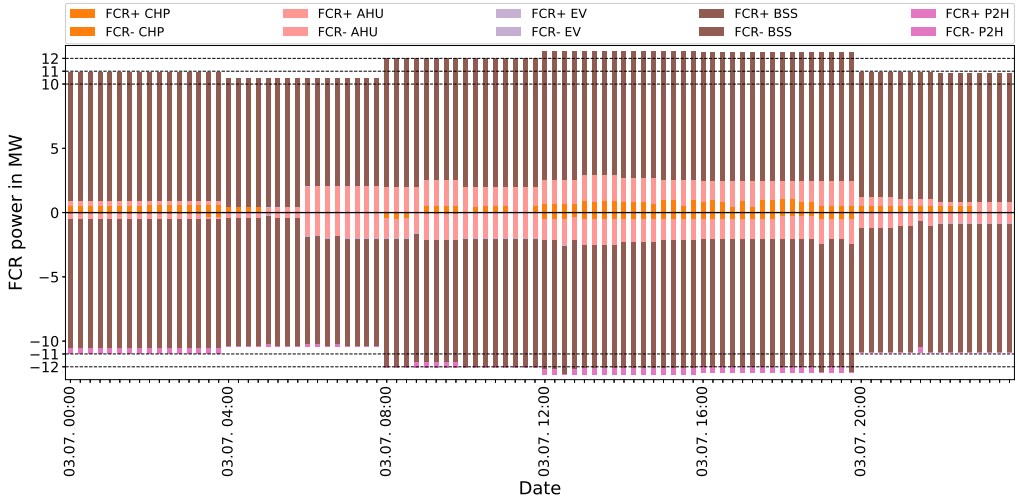

Figure 7.22: FCR provision on 3rd of July 2017 with constraints of Scenario 3

in further costs. Hence, it is always necessary to look at the total operational energy cost when comparing the different scenarios.
A great advantage of Scenario 1 lies in the run times. Due to the fewer possibilities of less aggregation, the optimization can be performed in much faster time.
In the following results are shown from a yearly optimization of Scenario 2 and 3.

7.3.2 Results from Scenario 2

Results from Scenario 2 are displayed in Figure 7.23. Energy costs can be reduced by 2.72 million EUR. Thus, this scenario performs slightly better than Scenario 1, as energy costs are lowered by another 57k EUR. The total savings compared to the reference scenario equal 12.4%. Nevertheless, the distribution of revenues gained from flexibility services is different from Scenario 1.
As opposed to Scenario 1, results from Scenario 2 in Figure 7.23 show lower EMO (decrease by 8.4%) and higher FCR revenues (increase of 60%). The main reason for this result is the lack of the aggregator fee for control reserve commercialization, which increases the competitiveness of flexibility services FCR and aFRR. As the aggregator fee is only 20% of capacity prices, the residual increase of FCR earnings must result from an intensified commercialization of flexibility as FCR. This also explains the decrease in earnings from the flexibility service EMO. While the use of the BSS for the flexibility service EMO decreased from 69% of the time to 59% of the time, the use for FCR increased from 26% to 35%.
aFRR revenues only increased slightly by 2.7% as opposed to Scenario 1. The capacity related revenues amounted to 247k EUR, which is only 4% higher than the capacity related revenues, although the aggregator fee (20%) was not accounted for in Scenario 2. A reason for the lower than expected aFRR revenues must lies in the condition of Scenario 2 that requires aFRR commercialized power to take on integer values. The commercialization of control reserve is further elaborated below in Section 7.3.4.

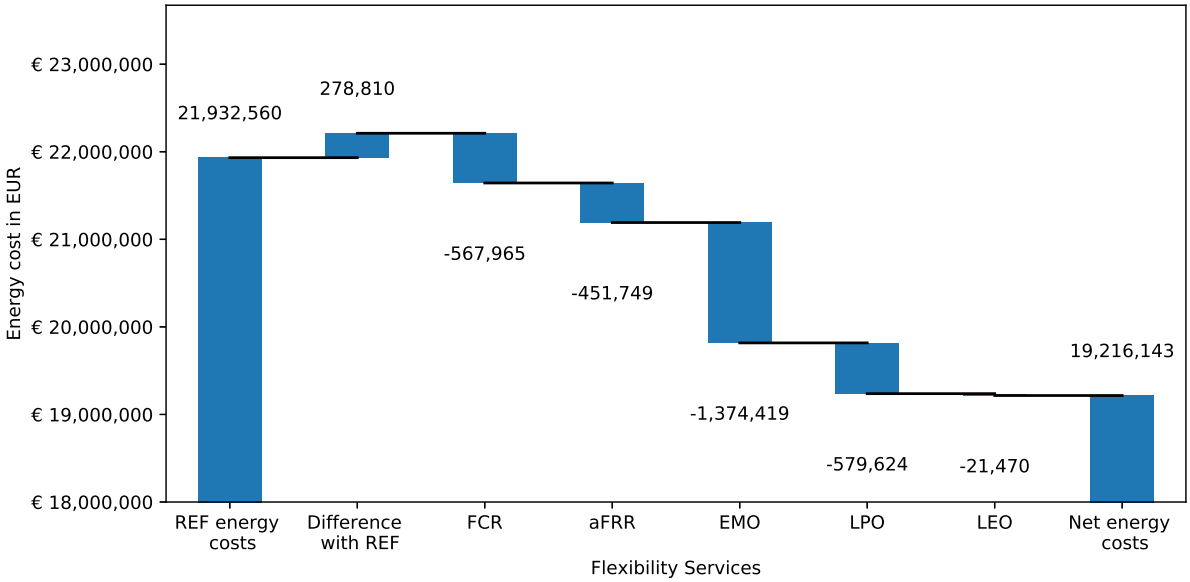

Figure 7.23: Energy cost and contribution of individual flexibility services for year 2017 with the optimization problem defined for Scenario 2

The local flexibility services LPO and LEO show similar revenues as opposed to Scenario 1 as almost the same peak reduction and energy im- and export is achieved.
Figures 7.24 to 7.26 display the commercialization of control reserve by energy technologies in Scenario 2; for example, Figure 7.24 shows the provision of FCR by individual technologies. Labels indicate the average power

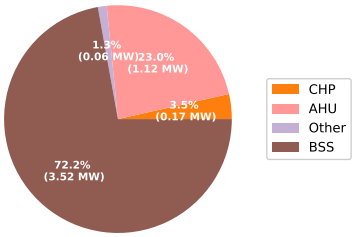

Figure 7.24: FCR provision in Scenario 2
Pie chart showing relative and average *FCR* power.

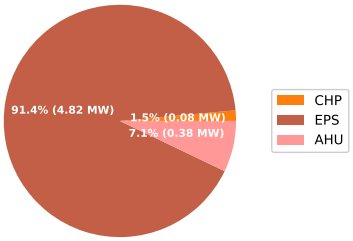

Figure 7.25: Positive aFRR provision in Scenario 2
Pie chart showing relative and average $aFRR^{+}$ power.

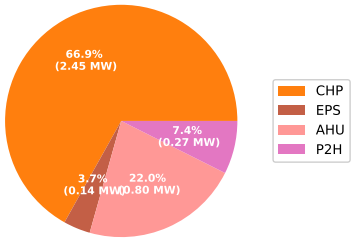

Figure 7.26: Negative aFRR provision in Scenario 2
Pie chart showing relative and average $aFRR^{-}$ power.

provision of FCR per week and the share of this power among all energy technologies. As in Scenario 1, the BSS provides the highest share of FCR. In Scenario 2, this share is the highest of all three scenarios. This supports the fact that devices of the technology BSS were more extensively used for the flexibility service FCR instead of the flexibility service EMO. Furthermore, it is visible that both the average power and the share of power by the second highest contributor, AHUs, decreased. A reason for this is the condition of integer values of FCR power. As all BSSs together provide 10 MW of FCR, the other devices have to be combined to provide an integer value of FCR, which is not always possible. An example of this behavior is visible in Figure 7.22. Furthermore, it might be beneficial to use the existing flexibility of AHUs to achieve integer values of aFRR provision instead.

For aFRR+, it is visible that, compared to Scenario 1, devices of the technology EPS provide less aFRR+ power. Again, due to the condition of integer values, the EPS needs to be combined with other devices to satisfy this criteria. The EPS is modeled as an On/Off operating device, i.e., it can either run at full power or be turned off. As nominal power values of the EPSs are not integer values, the EPSs can only offer aFRR if combined with other devices. As a result, Scenario 2 also displays a higher power by devices CHP and AHUs, which are combined with EPSs.

In Scenario 2, as in other scenarios, the majority of aFRR- is provided by a CHP. As opposed to aFRR+, the power commercialized as aFRR- actually increased, hinting at an increased commercialization due to higher capacity prices.

AHUs show increased utilization for all control reserve products in Scenario 2. Also this could point at the fact that the lack of the aggregator fee led to an better utilization of the available flexibility of AHUs.

7.3.3 Results from Scenario 3

Scenario 3 performs slightly better than Scenario 1 and slightly worse than Scenario 2: The reduction of total energy costs amounts to 2.69 million EUR (12.3%). Concerning the contribution of flexibility services, Scenario 3 shows higher revenues for flexibility services FCR and aFRR indicating that an internal aggregation of flexibility offers higher revenues for the provision of control reserves. FCR revenues increase by 5% and aFRR revenues increase by 7%, while revenues from flexibility service EMO remain almost the same.

The local flexibility services LPO and LEO show similar revenues as in Scenario 1, as almost the same peak reduction and energy im- and export are achieved.

Results from the flexibility service LEO show the greatest contribution between all scenarios. This indicates that the resulting schedule of Scenario 3 was able to consider moving the im- or exports from or to the public grid to less expensive times or to avoid penalties for electricity exports. A reason for this result can be the fact that this model is the least constrained model.

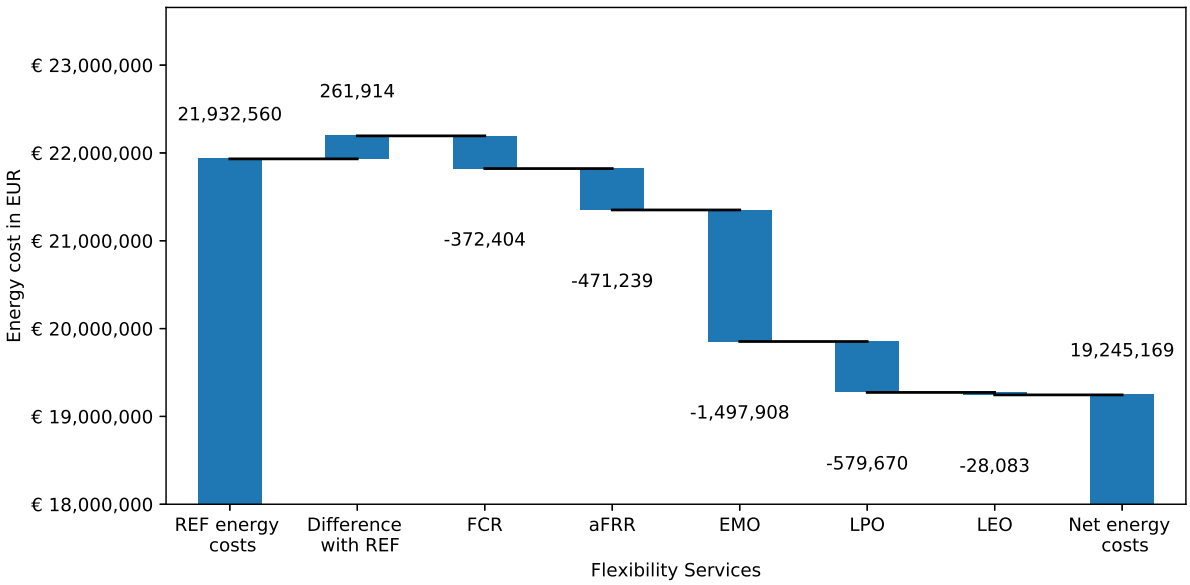

Figure 7.27: Energy cost and contribution of individual flexibility services for year 2017 with the optimization problem defined for Scenario 3

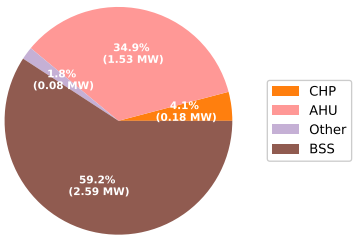

Figure 7.28: FCR provision in Scenario 3
Pie chart showing relative and average FCR power.

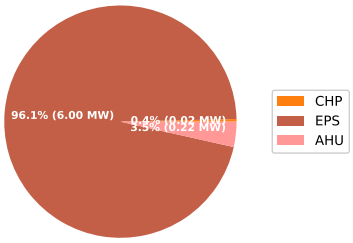

Figure 7.29: Positive aFRR provision in Scenario 3
Pie chart showing relative and average $aFRR^{+}$ power.

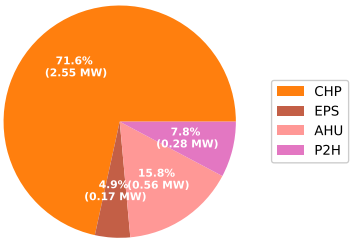

Figure 7.30: Negative aFRR provision in Scenario 3
Pie chart showing relative and average $aFRR^{-}$ power.

7.3.4 Comparison of control reserve power between all scenarios

Figure 7.31 displays the amount of power that is commercialized as control reserve for the individual scenarios. For FCR power, it is visible that Scenario 2 shows the highest FCR power levels (27% higher than Scenarios 1 and 20% higher than Scenario 3). This can be explained by the lack of the revenue share normally given to the aggregator in Scenario 2. Thus, the flexibility service FCR increases its competitiveness as compared with other flexibility services such as EMO. This is also visible by the comparison of Figures 7.16, 7.23, and 7.27: Compared to Scenarios 1 and 3, Scenario 2 shows lower revenues from flexibility service EMO.

A disadvantage of Scenario 2 can be seen in the commercialization of aFRR+. Scenarios 1 and 3 show 10% and 18% higher positive aFRR power. For Scenario 2, it seems to be difficult to combine different flexibility offers to satisfy the integer criteria. The same effect, however, is not visible for aFRR-.

For control reserve power, slightly higher revenues from flexibility services can be spotted between Scenario 1 and Scenario 3. This shows the benefit of an internal aggregation of control reserve power.

Figure 7.32 displays the advantages of Scenario 3 over Scenario 1 and Scenario 2. Scenario 3 shows the highest FCR commercialization of CHP plants. The FCR potential of CHPs varies greatly within 4-hours slots and in terms of symmetry. Scenario 3 is able to utilize this varying offer of flexibility best. Looking at the FCR power

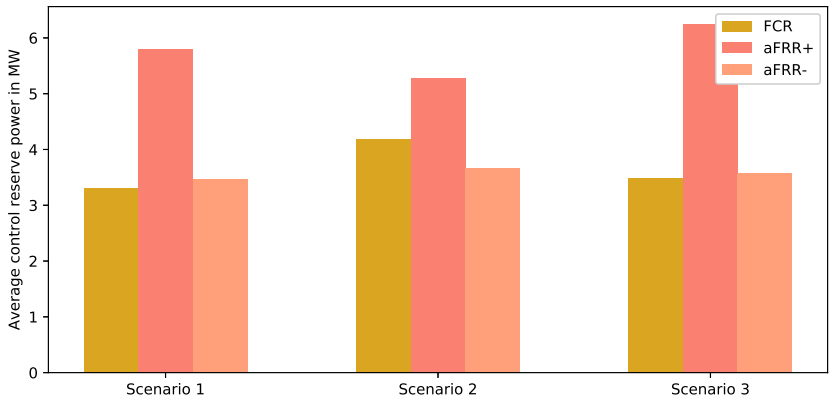

Figure 7.31: Average control reserve commercialization across Scenarios 1, 2, and 3

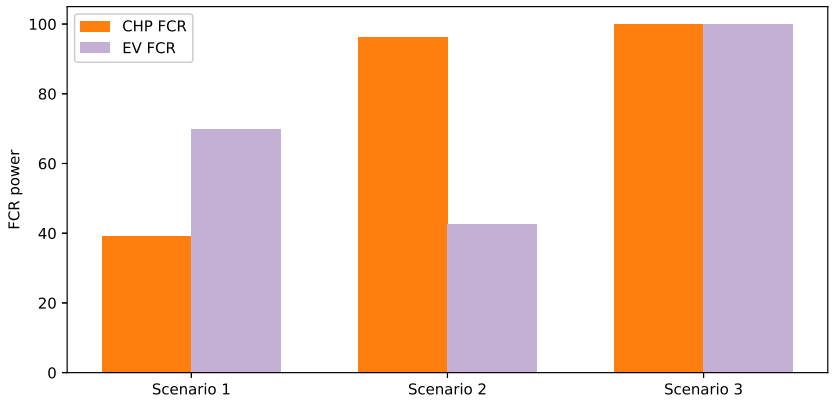

Figure 7.32: Relative FCR control reserve offers of CHPs and EVs across investigated scenarios. 100% equals maximum value of all three scenarios.

provided by EVs, Scenario 3 performs much better than Scenario 2. Scenario 2 has to combine given FCR offers by EVs with FCR offers of other devices to arrive at integer values. It is visible that this is only possible in around 40% of the cases.

We believe that for a scenario including a high number of energy devices from diverse energy technologies with varying availability and symmetry of FCR offers, Scenario 3 can yield higher revenues than Scenarios 1 and 2.

7.4 Discussion

7.4.1 Summary

The evaluation presented in this chapter displays results for the optimization model described in Chapter 6. By defining different scenarios, the contribution of flexibility services and the aggregation modes of control reserve offers is investigated. Simulations for the year 2017 are performed for the case study.

It is visible that flexibility services can lead to a reduction of energy costs by more than 12%. The flexibility service EMO, which is provided by devices of the energy technology BSS, yields the highest contributions to this reduction. Furthermore, flexibility services LPO, aFRR, and FCR contribute to further savings. The flexibility service LEO only leads to small reductions in energy costs.

Scenario 2, which is characterized by direct commercialization without an external aggregator, can realize the lowest energy costs due to substantial increases in earnings of flexibility services FCR and aFRR.

The internal aggregation of flexibility offers investigated in Scenario 3 shows slightly higher earnings for control reserve commercialization as opposed to Scenario 1; however, it needs to be pointed out that this increase is strongly dependent on the given configuration of energy devices and their operation.

7.4.2 Limitations

The performed simulation of the case study has the following limitations worth noting when considering the results. The case study has a device configuration that cannot be copied easily by other industrial plants. Especially the installation of wind power plants and battery storage systems is space- and capital intensive. The applied model of flexibility services; however, does not depend on the design of the industrial energy system. It can be applied to any site with flexible controllable energy devices. The modeling of the energy technologies offers typical models for different technologies.

The simulation includes perfect forecasts of energy demands as input data. It is, of course, impossible to achieve a perfect electricity and heating demand forecast for such a big manufacturing plant; however, tests showed that forecasts with a mean absolute percentage error of around 10% for electricity demand and around 20% for heating demand can be achieved; however, to correctly provide the flexibility service LPO, precise forecasts of the peak electricity demands are necessary. Without a perfect forecast, it is difficult to say if the set peak load will be exceeded during the optimization horizon. This will lead to higher peaks and less savings from the flexibility service LPO.

Furthermore, the modeling abstained from a thermodynamic model of the heating network. A model of the heating network as a possible heat storage might yield a more optimized operation of related devices. On the other side, it would increase the complexity and increase the run time of individual optimizations.

Furthermore, this thesis assumes perfect forecasts of prices on electricity and control reserve markets, which is not a trivial task. Next to accurate price forecasts, this thesis assumes perfect acceptance of bids on these markets. Concerning control reserve, the current market design which includes marginal pricing for FCR and MOL of power prices for aFRR allows industrial sites to take up a competitive market position, which would lead to high bid acceptance rates; however, continuous bid acceptance is not guaranteed on control reserve and electricity markets. In addition, the simulation runs have been performed with market data from the year 2017. Especially control reserve prices for FCR and aFRR have been decreasing further since 2017.

As the operational energy cost is optimized, no investment costs for energy devices are considered in this thesis. Moreover, Scenario 2 assumes direct market access for control reserve via an own virtual power plant by cutting out the middle man (aggregator). The operation of a VPP, nevertheless, is tied to investments, which were not considered.

Concerning the available technologies at the case study, the earnings can mainly be attributed to the BSS operating at the site. Here, it is to underline, that no limits on energy throughput or equivalent full cycle were set for the BSS. Especially the flexibility service EMO, which is responsible for the majority of earnings, requires more extreme power levels which can accelerate battery aging.

Therefore, the simulation can therefore be taken as an upper limit of potential savings. Still, a fraction of the displayed revenues acquired from the commercialization of flexibility would still be beneficial for industrial energy systems.

A part of the complete optimization problem has been implemented at the case study. This sub problem optimizes the schedule of the CHP plants, EPS, and AHUs based on actual day-ahead forecasts of energy demands in a dispatch problem combined with a model of flexibility services FCR, aFRR, and LPO. Energy demand forecasts are calculated based on weather forecasts and production schedules. First results showed feasible schedules that were realized at the case study plant and improved the provision of control reserve and lowered the peak power of the plant. An extension of the implemented model at the case study to match the optimization problem in Chapter

6 holds the possibility to further lower energy costs. Furthermore, the methodology could be implemented at different industrial sites that have a high number of controllable energy devices.

7.4.3 Future research

Future research could apply the described model at different industrial energy systems. Especially an industrial site with a higher number of devices could lead to a higher potential of local aggregation and increase earnings from control reserves for Scenarios 2 and 3.
Furthermore, a rolling horizon or rolling window optimization as done in [289] could have been implemented instead of setting strict start and end parameters at the beginning and end of the optimization horizon. For the BSS, for instance, a rolling horizon would be able to determine the optimal SOC at the end of the day by considering the situation of the following day.
Additionally, the application of the model with actual forecasts could display the sensitivity of the optimization model to forecasting errors. The model could be further extended to include measures of robustness against the deviation of electricity generation, energy price, or energy demand forecasts from actual values. Such robust optimization could include the use of stochastic optimization.
Moreover, the described model that solves the dispatch problem, on the one side, and the aggregator problem, on the other side, could be altered into a design problem. Especially, when looking at Scenario 2 that looks at the fulfillment of TSO criteria for the provision of control reserve bids, the composition of the pool of controllable devices is inherently important. When devices contribute different flexibility offers in a non-simultaneous way, it is important to install devices that complete bids by offering the correct amount of power at the correct time. When looking at results of Figure 7.32, at the current site, it is visible that at times aFRR+ offers lacked completion of Integer values. With a more optimized pool composition of devices, this could have been avoided.

8 Conclusion

This chapter provides a final summary of the thesis, which includes the discussion of proposed research questions.

8.1 Summary

A higher degree of decentralization of national energy systems and the proliferation of DERs lead to the conversion of electricity consumers to electricity prosumers. Especially industrial sites can benefit from the optimized control of generator, storage, and consumer devices to reduce operating energy costs and, furthermore, utilize the flexibility of the operation of these devices to provide local and external flexibility services. A flexibility service describes the use case that can be offered with the flexibility to adjust the electric load profile. This thesis defines an approach to model a combination of the dispatch problem that minimizes operational energy costs with the aggregator problem that maximizes revenues from the provision of flexibility services for industrial energy systems based on given flexibility offers and market conditions. These targets are combined in an optimization problem that results in an optimized schedule for the local and external flexibility utilization by various types of controllable devices.
To do so, this thesis reviews fundamental knowledge on energy systems, on the national electrical energy system in Germany, on the role of an industrial site within this electrical energy system, on energy technologies often encountered at industrial sites, and on mathematical modeling and optimization in Chapter 2. Chapter 3 defines the term flexibility of energy devices. Furthermore, it describes and assesses potential services that can be provided with the flexibility of devices at an industrial site. Chapter 4 presents an analysis of related work for modeling of energy systems, energy technologies, their application in models of dispatch or aggregator problems, and their ability to provide flexibility services. Chapter 5 provides simulation models for two flexibility services by a battery storage system, frequency control reserve and energy market optimization. Results are used to provide correct inputs for the optimization problem defined in the following chapter. The developed mathematical model in Chapter 6 describes a scheduling problem of controllable devices for an industrial site with individual mathematical models for each energy technology and flexibility service. The objective function of the constructed optimization problem intends to reduce operational energy costs through the economic dispatch to satisfy local energy demands and the utilization of flexibility to provide services within energy systems. Chapter 7 evaluates the developed model.

8.2 Conclusion

The following research questions have been answered along the thesis:

RQ 1 Flexibility services:
RQ 1.1: What are energy services that can be provided with the electrical flexibility of controllable devices of industrial sites?
RQ 1.2: How can the remuneration of the provision of these flexibility services be modeled?
In Chapter 3, several definitions of the term *flexibility* of energy systems are provided and compared. Based on these definitions, services that can be provided with the flexibility of devices within (local flexibility service) or outside of (external flexibility service) the energy system of the industrial site are identified. These flexibility services are arranged and introduced according to the solution that they offer within energy systems and the stakeholder that

they offer this value for. Based on this analysis, flexibility services are selected that are technologically feasible and economically viable to be provided by an industrial site such as the case study.
The method of remuneration of these flexibility services is discussed in detail in the second part of Chapter 3. The detailed mathematical model is then presented within Chapter 5 and Chapter 6.

RQ 2 Energy technologies:
RQ 2.1: How can controllable devices commonly found in industrial sites be modeled taking into account multiple energy carriers and interdependencies among them?
RQ 2.2: How can the flexibility of these controllable devices be modeled?
Energy technologies typically found at industrial sites are introduced in Chapter 2. Chapter 4 presents related work on the modeling of devices of these technologies and their ability to provide flexibility services. The detailed mathematical model applied in this work is then provided in Chapter 6. The mathematical model contains constraints of a MILP that represent the operation of the device as well as the contribution to the provision of flexibility services. The flexibility services FCR and EMO are modeled in detail for the energy technology BSS in Chapter 5 as the current state of the art lacks the estimation of economic benefits of the provision of these flexibility services. Naturally, not all available energy technologies at industrial sites are modeled in this work; however, Chapter 6 provides generic mathematical constraints that can be applied to a range of different technologies.

RQ 3 Benefits of flexibility use:
RQ 3.1: How can the provision of multiple flexibility services in combination with the economic dispatch problem be modeled for a microgrid in a joint optimization?
RQ 3.2: How can the ability of devices to provide multiple flexibility services ("multi-use") be modeled?
RQ 3.3: What is the contribution of flexibility services to the reduction of energy costs?
Related work on examples of microgrids that provide multiple flexibility services and simultaneously apply the objective function of the dispatch problem are presented in Chapter 4. Different approaches to model the provision of various flexibility services ("multi-use") of a BSS are shown and discussed. This work suggests to distinguish between simultaneous and serial provision of flexibility services as presented in Chapter 6. Furthermore, an approach to model the provision of multiple flexibility services in combination with the dispatch problem in presented in Chapter 6. A sum of the cost function of the economic dispatch problem and the revenues and costs associated with the flexibility services is used as a linear objective function for the optimization problem. The revenues and costs associated with individual flexibility services are modeled using a weighted sum. The weight is determined by changing market prices or penalties. This approach has the advantages to clearly reflect the apparent costs and is easy to adopt for other industrial sites. Using empirical data from the case study, Chapter 7 evaluates the monetary value that each flexibility service contributes to the reduction of energy costs in relation to a defined reference scenario. For the case study, a total energy cost reduction of 12% has been achieved. Flexibility services EMO and LPO displayed the highest contribution; however, the conclusion is drawn that the potential of flexibility services greatly depends upon the configuration of the industrial site and the existing regulation.

RQ 4 Flexibility aggregation:
RQ 4.1: What degrees of freedom in terms of aggregation of flexibility offers exist for the provision of control reserve?
RQ 4.2: What are possible aggregation models and which one proves most beneficial for the case study?
The degrees of freedom for aggregating control reserve offers according to the current regulation are presented in Chapter 6. Possibilities to aggregate flexibility offers exist in terms of bid size, time, and symmetry of the offer. Additionally, flexibility offers can be aggregated with or without the assistance of an external aggregator, which has implications on the earnings and bid size criteria to fulfill. Based on these degrees of freedom, three scenarios

have been defined that model either a device-by-device commercialization of control reserve (Scenario 1) or an aggregated commercialization of control reserve (Scenarios 2, 3) for an industrial site. Furthermore, market access with (Scenarios 1, 3) and without (Scenario 2) an external aggregator are assessed. Results for the case study show that Scenario 2 can provide the lowest operational energy costs due to higher earnings from control reserve provision. Although stricter constraints apply for Scenario 2 and make control reserve provision more complicated, higher earning per capacity lead to lower total energy costs.
The three main conclusions that can be drawn from this thesis are:

1. A multi-use model that combines the traditional economic dispatch problem and the aggregator problem can be modeled effectively and adequately in a mixed-integer linear program. The thesis provides an optimization problem of the use of an aggregate of multiple devices for the provision of multiple flexibility services that results in dispatch and commercialization decisions.
2. The provision of local and external flexibility services can greatly reduce energy costs of industrial sites. For battery storage systems a great potential lies in the optimization on short-term electricity markets, which up to now have often not been adequately modeled in literature.
3. Degrees of freedom in the aggregation control reserve bids offer the possibility to further increase earnings from control reserve provision. For the investigated case study, the local aggregation of control reserve bids and the direct commercialization without an external aggregator proves to be the most economic scenario.

8.3 Outlook

The work in this thesis can be extended by future work in multiple ways. Three relevant research topics are named in the following.
Firstly, an analysis of the implementation of the described generated device schedules at the case study would be of interest. As explained in Section 7.4 a part of the defined optimization problem is used at the case study to supply day-ahead schedules for the CHP plants, AHUs, and EPS at the plant to reduce the peak loads (LPS), lower electricity procurement costs (LEO) and provide control reserve (FCR, aFRR). An analysis of the actual savings as opposed to the previous years and the dependence on the quality of energy demand, and energy market forecasts would be of interest.
Secondly, the multi-use aspect of the modeling approach could be further evaluated. A comparison between different configurations of possible flexibility services per device shown in Table 6.2 would allow the reader to understand the advantage gained from different multi-use configurations. Additionally, the modeling and evaluation of more flexibility services mentioned in Table 3.6 that are currently not feasible or economical can be investigated.
Thirdly, for the field of aggregation of control reserve bids, other energy system configurations of industrial sites can be explored. These configurations can include different types and sizing of devices. Consequently, these might yield different results among the explored aggregation scenarios as pointed out in Section 7.3. Additionally, not just the control reserve bids of single energy system but of multiple energy system could be aggregated with the described model.
Next to future scientific research topic, it will be interesting to see what role industrial sites will play in national energy systems. To effectively achieve carbon emission targets in Germany, the participation of industrial sites in the provision of system services for the electrical energy system is inevitable. Using energy devices for flexible electricity generation, storage, and consumption, some industrial sites have gained the ability to actively adjust their own load profile. Due to the decreasing flexibility in electricity generation of renewable energy technologies wind and solar as compared to conventional generation, it is of utmost importance to increase the flexibility of traditional electricity consumers such as industrial sites. This work has shown that according to actual regulation energy cost reductions are possible using IT-assisted planning of energy resource operation.

Appendix

Below, the optimization problem is described that models trading fees and efficiencies for the provision of EMO with a BSS.

$$\max \sum_{t=1}^{t_{\max}} (\tau_t + \tau^{trading\_fee}) \cdot e_t^{buy} + (\tau_t - \tau^{trading\_fee}) \cdot e_t^{sell} \tag{A1a}$$

subject to

$$\underline{P}\Delta t \leq e_t^{disch} \leq 0, \forall t \in T \tag{A1b}$$

$$0 \leq e_t^{ch} \leq \overline{P}\Delta t, \forall t \in T \tag{A1c}$$

$$E_t = E_{t-1} + e_t^{ch} \cdot \eta ch - \frac{e_t^{disch}}{\eta^{disch}}, \forall t \in T \tag{A1d}$$

$$0 \leq E_t \leq \overline{E}, \forall t \in T \tag{A1e}$$

$$-V_t \leq e_t^{buy} - e_t^{sell} \leq V_t, \forall t \in T \tag{A1f}$$

$$x_t^{buy} + x^{buy} \leq 1, \forall t \in T \tag{A1g}$$

$$e_t^{planch} - e_t^{plandisch} + e_t^{buy} - e_t^{sell} = e_t^{ch} - e_t^{disch}, \forall t \in T \tag{A1h}$$

$$e_t^{buy} \leq x_t^{buy} \cdot \frac{(\overline{P} - \underline{P}) \cdot \Delta t}{\eta^{ch}}, \forall t \in T \tag{A1i}$$

$$e_t^{sell} \leq x_t^{buy} \cdot \frac{(\underline{P} - \overline{P}) \cdot \Delta t}{\eta^{disch}}, \forall t \in T \tag{A1j}$$

$$E^{start} = 0.5 \cdot \overline{E}, E^{end} = 0.5 \cdot \overline{E} \tag{A1k}$$

In the following, the variables and parameters introduced in the applied in the calculations, simulations, and optimization problems along the chapters will be introduced. For optimization problems in Chapters 5 and 6, variables are marked with a "V", parameters with a "P".

Table A1: Variables and parameters introduced in and related to Chapter 5

Variable	Description	Type	$\in$
$\overline{E}$	Capacity of BSS in MWh	-	$\mathbb{R}_{\geq 0}$
$\overline{P^{FCR}}$	Prequalified FCR power of the BSS in MW	-	$\mathbb{R}_{\geq 0}$
P_t^{FCR}	FCR bid at time step t for BSS in MW	-	$\mathbb{R}_{\geq 0}$
ν_t	Grid frequency at time step t in Hz	-	$\mathbb{R}$
$P_t^{FCR\_target}$	Target FCR power at time step t of BSS in MW	-	$\mathbb{R}$
P_t	Final power applied to BSS at time step t in MW	-	$\mathbb{R}$
SOC_t	SOC level at time step t in %	-	

$SOC^{l,POR}$	Lower SOC threshold that represents the end of the permissible operation range in %	-	
$SOC^{u,POR}$	Upper SOC threshold that represents the end of the permissible operation range in %	-	
$SOC^{l,MBC}$	Lower SOC threshold that triggers market-based charging in %	-	
$SOC^{u,MBC}$	Upper SOC threshold that triggers market-based charging in %	-	
SOC^{DOF}	Lower SOC threshold that allows the use of degrees of freedom in %	-	
SOC^{DU}	SOC threshold that allows the use of DOF deadband usage in %	-	
SOC^{OF}	SOC threshold that allows the use of DOF overfulfillment in %	-	
SOC^{GC}	SOC threshold that allows the use of DOF gradient control in %	-	
P_t^{DU}	Power change of FCR signal associated to DOF deadband usage in MW	-	$\mathbb{R}_{\geq 0}$
P_t^{OF}	Power change of FCR signal associated to DOF overfulfillment in MW	-	$\mathbb{R}_{\geq 0}$
P_t^{GC}	Power change of FCR signal associated to DOF gradient control in MW	-	$\mathbb{R}$
g_{max}	Maximum gradient of BSS in terms of $\Delta P/t$ in MW/s	-	
g_{min}	Maximum gradient of BSS in terms of $\Delta P/t$ in MW/s	-	
P_t^{MBC}	Power of market-based charging (discharging) at time step t in MW	-	$\mathbb{R}$
$P_t^{DOF\,ch}$	Power of degrees of freedom during BSS charging at time step t in MW	-	$\mathbb{R}$
$P_t^{DOF\,disch}$	Power of degrees of freedom during BSS charging at time step t in MW	-	$\mathbb{R}$
η^{ch}	Charging efficiency of BSS in %	-	
η^{disch}	Discharging efficiency of BSS in %	-	
$\underline{P}$	Minimum power of BSS in MW	P	
$\overline{P}$	Minimum power of BSS in MW	P	
e_t	Energy charged or discharged at time step t determined by current optimization in MWh	V	$\mathbb{R}$
e_t^{plan}	Energy charged or discharged at time step t determined by previous optimization in MWh	P	
E_t	Energy of BSS at time step t determined by current optimization in MWh	V	$\mathbb{R}$
E^{start}	Initial energy of BSS	P	
E^{end}	Final energy of BSS	P	
V_t	Tradable Volume at time step t and optimization u in MWh	P	
τ_t	Energy price of time step (product) t in optimization u in EUR/MWH	P	
e_t^{buy}	Energy bought at time step t determined by current optimization in MWh	V	$\mathbb{R}_{\geq 0}$
e_t^{sell}	Energy sold at time step t determined by current optimization in MWh	V	$\mathbb{R}_{\geq 0}$
e_t^{ch}	Energy charged at time step t determined by current optimization in MWh	V	$\mathbb{R}_{\geq 0}$
e_t^{disch}	Energy charged at time step t determined by current optimization in MWh	V	$\mathbb{R}_{\geq 0}$

Table A2: Variables and parameters introduced in Chapter 6

Variable	Description	Type	$\in$
$\underline{P}_{a,b}$	Minimum power of device b of energy technology a in MW	P	
$\check{P}_{a,b}$	Partial power of device b of energy technology a in MW	P	
$\overline{P}_{a,b}$	Maximum power of device b of energy technology a in MW	P	
$P_{a,b,t}$	Electric power level of device b of energy technology a in time step t in MW	V	$\mathbb{R}$
$x^{op}_{a,b,t}$	Operation state (on/off) of device b of energy technology a in time step t	V	$\{0,1\}$
$F^{-}_{a,b,t}$	Negative flexibility of device b of energy technology a in time step t in MW	V	$\mathbb{R}_{\geq 0}$
$F^{+}_{a,b,t}$	Positive flexibility of device b of energy technology a in time step t in MW	V	$\mathbb{R}_{\geq 0}$
$P^{FCR^{+}}_{a,b,t}$	Positive FCR bid of device b of energy technology a in time step t in MW	V	$\mathbb{R}_{\geq 0}$
$P^{aFRR^{+}}_{a,b,t}$	Positive aFRR bid of device b of energy technology a in time step t in MW	V	$\mathbb{R}_{\geq 0}$
$P^{FCR^{-}}_{a,b,t}$	Negative FCR bid of device b of energy technology a in time step t in MW	V	$\mathbb{R}_{\geq 0}$
$P^{aFRR^{-}}_{a,b,t}$	Negative aFRR bid of device b of energy technology a in time step t in MW	V	$\mathbb{R}_{\geq 0}$
$P^{FCR}_{a,b,t}$	Symmetric FCR bid of device b of energy technology a in time step t in MW	V	$\mathbb{R}_{\geq 0}$
P^{FCR}_{t}	Total FCR bid industrial site in time step t in MW	V	$\mathbb{R}_{\geq 0}/\mathbb{N}$
$P^{aFRR^{-}}_{t}$	Total negative aFRR bid of industrial site in time step t in MW	V	$\mathbb{R}_{\geq 0}/\mathbb{N}$
$P^{aFRR^{+}}_{t}$	Total positive aFRR bid of industrial site in time step t in MW	V	$\mathbb{R}_{\geq 0}/\mathbb{N}$
$x^{LFS}_{a,b,t}$	Binary variable for the decision for local flexibility services in serial model of flexibility services	V	$\{0,1\}$
$x^{FCR}_{a,b,t}$	Binary variable for the decision for FCR provision in serial model of flexibility services	V	$\{0,1\}$
$x^{EMO}_{a,b,t}$	Binary variable for the decision for EMO in serial model of flexibility services	V	$\{0,1\}$
r^{FCR}_{t}	Total revenues of FCR provision for industrial site in time step t in EUR	V	$\mathbb{R}_{\geq 0}$
υ^{FCR}_{t}	Capacity price of FCR provision in time step t in EUR/MW	P	
$r^{aFRR^{+}}_{t}$	Total revenues of positive aFRR provision for industrial site in time step t in EUR	V	$\mathbb{R}_{\geq 0}$
$\upsilon^{aFRR^{+}}_{t}$	Capacity price of positive aFRR provision in time step t in EUR/MW	P	
$p^{aFRR^{+}}_{a,b}$	Probability of positive aFRR call of device b of energy technology a in %	P	
$\tau^{aFRR^{+}}_{a,b}$	Selected energy price of positive aFRR call of device b of energy technology a in EUR/MWh	P	

$\gamma_{a,b}^{aFRR^+}$	Energy cost of positive aFRR call of device b of energy technology a in EUR/MWh	P	
$r_t^{aFRR^-}$	Total revenues of negative aFRR provision for industrial site in time step t in EUR	V	$\mathbb{R}_{\geq 0}$
$\upsilon_t^{aFRR^-}$	Capacity price of negative aFRR provision in time step t in EUR/MW	P	
$p_{a,b}^{aFRR^-}$	Probability of negative aFRR call of device b of energy technology a in %	P	
$\tau_{a,b}^{aFRR^-}$	Selected energy price of negative aFRR call of device b of energy technology a in EUR/MWh	P	
$\gamma_{a,b}^{aFRR^-}$	Energy cost of negative aFRR call of device b of energy technology a in EUR/MWh	P	
$\dot{P}_{a,b,t}$	Electric net power level after control reserve provision of device b of energy technology a in time step t in MW	V	$\mathbb{R}$
c^{LPO}	Cost of peak power level in EUR	V	$\mathbb{R}_{\geq 0}$
P^{peak}	Power above peak threshold of load profile in modeling approach 1 of LPO in MW	V	$\mathbb{R}_{\geq 0}$
$P_{GRID,t}^{+}$	Power from public grid in MW	V	$\mathbb{R}_{\geq 0}$
$\overline{P}_{GRID}^{+}$	Selected peak threshold for flexibility service LPO in MW	P	
P^{peak}	Maximum power level of load profile in modeling approach 1 of LPO in MW	V	$\mathbb{R}_{\geq 0}$
υ^{peak}	Capacity price of peak power in EUR/MW	P	
P_t^{peak}	Power above peak threshold of load profile for modeling approach 2 of LPO in time step t in MW	V	$\mathbb{R}_{\geq 0}$
P_t^{peak}	Power above additional peak threshold of load profile for modeling approach 2 of LPO in time step t in MW	V	$\mathbb{R}_{\geq 0}$
$\overline{P}_{GRID}^{+init}$	Initial peak threshold for flexibility service LPO at first optimization un MW	P	
υ^{peak_1}	Additional capacity price of peak power in EUR/MW	P	
r_t^{EMO}	Revenue of flexibility service EMO in EUR	V	$\mathbb{R}_{\geq 0}$
υ_t^{EMO}	Capacity price of peak power for predefined power level in time step t in EUR	P	
υ^{peak_1}	Additional capacity price of peak power in EUR/MW	P	
P_t^{RES}	Power generated by RES in time step t in MW	V	$\mathbb{R}_{\geq 0}$
P_t^{CONV}	Power generated by conventional power plants in time step t in MW	V	$\mathbb{R}_{\geq 0}$
$P_{GRID,t}^{-}$	Power exported to public grid in time step t in MW	V	$\mathbb{R}_{\geq 0}$
$P_t^{RES\_PEN}$	Penalized power for RES buffering in t in MW	V	$\mathbb{R}_{\geq 0}$

c_t^{LEO}	Cost related to flexibility service LEO in time step t in EUR	V	$\mathbb{R}$
$c_t^{LEO_{REF}}$	Cost related to flexibility service LEO of reference scenarios REF_LEO in time step t in EUR	V	$\mathbb{R}$
$\tau_{GRID,t}^{DA}$	Electricity prices from the EPEX Day-Ahead Auction in time step t in EUR/MWh	P	
τ_{GRID}^{fees}	Grid fees and surcharges for electricity import in EUR/MWh	P	
ϕ^{SB}	Fee for electricity export to the public grid in EUR/MWh	P	
ϕ^{RES}	Fee for electricity export of renewable energy to the public grid in EUR/MWh	P	
ϕ^{VPP}	Share of FCR and aFRR capacity-related revenues taken by the aggregator in %	P	
$c_{a,b,t}^{op}$	Operation cost of device b of energy technology a in time step t in EUR	V	$\mathbb{R}_{\geq 0}$
$c_{a,b}^{mt}$	Maintenance cost of device b of energy technology a in EUR	P	
$\check{c}_{a,b}^{var}$	Cost at minimum operation point of device b of energy technology a in EUR	P	
$\check{c}_{a,b}^{fuel}$	Cost related to fuel consumption at minimum operation point of device b of energy technology a in EUR/MWh	P	
$\check{c}_{a,b}^{sur}$	Cost related to surcharges at minimum operation point of device b of energy technology a in EUR/MWh	P	
$c_{a,b,t}^{grad}$	Gradient cost of device b of energy technology a in time step t in EUR	V	$\mathbb{R}_{\geq 0}$
$c_{a,b}^{lin.cost}$	Gradient cost development of device b of energy technology a	P	
$\bar{c}_{a,b}^{fuel}$	Cost related to fuel consumption at maximum operation point of device b of energy technology a in EUR/MWh	P	
$\bar{c}_{a,b}^{sur}$	Cost related to surcharges at maximum operation point of device b of energy technology a in EUR/MWh	P	
$c_{a,b,t}^{ramp}$	Ramping cost of device b of energy technology a in time step t in EUR	V	$\mathbb{R}_{\geq 0}$
$c_{a,b}^{on}$	Ramping up cost of device b of energy technology a in time step t in EUR	P	
$c_{a,b}^{off}$	Ramping down cost of device b of energy technology a in time step t in EUR	P	
$x_{a,b,t}^{on}$	Binary variable for the decision of ramping up device b of energy technology a in time step t	V	$\{0,1\}$
$x_{a,b,t}^{off}$	Binary variable for the decision of ramping down device b of energy technology a in time step t	V	$\{0,1\}$
$P_{DEM,t}$	Electricity demand	P	
$P_{WIND,t}$	Wind power generation	P	
$P_{a,b,t}^{charge}$	Charging power of device b of energy technology a in time step t in MW	V	$\mathbb{R}_{\geq 0}$

$P^{discharge}_{a,b,t}$	Charging power of device b of energy technology a in time step t in MW	V	$\mathbb{R}_{\geq 0}$
$P^{+}_{a,b,t}$	Positive local DR of device b of energy technology a in MW	V	$\mathbb{R}_{\geq 0}$
$P^{-}_{a,b,t}$	Negative local DR of device b of energy technology a in MW	V	$\mathbb{R}_{\geq 0}$
$P^{plan}_{a,b}$	Planned power profile of device b of energy technology a in MW	P	
$Q_{DEM,t}$	Heating demand	P	
$Q_{a,b,t}$	Heating power level of device b of energy technology a in MW	V	$\mathbb{R}_{\geq 0}$
$\overline{Q}_{a,b,t}$	Heating power level at maximum power of device b of energy technology a in MW	P	
$\check{Q}_{a,b,t}$	Heating power level at partial power of device b of energy technology a in MW	P	
$G_{a,b,t}$	Gas consumption of device b of energy technology a in MW	V	$\mathbb{R}_{\geq 0}$
$\overline{G}_{a,b}$	Gas consumption at maximum power of device b of energy technology a in MW	P	
$\check{G}_{a,b}$	Gas consumption at partial power of device b of energy technology a in MW	P	
$E_{a,b,t}$	Energy level of storage-restricted device b of energy technology a in MWh	V	$\mathbb{R}_{\geq 0}$
$\overline{E}_{a,b}$	Maximum energy level of storage-restricted device b of energy technology a in MWh	P	
$\underline{E}_{a,b}$	Minimum energy level of storage-restricted device b of energy technology a in MWh	P	
$E^{init}_{a,b}$	Initial storage level of device b of energy technology a in MWh or %	P	
$E^{final}_{a,b}$	Final storage level of device b of energy technology a in MWh or %	P	
η_{HN}	Efficiency of distribution network in %	P	
$\mu_{a,b}$	Power-to-heat ratio of device b of energy technology a in %	P	
$\eta^{tot}_{a,b}$	Total (electric + thermal) efficiency of device b of energy technology a in %	P	
$\overline{\eta}^{el}_{a,b}$	Electric efficiency at maximum power of device b of energy technology a in %	P	
$\check{\eta}^{el}_{a,b}$	Electric efficiency at partial power of device b of energy technology a in %	P	
$\overline{P^{FCR}}_{a,b}$	Prequalified FCR power of device b of energy technology a in MW	P	
$\overline{P^{aFRR}}_{a,b}$	Prequalified aFRR power of device b of energy technology a in MW	P	
γ^{EEG}	EEG surcharge (from 2017) in EUR/MWh	P	
$f^{EEG}_{a,b}$	EEG surcharge factor of device b of energy technology a in %	P	
$r^{sur}_{a,b}$	Subsidy of device b of energy technology a in EUR/MWh	P	
T^{l}_{a}	Operation hours for flexibility service l of energy technology a in h	P	
T^{refill}_{a}	Longest period until next refill of storage tank of energy technology a in h	P	
$t^{plug-in}_{EV,m}$	Time of plug-in of EV m as date	P	

$t_{EV,m}^{charge\_end}$	Time of end of charge of EV m as date	P	
$t_{EV,m}^{plug-out}$	Time of plug-in of EV m as date	P	
$T_{EV,m}^{charge}$	Charge duration of EV m as date	P	
$T_{EV,m}^{plug}$	Plug duration of EV m as date	P	
$T_{EV,m}^{flex}$	Idle duration of EV m as date	P	
$\eta_{a,b}^{discharge}$	Discharge efficiency of device b of energy technology a in %	P	
$\eta_{EV,m}^{charge}$	Charge efficiency of device b of energy technology a in %	P	
$E_{EV,m}^{charge}$	Charged energy of EV m in MWh	P	
$x_{EV,m,t}^{plug}$	Binary variable displaying plug status of EV m	P	$\{0,1\}$
θ_t	Temperature level in time step t in °C	P	
$\underline{\theta}$	Temperature threshold for winter operation of HVAC plants in °C	P	
$\overline{\theta}$	Temperature threshold for summer operation of HVAC plants in °C	P	
T_a^{LDR}	Flexibility interval for local DR measures of energy technology a in h	P	
$\eta_{a,b}^{-}$	Efficiency of negative local DR of device b of energy technology a in %	P	

List of Figures

List of Tables

Bibliography

[1] Khalid Abdulla, Julian Hoog, Valentin Muenzel, Frank Suits, Kent Steer, Andrew Wirth, and Saman Halgamuge. Optimal Operation of Energy Storage Systems Considering Forecasts and Battery Degradation. *IEEE Transactions on Smart Grid*, 9(3):2086–2096, May 2018.

[2] Lisias V. L. Abreu, Mohammad E. Khodayar, Mohammad Shahidehpour, and Lei Wu. Risk-Constrained Coordination of Cascaded Hydro Units With Variable Wind Power Generation. *IEEE Transactions on Sustainable Energy*, 3(3):359–368, July 2012.

[3] Jamshid Aghaei and Mohammad-Iman Alizadeh. Multi-objective self-scheduling of CHP (combined heat and power)-based microgrids considering demand response programs and ESSs (energy storage systems). *Energy*, 55:1044–1054, June 2013.

[4] Jamshid Aghaei, Mahdi Karami, Kashem M. Muttaqi, Heidarali A. Shayanfar, and Abdollah Ahmadi. MIP-Based Stochastic Security-Constrained Daily Hydrothermal Generation Scheduling. *IEEE Systems Journal*, 9(2):615–628, June 2015.

[5] Mohammad Reza Aghamohammadi and Hajar Abdolahinia. A new approach for optimal sizing of battery energy storage system for primary frequency control of islanded Microgrid. *International Journal of Electrical Power & Energy Systems*, 54(Supplement C):325–333, January 2014.

[6] René Aïd, Pierre Gruet, and Huyên Pham. An optimal trading problem in intraday electricity markets. *Mathematics and Financial Economics*, 10(1):49–85, January 2016.

[7] Nelson K. Akafuah, Sadegh Poozesh, Ahmad Salaimeh, Gabriela Patrick, Kevin Lawler, and Kozo Saito. Evolution of the Automotive Body Coating Process—A Review. *Coatings*, 6(2):24, June 2016.

[8] Ali T. Al-Awami and Eric Sortomme. Coordinating Vehicle-to-Grid Services With Energy Trading. *IEEE Transactions on Smart Grid*, 3(1):453–462, March 2012.

[9] Mubbashir Ali, Amir Safdarian, and Matti Lehtonen. Demand response potential of residential HVAC loads considering users preferences. *IEEE PES Innovative Smart Grid Technologies, Europe*, pages 1–6, October 2014.

[10] Florian Allerding. *Organic Smart Home - Energiemanagement für Intelligente Gebäude*. PhD Thesis, KIT Scientific Publishing, Karlsruhe, 2013. ISBN: 978-3-7315-0181-7.

[11] Monica Alonso, Hortensia Amaris, Jean Germain, Juan Galan, Monica Alonso, Hortensia Amaris, Jean Gardy Germain, and Juan Manuel Galan. Optimal Charging Scheduling of Electric Vehicles in Smart Grids by Heuristic Algorithms. *Energies*, 7(4):2449–2475, April 2014.

[12] Carlos Henggeler Antunes and Carla Oliveira Henriques. Multi-Objective Optimization and Multi-Criteria Analysis Models and Methods for Problems in the Energy Sector. In Salvatore Greco, Matthias Ehrgott, and José Rui Figueira, editors, *Multiple Criteria Decision Analysis: State of the Art Surveys*, pages 1067–1165. Springer New York, New York, NY, 2016.

[13] Nataly Banol Arias, Seyedmostafa Hashemi, Peter Bach Andersen, Chresten Traholt, and Ruben Romero. V2G enabled EVs providing frequency containment reserves: field results. *Proceedings of 2018 IEEE International Conference on Industrial Technology*, pages 1814–19, 2018.

[14] José M. Arroyo and Antonio J. Conejo. Optimal response of a thermal unit to an electricity spot market. *IEEE Transactions on Power Systems*, 15(3):1098–1104, August 2000.

[15] Ali Aydemir. Wärmepumpen. In Martin Wietschel, Sandra Ullrich, Peter Markewitz, Friedrich Schulte, and Fabio Genoese, editors, *Energietechnologien der Zukunft: Erzeugung, Speicherung, Effizienz und Netze*, pages 383–397. Springer Fachmedien, Wiesbaden, 2015.

[16] Ali Aydemir and Jan Steinbach. Raumlufttechnik und Klimakältesysteme. In Martin Wietschel, Sandra Ullrich, Peter Markewitz, Friedrich Schulte, and Fabio Genoese, editors, *Energietechnologien der Zukunft: Erzeugung, Speicherung, Effizienz und Netze*, pages 369–382. Springer Fachmedien Wiesbaden, Wiesbaden, 2015.

[17] X. Ayón, J. K. Gruber, B. P. Hayes, J. Usaola, and M. Prodanović. An optimal day-ahead load scheduling approach based on the flexibility of aggregate demands. *Applied Energy*, 198:1–11, July 2017.

[18] D. Azofra, E. Jiménez, E. Martínez, J. Blanco, and J. C. Saenz-Díez. Wind power merit-order and feed-in-tariffs effect: A variability analysis of the Spanish electricity market. *Energy Conversion and Management*, 83:19–27, July 2014.

[19] Sonja Babrowski. Bedarf und Verteilung elektrischer Tagesspeicher im zukünftigen deutschen Energiesystem. 2015. Publisher: KIT Scientific Publishing.

[20] Sonja Babrowski, Heidi Heinrichs, Patrick Jochem, and Wolf Fichtner. Load shift potential of electric vehicles in Europe. *Journal of Power Sources*, 255:283–293, June 2014.

[21] C. J. Baldwin, K. M. Dale, and R. F. Dittrich. A Study of the Economic Shutdown of Generating Units in Daily Dispatch. *Transactions of the American Institute of Electrical Engineers. Part III: Power Apparatus and Systems*, 78(4):1272–1282, December 1959.

[22] Prabir Barooah, Ana Buic, and Sean Meyn. Spectral Decomposition of Demand-Side Flexibility for Reliable Ancillary Services in a Smart Grid. In *2015 48th Hawaii International Conference on System Sciences*, pages 2700–2709, January 2015. ISSN: 1530-1605.

[23] Anthony Barré, Benjamin Deguilhem, Sébastien Grolleau, Mathias Gérard, Frédéric Suard, and Delphine Riu. A review on lithium-ion battery ageing mechanisms and estimations for automotive applications. *Journal of Power Sources*, 241:680–689, November 2013.

[24] Benedikt Battke and Tobias S. Schmidt. Cost-efficient demand-pull policies for multi-purpose technologies – The case of stationary electricity storage. *Applied Energy*, 155:334–348, October 2015.

[25] Benedikt Battke, Tobias S. Schmidt, David Grosspietsch, and Volker H. Hoffmann. A review and probabilistic model of lifecycle costs of stationary batteries in multiple applications. *Renewable and Sustainable Energy Reviews*, 25:240–250, September 2013.

[26] David Bauer, Stefan Kirschbaum, Gregor Wrobel, Julian Agudelo, and Philip Voll. Modellbasierte Optimierung von Energiesystemen. *GI-Jahrestagung*, 2015.

[27] Aliasghar Baziar and Abdollah Kavousi-Fard. Considering uncertainty in the optimal energy management of renewable micro-grids including storage devices. *Renewable Energy*, 59:158–166, November 2013.

[28] BDEW, German Association of Energy and Water Industries. *Technische Richtlinie Erzeugungsanlagen am Mittelspannungsnetz*. 2008. https://www.bdew.de/media/documents/20080529_TAB_Mittelspannung.pdf.

[29] BDEW, German Association of Energy and Water Industries. Smart Grid Traffic Light Concept. https://www.bdew.de/media/documents/Stn_20150310_Smart-Grids-Traffic-Light-Concept_english.pdf, 2015.

[30] BDEW, German Association of Energy and Water Industries. Anreizmechanismen Engpassmanagement VNB, January 2020. https://www.bdew.de/media/documents/Stn_20203001_Anreizmechanismen-Engpassmanagement.pdf.

[31] BDEW, German Association of Energy and Water Industries. BDEW-Strompreisanalyse Januar 2020, January 2020. https://www.bdew.de/media/documents/20200107_BDEW-Strompreisanalyse_Januar_2020.pdf.

[32] Dominik Becks, Michael Müller-Ruff, and Julian Rominger. Method for Providing Control Power for Stabilizing the Grid Frequency of a Power Grid and/or for Fulfilling a Power Schedule, Control Device for a Technical Installation, and Technical Installation, February 2019.

[33] Dominik Becks, Michael Müller-Ruff, and Julian Rominger. Verfahren zum Bereitstellen von Regelleistung für eine Netzfrequenzstabilisierung Stromnetzes und/oder für eine Erfüllung eines Leistungsfahrplans sowie Steuervorrichtung für eine technische Anlage, February 2019.

[34] Dominik Becks, Michael Müller-Ruff, Julian Rominger, and Tillmann Laux. Erbringung von Primärregelleistung, March 2018.

[35] Mahdi Behrangrad. A review of demand side management business models in the electricity market. *Renewable and Sustainable Energy Reviews*, 47:270–283, July 2015.

[36] Jörg Benze, Christian Hübner, and Andreas Kießling. Das intelligente Energiesystem als zukünftige Basis für ein nachhaltiges Energiemanagement. 2011. Accepted: 2018-11-27T09:59:07Z ISSN: 1617-5468.

[37] Joachim Bertsch, Simeon Hagspiel, and Lisa Just. Congestion management in power systems. *Journal of Regulatory Economics*, 50(3):290–327, December 2016.

[38] Valentin Bertsch and Wolf Fichtner. A participatory multi-criteria approach for power generation and transmission planning. *Annals of Operations Research*, 245(1):177–207, October 2016.

[39] Ricardo J. Bessa and Manuel A. Matos. The role of an aggregator agent for EV in the electricity market. pages 126–126, January 2010.

[40] Ricardo J. Bessa and Manuel A. Matos. Optimization Models for EV Aggregator Participation in a Manual Reserve Market. *IEEE Transactions on Power Systems*, 28(3):3085–3095, August 2013.

[41] Ricardo J. Bessa, Manuel A. Matos, Filipe J. Soares, and Joao. A. P. Lopes. Optimized Bidding of a EV Aggregation Agent in the Electricity Market. *IEEE Transactions on Smart Grid*, 3(1):443–452, March 2012.

[42] Michele Bianchi, Andrea De Pascale, Francesco Melino, and Antonio Peretto. Performance prediction of micro-CHP systems using simple virtual operating cycles. *Applied Thermal Engineering*, 71(2):771–779, October 2014.

[43] Ulf Birnbaum, Richard Bongartz, and Philipp Klever. Mikro-Kraftwärmekopplungsanlagen (Mikro-KWK). In Martin Wietschel, Sandra Ullrich, Peter Markewitz, Friedrich Schulte, and Fabio Genoese, editors, *Energietechnologien der Zukunft: Erzeugung, Speicherung, Effizienz und Netze*, pages 347–368. Springer Fachmedien Wiesbaden, Wiesbaden, 2015.

[44] Aldo Bischi, Leonardo Taccari, Emanuele Martelli, Edoardo Amaldi, Giampaolo Manzolini, Paolo Silva, Stefano Campanari, and Ennio Macchi. A rolling-horizon optimization algorithm for the long term operational scheduling of cogeneration systems. *Energy*, 184:73–90, October 2019.

[45] Andreas Bloess, Wolf-Peter Schill, and Alexander Zerrahn. Power-to-heat for renewable energy integration: A review of technologies, modeling approaches, and flexibility potentials. *Applied Energy*, 212:1611–1626, February 2018.

[46] BMW Group. BMW Group demonstriert Führungsrolle im Bereich Elektromobilität. October 2017. https://www.press.bmwgroup.com/deutschland/article/detail/T0275547DE/bmw-group-demonstriert-fuehrungsrolle-im-bereich-elektromobilitaet.

[47] BMW Group. Umwelterklärung 2017/2018: Werk Leipzig, 2018. https://www.bmwgroup-werke.com/content/dam/grpw/websites/bmwgroup-werke_com/leipzig/verantwortung/180709_Umwelterklaerung_Werk_Leipzig_2017-2018_final.pdf.

[48] BMW Group. Umwelterklärung BMW Werk München 2017/2018.pdf, 2018. https://www.bmwgroup-werke.com/content/dam/bmw-group-websites/werke_com/muenchen/verantwortung/Umwelterklaerung-2017-2018-BMW-Group-Werk-Muenchen.pdf.

[49] BMW Group. Start für Forschungsprojekt "Bidirektionales Lademanagement - BDL", 2019. https://www.press.bmwgroup.com/deutschland/article/detail/T0302526DE/start-fuer-forschungsprojekt-bidirektionales-lademanagement-bdl?language=de.

[50] Frieder Borggrefe and Ariette Nüßler. Auswirkungen fluktuierender Windverstromung auf Strommärkte und übertragungsnetze. *uwf UmweltWirtschaftsForum*, 17(4):333, November 2009.

[51] Jörg Böttcher and Peter Nagel. *Batteriespeicher: Rechtliche, technische und wirtschaftliche Rahmenbedingungen*. De Gruyter Oldenbourg, Boston/Berlin, 1 edition, February 2018.

[52] Diana Böttger, Mario Götz, Myrto Theofilidi, and Thomas Bruckner. Control power provision with power-to-heat plants in systems with high shares of renewable energy sources – An illustrative analysis for Germany based on the use of electric boilers in district heating grids. *Energy*, 82:157–167, March 2015.

[53] Stefano Bracco, Federico Delfino, Fabio Pampararo, Michela Robba, and Mansueto Rossi. A mathematical model for the optimal operation of the University of Genoa Smart Polygeneration Microgrid: Evaluation of technical, economic and environmental performance indicators. *Energy*, 64:912–922, January 2014.

[54] Fritz Braeuer, Julian Rominger, Russell McKenna, and Wolf Fichtner. Battery storage systems: An economic model-based analysis of parallel revenue streams and general implications for industry. *Applied Energy*, 239:1424–1440, April 2019.

[55] Marlon Alexander Braun. *Scalarized Preferences in Multi-objective Optimization*. PhD Thesis, Karlsruher Institut für Technologie (KIT), 2018.

[56] Sebastian Braun. Hydropower Storage Optimization Considering Spot and Intraday Auction Market. *Energy Procedia*, 87:36–44, January 2016.

[57] Sebastian Braun and Rainer Hoffmann. Intraday Optimization of Pumped Hydro Power Plants in the German Electricity Market. *Energy Procedia*, 87:45–52, January 2016.

[58] Sebastian M. Braun and Christoph Brunner. Price Sensitivity of Hourly Day-ahead and Quarter-hourly Intraday Auctions in Germany. *Zeitschrift für Energiewirtschaft*, 42(3):257–270, September 2018.

[59] Sebastian M. Braun and Michael Burkhardt. Trading of pumped storage hydropower plants on energy only and ancillary services markets. In *2015 International Conference on Renewable Energy Research and Applications (ICRERA)*, pages 649–653, November 2015.

[60] Timo Breithaupt, Thomas Leveringhaus, Torsten Rendel, and Lutz Hofmann. A MILP Approach for the Joint Simulation of Electric Control Reserve and Wholesale Markets. In *Proceedings of the 7th International Conference on Simulation and Modeling Methodologies, Technologies and Applications*, SIMULTECH 2017, pages 314–322, Madrid, Spain, July 2017. SCITEPRESS - Science and Technology Publications, Lda.

[61] Tom Brijs, Daniel Huppmann, Sauleh Siddiqui, and Ronnie Belmans. Auction-based allocation of shared electricity storage resources through physical storage rights. *Journal of Energy Storage*, 7:82–92, August 2016.

[62] Peter Bronski, Jon Creyts, Leia Guccione, Maite Madrazo, James Mandel, Bodhi Rader, Dan Seif, Peter Lilienthal, John Glassmire, Jeffrey Abromowitz, Mark Crowdis, John Richardson, Evan Schmitt, and Helen Tocco. *The Economics of Grid Defection - When and Where Distributed Solar generation plus Storage Competes with Traditional Utility Service*. January 2014.

[63] Thomas Bruckner, Igor Alexeyvich Bashmakov, Yacob Mulugetta, Helena Chum, A. De la Vega Navarro, James Edmonds, A. Faaij, B. Fungtammasan, A. Garg, and E. Hertwich. Energy systems Climate Change 2014: Mitigation of Climate Change. Contribution of Working Group III to the Fifth Assessment Report of the Intergovernmental Panel on Climate Change ed OR Edenhofer et al. *Cambridge and New York*, 2014.

[64] Bernd M. Buchholz. Aktive Energienetze im Kontext der Energiewende. *Anforderungen an künftige Übertragungs-und Verteilungsnetze unter Berücksichtigung von Marktmechanismen. Studie der Energietechnischen Gesellschaft im VDE (ETG). Frankfurt*, 2013.

[65] Bernd M. Buchholz and Zbigniew Styczynski. *Smart Grids – Fundamentals and Technologies in Electricity Networks*. Springer Vieweg, 2014.

[66] Bundesnetzagentur (BNetzA). Monitoringbericht 2017, 2017.

[67] Bundesnetzagentur (BNetzA). Beschluss BK6-17-234, May 2019. www.bundesnetzagentur.de/DE/Service-Funktionen/Beschlusskammern/1_GZ/BK6-GZ/2017/2017_0001bis0999/BK6-17-234/BK6-17-234_-beschluss_2019_05_02.pdf?__blob=publicationFile&v=2.

[68] Bundesnetzagentur (BNetzA). Monitoringbericht 2018, May 2019. https://www.bundesnetzagentur.de/SharedDocs/Mediathek/Monitoringberichte/Monitoringbericht2018.html.

[69] Duncan S. Callaway and Ian A. Hiskens. Achieving Controllability of Electric Loads. *Proceedings of the IEEE*, 99(1):184–199, January 2011.

[70] G. Cardoso, M. Stadler, M. C. Bozchalui, R. Sharma, C. Marnay, A. Barbosa-Póvoa, and P. Ferrão. Optimal investment and scheduling of distributed energy resources with uncertainty in electric vehicle driving schedules. *Energy*, 64:17–30, January 2014.

[71] Miguel Carrion and José M. Arroyo. A computationally efficient mixed-integer linear formulation for the thermal unit commitment problem. *IEEE Transactions on Power Systems*, 21(3):1371–1378, August 2006.

[72] Bo Chai, Alberto Costa, Selin D. Ahipasaoglu, Chau Yuen, and Zaiyue Yang. Optimal Meeting Scheduling in Smart Commercial Building for Energy Cost Reduction. *IEEE Transactions on Smart Grid*, 9(4):3060–3069, July 2018.

[73] Niangjun Chen, Gautam Goel, and Adam Wierman. Smoothed Online Convex Optimization in High Dimensions via Online Balanced Descent. *Conference On Learning Theory*, pages 1574–1594, July 2018.

[74] Yen-Haw Chen, Su-Ying Lu, Yung-Ruei Chang, Ta-Tung Lee, and Ming-Che Hu. Economic analysis and optimal energy management models for microgrid systems: A case study in Taiwan. *Applied Energy*, 103:145–154, March 2013.

[75] Jaephil Cho, Sookyung Jeong, and Youngsik Kim. Commercial and research battery technologies for electrical energy storage applications. *Progress in Energy and Combustion Science*, 48:84–101, June 2015.

[76] Christoph Maurer, Christian Zimmer, and Lion Hirth. Nodale und zonale Strompreissysteme im Vergleich, July 2018.

[77] Felix N. Claessen, Bert Claessens, Maarten. P. F. Hommelberg, Albert Molderink, Vincent Bakker, Hermen. A. Toersche, and Machteld. A. van den Broek. Comparative analysis of tertiary control systems for smart grids using the Flex Street model. *Renewable energy*, 69:260–270, September 2014.

[78] Kristien Clement-Nyns, Edwin Haesen, and Johan Driesen. The Impact of Charging Plug-In Hybrid Electric Vehicles on a Residential Distribution Grid. *IEEE Transactions on Power Systems*, 25(1):371–380, February 2010.

[79] Christopher M. Colson and M. Hashem Nehrir. A review of challenges to real-time power management of microgrids. In *2009 IEEE Power Energy Society General Meeting*, pages 1–8, July 2009.

[80] consentec GmbH. Beschreibung von Regelleistungskonzepten und Regelleistungsmarkt, 2014. https://www.regelleistung.net/ext/download/marktbeschreibung.

[81] consentec GmbH. Description of load-frequency control concept and market for control reserves, February 2014. http://www.consentec.de/wp-content/uploads/2014/08/Consentec_50Hertz_Regelleistungsmarkt_en__20140227.pdf.

[82] consentec GmbH. Verfahren zur dynamischen Bestimmung des Bedarfs für Sekundärregel- und Minutenreserve, July 2018. https://www.regelleistung.net/ext/tender/remark/download/128233055.

[83] consentec GmbH and Frontier Economics Ltd. Gutachten zur regulatorischen Behandlung unterschiedlicher Kostenarten vor dem Hintergrund der ARegV-Novelle für Verteilernetzbetreiber, July 2019. https://www.bundesnetzagentur.de/SharedDocs/Downloads/DE/Sachgebiete/Energie/Unternehmen_-Institutionen/Netzentgelte/Anreizregulierung/Gutachten/Kostenarten.pdf.

[84] Julian de Hoog, Khalid Abdulla, Ramachandra Rao Kolluri, and Paras Karki. Scheduling Fast Local Rule-Based Controllers for Optimal Operation of Energy Storage. *Proceedings of the Ninth International Conference on Future Energy Systems*, pages 168–172, 2018.

[85] Christof Deckmyn, Jan Van de Vyver, Tine L. Vandoorn, Bart Meersman, Jan Desmet, and Lieven Vandevelde. Day-ahead unit commitment model for microgrids. *Transmission Distribution IET Generation*, 11(1):1–9, 2017.

[86] Stephan Dempe and Heiner Schreier. *Operations Research: Deterministische Modelle und Methoden*. Studienbücher Wirtschaftsmathematik. Vieweg+Teubner Verlag, 2006.

[87] Chris J. Dent, Janusz W. Bialek, and Benjamin F. Hobbs. Opportunity Cost Bidding by Wind Generators in Forward Markets: Analytical Results. *IEEE Transactions on Power Systems*, 26(3):1600–1608, August 2011.

[88] Deutsche Energie-Agentur GmbH. dena-Studie Systemdienstleistungen 2030, February 2014. https://www.dena.de/themen-projekte/projekte/energiesysteme/dena-studie-systemdienstleistungen-2030.

[89] Deutscher Bundestag. Gesetz für den Ausbau erneuerbarer Energien (Erneuerbare-Energien-Gesetz - EEG 2014), 2014. http://www.bmwi.de/Redaktion/DE/Downloads/G/gesetz-fuer-den-ausbau-erneuerbarer-energien.html.

[90] Reinhilde D'hulst, Wouter Labeeuw, Bart Beusen, Sven Claessens, Geert Deconinck, and Koen Vanthournout. Demand response flexibility and flexibility potential of residential smart appliances: Experiences from large pilot test in Belgium. *Applied Energy*, 155:79–90, 2015.

[91] Marialaura Di Somma, Giorgio Graditi, Ehsan Heydarian-Forushani, Miadreza Shafie-khah, and Pierluigi Siano. Stochastic optimal scheduling of distributed energy resources with renewables considering economic and environmental aspects. *Renewable Energy*, 116:272–287, February 2018.

[92] Travis S. Dillon, K. W. Edwin, H. Kochs, and R. J. Taud. Integer Programming Approach to the Problem of Optimal Unit Commitment with Probabilistic Reserve Determination. *IEEE Transactions on Power Apparatus and Systems*, PAS-97(6):2154–2166, November 1978.

[93] DIN EN 50160:2011-02. *Merkmale der Spannung in öffentlichen Elektrizitätsversorgungsnetzen*. February 2011.

[94] Dong Ding, Jian Lin Li, Shui Li Yang, Xiao Gang Wu, and Zong Qi Liu. Capacity Configuration of BESS as an Alternative to Coal-Fired Power Units for Frequency Control. *Advanced Materials Research*, 953-954:743–747, 2014.

[95] Yuemin M. Ding, Seung H. Hong, and Xiao H. Li. A Demand Response Energy Management Scheme for Industrial Facilities in Smart Grid. *IEEE Transactions on Industrial Informatics*, 10(4):2257–2269, November 2014.

[96] Wolfgang Domschke, Andreas Drexl, Robert Klein, and Armin Scholl. *Einführung in Operations Research*. Gabler Verlag, 9 edition, 2015.

[97] Stefan Döring. Zusammensetzung des Strompreises und dessen Entwicklung. In Stefan Döring, editor, *Energieerzeugung nach Novellierung des EEG: Konsequenzen für regenerative und nicht regenerative Energieerzeugungsanlagen*, pages 27–47. Springer Berlin Heidelberg, Berlin, Heidelberg, 2015.

[98] Patrick Dossow and Serafin von Roon. Merit Order der konventionellen Kraftwerke in Deutschland (2018), 2019.

[99] Daniel H. Doughty, Paul C. Butler, Abbas A. Akhil, Nancy H. Clark, and John D. Boyes. Batteries for Large-Scale Stationary Electrical Energy Storage. *The Electrochemical Society Interface*, 19(3):49–53, January 2010.

[100] Energietechnischen Gesellschaft im VDE. *Batteriespeicher in der Nieder- und Mittelspannungsebene*. 2015. https://www.vde.com/de/etg/publikationen/studien/vde-studie-powertoheat.

[101] Daniel Engelbrecht. Engpassmanagement und Redispatch mit Anlagen im Verteilnetz, September 2017.

[102] Stefan Englberger, Holger Hesse, Nina Hanselmann, and Andreas Jossen. SimSES Multi-Use: A simulation tool for multiple storage system applications. In *2019 16th International Conference on the European Energy Market (EEM)*, pages 1–5, September 2019. ISSN: 2165-4093.

[103] ENTSO-E. Network Code on Load-Frequency Control and Reserves. June 2013. https://www.acer.europa.eu/Official_documents/Acts_of_the_-Agency/Annexes/The%20Network%20Code%20on%20Load-Frequency%20Control%20and%20Reserves%20submitted%

[104] ENTSO-E. Consultation Report "FCR Cooperation", May 2017. https://www.entsoe.eu/network_-codes/eb/fcr.

[105] ENTSO-E. Capacity Calculation: Risks linked to a pan-European threshold- Focus on CACM implementation & more transparency, 2018. https://www.entsoe.eu/news/2018/07/05/capacity-calculation-risks-linked-to-a-pan-european-threshold-focus-on-cacm-implementation-more-transparency.

[106] EPEX SPOT SE. Day-Ahead-Auktion, 2017. http://www.epexspot.com/de/produkte/auktionshandel/deutschland-oesterreich.

[107] EPEX SPOT SE. Epex Spot Operational Rules, 2018. https://www.epexspot.com/document/39298/EPEX%20SPOT%20Market%.zip.

[108] EPEX SPOT SE. Kontinuierlicher Intraday-Markt, 2018. https://www.epexspot.com/de/produkte/intradaycontinuous/deutschland

[109] EPEX SPOT SE. Nominale volumengewichtete Durchschnittspreise, 2018. https://www.epexspot.com/en/market-data/market_data_offers.

[110] EURELECTRIC. Flexibility and Aggregation: Requirements for their interaction in the market. *Eurelectric: Brussels, Belgium*, 2014. https://www.usef.energy/app/uploads/2016/12/EURELECTRIC-Flexibility-and-Aggregation-jan-2014.pdf.

[111] European Parliament. Directive (EU) 2019/944 of the European Parliament and of the Council of 5 June 2019 on common rules for the internal market for electricity and amending Directive 2012/27/EU (Text with EEA relevance.), June 2019.

[112] Farnaz Farzan, Mohsen A. Jafari, Ralph Masiello, and Yan Lu. Toward Optimal Day-Ahead Scheduling and Operation Control of Microgrids Under Uncertainty. *IEEE Transactions on Smart Grid*, 6(2):499–507, March 2015.

[113] Federal Ministry for Economics Affairs and Energy. Moderne Verteilernetze für Deutschland, 2014. https://www.bmwi.de/Redaktion/DE/Publikationen/Studien/verteilernetzstudie.pdf?__blob=publicationFile&v=5.

[114] Federal Ministry for Economics Affairs and Energy. Ein Strommarkt für die Energiewende - Ergebnispapier des Bundesministeriums für Wirtschaft und Energie (Weißbuch), July 2015. https://www.bmwi.de/Redaktion/DE/Publikationen/Energie/weissbuch.html.

[115] Federal Ministry for Economics Affairs and Energy. Verordnungspaket Intelligente Netze, February 2015. https://www.bmwi.de/Redaktion/DE/Downloads/E/eckpunkte-fuer-das-verordnungspaket-intelligente-netze.pdf?__blob=publicationFile&v=1.

[116] Federal Ministry for Economics Affairs and Energy. Gesetz zur Beschleunigung des Energieleitungsausbaus, December 2018. https://www.bmwi.de/Redaktion/DE/Artikel/Service/Gesetzesvorhaben/gesetz-zur-beschleunigung-des-energieleitungsausbaus.html.

[117] Federal Ministry for Economics Affairs and Energy. Competition and Regulation, 2019. https://www.bmwi.de/Redaktion/EN/Textsammlungen/Energy/comtetition-and-regualtion.html?cms_artId=255910.

[118] Federal Ministry for Economics Affairs and Energy. EEG-Umlage 2020: Fakten & Hintergründe, October 2019. https://www.bmwi.de/Redaktion/DE/Downloads/XYZ/zahlen-fakten-eeg.pdf?__blob=publicationFile&v=4.

[119] Federal Ministry for Economics Affairs and Energy. Kapazitätsreserveverordnung, February 2019. https://www.bmwi.de/Redaktion/DE/Artikel/Service/Gesetzesvorhaben/kapazitaetsreserveverordnung.html.

[120] Federal Ministry for Economics Affairs and Energy. State-imposed components of the electricity price, 2019. https://www.bmwi.de/Redaktion/EN/Artikel/Energy/electircity-price-components-state-imposed.html.

[121] Federal Ministry for the Environment, Nature Conservation and Nuclear Safety. Klimaschutz in Zahlen, May 2018. https://www.bmu.de/fileadmin/Daten_BMU/Pools/Broschueren/klimaschutz_in_zahlen_2018_-bf.pdf.

[122] Federal Ministry of Justice and Consumer Protection. § 19 Sonderformen der Netznutzung, StromNEV, 2012. https://www.gesetze-im-internet.de/stromnev/__19.html.

[123] Federal Ministry of Justice and Consumer Protection. § 61e, EEG 2017, 2017. https://www.gesetze-im-internet.de/eeg_2014/__61e.html.

[124] J. Fedjaev, S. A. Amamra, and B. Francois. Linear programming based optimization tool for day ahead energy management of a lithium-ion battery for an industrial microgrid. In *2016 IEEE International Power Electronics and Motion Control Conference (PEMC)*, pages 406–411, September 2016.

[125] Baptiste Feron and Antonello Monti. Domestic Battery and Power-to-Heat Storage for Self-Consumption and Provision of Primary Control Reserve. *2018 Power Systems Computation Conference (PSCC)*, pages 1–6, June 2018.

[126] Fingrid. Determining the transmission capacities, 2018. https://www.fingrid.fi/en/electricity-market/cross-border-transmission/determining-the-transmission-capacities.

[127] Marco Giacomo Flammini, Giuseppe Prettico, Andreea Julea, Gianluca Fulli, Andrea Mazza, and Gianfranco Chicco. Statistical characterisation of the real transaction data gathered from electric vehicle charging stations. *Electric Power Systems Research*, 166:136–150, January 2019.

[128] Johannes Fleer and Peter Stenzel. Impact analysis of different operation strategies for battery energy storage systems providing primary control reserve. *Energy Storage*, 8:320–338, November 2016.

[129] FNN Forum Netztechnik/ Netzbetrieb im VDE. Technische Anforderungen an die automatische Frequenzentlastung, June 2012. https://www.vde.com/resource/blob/824818/f74bd2fc3d1ca4abcc7937927fb905d6/fnn-th-lastabwurf-2012-07-05-data.pdf.

[130] FNN Forum Netztechnik/ Netzbetrieb im VDE. FNN-Studie: Statische Spannungshaltung, 2015. https://www.vde.com/resource/blob/775184/e32178f5639afae93a835042c1f59445/vde-fnn-studie-statische-spannungshaltung-kurz-gefasst-pdf-data.pdf.

[131] Fraunhofer ISE. Net public electricity generation in Germany in 2019, 2020. https://www.energy-charts.de/energy_pie.htm?year=2019.

[132] Nele Friedrichsen. Verbrauchssteuerung. In Martin Wietschel, Sandra Ullrich, Peter Markewitz, Friedrich Schulte, and Fabio Genoese, editors, *Energietechnologien der Zukunft: Erzeugung, Speicherung, Effizienz und Netze*, pages 417–443. Springer Fachmedien, Wiesbaden, 2015.

[133] Alexander Funke, Jens Berger, and Julian Rominger. System for Reducing Load Peaks in an Electrical System, January 2019.

[134] Matthias D. Galus, Stephan Koch, and Göran Andersson. Provision of Load Frequency Control by PHEVs, Controllable Loads, and a Cogeneration Unit. *IEEE Transactions on Industrial Electronics*, 58(10):4568–4582, October 2011.

[135] Carlos Gamarra and Josep M. Guerrero. Computational optimization techniques applied to microgrids planning: A review. *Renewable and Sustainable Energy Reviews*, 48:413–424, August 2015.

[136] Satoshi Gamou, Ryohei Yokoyama, and Koichi Ito. Optimal unit sizing of cogeneration systems in consideration of uncertain energy demands as continuous random variables. *Energy Conversion and Management*, 43(9):1349–1361, June 2002.

[137] Jesse M. Gantz, S. Massoud Amin, and Anthony M. Giacomoni. Optimal Capacity Partitioning of Multi-Use Customer-Premise Energy Storage Systems. *IEEE Transactions on Smart Grid*, 5(3):1292–1299, May 2014.

[138] Javier García-González, Ernesto Parrilla, and Alicia Mateo. Risk-averse profit-based optimal scheduling of a hydro-chain in the day-ahead electricity market. *European Journal of Operational Research*, 181(3):1354–1369, September 2007.

[139] Erik Gawel and Alexandra Purkus. Die Marktprämie im EEG 2012: Ein sinnvoller Beitrag zur Markt- und Systemintegration erneuerbarer Energien? *Zeitschrift für Energiewirtschaft*, 37(1):43–61, March 2013.

[140] Linas Gelazanskas and Kelum A. A. Gamage. Demand side management in smart grid: A review and proposals for future direction. *Sustainable Cities and Society*, 11:22–30, February 2014.

[141] Clark W. Gellings. The concept of demand-side management for electric utilities. *Proceedings of the IEEE*, 73(10):1468–1470, October 1985.

[142] Michel Gendreau and Jean-Yves Potvin. *Handbook of metaheuristics*, volume 2. Springer, 2010.

[143] German Environment Agency. Umweltbundesamt - Indicator: Greenhouse gas emissions, March 2020. https://www.umweltbundesamt.de/en/indicator-greenhouse-gas-emissions.

[144] Marte K. Gerritsma, Tarek A. AlSkaif, Henk A. Fidder, and Wilfried G. J. H. M. van Sark. Flexibility of Electric Vehicle Demand: Analysis of Measured Charging Data and Simulation for the Future. *World Electric Vehicle Journal*, 10(1):14, March 2019.

[145] M. Giuntoli and D. Poli. Optimized Thermal and Electrical Scheduling of a Large Scale Virtual Power Plant in the Presence of Energy Storages. *IEEE Transactions on Smart Grid*, 4(2):942–955, June 2013.

[146] Christoph Goebel and Hans-Arno Jacobsen. Aggregator-Controlled EV Charging in Pay-as-Bid Reserve Markets With Strict Delivery Constraints. *IEEE Transactions on Power Systems*, 31(6):4447–4461, November 2016.

[147] Christoph Goebel and Hans-Arno Jacobsen. Bringing Distributed Energy Storage to Market. *IEEE Transactions on Power Systems*, 31(1):173–186, January 2016.

[148] Andreas Goldthau. Rethinking the governance of energy infrastructure: Scale, decentralization and polycentrism. *Energy Research & Social Science*, 1:134–140, March 2014.

[149] Pablo González, José Villar, Cristian A. Díaz, and Fco Alberto Campos. Joint energy and reserve markets: Current implementations and modeling trends. *Electric Power Systems Research*, 109:101–111, April 2014.

[150] Sebastian Gottwalt, Johannes Gärttner, Hartmut Schmeck, and Christoph Weinhardt. Modeling and Valuation of Residential Demand Flexibility for Renewable Energy Integration. *IEEE Transactions on Smart Grid*, 8(6):2565–2574, November 2017.

[151] Dietmar Richard Graeber. *Handel mit Strom aus erneuerbaren Energien*. Springer, 2014.

[152] Eric Granryd, Ingvar Ekroth, Per Lundqvist, Ake Melider, Bjorn Palm, and Peter Rohlin. *Refrigeration Engineering*. 2011.

[153] Sebastian Groß. *Untersuchung der Speicherfähigkeit von Fernwärmenetzen und deren Auswirkungen auf die Einsatzplanung von Wärmeerzeugern*. PhD thesis, Technische Universität Dresden, March 2013.

[154] Anna Gruber, Serafin Von Roon, and Steffen Fattler. *Wissenschaftliche Projektbegleitung des Projektes DSM Bayern*. 2016.

[155] Josep M. Guerrero, Mukul Chandorkar, Tzung-Lin Lee, and Poh Chiang Loh. Advanced Control Architectures for Intelligent Microgrids—Part I: Decentralized and Hierarchical Control. *IEEE Transactions on Industrial Electronics*, 60(4):1254–1262, April 2013. Conference Name: IEEE Transactions on Industrial Electronics.

[156] Gurobi. MPS format. https://www.gurobi.com/documentation.

[157] Guillermo Gutiérrez-Alcaraz, Eric Galván, Nestor González-Cabrera, and Mohammad S. Javadi. Renewable energy resources short-term scheduling and dynamic network reconfiguration for sustainable energy consumption. *Renewable and Sustainable Energy Reviews*, 52:256–264, December 2015.

[158] Juha Haakana, Ville Tikka, Jukka Lassila, and Jarmo Partanen. Methodology to analyze combined heat and power plant operation considering electricity reserve market opportunities. *Energy*, 127:408–418, May 2017.

[159] Juha Haakana, Ville Tikka, Jukka Lassila, Jarmo Partanen, and Samuli Rinne. Opportunities of bioenergy-based CHP production in balancing renewable power production. *2016 13th International Conference on the European Energy Market (EEM)*, pages 1–5, June 2016.

[160] David Haberschusz, Monika Kwiecien, Julia Badeda, Dominik Schulte, and Florian Jöris. *Zwischenbericht Projekt BSMS*. September 2016.

[161] Simon Hagemann. Price Determinants in the German Intraday Market for Electricity: An Empirical Analysis. October 2013.

[162] S. M. Hakimi and S. M. Moghaddas-Tafreshi. Optimal Planning of a Smart Microgrid Including Demand Response and Intermittent Renewable Energy Resources. *IEEE Transactions on Smart Grid*, 5(6):2889–2900, November 2014.

[163] Junqiao Han and Mary Piette. Solutions for summer electric power shortages: Demand response and its application in air conditioning and refrigerating systems. *Refrigeration, Air Conditioning, & Electric Power Machinery*, 29(1):1–4, 2008.

[164] Sekyung Han, Soohee Han, and Kaoru Sezaki. Development of an Optimal Vehicle-to-Grid Aggregator for Frequency Regulation. *IEEE Transactions on Smart Grid*, 1(1):65–72, June 2010.

[165] He Hao, Anupama Kowli, Yashen Lin, Prabir Barooah, and Sean Meyn. Ancillary service for the grid via control of commercial building HVAC systems. *2013 American Control Conference*, pages 467–472, June 2013.

[166] He Hao, Borhan M. Sanandaji, Kameshwar Poolla, and Tyrone L. Vincent. Aggregate Flexibility of Thermostatically Controlled Loads. *IEEE Transactions on Power Systems*, 30(1):189–198, January 2015.

[167] He Hao, Abhishek Somani, Jianming Lian, and Thomas E. Carroll. Generalized aggregation and coordination of residential loads in a smart community. *2015 IEEE International Conference on Smart Grid Communications (SmartGridComm)*, pages 67–72, November 2015.

[168] He Hao, Di Wu, Jianming Lian, and Tao Yang. Optimal Coordination of Building Loads and Energy Storage for Power Grid and End User Services. *IEEE Transactions on Smart Grid*, 9(5):4335–4345, September 2018.

[169] Niklas Hartmann, Noha Saad Hussein, Michael Taumann, Verena Jülch, and Thomas Schlegl. Stromerzeugung aus Windenergie. In Martin Wietschel, Sandra Ullrich, Peter Markewitz, Friedrich Schulte, and Fabio Genoese, editors, *Energietechnologien der Zukunft: Erzeugung, Speicherung, Effizienz und Netze*, pages 103–122. Springer Fachmedien Wiesbaden, Wiesbaden, 2015.

[170] Niklas Hartmann, Jessica Thomsen, and Natapon Wanapinit. Using demand side management and CHP in renewable dominated decentral energy systems: a case study. *Computer Science - Research and Development*, 33(1):193–198, February 2018.

[171] Md Umar Hashmi, Wael Labidi, Ana Bušić, Salah-Eddine Elayoubi, and Tijani Chahed. Long-Term Revenue Estimation for Battery Performing Arbitrage and Ancillary Services. In *2018 IEEE International Conference on Communications, Control, and Computing Technologies for Smart Grids (SmartGridComm)*, pages 1–7, October 2018.

[172] A. D. Hawkes and M. A. Leach. Modelling high level system design and unit commitment for a microgrid. *Applied Energy*, 86(7):1253–1265, July 2009.

[173] Xian He, Erik Delarue, William D'haeseleer, and Jean-Michel Glachant. A novel business model for aggregating the values of electricity storage. *Energy Policy*, 39(3):1575–1585, March 2011.

[174] Xian He, Raphael Lecomte, Andrei Nekrassov, Erik Delarue, and Eric Mercier. Compressed air energy storage multi-stream value assessment on the french energy market. *2011 IEEE Trondheim PowerTech*, pages 1–6, June 2011.

[175] Rasmus Elbæk Hedegaard, Theis Heidmann Pedersen, and Steffen Petersen. Multi-market demand response using economic model predictive control of space heating in residential buildings. *Energy and Buildings*, 150:253–261, September 2017.

[176] Stefan Henninger, Markus Schroeder, and Johann Jaeger. Combining Frequency Containment Reserves and Renewable Power Leveling in Energy Storage Systems. *Energy Procedia*, 99(Supplement C):147–156, November 2016.

[177] Wilfried Hennings and Jochen Linssen. Elektromobilität. In Martin Wietschel, Sandra Ullrich, Peter Markewitz, Friedrich Schulte, and Fabio Genoese, editors, *Energietechnologien der Zukunft: Erzeugung, Speicherung, Effizienz und Netze*, pages 447–473. Springer Fachmedien Wiesbaden, Wiesbaden, 2015.

[178] Carlos A. Hernandez-Aramburo, Tim C. Green, and Nicolas Mugniot. Fuel consumption minimization of a microgrid. *IEEE Transactions on Industry Applications*, 41(3):673–681, May 2005.

[179] Holger C. Hesse, Michael Schimpe, Daniel Kucevic, and Andreas Jossen. Lithium-Ion Battery Storage for the Grid—A Review of Stationary Battery Storage System Design Tailored for Applications in Modern Power Grids. *Energies*, 10(12):2107, December 2017.

[180] Caroline Hirsch. Bewertung von Methoden zur Lastprognose für eine industrielle Liegenschaft im Automobilsektor, Master Thesis, supervised by Julian Rominger. *Institute of Applied Informatics and Formal Description Methods, Karlsruhe Institute of Technology*, October 2017.

[181] Lion Hirth. Die Inc-Dec-Strategie, September 2019.

[182] Lion Hirth and Inka Ziegenhagen. Balancing power and variable renewables: Three links. *Renewable and Sustainable Energy Reviews*, 50:1035–1051, October 2015.

[183] Wai Shin Ho, Sandro Macchietto, Jeng Shiun Lim, Haslenda Hashim, Zarina Ab. Muis, and Wen Hui Liu. Optimal scheduling of energy storage for renewable energy distributed energy generation system. *Renewable and Sustainable Energy Reviews*, 58:1100–1107, May 2016.

[184] Raphael Hollinger, Luis M. Diazgranados, Felix Braam, Thomas Erge, Georg Bopp, and Bernd Engel. Distributed solar battery systems providing primary control reserve. *IET Renewable Power Generation*, 10(1):63–70, 2016.

[185] Raphael Hollinger, Luis M. Diazgranados, Christof Wittwer, and Bernd Engel. Optimal Provision of Primary Frequency Control with Battery Systems by Exploiting All Degrees of Freedom within Regulation. *Energy Procedia*, 99(Supplement C):204–214, November 2016.

[186] S. Horii, Kyoko Ito, and Yoshikazu Suzuki. A computer-aided planning (CAP) system for the gas engine co-generation plant. *International Journal of Energy Research*, 11(4):491–505, October 1987.

[187] Hanspeter Höschle. *Capacity Mechanisms in Future Electricity Markets*. PhD thesis, KU Leuven, 2018.

[188] Wuhua Hu, Ping Wang, and Hoay Beng Gooi. Assessing the economics of customer-sited multi-use energy storage. In *2016 IEEE Region 10 Conference (TENCON)*, pages 651–654, November 2016. ISSN: 2159-3450.

[189] Wei Huang, Miao Lu, and Li Zhang. Survey on Microgrid Control Strategies. *Energy Procedia*, 12:206–212, January 2011.

[190] Institut für Stromrichtertechnik und Elektrische Antriebe - RWTH Aachen. *Wissenschaftliches Mess- und Evaluierungsprogramm Solarstromspeicher 2.0 - Jahresbericht 2018*. 2018.

[191] International Electrotechnical Commission. IEC 61851–1 - Electric vehicle conductive charging system – Part 1: General requirements., 2010.

[192] International Energy Agency. Germany 2020 - Energy Policy Review, 2020. https://www.bmwi.de/Redaktion/DE/Downloads/G/germany-2020-energy-policy-review.pdf?__-blob=publicationFile&v=4.

[193] International Renewable Energy Agency (IRENA). Electricity storage and renewables: Costs and markets to 2030, 2017. http://www.irena.org/-/media/Files/IRENA/Agency/Publication/2017/Oct/IRENA_Electricity_Storage_Costs_2017_Summary.pdf?la=en&hash=2FDC44939920F8D2BA29CB762C607BC9E882D4E9.

[194] Koichi Ito, Ryohei Yokoyama, and T. Shiba. Optimal Operation of a Diesel Engine Cogeneration Plant Including a Heat Storage Tank. *Journal of Engineering for Gas Turbines and Power*, 114(4):687–694, October 1992.

[195] Hussein Jumma Jabir, Jiashen Teh, Dahaman Ishak, and Hamza Abunima. Impacts of Demand-Side Management on Electrical Power Systems: A Review. *Energies*, 11(5):1050, May 2018.

[196] Jenbacher. Jenbacher Baureihe 6, 2019. https://www.energas-gmbh.de/wp-content/uploads/2019/05/INNIO_BR_T6_Update_A4_DE_2019_Screen.pdf.

[197] Ping Ji, Xiao Xin Zhou, and ShouYuan Wu. Review on sustainable development of island microgrid. In *2011 International Conference on Advanced Power System Automation and Protection*, volume 3, pages 1806–1813, October 2011.

[198] Linni Jian, Yanchong Zheng, Xinping Xiao, and C. C. Chan. Optimal scheduling for vehicle-to-grid operation with stochastic connection of plug-in electric vehicles to smart grid. *Applied Energy*, 146:150–161, May 2015.

[199] A. Jindal, N. Kumar, and J. J. P. C. Rodrigues. A Heuristic-Based Smart HVAC Energy Management Scheme for University Buildings. *IEEE Transactions on Industrial Informatics*, 14(11):5074–5086, November 2018.

[200] Patrick Jochem, Thomas Kaschub, and Wolf Fichtner. How to Integrate Electric Vehicles in the Future Energy System? In Michael Hülsmann and Dirk Fornahl, editors, *Evolutionary Paths Towards the Mobility Patterns of the Future*, Lecture Notes in Mobility, pages 243–263. Springer, Berlin, Heidelberg, 2014.

[201] Patrick Jochem, Thomas Kaschub, Alexandra-Gwyn Paetz, and Wolf Fichtner. Integrating Electric Vehicles into the German Electricity Grid – an Interdisciplinary Analysis. *World Electric Vehicle Journal*, 5(3):763–770, September 2012.

[202] Patrick Jochem, Martin Schönfelder, and Wolf Fichtner. An efficient two-stage algorithm for decentralized scheduling of micro-CHP units. *European Journal of Operational Research*, 245(3):862–874, September 2015.

[203] Lewis Johnston, Francisco Díaz-González, Oriol Gomis-Bellmunt, Cristina Corchero-García, and Miguel Cruz-Zambrano. Methodology for the economic optimisation of energy storage systems for frequency support in wind power plants. *Applied Energy*, 137:660–669, January 2015.

[204] Julien Jomaux, Thomas Mercier, and Emmanuel De Jaeger. Provision of frequency containment reserves with batteries and power-to-heat. *2017 IEEE Manchester PowerTech*, pages 1–6, June 2017.

[205] Ami Joseph and Mohammad Shahidehpour. Battery storage systems in electric power systems. *2006 IEEE Power Engineering Society General Meeting*, June 2006.

[206] Marc Jüdes, Stefan Vigerske, and George Tsatsaronis. Optimization of the Design and Partial-Load Operation of Power Plants Using Mixed-Integer Nonlinear Programming. In Josef Kallrath, Panos M. Pardalos, Steffen Rebennack, and Max Scheidt, editors, *Optimization in the Energy Industry*, Energy Systems, pages 193–220. Springer Berlin Heidelberg, Berlin, Heidelberg, 2009.

[207] Sebastian Just. The German Market for System Reserve Capacity and Balancing. *EWL Working Paper*, 6(2015), September 2015.

[208] Sebastian Just and Christoph Weber. Pricing of reserves: Valuing system reserve capacity against spot prices in electricity markets. *Energy Economics*, 30(6):3198–3221, November 2008.

[209] Josef Kallrath. *Gemischt-ganzzahlige Optimierung: Modellierung in der Praxis: Mit Fallstudien aus Chemie, Energiewirtschaft, Papierindustrie, Metallgewerbe, Produktion und Logistik*. Springer Vieweg, 2 edition, 2013.

[210] Hamidreza Kamankesh, Vassilios G. Agelidis, and Abdollah Kavousi-Fard. Optimal scheduling of renewable micro-grids considering plug-in hybrid electric vehicle charging demand. *Energy*, 100:285–297, April 2016.

[211] Fatih Karanfil and Yuanjing Li. The Role of Continuous Intraday Electricity Markets: The Integration of Large-Share Wind Power Generation in Denmark. *Energy Journal*, 38(2):107–130, March 2017.

[212] Thomas Kaschub. Batteriespeicher in Haushalten unter Berücksichtigung von Photovoltaik, Elektrofahrzeugen und Nachfragesteuerung. 2017.

[213] Thomas Kaschub, Patrick Jochem, and Wolf Fichtner. Solar energy storage in German households: profitability, load changes and flexibility. *Energy Policy*, 98:520–532, November 2016.

[214] Faridaddin Katiraei, Mohammad Reza Iravani, and Peter W. Lehn. Micro-grid autonomous operation during and subsequent to islanding process. *IEEE Transactions on Power Delivery*, 20(1):248–257, January 2005.

[215] Genku Kayo, Ala Hasan, and Kai Siren. Energy sharing and matching in different combinations of buildings, CHP capacities and operation strategy. *Energy and Buildings*, 82:685–695, October 2014.

[216] S. Jalal Kazempour, M. Parsa Moghaddam, M. R. Haghifam, and G. Reza Yousefi. Risk-constrained dynamic self-scheduling of a pumped-storage plant in the energy and ancillary service markets. *Energy Conversion and Management*, 50(5):1368–1375, May 2009.

[217] Wolfgang Kempkens. Allgäuer Hybridkraftwerk mit der Lizenz zu regeln, June 2019.

[218] Cornelia Kermel and Jan Dinter. Gesetz zur Digitalisierung der Energiewende: Das Messstellenbetriebsgesetz im überblick. *Recht der Energiewirtschaft*, 95(4-5):158–164, April 2016. Publisher: Wolters Kluwer Deutschland Section: Recht der Energiewirtschaft.

[219] Kashif Hesham Khan, Caspar Ryan, and Ermyas Abebe. Day Ahead Scheduling to Optimize Industrial HVAC Energy Cost Based ON Peak/OFF-Peak Tariff and Weather Forecasting. 5:21684–21693, 2017.

[220] Mariam Khattabi, Andreas Kießling, and Jan Ringelstein. A novel agent based system architecture for smart grids including market and grid aspects. *2011 IEEE Power and Energy Society General Meeting*, pages 1–8, July 2011.

[221] Mohammad E. Khodayar, Mohammad Shahidehpour, and Lei Wu. Enhancing the Dispatchability of Variable Wind Generation by Coordination With Pumped-Storage Hydro Units in Stochastic Power Systems. *IEEE Transactions on Power Systems*, 28(3):2808–2818, August 2013. Conference Name: IEEE Transactions on Power Systems.

[222] Il-Song Kim. The novel state of charge estimation method for lithium battery using sliding mode observer. *Journal of Power Sources*, 163(1):584–590, December 2006.

[223] Ki Hong Kim, Young Jae Han, Sugil Lee, Sung Won Cho, and Chulung Lee. Text Mining for Patent Analysis to Forecast Emerging Technologies in Wireless Power Transfer. *Sustainability*, 11(22):6240, January 2019.

[224] Young-Jin Kim, Leslie K. Norford, and James L. Kirtley. Modeling and Analysis of a Variable Speed Heat Pump for Frequency Regulation Through Direct Load Control. *IEEE Transactions on Power Systems*, 30(1):397–408, January 2015.

[225] Sebastian Kochanneck. *Systemdienstleistungserbringung durch intelligente Gebäude*. PhD Thesis, Karlsruher Institut für Technologie (KIT), 2019.

[226] Michael Koller, Theodor Borsche, Andreas Ulbig, and Göran Andersson. Review of grid applications with the Zurich 1MW battery energy storage system. *Electric Power Systems Research*, 120:128–135, March 2015.

[227] Lukas König, Friederike Pfeiffer-Bohnen, and Hartmut Schmeck. *Theoretische Informatik - ganz praktisch*. De Gruyter Oldenbourg, Berlin, Boston, 2016.

[228] Marcel Konstantinov. Identifizierung und Evaluation von Anwendungen gewerblicher Vanadium Redox-Flow-Batteriespeicher in internationalen Märkten, Master Thesis, supervised by Julian Rominger. *Institute of Applied Informatics and Formal Description Methods, Karlsruhe Institute of Technology*, 2018.

[229] Katrin Köper. Detailanalyse des kontinuierlichen Intradayhandels insbesondere hinsichtlich des Erlöspotentials von Flexibilitätsoptionen, Master Thesis, supervised by Julian Rominger. *Institute of Applied Informatics and Formal Description Methods, Karlsruhe Institute of Technology*, 2018.

[230] Emil Kraft, Julian Rominger, Vincent Mohiuddin, and Dogan Keles. Forecasting of Frequency Containment Reserve Prices Using Econometric and Artificial Intelligence Approaches [in press]. *11. Internationale Energiewirtschaftstagung an der TU Wien, Vienna, Austria, 13. - 15. Februar 2019*, 2019.

[231] Sophia Kraft. Smart Markets für regionale Systemdienstleistungen: Entwicklung eines Marktdesigns, September 2017.

[232] Philipp Kuhn. Mathematische Optimierungsstrategien zur kurzfristigen Kraftwerkseinsatzplanung, Diplomarbeit am Lehrstuhl für Energiewirtschaft und Anwendungstechnik der Technischen Universität München, München. 2005.

[233] Philipp Kuhn. *Iteratives Modell zur Optimierung von Speicherausbau und-betrieb in einem Stromsystem mit zunehmend fluktuierender Erzeugung*. PhD thesis, Technische Universität München (TUM), 2012.

[234] P. Kundur, J. Paserba, V. Ajjarapu, G. Andersson, A. Bose, C. Canizares, N. Hatziargyriou, D. Hill, A. Stankovic, C. Taylor, T. Van Cutsem, and V. Vittal. Definition and classification of power system stability IEEE/CIGRE joint task force on stability terms and definitions. *IEEE Transactions on Power Systems*, 19(3):1387–1401, August 2004. Conference Name: IEEE Transactions on Power Systems.

[235] H. J. Kunisch, Kevin G. Kramer, and H. Dominik. Battery Energy Storage Another Option for Load-Frequency-Control and Instantaneous Reserve. *IEEE Transactions on Energy Conversion*, EC-1(3):41–46, September 1986.

[236] Friedrich Kunz. Improving Congestion Management: How to Facilitate the Integration of Renewable Generation in Germany. *The Energy Journal*, 34(4):55–78, 2013.

[237] Andrew Kusiak and Guanglin Xu. Modeling and optimization of HVAC systems using a dynamic neural network. *Energy*, 42(1):241–250, June 2012.

[238] S. Lee, S. Iyengar, D. Irwin, and P. Shenoy. Shared solar-powered EV charging stations: Feasibility and benefits. *2016 Seventh International Green and Sustainable Computing Conference (IGSC)*, pages 1–8, November 2016.

[239] Young M. Lee, Raya Horesh, and Leo Liberti. Optimal HVAC Control as Demand Response with On-site Energy Storage and Generation System. *Energy Procedia*, 78:2106–2111, November 2015.

[240] Bo Lei, Xin Ran Li, Ji Yuan Huang, and Shao Jie Tan. Droop Configuration and Operational Mode Setting of Battery Energy Storage System in Primary Frequency Regulation. *Applied Mechanics and Materials*, 448-453:2235–2238, 2014.

[241] Elisabeth Lemaire, Nicolas Martin, Per Nørg\a ard, Erik de Jong, Roald de Graaf, Jasper Groenewegen, Efstathia Kolentini, and Stathis Tselepis. *European white book on grid-connected storage*. 2011.

[242] Han Li, Abinet Tesfaye Eseye, Jianhua Zhang, and Dehua Zheng. Optimal energy management for industrial microgrids with high-penetration renewables. *Protection and Control of Modern Power Systems*, 2(1):12, April 2017.

[243] Yashen Lin, Prabir Barooah, Sean Meyn, and Timothy Middelkoop. Experimental Evaluation of Frequency Regulation From Commercial Building HVAC Systems. *IEEE Transactions on Smart Grid*, 6(2):776–783, March 2015. Conference Name: IEEE Transactions on Smart Grid.

[244] Da Liu, Guowei Zhang, Baohua Huang, and Weiwei Liu. Optimum Electric Boiler Capacity Configuration in a Regional Power Grid for a Wind Power Accommodation Scenario. *Energies*, 9(3):144, March 2016.

[245] Guodong Liu, Michael Starke, Bailu Xiao, and Kevin Tomsovic. Robust optimisation-based microgrid scheduling with islanding constraints. *Transmission Distribution IET Generation*, 11(7):1820–1828, 2017. Conference Name: Transmission Distribution IET Generation.

[246] Guodong Liu, Yan Xu, and Kevin Tomsovic. Bidding strategy for microgrid in day-ahead market based on hybrid stochastic/robust optimization. *IEEE Transactions on Smart Grid*, 7(1), January 2016.

[247] Liansheng Liu, Fanxin Kong, Xue Liu, Yu Peng, and Qinglong Wang. A review on electric vehicles interacting with renewable energy in smart grid. *Renewable and Sustainable Energy Reviews*, 51:648–661, November 2015.

[248] João A. Peças Lopes, Filipe Joel Soares, and Pedro M. Rocha Almeida. Integration of Electric Vehicles in the Electric Power System. *Proceedings of the IEEE*, 99(1):168–183, January 2011. Conference Name: Proceedings of the IEEE.

[249] Manuel Lösch. *Utilization of Electric Prosumer Flexibilities at Electricity and Reserve Markets [to be published]*. PhD thesis, Karlsruhe Institut für Technologie (KIT), Karlsruhe.

[250] Manuel Lösch. Sekundärregelleistung: Preise, Abrufcharakteristika & Nachholmanagement für alternative SRL-Erbringer, June 2017.

[251] Manuel Lösch, Julian Rominger, Sandeep Nainappagari, and Hartmut Schmeck. Optimizing Bidding Strategies for the German Secondary Control Reserve Market: The Impact of Energy Prices. *2018 15th International Conference on the European Energy Market (EEM)*, pages 1–5, 2018.

[252] N. Lu. An Evaluation of the HVAC Load Potential for Providing Load Balancing Service. *IEEE Transactions on Smart Grid*, 3(3):1263–1270, September 2012.

[253] N. Lu and Y. Zhang. Design Considerations of a Centralized Load Controller Using Thermostatically Controlled Appliances for Continuous Regulation Reserves. *IEEE Transactions on Smart Grid*, 4(2):914–921, June 2013.

[254] Patrick Ludwig. Entwicklung eines Nachlademanagements für einen stationären Batteriespeicher zur Regelleistungserbringung mittels flexibler Erzeuger und Verbraucher. November 2017.

[255] Chenjie Ma, Juha Rautiainen, Dirk Dahlhaus, Akhilesh Lakshman, J. Christian Toebermann, and Martin Braun. Online Optimal Charging Strategy for Electric Vehicles. *Energy Procedia*, 73:173–181, June 2015.

[256] Mehdi Maasoumy, Jorge Ortiz, David Culler, and Alberto Sangiovanni-Vincentelli. Flexibility of Commercial Building HVAC Fan as Ancillary Service for Smart Grid. *arXiv:1311.6094 [cs]*, November 2013. arXiv: 1311.6094.

[257] L. Majić, Ivana Krželj, and Marko Delimar. Optimal scheduling of a CHP system with energy storage. In *2013 36th International Convention on Information and Communication Technology, Electronics and Microelectronics (MIPRO)*, pages 1253–1257, May 2013.

[258] Tanmoy Malakar, Swapan K. Goswami, and Avinash K. Sinha. Optimum scheduling of micro grid connected wind-pumped storage hydro plant in a frequency based pricing environment. *International Journal of Electrical Power & Energy Systems*, 54:341–351, January 2014.

[259] Abhishek Malhotra, Benedikt Battke, Martin Beuse, Annegret Stephan, and Tobias Schmidt. Use cases for stationary battery technologies: A review of the literature and existing projects. *Renewable and Sustainable Energy Reviews*, 56:705–721, April 2016.

[260] Pawel Malysz, Shahin Sirouspour, and Ali Emadi. MILP-based rolling horizon control for microgrids with battery storage. *IECON 2013 - 39th Annual Conference of the IEEE Industrial Electronics Society*, pages 2099–2104, November 2013.

[261] Devin J. Marshman, Terrance Chmelyk, Mohandeep S. Sidhu, R. B. Gopaluni, and G. A. Dumont. Energy optimization in a pulp and paper mill cogeneration facility. *Applied Energy*, 87(11):3514–3525, November 2010.

[262] Henry Martin and Scott Otterson. German Intraday Electricity Market Analysis and Modeling Based on the Limit Order Book. *2018 15th International Conference on the European Energy Market (EEM)*, pages 1–6, June 2018.

[263] Elaheh Mashhour and Seyed Masoud Moghaddas-Tafreshi. Bidding Strategy of Virtual Power Plant for Participating in Energy and Spinning Reserve Markets—Part II: Numerical Analysis. *IEEE Transactions on Power Systems*, 26(2):957–964, May 2011.

[264] Brian Vad Mathiesen and Henrik Lund. Comparative analyses of seven technologies to facilitate the integration of fluctuating renewable energy sources. *IET Renewable Power Generation*, 3(2):190, 2009.

[265] Ingo Mauser. *Multi-modal Building Energy Management*. PhD Thesis, Karlsruher Institut für Technologie (KIT), 2017.

[266] Ingo Mauser, Jan Müller, Kevin Förderer, and Hartmut Schmeck. Definition, Modeling, and Communication of Flexibility in Smart Buildings and Smart Grid. In *ETG Congress 2017 – Die Energiewende, Bonn, November 28 – 29, 2017*, ETG-Fachberichte, pages 605–610. VDE VERLAG, 2017.

[267] Jan Meese, Benedikt Dahlmann, Markus Zdrallek, and Andy Voelschow. Intraday Redispatch - Optimal Scheduling of industrial processes at day-ahead and continuous intraday market. In *International ETG Congress 2017*, pages 1–6, November 2017.

[268] Olivier Megel. Storage in Power Systems: Frequency Control, Scheduling of Multiple Applications, and Computational Complexity. 2017.

[269] Eugenia D. Mehleri, Haralambos Sarimveis, Nikolaos C. Markatos, and Lazaros G. Papageorgiou. Optimal design and operation of distributed energy systems: Application to Greek residential sector. *Renewable Energy*, 51:331–342, March 2013.

[270] Rahul Mehta, D. Srinivasan, and Anupam Trivedi. Optimal charging scheduling of plug-in electric vehicles for maximizing penetration within a workplace car park. *2016 IEEE Congress on Evolutionary Computation (CEC)*, pages 3646–3653, July 2016.

[271] Rodrigo Mena, Martin Hennebel, Yan-Fu Li, Carlos Ruiz, and Enrico Zio. A risk-based simulation and multi-objective optimization framework for the integration of distributed renewable generation and storage. *Renewable and Sustainable Energy Reviews*, 37:778–793, September 2014.

[272] Pascal Mercier, Rachid Cherkaoui, and Alexandre Oudalov. Optimizing a Battery Energy Storage System for Frequency Control Application in an Isolated Power System. *IEEE Transactions on Power Systems*, 24(3):1469–1477, August 2009.

[273] Frank Merten, Christine Krüger, Arjuna Nebel, Dietmar Schüwer, and Stefan Lechtenböhmer. Klimapolitischer Beitrag kohlenstoffarmer Energieträger in der dezentralen Stromerzeugung sowie ihre Integration als Beitrag zur Stabilisierung der elektrischen Versorgungssysteme: Endbericht, 2015.

[274] Zoltan Meszaros. Hybridspeicher - Kraftwerk Gasturbine und Batterie, December 2018.

[275] Dennis Metz and João Tomé Saraiva. Simultaneous co-integration of multiple electrical storage applications in a consumer setting. *Energy*, 143:202–211, January 2018.

[276] Christian Milan, Michael Stadler, Gonçalo Cardoso, and Salman Mashayekh. Modeling of non-linear CHP efficiency curves in distributed energy systems. *Applied Energy*, 148:334–347, June 2015.

[277] Saeed Misaghian, Mohammadali Saffari, Mohsen Kia, Alireza Heidari, Miadreza Shafie-khah, and Joao P. S. Catalão. Tri-level optimization of industrial microgrids considering renewable energy sources, combined heat and power units, thermal and electrical storage systems. *Energy*, 161:396–411, October 2018.

[278] MITNETZ. *Netzentgelte für Entnahmen mit Leistungsmessung*. 2019. https://www.mitnetz-strom.de/Media/docs/default-source/datei-ablage/ne_2018_mns_pb1_rlm.pdf?sfvrsn=1c02acf9_4.

[279] Sumit Mitra, Lige Sun, and Ignacio E. Grossmann. Optimal scheduling of industrial combined heat and power plants under time-sensitive electricity prices. *Energy*, 54:194–211, June 2013.

[280] Hadi Moghimi, Abdollah Ahmadi, J. Aghaei, and Atefeh Rabiee. Stochastic techno-economic operation of power systems in the presence of distributed energy resources. *International Journal of Electrical Power & Energy Systems*, 45(1):477–488, February 2013.

[281] Hadi Moghimi Ghadikolaei, Abdollah Ahmadi, Jamshid Aghaei, and Meysam Najafi. Risk constrained self-scheduling of hydro/wind units for short term electricity markets considering intermittency and uncertainty. *Renewable and Sustainable Energy Reviews*, 16(7):4734–4743, September 2012.

[282] Faisal A. Mohamed and Heikki N. Koivo. System modelling and online optimal management of MicroGrid using Mesh Adaptive Direct Search. *International Journal of Electrical Power & Energy Systems*, 32(5):398–407, June 2010.

[283] Faisal A. Mohamed and Heikki N. Koivo. Multiobjective optimization using Mesh Adaptive Direct Search for power dispatch problem of microgrid. *International Journal of Electrical Power & Energy Systems*, 42(1):728–735, November 2012.

[284] Sirus Mohammadi, Soodabeh Soleymani, and Babak Mozafari. Scenario-based stochastic operation management of MicroGrid including Wind, Photovoltaic, Micro-Turbine, Fuel Cell and Energy Storage Devices. *International Journal of Electrical Power & Energy Systems*, 54:525–535, January 2014.

[285] Vincent Mohiuddin. Short-term Prognosis of Control Power Prices, Master Thesis, supervised by Julian Rominger. *Institute for Industrial Production, Karlsruhe Institute of Technology*, October 2018.

[286] Mohammad H. Moradi and A. Khandani. Evaluation economic and reliability issues for an autonomous independent network of distributed energy resources. *International Journal of Electrical Power & Energy Systems*, 56:75–82, March 2014.

[287] Rodrigo Moreno, Roberto Moreira, and Goran Strbac. A MILP model for optimising multi-service portfolios of distributed energy storage. *Applied Energy*, 137:554–566, January 2015.

[288] Naoya Motegi, Mary Ann Piette, David S. Watson, Sila Kiliccote, and Peng Xu. Introduction to commercial building control strategies and techniques for demand response. *Lawrence Berkeley National Laboratory LBNL-59975*, May 2007.

[289] Jan Müller. *Optimization Under Uncertainty in Building Energy Management*. PhD Thesis, Karlsruher Institut für Technologie (KIT), 2019.

[290] Jan Müller, Matthias März, Ingo Mauser, and Hartmut Schmeck. Optimization of Operation and Control Strategies for Battery Energy Storage Systems by Evolutionary Algorithms. *19th European Conference - Applications of Evolutionary Computation (EvoApplications), Porto, Portugal, March 30 - April 1, 2016, Part 1. Ed.: G. Squillero*, 9597:507–522, 2016.

[291] Michael Müller-Ruff and Julian Rominger. Simultane Erbringung und Sicherstellung von asymmetrischer Primär- und negativer Sekundärregelleistung durch eine Kraft-Wärme-Kopplungsanlage (KWK) [to be published].

[292] Marc Mültin. *Das Elektrofahrzeug als flexibler Verbraucher und Energiespeicher im Smart Home*. PhD Thesis, KIT, Karlsruhe, 2014.

[293] Waqaas Munawar. *Model-Based Design, Analysis, and Implementations for Power and Energy-Efficient Computing Systems*. PhD Thesis, Karlsruher Institut für Technologie (KIT), 2019.

[294] Ilham Naharudinsyah and Steffen Limmer. Optimal Charging of Electric Vehicles with Trading on the Intraday Electricity Market. *Energies*, 11(6):1416, June 2018. Number: 6 Publisher: Multidisciplinary Digital Publishing Institute.

[295] Pavan Kumar Naraharisetti, I. A. Karimi, Abhay Anand, and Dong-Yup Lee. A linear diversity constraint – Application to scheduling in microgrids. *Energy*, 36(7):4235–4243, July 2011.

[296] Nationale Plattform Elektromobilität. Fortschrittsbericht der Nationalen Plattform Elektromobilität (Dritter Bericht). *Gemeinsame Geschäftsstelle Elektromobilität der Bundesregierung (GGEMO), Berlin*, 2012.

[297] Myriam Neaimeh, Robin Wardle, Andrew M. Jenkins, Jialiang Yi, Graeme Hill, Padraig F. Lyons, Yvonne Hübner, Phil T. Blythe, and Phil C. Taylor. A probabilistic approach to combining smart meter and electric vehicle charging data to investigate distribution network impacts. *Applied Energy*, 157:688–698, November 2015.

[298] Bijay Neupane, Laurynas Šikšnys, and Torben Bach Pedersen. Generation and Evaluation of Flex-Offers from Flexible Electrical Devices. *Proceedings of the Eighth International Conference on Future Energy Systems*, pages 143–156, 2017. event-place: Shatin, Hong Kong.

[299] Linna Ni, Fushuan Wen, Weijia Liu, Jinling Meng, Guoying Lin, and Sanlei Dang. Congestion management with demand response considering uncertainties of distributed generation outputs and market prices. *Journal of Modern Power Systems and Clean Energy*, 5(1):66–78, January 2017.

[300] Stefan Nickel, Oliver Stein, and Karl-Heinz Waldmann. *Operations Research*. Springer-Lehrbuch. Gabler Verlag, 2 edition, 2014.

[301] Taher Niknam, Rasoul Azizipanah-Abarghooee, and Mohammad Rasoul Narimani. An efficient scenario-based stochastic programming framework for multi-objective optimal micro-grid operation. *Applied Energy*, 99:455–470, November 2012.

[302] Seyyed Mostafa Nosratabadi, Rahmat-Allah Hooshmand, and Eskandar Gholipour. A comprehensive review on microgrid and virtual power plant concepts employed for distributed energy resources scheduling in power systems. *Renewable and Sustainable Energy Reviews*, 67:341–363, January 2017.

[303] Björn Nykvist and Måns Nilsson. Rapidly falling costs of battery packs for electric vehicles. *Nature Climate Change*, 5(4):329–332, April 2015. Number: 4 Publisher: Nature Publishing Group.

[304] Frauke Oldewurtel, Theodor Borsche, Matthias Bucher, Philipp Fortenbacher, Marina González Vayá Tobias Haring, Tobias Haring, Johanna L. Mathieu, Olivier Mégel, Evangelos Vrettos, and Göran Andersson. A framework for and assessment of demand response and energy storage in power systems. *2013 IREP Symposium Bulk Power System Dynamics and Control - IX Optimization, Security and Control of the Emerging Power Grid*, pages 1–24, August 2013.

[305] Pol Olivella-Rosell, Pau Lloret-Gallego, Íngrid Munné-Collado, Roberto Villafafila-Robles, Andreas Sumper, Stig Ødegaard Ottessen, Jayaprakash Rajasekharan, and Bernt A. Bremdal. Local Flexibility Market Design for Aggregators Providing Multiple Flexibility Services at Distribution Network Level. *Energies*, 11(4):822, April 2018.

[306] Alexandra-Gwyn Paetz, Thomas Kaschub, Patrick Jochem, and Wolf Fichtner. Load-shifting potentials in households including electric mobility - A comparison of user behaviour with modelling results. *2013 10th International Conference on the European Energy Market (EEM)*, pages 1–7, May 2013.

[307] Peter Palensky and Dietmar Dietrich. Demand Side Management: Demand Response, Intelligent Energy Systems, and Smart Loads. *IEEE Transactions on Industrial Informatics*, 7(3):381–388, August 2011.

[308] Stefanos V. Papaefthymiou and Stavros A. Papathanassiou. Optimum sizing of wind-pumped-storage hybrid power stations in island systems. *Renewable Energy*, 64:187–196, April 2014.

[309] Markos Papageorgiou, Marion Leibold, and Martin Buss. *Optimierung: Statische, dynamische, stochastische Verfahren für die Anwendung*. Springer Vieweg, 4 edition, 2015.

[310] Christian Pape, Simon Hagemann, and Christoph Weber. Are fundamentals enough? Explaining price variations in the German day-ahead and intraday power market. *Energy Economics*, 54:376–387, February 2016.

[311] Moein Parastegari, Rahmat-Allah Hooshmand, and Majid Moazzami. Coordinated Scheduling of Renewable Energy Sources in the Unit Commitment Problem: A Review of Recent Literature. *Iranian Journal of Science and Technology, Transactions of Electrical Engineering*, 43(1):15–37, July 2019.

[312] Moritz Paulus and Frieder Borggrefe. The potential of demand-side management in energy-intensive industries for electricity markets in Germany. *Applied Energy*, 88(2):432–441, February 2011.

[313] Dominik Pelzer, David Ciechanowicz, Heiko Aydt, and Alois Knoll. A price-responsive dispatching strategy for Vehicle-to-Grid: An economic evaluation applied to the case of Singapore. *Journal of Power Sources*, 256:345–353, June 2014.

[314] Cristian Perfumo, Ernesto Kofman, Julio H. Braslavsky, and John K. Ward. Load management: Model-based control of aggregate power for populations of thermostatically controlled loads. *Energy Conversion and Management*, 55:36–48, March 2012.

[315] Mette K. Petersen, Kristian Edlund, Lars Henrik Hansen, Jan Bendtsen, and Jakob Stoustrup. A taxonomy for modeling flexibility and a computationally efficient algorithm for dispatch in smart grids. *American Control Conference (ACC), 2013*, pages 1150–1156, 2013.

[316] Philipp Maria Pfeifroth. *Modellierung der Einsatzplanung funktionaler Stromspeicher für Strom-und Regelleistungsmärkte*. PhD thesis, Technische Universität München (TUM), 2015.

[317] Dragana H. Popovic, David J. Hill, and Qiang Wu. Coordinated Static and Dynamic Voltage Control in Large Power Systems. *Bulk Power System Dynamics and Control IV - Re-structuring*, 1998.

[318] Joachim Pott. Jenbacher Produkte und Anwendungen, September 2015. https://www.technologieforum-osmo.com/fileadmin/data/pdf/V9_Jenbacher_Einsatzbereiche_der_Kraft-Waerme-Kopplung.pdf.

[319] Press and Information Office of the Federal Government. Climate change will determine our fate, November 2017. https://www.bundesregierung.de/breg-en/issues/sustainability/climate-change-will-determine-our-fate-434242.

[320] Volker V. Quaschning. *Renewable energy and climate change*. Wiley, 2019.

[321] Daniel Quiggin, Sarah Cornell, Michael Tierney, and Richard Buswell. A simulation and optimisation study: Towards a decentralised microgrid, using real world fluctuation data. *Energy*, 41(1):549–559, May 2012.

[322] Andreas Franz Alois Raab. Operational planning, modeling and control of virtual power plants with electric vehicles. 2018. Accepted: 2018-02-05T09:54:42Z.

[323] Abdorreza Rabiee, Mohammad Sadeghi, Jamshid Aghaeic, and Alireza Heidari. Optimal operation of microgrids through simultaneous scheduling of electrical vehicles and responsive loads considering wind and PV units uncertainties. *Renewable and Sustainable Energy Reviews*, 57:721–739, May 2016.

[324] Alireza Rezvani, Majid Gandomkar, Maziar Izadbakhsh, and Abdollah Ahmadi. Environmental/economic scheduling of a micro-grid with renewable energy resources. *Journal of Cleaner Production*, 87:216–226, January 2015.

[325] Peter Richardson, Damian Flynn, and Andrew Keane. Optimal Charging of Electric Vehicles in Low-Voltage Distribution Systems. *IEEE Transactions on Power Systems*, 27(1):268–279, February 2012.

[326] Julian Rominger. muse_industry, 2020. https://github.com/julianrominger/muse_industry.

[327] Julian Rominger and Csaba Farkas. Public charging infrastructure in Japan – A stochastic modelling analysis. *International Journal of Electrical Power & Energy Systems*, 90:134–146, September 2017.

[328] Julian Rominger, Fabian Kern, and Hartmut Schmeck. Provision of frequency containment reserve with an aggregate of air handling units. *Computer Science - Research and Development*, 33(1):215–221, February 2018.

[329] Julian Rominger, Manuel Loesch, and Hartmut Schmeck. Utilization of Electric Vehicle Charging Flexibility to Lower Peak Load by Controlled Charging (G2V and V2G) [to be published]. *IFAC Workshop on Control of Smart Grid and Renewable Energy Systems (CSGRES 2019)*, 2019.

[330] Julian Rominger, Manuel Lösch, Sebastian Steuer, Katrin Köper, and Hartmut Schmeck. Analysis of the German Continuous Intraday Market and the Revenue Potential for Flexibility Options. *2019 16th International Conference on the European Energy Market (EEM)*, pages 1–6, September 2019.

[331] Julian Rominger, Patrick Ludwig, Fabian Kern, Manuel Lösch, and Hartmut Schmeck. Utilization of Local Flexibility for Charge Management of a Battery Energy Storage System Providing Frequency Containment Reserve. *Energy Procedia*, 155:443–453, November 2018.

[332] Michael Ross, Chad Abbey, Franois Bouffard, and Gza Jos. Multiobjective Optimization Dispatch for Microgrids With a High Penetration of Renewable Generation. *IEEE Transactions on Sustainable Energy*, 6(4):1306–1314, October 2015. Conference Name: IEEE Transactions on Sustainable Energy.

[333] Nasrin Sadeghianpourhamami, N. Refa, Matthias Strobbe, and Chris Develder. Quantitive analysis of electric vehicle flexibility: A data-driven approach. *International Journal of Electrical Power & Energy Systems*, February 2018.

[334] Cem Sahin, Mohammad Shahidehpour, and Ismet Erkmen. Generation risk assessment in volatile conditions with wind, hydro, and natural gas units. *Applied Energy*, 96:4–11, August 2012.

[335] Eleonora Riva Sanseverino, Maria Luisa Di Silvestre, Mariano Giuseppe Ippolito, Alessandra De Paola, and Giuseppe Lo Re. An execution, monitoring and replanning approach for optimal energy management in microgrids. *Energy*, 36(5):3429–3436, May 2011.

[336] Mushfiqur R. Sarker, Y. Dvorkin, and Miguel A. Ortega-Vazquez. Optimal Participation of an Electric Vehicle Aggregator in Day-Ahead Energy and Reserve Markets. *IEEE Transactions on Power Systems*, 31(5):3506–3515, September 2016.

[337] Mushfiqur R. Sarker, Matthew D. Murbach, Daniel T. Schwartz, and Miguel A. Ortega-Vazquez. Optimal operation of a battery energy storage system: Trade-off between grid economics and storage health. *Electric Power Systems Research*, 152:342–349, November 2017.

[338] Rick Scharrenberg, Bram Vonk, and Phuong H. Nguyen. EV stochastic modelling and its impacts on the Dutch distribution network. *2014 International Conference on Probabilistic Methods Applied to Power Systems (PMAPS)*, pages 1–6, July 2014.

[339] Johannes Schäuble, Thomas Kaschub, Axel Ensslen, Patrick Jochem, and Wolf Fichtner. Generating electric vehicle load profiles from empirical data of three EV fleets in Southwest Germany. *Journal of Cleaner Production*, 150:253–266, May 2017.

[340] Fabian Scheller, Simon Johanning, Stephan Seim, Kerstin Schuchardt, Jonas Krone, Rosa Haberland, and Thomas Bruckner. Legal Framework of Decentralized Energy Business Models in Germany: Challenges and Opportunities for Municipal Utilities. *Zeitschrift für Energiewirtschaft*, 42(3):207–223, September 2018.

[341] Jonas Schlund, Ronny Steinert, and Marco Pruckner. Coordinating E-Mobility Charging for Frequency Containment Reserve Power Provision. *Proceedings of the Ninth International Conference on Future Energy Systems*, pages 556–563, 2018.

[342] Alexander Schuller, Christoph M. Flath, and Sebastian Gottwalt. Quantifying load flexibility of electric vehicles for renewable energy integration. *Applied Energy*, 151:335–344, August 2015.

[343] Adolf J. Schwab. *Elektroenergiesysteme: Erzeugung, Transport, Übertragung und Verteilung elektrischer Energie*. Springer-Verlag, Berlin Heidelberg, 2 edition, 2009.

[344] Katrin Seddig, Patrick Jochem, and Wolf Fichtner. Two-stage stochastic optimization for cost-minimal charging of electric vehicles at public charging stations with photovoltaics. *Applied Energy*, 242:769–781, May 2019.

[345] T. Seeger and Johannes Verstege. Short term scheduling in cogeneration systems. *[Proceedings] Conference Papers 1991 Power Industry Computer Application Conference*, pages 106–112, May 1991.

[346] Karsten Senkel. Wieviel Batteriegroßspeicher verträgt der Primärregelleistungsmarkt?, 2017.

[347] Yingying Seow and Shahin Rahimifard. A framework for modelling energy consumption within manufacturing systems. *CIRP Journal of Manufacturing Science and Technology*, 4(3):258–264, January 2011.

[348] M. Shafie-khah, E. Heydarian-Forushani, M. E. H. Golshan, P. Siano, M. P. Moghaddam, M. K. Sheikh-El-Eslami, and J. P. S. Catalão. Optimal trading of plug-in electric vehicle aggregation agents in a market environment for sustainability. *Applied Energy*, 162:601–612, January 2016.

[349] Jingshuang Shen, Chuanwen Jiang, Yangyang Liu, and Jie Qian. A Microgrid Energy Management System with Demand Response for Providing Grid Peak Shaving. *Electric Power Components and Systems*, 44(8):843–852, May 2016.

[350] Lukas Sigrist, Enrique Lobato, and Luis Rouco. Energy storage systems providing primary reserve and peak shaving in small isolated power systems: An economic assessment. *International Journal of Electrical Power & Energy Systems*, 53(Supplement C):675–683, December 2013.

[351] Peter Sorknæs, Henrik Lund, Anders N. Andersen, and Peter Ritter. Small-scale combined heat and power as a balancing reserve for wind – The case of participation in the German secondary control reserve. *International Journal of Sustainable Energy Planning and Management*, 4:31–42, 2014.

[352] Ingo Stadler. *Demand Response: Nichtelektrische Speicher für Elektrizitätsversorgungssysteme mit hohem Anteil erneuerbarer Energien*. Winter Industries, Berlin, March 2006.

[353] Ingo Stadler. Power grid balancing of energy systems with high renewable energy penetration by demand response. *Utilities Policy*, 16(2):90–98, June 2008.

[354] Statkraft. Statkraft und REstore planen Deutschlands ersten Primärregelleistungspool aus Batteriespeicher und industriellen Verbrauchern, September 2017. https://www.statkraft.de/presse/Pressemitteilungen/Pressemitteilungen-archiv/2017/statkraft–restore.

[355] David Steber, Marco Pruckner, Peter Bazan, and Reinhard German. SWARM — Providing 1 MW FCR power with residential PV-battery energy storage — Simulation and empiric validation. *2017 IEEE Manchester PowerTech*, pages 1–6, June 2017.

[356] Michael Horst Emil Steck. Mikro-KWK und virtuelle Kraftwerke – Neue Energielandschaften, October 2010.

[357] Michael Horst Emil Steck. *Entwicklung und Bewertung von Algorithmen zur Einsatzplanerstellung virtueller Kraftwerke*. PhD thesis, Technische Universität München (TUM), 2013.

[358] Oliver Stein. *Grundzüge der Globalen Optimierung*. Springer Spektrum, 2018.

[359] Oliver Stein. Restringierte Optimierung. In Oliver Stein, editor, *Grundzüge der Nichtlinearen Optimierung*, pages 111–212. Springer, Berlin, Heidelberg, 2018.

[360] Peter Stenzel, Johannes Fleer, and Jochen Linssen. Elektrochemische Speicher. In Martin Wietschel, Sandra Ullrich, Peter Markewitz, Friedrich Schulte, and Fabio Genoese, editors, *Energietechnologien der Zukunft: Erzeugung, Speicherung, Effizienz und Netze*, pages 157–214. Springer Fachmedien Wiesbaden, Wiesbaden, 2015.

[361] Annegret Stephan, Benedikt Battke, Martin D. Beuse, J. H. Clausdeinken, and Tobias S. Schmidt. Limiting the public cost of stationary battery deployment by combining applications. *Nature Energy*, 1(7):16079, July 2016.

[362] P. Stluka, D. Godbole, and T. Samad. Energy management for buildings and microgrids. In *2011 50th IEEE Conference on Decision and Control and European Control Conference*, pages 5150–5157, December 2011.

[363] Gernot Stoeglehner, Nora Niemetz, and Karl-Heinz Kettl. Spatial dimensions of sustainable energy systems: new visions for integrated spatial and energy planning. *Energy, Sustainability and Society*, 1(1):2, November 2011.

[364] Wencong Su, Jianhui Wang, and Jaehyung Roh. Stochastic Energy Scheduling in Microgrids With Intermittent Renewable Energy Resources. *IEEE Transactions on Smart Grid*, 5(4):1876–1883, July 2014.

[365] Stjepan Sučić, Tomislav Dragičević, Tomislav Capuder, and Marko Delimar. Economic dispatch of virtual power plants in an event-driven service-oriented framework using standards-based communications. *Electric Power Systems Research*, 81(12):2108–2119, December 2011.

[366] Olle Sundstrom and Carl Binding. Flexible Charging Optimization for Electric Vehicles Considering Distribution Grid Constraints. *IEEE Transactions on Smart Grid*, 3(1):26–37, March 2012.

[367] Maciej Swierczynski, Daniel-Ioan Stroe, Ana-Irina Stan, Remus Teodorescu, Rasmus Lærke, and Philip Carne Kjær. Field tests experience from 1.6MW/400kWh Li-ion battery energy storage system providing primary frequency regulation service. *IEEE PES ISGT Europe 2013*, pages 1–5, October 2013.

[368] Sajad Tabatabaee, Seyed Saeedallah Mortazavi, and Taher Niknam. Stochastic energy management of renewable micro-grids in the correlated environment using unscented transformation. *Energy*, 109:365–377, August 2016.

[369] P. A. Taylor. Update on the Puerto Rico electric power authority's spinning reserve battery system. In *Proceedings of 11th Annual Battery Conference on Applications and Advances*, pages 249–252, January 1996.

[370] Jen-Hao Teng, Shang-Wen Luan, Dong-Jing Lee, and Yong-Qing Huang. Optimal Charging/Discharging Scheduling of Battery Storage Systems for Distribution Systems Interconnected With Sizeable PV Generation Systems. *IEEE Transactions on Power Systems*, 28(2):1425–1433, May 2013.

[371] TenneT TSO GmbH. Haushalte ersetzen Kraftwerke - sonnen nimmt größte, virtuelle Batterie für das Stromnetz der Zukunft in Betrieb, December 2018. https://www.tennet.eu/de/news/news/haushalte-ersetzen-kraftwerke-sonnen-nimmt-groesste-virtuelle-batterie-fuer-das-stromnetz-der-zukunf.

[372] TenneT TSO GmbH. Blockchain-Pilot zeigt Potenzial von dezentralen Heimspeichern für das Energiesystem von morgen, May 2019. https://www.tennet.eu/de/news/news/blockchain-pilot-zeigt-potenzial-von-dezentralen-heimspeichern-fuer-das-energiesystem-von-morgen-1.

[373] TenneT TSO GmbH. Märkte in C/sells: Netzdienstleistungen - YouTube, July 2019. https://www.youtube.com/watch?v=joY2qDRIjUY&t=405s.

[374] TenneT TSO GmbH. Status Bilanzkreise, July 2019. https://www.tennet.eu/de/strommarkt/strommarkt-in-deutschland/bilanzkreise/.

[375] The German Energy Storage Association. *Faktenpapier Energiespeicher. Rechtsrahmen. Geschäftsmodelle. Forderungen.* 2017. http://www.bves.de/wp-content/uploads/2017/05/Faktenpapier_2017.pdf.

[376] Sebastian M Thiem. *Multi-modal on-site energy systems*. PhD thesis, Technische Universität München (TUM), January 2017.

[377] Tjark Thien, Daniel Schweer, Denis vom Stein, Albert Moser, and Dirk Uwe Sauer. Real-world operating strategy and sensitivity analysis of frequency containment reserve provision with battery energy storage systems in the german market. *Journal of Energy Storage*, 13:143–163, October 2017.

[378] Dan T. Ton and Merrill A. Smith. The U.S. Department of Energy's Microgrid Initiative. *The Electricity Journal*, 25(8):84–94, October 2012.

[379] TransnetBW. Regelenergie Bedarf und Abruf, 2019.

[380] J. Trefke, S. Rohjans, M. Uslar, S. Lehnhoff, L. Nordström, and A. Saleem. Smart Grid Architecture Model use case management in a large European Smart Grid project. *IEEE PES ISGT Europe 2013*, pages 1–5, October 2013.

[381] Cong Nam Truong, Michael Schimpe, Uli Bürger, Holger C. Hesse, and Andreas Jossen. Multi-Use of Stationary Battery Storage Systems with Blockchain Based Markets. *Energy Procedia*, 155:3–16, November 2018.

[382] Anna S. Tsagkou, Evangelos D. Kerasidis Dimitrios I. Doukas, Dimitris P. Labridis, Antonis G. Marinopoulos, and Tomas Tengnér. Stacking grid services with energy storage techno-economic analysis. *2017 IEEE Manchester PowerTech*, pages 1–6, June 2017.

[383] C.-L. Tseng and W. Zhu. Optimal self-scheduling and bidding strategy of a thermal unit subject to ramp constraints and price uncertainty. *Transmission Distribution IET Generation*, 4(2):125–137, February 2010. Conference Name: Transmission Distribution IET Generation.

[384] Tea Tušar, Laurynas Šikšnys, Torben Bach Pedersen, Erik Dovgan, and Bogdan Filipic. Using aggregation to improve the scheduling of flexible energy offers. *Proc. of BIOMA*, pages 347–358, 2012.

[385] Universal Smart Energy Framework. *USEF: the framework explained.* November 2015.

[386] Universal Smart Energy Framework. *USEF: The framework specifications*. November 2015.

[387] Mart van der Kam and Wilfried van Sark. Smart charging of electric vehicles with photovoltaic power and vehicle-to-grid technology in a microgrid; a case study. *Applied Energy*, 152:20–30, August 2015.

[388] Stijn Vandael, Bert Claessens, Damien Ernst, Tom Holvoet, and Geert Deconinck. Reinforcement Learning of Heuristic EV Fleet Charging in a Day-Ahead Electricity Market. *IEEE Transactions on Smart Grid*, 6(4):1795–1805, July 2015.

[389] VDE - Verband der Elektrotechnik Elektronik Informationstechnik e. V. Erzeugungsanlagen am Niederspannungsnetz (VDE-AR-N 4105), 2011. https://www.vde.com/de/fnn/themen/tar/tar-niederspannung/erzeugungsanlagen-am-niederspannungsnetz-vde-ar-n-4105.

[390] Verband der Netzbetreiber. *TransmissionCode 2007 - Netz- und Systemregeln der deutschen Übertragungsnetzbetreiber*. 2007. https://www.regelleistung.net/ext/download/transmission2007.

[391] Verband der Netzbetreiber. Eckpunkte und Freiheitsgrade bei Erbringung von Primärregelleistung, 2014. https://www.regelleistung.net/ext/download/eckpunktePRL.

[392] Verband der Netzbetreiber. Anforderungen an die Speicherkapazität bei Batterien für die Primärregelleistung, 2015. https://www.regelleistung.net/ext/download/anforderungBatterien.

[393] Verband der Netzbetreiber. Aktuelles und zukünftiges Rollenverständnis der übertragungsnetzbetreiber insbesondere hinsichtlich der Zusammenarbeit mit Verteilnetzbetreibern, August 2017. https://www.amprion.net/Dokumente/Dialog/Downloads/Stellungnahmen/2017_08_30_langfassung_-positionspapier_tsodso.pdf.

[394] Verband der Netzbetreiber. Ausschreibungsübersicht auf Regelleistung.net, 2018. https://www.regelleistung.net/ext/tender/.

[395] Verband der Netzbetreiber. Präqualifizierte Leistung in Deutschland, 2018. https://www.regelleistung.net/ext/download/pq_capacity.

[396] Verband der Netzbetreiber. Systemschutzplan der vier deutschen übertragungsnetzbetreiber, December 2018. https://www.netztransparenz.de/portals/1/Content/EU-Network-Codes/ER-VErordnung/Systemschutzplan%20der%20%C3%9CNB%20-%20Hauptdokument.pdf.

[397] Verband der Netzbetreiber. Weitere Informationen zum Workshop zum neuen Dimensionierungsverfahren, 2018. https://www.regelleistung.net/ext/tender/remark/news/345.

[398] Verband der Netzbetreiber. Internetplattform zur Vergabe von Regelleistung, 2019. https://www.regelleistung.net/ext/tender/.

[399] Verband der Netzbetreiber. Prequalification Process for Balancing Service Providers (FCR, aFRR, mFRR) in Germany ("PQ conditions"), May 2019. https://www.regelleistung.net/ext/download/Ergebnis_Konsultation_Mai_2018.

[400] Verband der Netzbetreiber. Quartalsbericht zu Netz- und Systemsicherheitsmaßnahmen Gesamtjahr und Viertes Quartal 2018, August 2019. https://www.bundesnetzagentur.de/SharedDocs/Downloads/DE/Allgemeines/Bundesnetzagentur/Publikationen/Berichte/2019/Q
Q4_2018.pdf?__blob=publicationFile&v=6.

[401] Verband der Netzbetreiber. Systembilanzabweichung Juni 2019, 2019. https://www.regelleistung.net/ext/download/JuniSystemBilanz.

[402] Verband der Netzbetreiber. Untersuchung von Systembilanzungleichgewichten in Deutschland im Juni 2019, November 2019. https://www.regelleistung.net/ext/download/STUDIE_JUNI2019.

[403] Verband der Netzbetreiber. Anbieterworkshop der deutschen übertragungsnetzbetreiber zum Regelarbeitsmarkt, January 2020. https://www.regelleistung.net/ext/tender/remark/download/128315996.

[404] Jens Vetter, P. Novák, Markus R. Wagner, C. Veit, Kai Christian Möller, J. O. Besenhard, M. Winter, M. Wohlfahrt-Mehrens, C. Vogler, and A. Hammouche. Ageing mechanisms in lithium-ion batteries. *Journal of Power Sources*, 147(1):269–281, September 2005.

[405] Olli Vilppo, Antti Rautiainen, Jenni Rekola, Joni Markkula, Kai Vuorilehto, and Pertti Järventausta. Profitable Multi-Use of Battery Energy Storage in Outage Mitigation and as Frequency Reserve. *International Review of Electrical Engineering (IREE)*, 13(3):185, June 2018.

[406] Thorsten Vogt, Julia Badeda, Joachim Böcker, and Dirk Uwe Sauer. Consideration on primary control reserve provision by industrial microgrids in grid-coupled operation. In *2017 IEEE 12th International Conference on Power Electronics and Drive Systems (PEDS)*, pages 105–113, December 2017. ISSN: 2164-5264.

[407] Katharina Volk, Christian Lakenbrink, Linda Rupp, Joe Imfeld, Peter Stolle, Dr. Daniel Zech, Florian Wellmann, Steffen Pfendtner, Dr. Sebastian Kochanneck, Kevin Förderer, Dr. Pascal Wiest, Daniel Groß, Simon Eberlein, Daniel Contreras, Dr. Tobias Mirbach, and Jakub Vancura. Abschlussbericht grid control, June 2019.

[408] Evangelos Vrettos, Stephan Koch, and Göran Andersson. Load frequency control by aggregations of thermally stratified electric water heaters. *2012 3rd IEEE PES Innovative Smart Grid Technologies Europe (ISGT Europe)*, pages 1–8, October 2012.

[409] Evangelos Vrettos, Frauke Oldewurtel, Fengtian Zhu, and Göran Andersson. Robust Provision of Frequency Reserves by Office Building Aggregations. *IFAC Proceedings Volumes*, 47(3):12068–12073, January 2014.

[410] Timo Wagner. Energy market crawlers rmarketcrawlR, emarketcrawlR, and entsoecrawlR, 2019. https://github.com/wagnertimo.

[411] Fabian Wandelt, Dennis Gamrad, Deis Wolfgang, and Johanna Myrzik. Vergleich und Einsatzmöglichkeiten verschiedener Technologien zur Regelleistungserbringung. 2015.

[412] Zongfei Wang, Patrick Jochem, and Wolf Fichtner. A scenario-based stochastic optimization model for charging scheduling of electric vehicles under uncertainties of vehicle availability and charging demand. *Journal of Cleaner Production*, 254:119886, May 2020.

[413] Prof. Dr. Christoph Weber. Berücksichtigung von Intraday-Optionalitäten im Rahmen der Redispatch-Vergütung, August 2015.

[414] M. de Weerdt, G. Morales-Espana, and K. van der Linden. Optimal Non-Zero Price Bids for EVs in Energy and Reserves Markets Using Stochastic Optimization. *2018 15th International Conference on the European Energy Market (EEM)*, pages 1–5, June 2018.

[415] WEMAG. Batteriespeicher testet erfolgreich Schwarzstart nach Blackout, August 2017. https://www.wemag.com/aktuelles-presse/wemag-batteriespeicher-testet-erfolgreich-schwarzstart-nach-blackout.

[416] Günther Westner and Reinhard Madlener. Development of cogeneration in Germany: A mean-variance portfolio analysis of individual technology's prospects in view of the new regulatory framework. *Energy*, 36(8):5301–5313, August 2011.

[417] Holger Wiechmann. *Neue Betriebsführungsstrategien für unterbrechbare Verbrauchseinrichtungen: Ein Modell für eine markt- und erzeugungsorientierte Regelung der Stromnachfrage über ein zentrales Lastmanagement*. PhD thesis, Karlsruhe Institut für Technologie (KIT), 2008.

[418] Adam Wierman. Online Optimization & Energy, October 2019.

[419] Bernhard Wille-Haussmann, Thomas Erge, and Christof Wittwer. Decentralised optimisation of cogeneration in virtual power plants. *Solar Energy*, 84(4):604–611, April 2010.

[420] Lukas Wolf. Effects of Bi-Directional Charging on the Components of an Electrical Vehicle for different Use Cases, Master Thesis, partly supervised by Julian Rominger. *Institute for Electrical Energy Storage Technology, TU Munich*, September 2019.

[421] Di Wu, Dionysios C. Aliprantis, and Lei Ying. Load Scheduling and Dispatch for Aggregators of Plug-In Electric Vehicles. *IEEE Transactions on Smart Grid*, 3(1):368–376, March 2012.

[422] Di Wu, Chunlian Jin, Patrick Balducci, and Michael Kintner-Meyer. An energy storage assessment: Using optimal control strategies to capture multiple services. In *2015 IEEE Power Energy Society General Meeting*, pages 1–5, July 2015. ISSN: 1932-5517.

[423] Philip Würfel. *Unter Strom: Die neuen Spielregeln der Stromwirtschaft*. Springer Spektrum, 2015.

[424] Hasan Ümitcan Yilmaz, Dogan Keles, Alessandro Chiodi, Rupert Hartel, and Martina Mikulić. Analysis of the power-to-heat potential in the European energy system. *Energy Strategy Reviews*, 20:6–19, April 2018.

[425] Ryohei Yokoyama, Yasushi Hasegawa, and Koichi Ito. A MILP decomposition approach to large scale optimization in structural design of energy supply systems. *Energy Conversion and Management*, 43(6):771–790, April 2002.

[426] Ryohei Yokoyama and Koichi Ito. Operational Strategy of a Cogeneration System Under a Complex Utility Rate Structure. *Journal of Energy Resources Technology*, 118(4):256–262, December 1996.

[427] Ryohei Yokoyama, Yuji Shinano, Syusuke Taniguchi, Masashi Ohkura, and Tetsuya Wakui. Optimization of energy supply systems by MILP branch and bound method in consideration of hierarchical relationship between design and operation. *Energy Conversion and Management*, 92:92–104, March 2015.

[428] Alireza Zakariazadeh, Shahram Jadid, and Pierluigi Siano. Stochastic multi-objective operational planning of smart distribution systems considering demand response programs. *Electric Power Systems Research*, 111:156–168, June 2014.

[429] Ali Ghahgharaee Zamani, Alireza Zakariazadeh, and Shahram Jadid. Day-ahead resource scheduling of a renewable energy based virtual power plant. *Applied Energy*, 169:324–340, May 2016.

[430] Alexander Zeh, Marcus Mueller, Holger C. Hesse, Andreas Jossen, and Rolf Witzmann. Operating a Multitasking Stationary Battery Storage System for Providing Secondary Control Reserve on Low-Voltage Level. In *International ETG Congress 2015; Die Energiewende - Blueprints for the new energy age*, pages 1–8, November 2015.

[431] Linfeng Zhang, Nicolae Gari, and Lawrence V. Hmurcik. Energy management in a microgrid with distributed energy resources. *Energy Conversion and Management*, 78:297–305, February 2014.

[432] T. Zhang, W. Chen, Z. Han, and Z. Cao. Charging Scheduling of Electric Vehicles With Local Renewable Energy Under Uncertain Electric Vehicle Arrival and Grid Power Price. *IEEE Transactions on Vehicular Technology*, 63(6):2600–2612, July 2014.

[433] X. Zhang, R. Sharma, and Yanyi He. Optimal energy management of a rural microgrid system using multi-objective optimization. *2012 IEEE PES Innovative Smart Grid Technologies (ISGT)*, pages 1–8, January 2012.

[434] Y. Zhang and N. Lu. Demand-side management of air conditioning cooling loads for intra-hour load balancing. *2013 IEEE PES Innovative Smart Grid Technologies Conference (ISGT)*, pages 1–6, February 2013.

[435] Changhong Zhao, Ufuk Topcu, Na Li, and Steven Low. Design and Stability of Load-Side Primary Frequency Control in Power Systems. *IEEE Transactions on Automatic Control*, 59(5):1177–1189, May 2014.

[436] Peng Zhao, Gregor P. Henze, Michael J. Brandemuehl, Vincent J. Cushing, and Sandro Plamp. Dynamic frequency regulation resources of commercial buildings through combined building system resources using a supervisory control methodology. *Energy and Buildings*, 86:137–150, January 2015.

[437] Muhammad Fahad Zia, Elhoussin Elbouchikhi, and Mohamed Benbouzid. Microgrids energy management systems: A critical review on methods, solutions, and prospects. *Applied Energy*, 222:1033–1055, July 2018.